REPUBLIC OF BENIN

------000------

MINISTRY OF HIGHER EDUCATION AND SCIENTIFIC RESEARCH

------000------

UNIVERSITY OF ABOMEY - CALAVI

------000------

DOCTORAL SCHOOL OF LIFE AND EARTH SCIENCES

------000------

Registered under N°:416

A DISSERTATION

Submitted

In partial fulfillment of the requirements for the degree of

DOCTOR of Philosophy (PhD) of the University of Abomey-Calavi

In the framework of the

Graduate Research Program on Climate Change and Water Resources (GRP-CCWR)

By

Amichiatchi N'da Jocelyne Maryse Christine

Public defense on: 05/22/2024

======

ASSESSMENT OF THE IMPACT OF CLIMATE CHANGE ON HYDROLOGICAL EXTREMES IN COTE D'IVOIRE

Supervisors:

LAWIN Agnidé Emmanuel	Full Professor	University of ABOMEY-CALAVI, Benin
GOULA Bi Tie Albert	Full Professor	University of NANGUI ABROGOUA, Cote d'Ivoire

Reviewers:

FADIKA Vamoryba,	Associate Professor	University of NANGUI ABROGOUA, Cote d'Ivoire
ALAMOU Adéchina Eric,	Full Professor	University of ABOMEY-CALAVI, Benin
NGOUNOU NGATCHA Benjamin	Full Professor	University of NGAOUNDERE, Cameroon

JURY

KELOME Nelly	Professeur titulaire, Université d'ABOMEY-CALAVI, Benin	President
FADIKA Vamoryba	Maitre de Conferences, Université de NANGUI ABROGOUA, Cote d'Ivoire	Reviewer
ALAMOU Adéchina Eric	Professeur titulaire, Université d'ABOMEY-CALAVI, Benin	Reviewer
NGOUNOU NGATCHA Benjamin	Professeur titulaire, Université de NGAOUNDERE, Cameroon	Reviewer
GUEDJE Kossi François	Maitre de Conferences, Université d'ABOMEY-CALAVI, Benin	Examiner
LAWIN Agnidé Emmanuel	Professeur titulaire, Université d'ABOMEY-CALAVI, Benin	Supervisor
GOULA Bi Tie Albert	Professeur titulaire, Université de NANGUI ABROGOUA, Cote d'Ivoire	Co- Supervisor
SORO Gneneyougo Emile	Maitre de Conferences, Université de NANGUI ABROGOUA, Cote d'Ivoire	Advisor

WASCAL West African Science Service Centre on Climate Change and Adapted Land Use

Federal Ministry of Education and Research

REPUBLIQUE DU BENIN

------000------

MINISTERE DE L'ENSEIGNEMENT SUPERIEUR ET DE LA RECHERCHE SCIENTIFIQUE

------000------

UNIVERSITE D'ABOMEY - CALAVI

------000------

ECOLE DOCTORALE SCIENCES DE LA VIE ET DE LA TERRE

------000------

Enregistrée sous N°: 416

THESE

Soumise pour obtenir le grade de

DOCTEUR de l'Université d'Abomey-Calavi

Dans la Spécialité:

Changement climatique et Ressources en Eau

Par

Amichiatchi N'da Jocelyne Maryse Christine

Soutenue publiquement le: 22/05/2024

ASSESSMENT OF THE IMPACT OF CLIMATE CHANGE ON HYDROLOGICAL EXTREMES IN COTE D'IVOIRE

======

Directeurs de thèse:

LAWIN Agnidé Emmanuel	Professeur titulaire,	Université d'ABOMEY-CALAVI, Benin
GOULA Bi Tie Albert	Professeur titulaire	Université de NANGUI ABROGOUA, Cote d'Ivoire

Rapporteurs:

FADIKA Vamoryba	Maitre de Conferences	Université de NANGUI ABROGOUA, Cote d'Ivoire
ALAMOU Adéchina Eric	Professeur titulaire	Université d'ABOMEY-CALAVI, Benin
NGOUNOU NGATCHA Benjamin	Professeur titulaire	Université de NGAOUNDERE, Cameroon

JURY

KELOME Nelly	Professeur titulaire, Université d'ABOMEY-CALAVI, Benin	Presidente
FADIKA Vamoryba	Maitre de Conferences, Université de NANGUI ABROGOUA, Cote d'Ivoire	Rapporteur
ALAMOU Adéchina Eric	Professeur titulaire, Université d'ABOMEY-CALAVI, Benin	Rapporteur
NGOUNOU NGATCHA Benjamin	Professeur titulaire, Université de NGAOUNDERE, Cameroon	Rapporteur
GUEDJE Kossi François	Maitre de Conferences, Université d'ABOMEY-CALAVI, Benin	Examinateur
LAWIN Agnidé Emmanuel	Professeur titulaire, Université d'ABOMEY-CALAVI, Benin	Superviseur
GOULA Bi Tie Albert	Professeur titulaire, Université de NANGUI ABROGOUA, Cote d'Ivoire	Co- Superviseur
SORO Gneneyougo Emile	Maitre de Conferences, Université de NANGUI ABROGOUA, Cote d'Ivoire	Membre Encadrement

WASCAL West African Science Service Centre on Climate Change and Adapted Land Use

Federal Ministry of Education and Research

Dedication

I dedicate this work to God Almighty and my parents who kept me and gave me the education.

I am very grateful.

Acknowledgment

This PhD project is carried out within the context of the West African Science Service Center on Climate Change and Adapted Land Use (WASCAL) and is supported by the German Ministry of Education and Research (BMBF) in partnership with the Benin Ministry of High Education and Scientific Research (MESRS).

Completing this PhD thesis has been a long, exciting, and great trip that has allowed me to work and interact with a wide range of people. To my supervisors, Lawin Agnide Emmanuel (Université d'Abomey Calavi) and Goula Bi Tie Albert (Université de Nangui Abrogoua), as well as my advisor, Dr. Soro Gneneygo Emile (Université de Nangui Abrogoua), for their encouragement, devotion, and assistance throughout this research project. I can't express how much you have all influenced my life and assisted my scientific studies.

I would also like to offer my gratitude to the administration of the WASCAL research program at the University of Abomey Calavi, as well as all my colleagues, for their aid in.

Finally, and most importantly, I would like to express my sincere gratitude to my family and friends, especially my dear parents (AMICHIATCHI Anatole and KOUADIO Adjoua), my siblings, the family of Dr. Isaac Larbi, Dr. Andrew Limantol, Dr Hounkpè Jean and my friend and colleague Dr YAO Ble Anouma Fhorest, Dr DEGUI Attoungbré for their support, prayers, and encouragement both while I was away from home and throughout the study.

Synthèse de la Thèse

Les conditions hydrométéorologiques extrêmes, en particulier les inondations et les sécheresses, sont devenues des catastrophes naturelles annuelles en Côte d'Ivoire, causant des dommages matériels importants, des décès, et l'évacuation de la population, avec très souvent des difficultés pour l'approvisionnement en eau potable aux populations. Cette étude évalue l'impact du changement climatique sur les extrêmes hydrologiques (précipitations et débit) dans les différentes zones climatiques de la Côte d'Ivoire. Les objectifs de ce travail sont: (i) d'analyser les tendances hydro-climatiques historiques (précipitations et débits) de 1970 à 2017 et de connaitre l'effet de la variabilité des précipitations sur les débits d'étiage et de crue des bassins hydrographiques; (ii) d'étudier la performance des modèles hydrologiques GR4J, GR5J et HEC-HMS à simuler les débits d'étiage et de crue des bassins d'étude; (iii) d'examiner l'impact du changement climatique sur des phénomènes hydro-climatiques extrêmes selon les scénarios climatiques RCP4.5 et RCP8.5 pour la période de 2020 à 2050 avec les models climatiques suivants CM54,CNRM et MPI. Les données journalières de pluie, de débit, d'évapotranspiration (observées et futures) et les images satellitaires ont été les principales données de cette recherche. Ainsi, pour atteindre nos objectifs, plusieurs méthodes ont été utilisées. D'abord, l'extraction des différents indices des extrêmes hydro-climatiques, suivi de l'analyse de leurs fluctuations interannuelles par élimination des variations saisonnières à l'aide du filtre Hanning passe-bas d'ordre 2. Ensuite, l'analyse des tendances à l'aide du test Mann-Kendall modifié (MMK) et la détection d'homogénéité par le test d'homogénéité normale standard (SNHT) à un niveau de confiance de 0,05. Enfin, la simulation des extrêmes hydrologiques et l'étude des impacts du changement climatique futur par la modélisation hydrologique. Les résultats obtenus montrent que les indices d'extrêmes pluviométriques et les extrêmes hydrologiques de crue ont connu une tendance à la baisse, tandis que ceux des étiages, une tendance à la hausse. Les modèles hydrologiques, quant à eux, ont pu montrer une bonne performance à la calibration et à la validation avec des valeurs de Nash comprises entre 0.7 et 0.9. Le modèle GR5J, ayant montré la meilleure performance (valeurs de Nash comprises entre 0.7 et 0.9 en calage) sur tous les bassins d'études, a donc été utilisé dans la simulation des débits futurs sur ces différents bassins. Sous le scénario RCP 4.5 et selon les modèles climatiques CNRM, MPI, et ENSEMBLE, les indices pluviométriques pourraient connaître des tendances non-significatives à l'horizon 2020-2050. Sous le scénario RCP 8.5 et selon les modèles CM5A

et CNRM, les indices Pmaxan et Rx5days connaitront une tendance significative à la hausse. Une tendance non-significative a été observée dans les modèles MPI et ENSEMBLE. Les indices de débits extrêmes à l'horizon 2020-2050 pourraient connaître une tendance non-significative dans leur ensemble. Cependant, sous le scénario RCP4.5, l'indice de crue QMAXAN connaitra une hausse significative sur le bassin versant de la Bagoue, et sous le scénario RCP 8.5, les indices de crue QMAXAN, QX5days enregistreraient une baisse significative dans le nord du pays. Les indices d'étiage pris dans leur ensemble sous les scénarios RCP 4.5 et RCP 8.5 connaitront une baisse significative à l'horizon 2020-2050 sur les différents bassins d'étude. Aussi, l'évaluation de la dynamique de l'occupation du sol sur les extrêmes a été mise en évidence par plusieurs méthodes. Elle a relevé que du sud au nord et de l'ouest à l'est de la Côte d'Ivoire, on observe une bonne régression de la forêt ou de la savane, des ressources en eau, et une augmentation de l'habitat et des zones cultivées d'un endroit à l'autre. En outre, la relation entre l'évolution de l'indice de végétation (NDVI) et les indices extrêmes de pluie a montré une corrélation négative non-significative en général sur les bassins versants étudiés. De même, cette analyse a révélé une corrélation positive entre les indices de végétation (NDVI) et les indices extrêmes de débits dans son ensemble. De plus, l'impact du changement climatique affectera les paramètres avec une diminution dans les moyennes de pluies annuelles, les débits moyens, l'évapotranspiration, et une augmentation des températures. Ce travail a permis de comprendre le comportement hydrologique à travers l'étude et l'évaluation des performances de certains modèles hydrologiques par la simulation et l'évaluation de l'impact du changement climatique sur certains paramètres climatiques et des indices extrêmes hydro-climatiques. Ces connaissances seront utilisées pour planifier des politiques et des stratégies afin de se préparer aux défis potentiels qui résulteront des impacts du changement climatique dans les zones étudiées.

Mots clé: Variabilité climatique, changement climatique, impacts, modèles hydrologiques, pluie, débits, température, crues, Côte d'Ivoire.

INTRODUCTION

Dans de nombreuses régions de la planète, les températures augmentent, les forêts s'embrasent, des pluies torrentielles tombent, les inondations font des ravages et des sècheresses s'intensifient chaque année. Non seulement ces phénomènes s'aggravent, mais ils se répandent dans le monde entier et causent de nombreux dégâts matériels, humains et dégradent la qualité de l'environnement ces dernières décennies.

L'Afrique de l'ouest comme toutes les régions du monde est devenue plus vulnérable aux effets de ces évènements extrêmes à cause de l'ampleur des dégâts observés ces deux dernières décennies (2003-2023). Aujourd'hui, la partie Nord de l'Afrique est confrontée de plus en plus à des conditions hydrométéorologiques extrêmes dont les sècheresses (Donat et al., 2014). La partie Sud, surtout en zones côtières quant à elle est soumise à une récurrence d'événements extrêmes pluviométriques. Notons aussi que le Mali et le Niger sont aujourd'hui confrontés aux phénomènes d'inondations dû en partie aux impacts du changement climatique (Fofana et al., 2022); Oser et al.,2017; Abiodum et al.,2017). Au Ghana, les études de Larbi et al. (2022) ont montré une fréquence et une intensité élevées des conditions hydrométéorologiques.

Ces constats sont aussi réels en Côte d'Ivoire, comme tous ces pays du sud-ouest africain qui subissent l'impact de ces extrêmes hydrométéorologiques dus en partie aux conséquences du changement climatique. Ainsi, les conditions hydrométéorologiques extrêmes, en particulier les inondations et les sécheresses sont devenues des catastrophes naturelles annuelles en Côte d'Ivoire, causant des dommages matériels importants, des décès et le déplacement des populations de leurs lieux de vie habituels (Kouassi et al., 2021); (Assoma et al., 2016). Par exemple, dans le district d'Abidjan, l'étude d'OCHA (2013) révèle que 80000 personnes résident dans des zones inondables, dont 40000 à Cocody, 12500 à Abobo, 10000 à Adjamé, 9500 à Yopougon et 8000 à Attécoubé. Et aussi, selon le rapport de la RNC pour 2021, plusieurs villes ivoiriennes sont confrontées chaque année à des phénomènes hydrologiques extrêmes avec des inondations dévastatrices. Des études réalisées par (Assoko et al., 2020) ont révélé que de nombreuses villes en Côte d'Ivoire (Bouaké, Korhogo, Tiébissou, Niakaramandougou, Odienné) ont connu des épisodes prolongés de sécheresse qui se soldent par des assèchements de lacs utilisés pour l'approvisionnement en eau potable de la population. Par ailleurs, de nombreux barrages hydro-électriques dont Buyo et Kossou ont connu un assèchement de leur plan d'eau,

qui a causé des difficultés dans le pays pour l'approvisionnement en eau potable aux populations de ces villes et des délestages pour la fourniture en électricité. Il est donc urgent pour la Côte d'Ivoire de mieux comprendre la dynamique des phénomènes hydrométéorologiques extrêmes afin de minimiser leurs conséquences par des analyses tendancielles desdits phénomènes passés en suivant leur évolution dans un futur proche, surtout dans toutes ces villes à risque en raison des zones climatiques auxquelles ils appartiennent. Cette analyse apparait plus importante car elle offre la possibilité de connaître l'évolution à court, moyen et long terme des extrêmes hydrologiques afin de fournir des solutions adaptatives pour réduire la vulnérabilité des personnes à faible revenu. En outre, la prévention des inondations et des sécheresses désastreuses exige une meilleure compréhension des changements futurs prévus dans les ressources en eau en ce qui concerne les variables extrêmes.

L'objectif global de cette étude est d'évaluer les effets du changement climatique sur les extrêmes hydrométéorologiques à travers les différentes zones climatiques en Côte d'Ivoire. De manière spécifique, il s'agit d'abord d'analyser les tendances dans les extrêmes hydrométéorologiques historiques (précipitations et débits) de 1970 à 2017, et évaluer l'effet de la variabilité des précipitations sur les débits d'étiage et de crue dans quelques bassins hydrographiques sélectionnés. Ensuite, l'analyse de l'efficacité de quelques modèles hydrologiques pour la simulation des faibles débits et des inondations dans quelques bassins hydrographiques choisis sera faite. Et enfin, les tendances des extrêmes hydrométéorologiques selon les scénarios climatiques RCP4.5 et RCP8.5 pour la période de 2020 à 2050 seront déduites.

- **Zone d'étude**

La Côte d'Ivoire est un pays situé en Afrique de l'Ouest, bordé par le Libéria, la Guinée, le Mali, le Burkina Faso et le Ghana où cinq bassins versants (N'zo, Lobo Agneby, Bagoue et Baya) ont été sélectionnés en fonction des zones climatiques pour mener cette étude.

Le bassin versant de N'zo est situé dans la partie ouest du pays, près de la frontière du Libéria, entre les latitudes 6°50' et 7°50' nord et les longitudes 7°15' et 8°05' ouest (Kouassi et al., 2021). Il couvre une superficie d'environ 4300 km^2 (Oularé et al., 2017).

Le bassin versant de Lobo est situé entre 6°05'W et 6°55 W et entre 6°02'N et 7°55'N de latitude Nord, dans la région du centre-ouest de la Côte d'Ivoire avec une superficie de 12 723 km^2 (Deguy, 2021).

Le bassin hydrographique d'Agneby est situé dans la partie sud du pays et couvre une superficie d'environ 4000 km^2 (Ministère de l'Eau et des Forêts, 2018). Le bassin côtier de l'Agnéby est localisé au sud-est de la Côte d'Ivoire entre les longitudes 4°45' et 3°43' ouest et les latitudes 5°18' et 6°56' nord (Koudou et al., 2018).

Le bassin versant de Bagoue est situé dans la partie nord du pays et couvre une superficie d'environ 33 430 km^2 qui s'étend de la Côte d'Ivoire, au Mali et au Niger (N'da et al., 2018). Le bassin est situe entre latitudes 9°30' et 10°00' nord et entre longitudes -7°30' et -6°00' west.

Le bassin versant Baya est situé dans le nord-est du pays et couvre une superficie d'environ 6324 km^2 (Mangoua et al., 2015). Le bassin est limité à l'est par la République du Ghana, qui est située entre 2°38 et 3°33' de longitude ouest et 6°35 et 8°26' de latitude nord.

Dans l'ensemble, ces cinq bassins versants en Côte d'Ivoire sont importants pour leur valeur écologique, économique et sociale (ministère de l'Eau et des Forêts, 2018). Ils fournissent un habitat important pour la faune, soutiennent l'agriculture et d'autres activités économiques, et sont d'importantes sources d'eau pour les populations et les écosystèmes (ministère de l'Eau et des Forêts, 2018). Cependant, ils font également face à de nombreux défis, y compris le changement climatique, la pollution et la déforestation, qui peuvent avoir des impacts négatifs sur leur valeur écologique et sociale (ministère de l'Eau et des forêts, 2018).

- **Matériel et méthodes**

Les données de précipitations et de débits journaliers ont été utilisé pour l'analyse des tendances hydro climatiques historiques (précipitations et débits) de 1970 à 2017 et l'effet de la variabilité des précipitations sur les débits de crue et d'étiage dans les cinq bassins hydrographiques sélectionnés. La méthodologie a d'abord, consisté à filtrer les données pour éliminer les variations saisonnières afin de mieux visualiser les périodes de déficit et d'excédant sur une échelle interannuelle à l'aide d'un filtre Hanning passe-bas d'ordre 2 (moyenne mobile pondérée). Ensuite, l'extraction des indices hydro climatiques extrêmes a été faite. Les indices des extrêmes de pluie déduits sont la pluviométrie annuelle maximale (Pmaxan), les jours secs

consécutifs (CDD), la pluviométrie maximale de 5 jours (Rx5days) et la pluviométrie très humide (R95p) pour tous les bassins d'étude. Les indices de débits extrêmes qui sont au nombre de sept (7) indices à savoir le débit maximal sur 5 jours (QX5 jours), le débit maximal (Qmaxan), le débit maximal mensuel (VCX30), le débit minimal annuel (Qminan), le débit moyen mensuel (QMNA), le débit quotidien (VCN7) et la caractéristique de basse eau (DCE) ont été sélectionnés. Ces différents indices extrêmes ont été soumis à différents tests statistiques à savoir, un test d'homogénéité normale standard (SNHT), appliqué pour la détection des ruptures dans la série et une analyse des tendances à l'aide du test de Mann-Kendall modifié.

Les données journalières de pluie, de débit, d'évapotranspiration et le modèle numérique du terrain de chaque bassin ont servi de données d'entrée des modèles hydrologiques GR4J, GR5J et HEC-HMS dans l'évaluation de l'efficacité de ces modèles dans la simulation des débits d'étiage et les débits de crue des bassins hydrographiques choisis. Des calages et des validations pour chaque bassin ont été fait sur différentes années allant de 3 ans à 5 ans (voir 10 ans) pour les modèles utilisés. L'évaluation de la performance des modèles a été fait à l'aide du coefficient de Nash-Sutcliffe (NSE), l'Efficacité de Kling-Gupta (KGE) et le pourcentage de biais (PBIAS). Les moyennes d'ensemble des modèles climatiques pour chacun des scénarios RCP4.5 et RCP8.5 ont été utilisée pour évaluer l'impact du changement climatique (2020-2050) sur les différents bassins.

R Package "*qmap*" programme a été utilisé avec comme technique de réduction des biais par la méthode de distribution de cartographie du quantile. Les paramètres d'ajustement pour la période future pour les scénarios RCP4.5 et RCP8.5 des models climaques CM5A, CNRM et MPI sont calculés par R Package "*qmap*" programme en utilisant la technique de chevauchement des données de pluie observées et simulées (les scénarios historiques et futurs). Une méthode statistique d'évaluation du rendement du modèle qui comprend l'erreur absolue moyenne (MAE) et le pourcentage de biais (PBIAS), a été utilisé pour évaluer l'efficacité de la MCR (Model Climatique Regional). Enfin, l'analyse de l'impact du changement climatique a été évaluée par une étude comparative entre les paramètres climatique futur et les paramètres climatiques observés.

- **Résultats et discussion**

Les résultats obtenus en appliquant le filtre passe-bas de second ordre de Hanning sur les précipitations et les débits observés indiquent une grande irrégularité interannuelle des précipitations et des débits dans chaque zone climatique du pays.

Le test d'homogénéité appliqué aux indices des extrêmes hydro climatiques a montré en général, des périodes de rupture différente d'une station à l'autre et d'un bassin hydrographique à l'autre. Mais, la période de rupture de 2008 a été observée dans les zones climatiques II et III comme une période commune pour les indices de débits d'étiage et de crue. Dans les zones climatiques I et IV, c'est seulement le débit d'étiage qui a montré un nombre signifiant de période de rupture.

Le test de Mann-Kendall modifié appliqué aux indices des extrêmes a montré une tendance significative à la baisse dans chaque zone climatique. En ce qui concerne les débits extrêmes, le test nous a permis de constater une tendance non significative pour la plupart des indices extrêmes de débits de crue. Les débits d'étiage ont tous connus une tendance significative à la hausse pour la plupart des indices extrêmes et dans les zones climatiques d'études.

Les simulations des modèles GR4J, GR5J et HEC-HMS ont montré dans l'ensemble un résultat satisfaisant sur les différents bassins. Le processus de calage a donné une valeur de Nash assez bonne comprise entre 0.58-0.94 pour GR4J et 0.56-0.90 pour GR5J. En ce qui concerne la validation, les valeurs de Nash étaient entre 0.09-0.90 pour GR4J et 0.39-0.56 pour GR5J. HEC HMS quant à lui, lors du processus de calibration, a présenté un résultat insatisfaisant avec des valeurs de Nash allant de -0.86-0.57 et des valeurs de Nash de -3.9-0.49 pour les différentes périodes de validation.

L'évaluation de la performance des modèles hydrologiques a été éprouvée par trois fonctions objectives, Nash, KGE et PBAIS. L'évaluation donnée par le Nash a présenté une bonne performance en calibration et en validation avec des valeurs générales comprise entre 0.58-0.94 pour GR4J et 0.56-0.90 pour GR5J en calibration et 0.09-0.90 pour GR4J et 0.39-0.56 pour GR5J en validation. L'évaluation du KGE a aussi donné une bonne performance dans le même ordre que le Nash en calibration et en validation. La valeur PBIAS a plus servi dans l'évaluation de la performance du modèle hydrologique HEC-HMS. Il a montré quelques valeurs négatives et

positives mettant en évidence une sous-estimation ou une surestimation du modèle dans la simulation.

Et enfin, pour ce qui est de l'analyse de l'impact du changement climatique sous les scenarios RCP 4.5 et RCP 8.5, le résultat a montré une diminution dans les pluies annuelles, une augmentation dans la température moyenne, une alternance de diminution et d'augmentation dans l'évapotranspiration analysées et une diminution du débit moyens annuels sur l'ensemble des bassins d'étude pour quelques différents paramètres climatiques.

Les indices de débits extrêmes sous les scenarios RCP 4.5 et RCP 8.5 à l'horizon 2020-2050 ont montré une tendance non-significative dans leur ensemble. Cependant, sous le scenario RCP4.5, l'indice de crue QMAXAN connaitra une hausse significative dans le bassin versant de la Bagoue. Et sous le scenario RCP 8.5, les indices de crue QMAXAN, QX5days une baisse significative dans le nord du pays. Les indices d'étiage pris dans leur ensemble sous les scenarios RCP 4.5 et RCP 8.5, connaitront une baisse significative à l'horizon 2020-2050 sur les différents bassins d'étude.

L'évaluation de la dynamique de l'occupation du sol sur les extrêmes a été mise en évidence par plusieurs méthodes. Elle a relevé que du sud, au nord, de l'ouest à l'est de la Côte d'Ivoire ; on observe une régression de la forêt ou de la savane, des ressources en eau, et une augmentation de l'habitat et des zones cultivées d'un endroit à l'autre. Aussi, la relation mise en œuvre entre l'évolution de l'indice de végétation (NDVI) et les indices extrêmes de pluie a montré une corrélation négative non significative en générale sur les bassins versants d'étude. De même, cette analyse a révélé une corrélation positive entre les indices de végétation (NDVI) et les indices extrêmes de débits dans son ensemble.

➢ Conclusion

Cette étude montre d'abord que les paramètres hydro climatiques sont influencés par une grande irrégularité interannuelle dans chaque zone climatique du pays. Ensuite, le test d'homogénéité appliqué aux indices de précipitations et débits au niveau de confiance de 0,05 montre en général, des périodes de rupture différente d'une station à l'autre et d'un bassin hydrographique à l'autre. Aussi, le test modifié de Mann-Kendall appliqué aux indices de débits et de précipitations montre une tendance à la baisse significative sous chaque zone climatique

pour les indices de précipitations extrêmes. Concernant les indices extrêmes de débits de crue, le test révèle une tendance non-significative sur tous les bassins d'études. Les indices extrêmes de débits d'étiage ont tous connu une tendance significative à la hausse dans les zones climatiques d'études.

Sous le scenario RCP 4.5, les modèles climatiques CNRM, MPI et ENSEMBLE présentent une tendance non-significative dans les indices de pluie extrêmes à l'horizon 2050. Le modèle CM5A donne une tendance significative à la hausse pour les indices Pmaxan, Rx5days et R95p. Sous le scenario RCP 8.5, les modèles CM5A et CNRM montrent une tendance significative à la hausse dans les indices Pmaxan et Rx5days à l'horizon 2050. Une tendance non-significative s'observe dans les modèles MPI et ENSEMBLE. Aussi, les régressions dans l'ensemble du couvert végétal et la dynamique de l'occupation du sol sur ses différents bassins ont beaucoup impacté la fréquence des crues et sécheresses en Côte d'Ivoire.

L'impact du changement climatique affecte certains paramètres du climat dans l'ensemble des bassins d'étude en termes de hausse de la température, de diminution des débits, des pluie moyennes annuelles et de l'évapotranspiration.

Table of Contents

List of Acronyms

IPCC	:	Intergovernmental Panel on Climate Change
CCl	:	Commission for Climatology
CORDEX	:	Coordinated Regional Downscaling Experiment
ECOWAS	:	Economic Community of West African States
ETCCDI	:	Expert Team on Climate Change Detection and Monitoring
ETCRSCI	:	Expert Team on Climate Risk and Sector-Specific Indices
INS	:	Institut National de la Statistique
OCHA	:	Office for the Coordination of Humanitarian Affairs
RGPH	:	Recensement Général de la Population et de l'Habitat
RNC	:	Rapport National de Consultation
SODEXAM	:	Société d'Exploitation et de Développement Aéroportuaire Aéronautique et Météorologique
UNDP	:	United Nations Development Programme
WAM	:	Mousson d'Afrique de l'Ouest
WASCAL	:	West Africa Science Service Center on Climate Change and Adapted Landuse
WMO	:	World Meteorological Organization

List of figures

List of Tables

CHAPTER 1 : GENERAL INTRODUCTION

The general introduction gives a general overview of the thesis. It describes the content of the dissertation, starting with the context and the issue raised in Section 1.1. The paragraph 1.2 is the literature review, which gives an overview of the state of the art on hydrological extreme events in Cote d'Ivoire. Section 1.3 focuses on the research questions of the thesis, while sections 1.4 and 1.5 focus on the objectives and novelty. The scope of the thesis of the thesis is detailed in Section 1.6. Section 1.8 discusses the expected results.

1.1 Context and problem statement

Water is one of the most vital sources for all living organisms. We need water for a variety of purposes, including growing crops, generating electricity, and, above all for human survival. However, with the negative effect of climate change, this source of life has become a natural disaster that is causing thousands of casualties around the world due to hydrological extreme events. These hydrological risks have become a major concern regarding the use of land planning and management for the well-being of living beings (Saley et al., 2005). In recent past, more frequent extreme hydrological events have occurred, affecting socio-economic global activities and livelihood. The extreme hydrological events are caused by a variety of natural and man-made variables that are currently having an impact on water resources. For example, river flows are either increasing, leading to significant floods, or decreasing, in some locations, with alarming socioeconomic harm. In addition, a rise in the frequency of extreme weather events in many regions around the world has also been attributed to the global warming (IPCC, 2001).

Like the other continents, Africa has faced extreme weather occurrences for decades, causing catastrophic damage. For example, the northern part of Africa is confronted with increasingly dry trends, although these trends are not significant (Donat et al., 2014). Also, in the sub-Saharan region, extreme climatic conditions have been the subject of various research projects. Extreme cases have been reported in Niger (Bigi et al., 2018), Burkina Faso (Okafor et al., 2021b), Nigeria (Adeyeri et al., 2019), and Côte d'Ivoire (Fabrice et al., 2020). In contrast, decreasing trends in extremes are reported in Nigeria (Oguntunde et al., 2011), Guinea-Conakry (Aguilar et al., 2009), eastern Niger (Ozer et al., 2017), and Côte d'Ivoire by (Soro et al., 2016). These

studies indicate a contrasting evolution of climate extremes over the West African region, which requires a detailed assessment of the trends of extremes over the region.

In Cote d'Ivoire, extreme weather conditions, especially floods, have become a natural disaster causing major property damage, fatalities, and population displacements (Kouassi et al., 2020; Assoma et al. 2016). For instance, in the district of Abidjan, about 80,000 people reside in flood-prone areas; 40,000 in Cocody, 12,500 in Abobo, 10,000 in Adjame, 9,500 in Yopougon, and 8,000 in Attecoube (OCHA, 2013). The RNC report for 2021 revealed that several Ivorian cities face extreme hydrological phenomena each year with devastating floods. For example, in June 2018, the cities of Floods with devastating damage occurred at Zuenoula, Bouaflé, Tiassalé, Touleupleu, N'douci, Sassandra, Fresco, Gagnoa, Korhogo, Ferké, Aboisso, and Agboville, 3115 families affected, and 34 deaths. Hydrological extremes in October 2019 hit the cities of Abidjan, Aboisso, Grand Bassam, Ayamé, and the city of Man where 12,900 people were affected, 202 homes were fully inundated, 72 homes were demolished, 32 people were injured, and 12 people died. Many cities in Côte d'Ivoire including, Bouaké, Korhogo, Tiébissou, Niakaramandougou and Odienné, have experienced prolonged periods of drought, resulting in the drying up of lakes causing acute water shortages (Assoko et al., 2020). In addition, the Buyo and Kossou hydroelectric dams have experienced decreased water levels, which has caused serious damages leading to inadequate supply of drinking water to the populations living in these areas. In contrast to the reported flooding that causes significant damage every year in several cities in the country, (Guessan et al., 2014); (Gauze et al., 2018); (Koffi et al., 2020); (Allechy et al., 2020) and (Anouman et al., 2019) there are only a few examples of the numerous studies on the effects of climatic variability that have been conducted in Côte d'Ivoire. In addition, little research has been done on the effects of climate change on hydrological extremes, despite the frequency of floods and droughts in most cities across the nation (Dibi-Anoh et al., 2023); (Kouakou et al., 2016). Therefore, it is urgent for the country to better understand the dynamics of extreme phenomena in order to minimize their consequences by analyzing the trends of past data and monitoring their evolution in the near future, especially in all these cities at risk due to the climatic zones. Trend analysis is important and offers the possibility of knowing the short-, medium-, and long-term evolution of hydrological extremes in order to provide adaptive solutions to reduce the vulnerability of low-income people. One of the crucial areas to research is the effect of climate change on hydrological extremes in Cote d'Ivoire. In addition, preventing

disastrous floods and droughts requires a better understanding of anticipated future changes in water resources with regard to extreme variables. Supporting the creation of specific measures is also crucial.

1.2 Literature review

1.2.1 Definition of the hydrological concepts

In its 2007 annual report, the Intergovernmental Panel on Climate Change (IPCC) describes a "extreme" climate event as "an uncommon event that happens at a time of year." Although the term "rare" has several meanings depending on context, a severe meteorological occurrence is typically as rare as or even rarer than the 10th or 90th percentile of the observed probability density function. (Décamps, 2010) claims that "extreme" climatic event is a unique occurrence brought on by the remarkable levels that one or more parameters (such as temperature or rainfall) reach in a specific area. These values can occur suddenly or spread over time like extreme climatic phenomena, which essentially group together the phenomena of "storms", which cause gusts of wind and precipitation (rain, snow, or hail) over very variable areas and durations. Extreme climatic phenomena are also defined by (Goubanova, 2007) as climatic phenomena that differ from the climatological normal. From a statistical point of view, the climatic parameters (e.g., rainfall, temperature, etc.) can be characterized by a probability distribution. The “distribution tails” then constitute what are called “extreme climatic events”, that is to say, weather anomalies whose probability of occurrence is low (less than 10%) As far as **extreme hydrological events** are concerned, they are essentially floods in the river courses, followed by the flooding of the plains after excess rainfall or low water levels due to dry rainfall. According to the (WMO, 2006) and (Vissin, 2007), river floods occur when the volume of the watercourse is exceeded and overflows into the floodplain due to torrential rains in the affected sectors, especially upstream of the watercourse. Their advent is sometimes favored by the forms of land use and the seasonal variations in vegetation (Draman-donou et al., 2015). For our purposes, an extreme hydroclimatic event is any event that refers to exceptional hydroclimatic conditions and, if necessary, causes damage or has an impact on river flows and the hydrological dynamics of a catchment area.

Flooding: This is a basic hydrological phenomenon affecting the river. It results in an increase in its flow, height, and velocity. The flood, if it is large enough, can result in the flooding of an area. It can also be the overflowing of a stream's or another body of water's typical boundary or

the buildup of water over places that aren't typically submerged. Fluvial (river) flooding, flash flooding, urban flooding, pluvial flooding, sewage flooding, coastal flooding, and glacial lake outburst flooding are different types of flooding (IPCC, 2012).

Low-flow: Etymologically, "low water" would have been derived from the word "either", a term that refers to the canal that brings seawater to the salt marshes (Dacharry, 1996). The low water level thus corresponded to the state of the river following water withdrawal. The International Glossary of Hydrology (1992) describes low-water levels as the "lowest level reached by a river or lake" without specifying the time, whereas the French Dictionary of Surface Hydrology (Roche, 1986) places this event in an annual context: "the lowest annual level reached by a river at a given point". Low-water levels are also defined as hydrological events with slow dynamics that can extend over long periods of time. For a complete description of the phenomenon, low water levels should therefore be understood not only in terms of the levels reached, but also in terms of processes and duration. It is true that low water levels with long-term low flows can do more damage than very low flows with short-term low flows. The statistical definitions of low water levels make it possible to integrate these different elements and also offer a characterization of the events in terms of severity. In this same statistical definition, they will say that low water levels are difficult to characterise because the identification of low water flows is not subject to established rules, which is explained by the original character that these events can take from one year to the next. Thus, low water flows can be defined on the basis of daily flows, monthly flows, or moving averages calculated over several days. It is also possible to characterise low water levels from a threshold flow by counting the number of days below this threshold, or the volume deficit. The definition of low water levels from a statistical point of view imposes a choice of descriptive variables, which will therefore depend on the objectives of the work but may also result from a constraint imposed by a legislative framework if the study is carried out in an operational context.

1.2.2 Climate change impacts on extremes

The community of climatologists and water managers has become significantly more active over the past decade as a result of the study of how climate change affects the water cycle (Carroget et al., 2017). A major area of exploitation for the future community is quantifying the effects of changes in climate factors on natural resources in a specific place (Oguntunde et al., 2006). Thus,

the analysis of past changes is based on climatic and hydrological observations and the study of their potential links with climate (Renard, 2006). The (IPCC, 2001) found that global warming has increased the frequency of extreme weather occurrences in many parts of the world, and this increase in extreme phenomena is felt every year through floods and droughts everywhere, causing thousands of dollars in damage and taking thousands of human lives. In Africa, these extremes have become annual natural disasters with thousands of human losses and deplorable damage. In Cote d'Ivoire, where these disasters are common, the effect of climate change on hydrological extremes have been extensively studied. A study by Kouassi (Kouassi et al., 2018) on the impact of climate change on water stress in West Africa, revealed that the N'zi watershed's vulnerability to high water levels was highlighted by the determined flows of severity levels, with the Fétékro sub-watershed being more exposed to this vulnerability. Another study by Goula and colleagues (Goula et al., 2009) found that the N'zi watershed in Dimbokro and the N'zo watershed in Kahin both experienced a decrease in rainfall, respectively between 1969 and 2000 with a 13% deficit and between 1967 and 1993 with a 14% deficit. Also, studies by Anounman and colleagues (Anouman et al., 2019) on Sassandra River watershed discovered that the Mann-Kendall trend test statistics had a 67% of the hydrological stations (8 out of a total of 12 stations) presented an increased low flow trend, while the other stations had an insignificant trend. Further, a study conducted N'gnessan (N'gnessan Bi al., 2017) to analyze the hydrological dynamics of river revealed that the Marahoué river regime breaks down into a single long-duration flood phase and a short-duration recession phase with a synchronous trend throughout the study period. On the Bandama, studies by Assoko (Assoko et al., 2020) on statistical modelling of low flows and determination of low water thresholds in the Marahoué watershed (Bandama, Côte d'Ivoire), showed that the QMNA of Marahoué was better adjusted by the Gamma law. (Atcheremi et al.,2018) made it possible to monitor the evolution of rainfall extremes and thermal extremes at three synoptic rainfall stations (Daloa, Gagnoa, and Sassandra stations) in the Da**v**o basin. His analysis showed a decrease in most rainfall indices and during the same time period, the study basin's temperature indices increased.(Allechy et al., 2020) focused on trends in central Côte d'Ivoire through their studies on "West-central United States severe precipitation trend The Lobo Watershed Case in Côte d'Ivoire", and their analysis reveals that, overall, the number of consecutive wet days, the number of rainy days, and the total quantity of annual precipitation are all declining, with the exception of consecutive dry days,

which are rising across the whole study area. (Kouadio et al.,2018) made it possible to understand the origins of flooding in the Agneby basin through their study on "What causes Agboville, Côte d'Ivoire, to flood frequently?" Identification of the origins of flooding in Agboville and in the upstream catchment of the Agneby River. The hydrological modelling of the Agneby catchment revealed that forest dynamics resulted in a decrease in evapotranspired and infiltrated water on the one hand and an increase in water flowing out on the other. (Kouman et al., 2022), Have seen the Spatio-Temporal Trends of Precipitation and Temperature Extremes in the North-East Area of Côte d'Ivoire from 1981 to 2020. They discovered non-significant statistical trends in the extreme precipitation as well as a decrease in the annual total precipitation PRCPTOT, daily precipitation intensity SDII, and consecutive wet days CWD, all of which point to a reduction in rainfall in the area. Additionally, the research by (Konin et al., 2022) enables the analysis of the effects of rainfall trends on flooding in the Agnéby watershed, where they discovered a dynamic upward evolution of extreme rainfall and a decline in the length of consecutive rainy episodes, the number of rainy episodes, and the flows feeding the main watercourse.

In this situation, the research will assess how climate change may affect hydrological extremes (rainfall and outflow) in the five climatic zone of Côte d'Ivoire.

1.2.3 Hydrological modeling

Water is life; it is a major and precious natural resource in life that needs to be protected, nourished, and monitored. Models that attempt to represent the physical processes observed between natural resources and the real world are needed. These models typically include surface runoff, subsurface flow, evapotranspiration, and channel flow, although they can be far more complex. Hence, conceptual representations of a specific aspect of the hydrologic cycle are simplified in hydrologic models. Moreover, they are typically created to produce stream flow data to: complete gaps in present records; estimate current and/or natural flows and yields for ungauged sections of a catchment; create long-term data to develop statistics and estimates of yield reliability; input data for additional research, such as environmental flow or scenario or forecast modeling (Zhu et al., 2018). But modern water resource management requires reliable hydrological data on watershed water availability, the extent of existing water usage, and environmental water needs. Hence, hydrological models mathematical formulations for

determining the runoff signal that departs a watershed from the rainfall signal that this watershed receives can be used, have become a useful tool for water resources assessment, understanding hydrological processes, and prediction (Wagener et al., 2003). It has been widely used in most fields of water resources in West Africa, with a good representation of the water cycle and models involved (Djellouli et al., 2016); (Kodja et al.,2018) and (Awotwi et al., 2021).

Among these models are the GR4J model (4-parameter daily model), which is a conceptual rainfall-runoff model with reservoirs; the GR5J model, a rainfall-runoff model that emphasizes soil moisture partitioning (Le Moine, 2008); (De Lavenne et al., 2016); and HEC-HMS (Hydrologic Engineering Center's Hydrological Modeling System) semi-distributed models that are free and flexible and offer the advantage of simulating single and continuous events. They will be used throughout this thesis.

1.3 Research questions

1. How have the hydro-climatic variables extremes varied over the period 1970-2017, and how has discharge been affected by the variability in rainfall?
2. What is the effectiveness of various hydrological models in simulating high and low flows?
3. What are the projected trends for hydro-climatic extremes from 2020 to 2050 under the RCP4.5 and RCP8.5 warming scenarios?

1.4 Thesis objectives

The study's goal is to evaluate the effects of climate change on hydroclimatic extremes across Côte d'Ivoire's climatic zones.

1.4.1 Specific objectives

This study specifically attempts to:

1. Analyze historical hydro-climatic extremes patterns from 1970 to 2017 and the effect of rainfall variability on low and high flows in a few selected river basins.

2. Analyze the effectiveness of several hydrological models in simulating low flows and floods in a few chosen river basins.

3. Examine the patterns and trends in hydro-climatic extremes under the RCP4.5 and RCP8.5 climate scenarios for the period of 2020 to 2050.

1.5 Novelty

Some studies have looked at the effect of climate change on hydrological extremes, but they did so at the watershed level. Using extremes indexes for data on rainfall and discharge, this study examined how climate change has affected hydrological extremes across the Cote d'Ivoire climatic zone. It will offer the possibility to see

- intercomparison of the extreme rainfall and discharge indexes on watersheds with different climatic patterns in Côte d'Ivoire.

- use of multi modelling approach for future projection of hydroclimatic extremes.

1.6 Scope of the thesis

In this thesis, the assessment of climate change's effects on extreme flows in Côte d'Ivoire is the main topic. In addition, historical hydro-climatic (rainfall and discharge) patterns for low and high flows in the chosen river basin are evaluated. In order to analyze future patterns and trends in hydro-climatic extremes under two representative concentration pathways, it is necessary to compare how well different hydrological models perform when simulating low-flows and floods.

1.7 Expected results and benefits

This study's findings would include: (i) trends analysis on hydrological extreme indexes over each climatic zone for past and future data (rainfall and discharge). (ii) understanding the impact of climate change using multiple hydrological models to simulate low flows and floods in some selected river basins. (iii)The study also includes data on the current and future status of the climate under the RCP4.5 and RCP8.5 climatic scenarios, which is important for minimizing the harm caused by extreme events.

1.8 Outline of the thesis

Chapter 1 provides a summary of the broad introduction and literature study on the subject. This chapter explored the definition of hydrological concepts, climate change impacts on extremes, and hydrological modeling. Furthermore, the problem statement, justification of the study, objectives, and expected results are covered.

Chapter 2 covers the description of the study area and its physical characteristics.

Chapter 3 describes the data collection procedures.

Chapter 4 describes the trend analysis.

In order to analyze trends at the annual and monthly timescales, Hanning's second-order low-pass filter for interannual variability and the Modified Mann-Kendall test were applied to the data. The Standard Normal Homogeneity Test was used to assess the data's homogeneity.

Chapter 5 detailed the examination of the effectiveness of various hydrological models in simulating low-flows and floods in a few chosen river basins.

In Chapter 6, projected patterns and trends in hydroclimatics extremes under the RCP4.5 and RCP8.5 warming scenarios from 2020 to 2050 were analyzed.

Chapter 7 summarizes the results and concludes the thesis.

CHAPTER 2: STUDY AREA

Chapter 2 provides a description of the research areas. The first section discusses topography, the second covers climate, the third addresses hydrology, the fourth talks about land cover and land use, and the final section goes over the socioeconomic characteristics of each catchment.

2.1 Location

Côte d'Ivoire is located in West Africa in the intertropical zone between the equator and the Tropic of Cancer, between latitudes 4°30' and 10°30' North and longitudes 8°30' and 2°30' West. Côte d'Ivoire is a very flat country, with the exception of the Man region in the west, where some peaks soar beyond 1,000 meters. In the south, some undulating plains rise gradually from south to north through the country's center. Between 1975 and 2013, land use and land cover in Côte d'Ivoire changed dramatically,agriculture has grown the most, with a net gain of 84%. (31,600 sq km) (Ehuitché ,2015). Five watershed areas were chosen for this study based on the four climatic zones and the presence or lack of hydraulic infrastructure in these defined watershed areas. The climatic zones and the five selected watersheds (N'zo, Lobo, Agneby, Bagoue, and Baya) are depicted in Figure 1 and Table 1. The N'zo watershed is located in the western part of the country, near the border with Liberia and situated between latitudes 6°50' and 7°50' North and longitudes 7°15' and 8°05' West (Michel et al., (2021). It covers an area of approximately 4,300 km^2 (Oularé, et al., 2017). The Lobo watershed in Nibéhibé is situated between 6°17' and 6°44' West longitude and 6°46' and 7°41' North latitude in the central-western region of Côte d'Ivoire with an area of 6,923 km2 (Toure et al. 2022). The Agneby watershed is located in the south part of the country, covering an area of approximately 8,420 km^2. The Bagoue watershed is located in the northern part of the country, covering an area of 4,825 km^2. The Baya watershed is located in the northeastern part of the country, covering an area of 2,266 km^2.

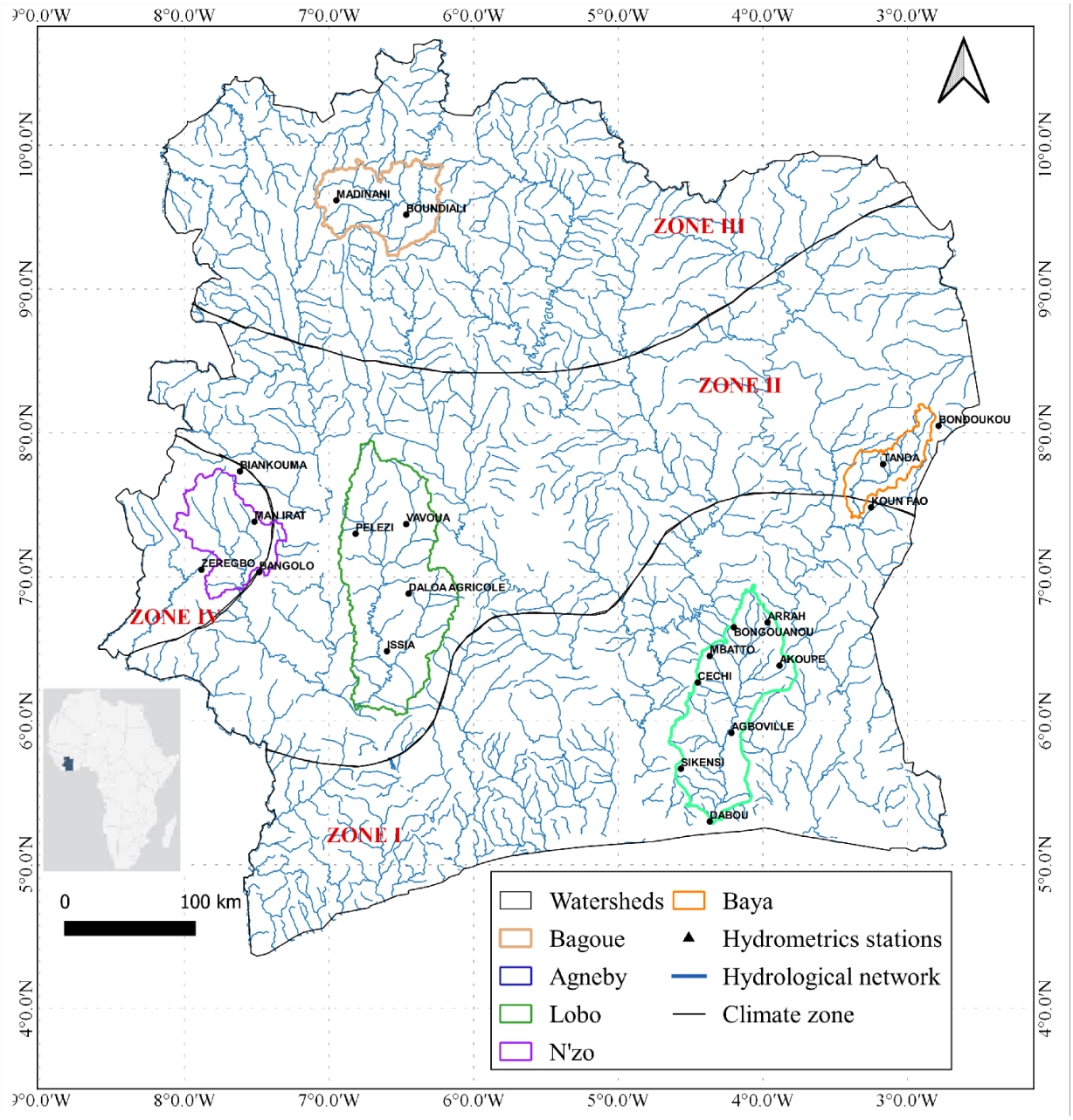

Figure 1: Location of the study area. **Source**: Goula et al., 2007 (For the climate zone)

Table 1: Characteristics of each climatic zone

Climate Zone	**Watersheds**	**Area (km^2)**	**Climate**	**Characteristics**
Zone I **Attieen climate (transitional equatorial regime)**	Agneby	8420	equatorial transition	- Two dry (December-March and July-September) and two wet seasons total four (April-July, which is more important, and September-November, which is very irregular). - annual precipitation of 1400 to 2500 mm
Zone II **Equatorial transitional regime** **attenuated**	Baya	2266.6	The humid tropical climate is characterized by watersheds.	- Maximum annual rainfall of 1200 m; seasons divided into three parts: a significant rainy season (April–June), a brief dry season, and a

(Baouleen climate)				substantially dry season (November–March) (July-August).
	Lobo	12,660	The sub-equatorial climate is represented by transitional equatorial twatershedsshed.	- With a dry season from November to February and a rainy season from March to October, the average annual rainfall is 1238.2 mm.
Zone III **Tropical regime in transition (Sudanese climate)**	Bagoue	4825.7	soudano-guinea	April through October is a single rainy season.
Zone IV **Mountain** **regime**	N’zo	4458.6	Mountain has two distinct seasons: a long wet season (8 months long) and a short dry season (4 months long).	- two major seasons with varying lengths - between 1600 and 2000 mm of rainfall every year.

2.2 Vegetation

Côte d'Ivoire's vegetation is made up of two major natural environments : the forest and the savannah. These two major formations are well distributed throughout Côte d'Ivoire. There are two (02) main types of forest: the dense or ombrophilous forest found in the south and west of Côte d'Ivoire with the presence of lianas and large trees with foliage that is always green

because of the abundant rainfall, and the mesophilous open forest found in the centre of Côte d'Ivoire. The savannah is the domain of grasses and is found throughout the north and centre of Côte d'Ivoire. There are four (04) types of savannah: wooded savannah, tree savannah, shrub savannah and grassy savannah (Adjanohoun et al.,1971).

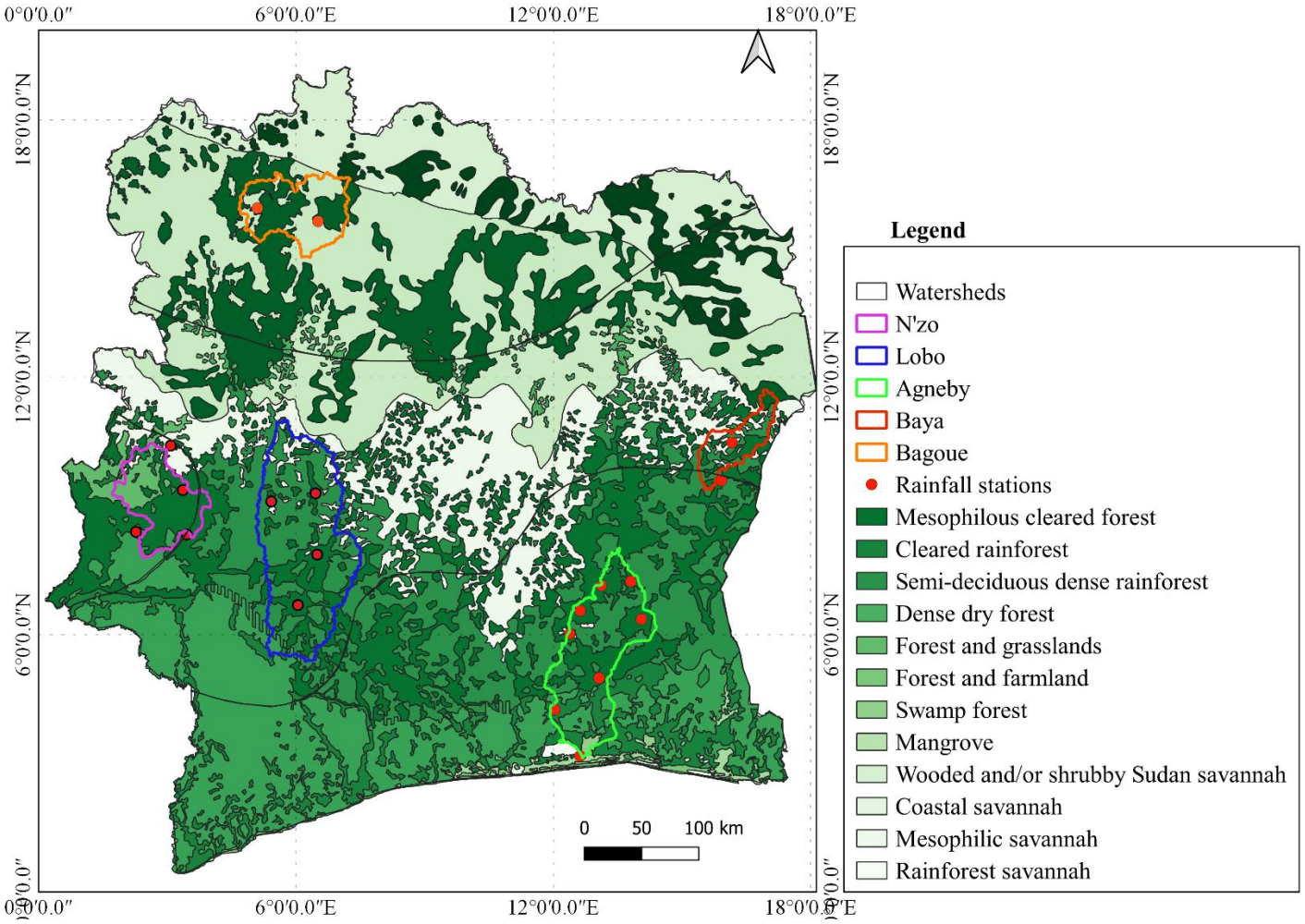

Figure 2: Vegetation of Cote d'Ivoire

2.3. Geology

Côte d'Ivoire's geology relates to West Africa's old precambrian shield and is defined by two major geological units: a precambrian basement occupying 97.5% of the Ivorian area and a secondary-tertiary sedimentary basin covering 2.5% (Moatti, 2006).

a. Agneby watershed

Located between latitudes 5°18' and 6°56' north and longitudes 4°45' and 3°43' west, Agneby watershed is a coastal catchment area with a surface area of 8,420 km² and extends over soils of fairly good quality in terms of water retention capacity (Figure 3). The relief is dominated by very hilly plains in a more classical and monotonous series of low elevations (20-140 m) marked by an alignment of shale hills reaching 560 m (Assoma et al., 2016). The basin belongs to a group formed by two geological units: the sedimentary basin in the south and the crystalline and crystallophyllous basement in the north, made up of volcano-sedimentary rocks. The formations of the basement, consisting of birimian formations such as schists, metaarenites, and metasiltones, outcrop in the region and are attributed to the Paleoproterozoic (Kouamelan et al., 1997). The basement is generally inclined from north to south towards the Atlantic Ocean, with a slope that varies between 6 and 9% (Ahoussi et al., 2013).

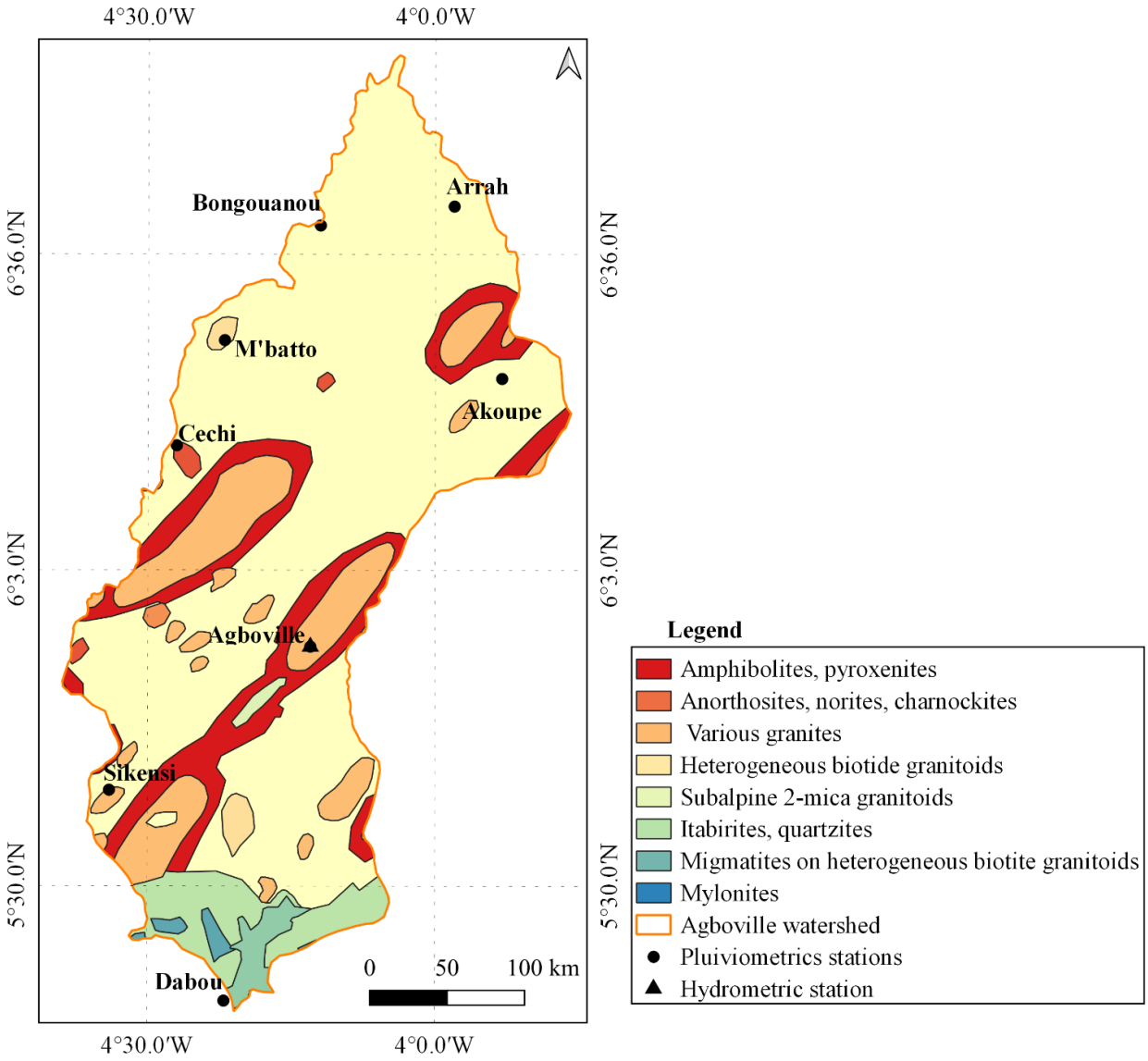

Figure 3: Geology of Agneby watershed

b. Bagoue watershed

The Bagoue watershed is a tributary of the Niger River and contains the Kouto sub-catchment. It is located between latitudes 9°30' and 10°00' north and longitudes -7°30' and -6°00' west. The topography is monotonous, with heights ranging from 300 to 400 m on average; nevertheless, granitic inselbergs occasionally climb to elevations of more than 500 m (N'guessan et al., 2015). The geology of the area (Figure 4) consists of solitary domes of granitic, metamorphosed, or granitic intrusive and metasomatized rocks. Metasediments, schists, greywackes, and metavulcanites are also present, as are old migmatites, migmatitic granites, gneisses, and gabbros (Miessan et al., 2019).

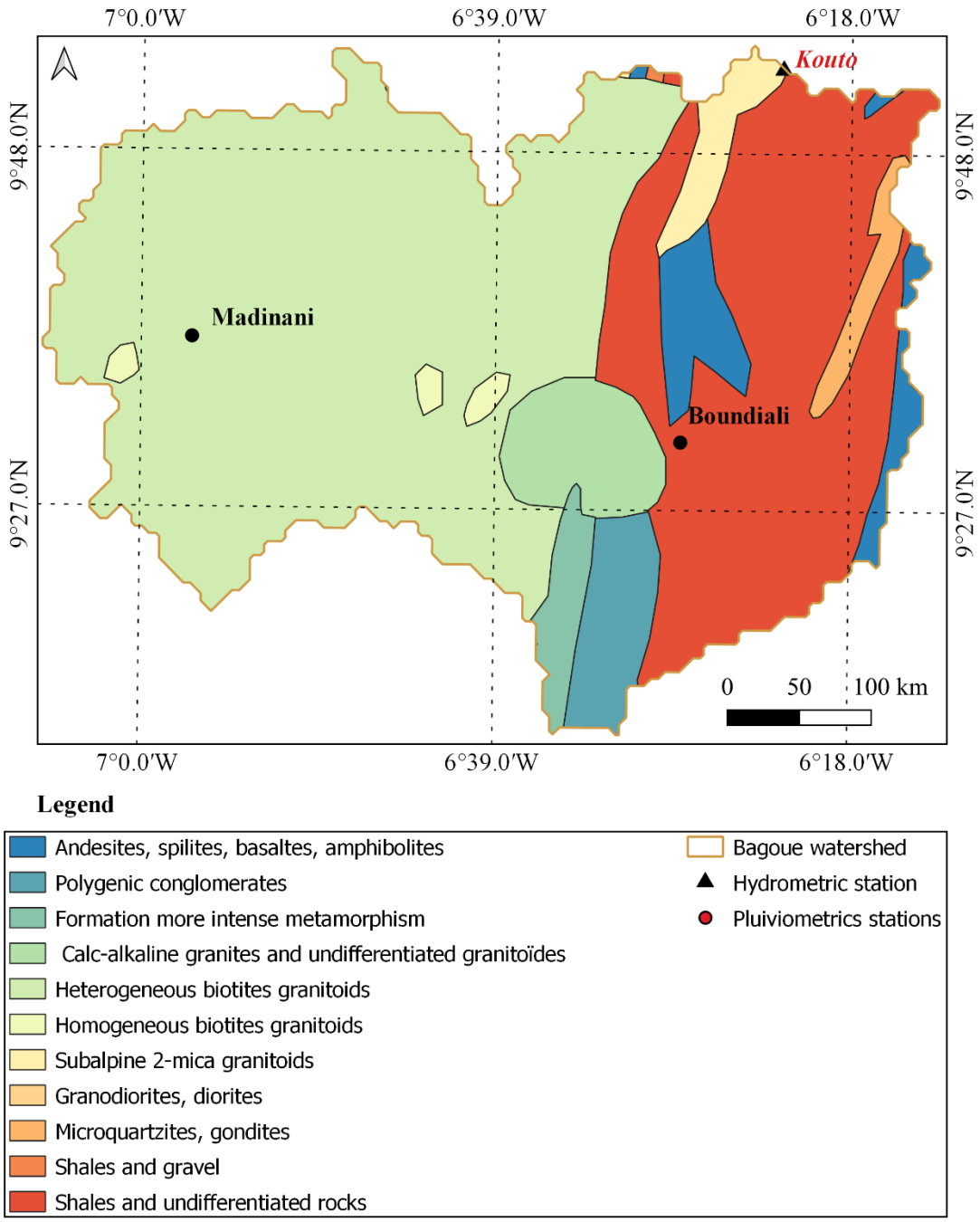

Figure 4: Geology of Bagoue watershed

c. Baya watershed

The Baya watershed is located to the east by the Republic of Ghana and is between 2°38 and 3°33' west longitude and 6°35 and 8°26' north latitude. The basin's geography consists of a series of terraced plateaus with flattened surfaces that range in altitude from 400 meters to 500 meters (N'guettia, 2021). The geological formations (Figure 5) are classified into three types: intrusive formations, which are discordant and circumscribed granites with alkaline granites, granodiorites, and veins of pegmatites and granophyres inside them (Touré et al., 2007), secondary formations, and tertiary formations. Second, the volcano-sedimentary formations are composed of coarser strata that immediately outcrop in the Zanzan Mountains, which rise to an elevation of more than 500 meters. They contain diverse lithic materials (David et al., 2022). Finally, volcanic Tarkwaan formations are found almost across the catchment region, from south to north, deposited in a sedimentation basin prone to severe compressive deformations (Touré et al., 2007).

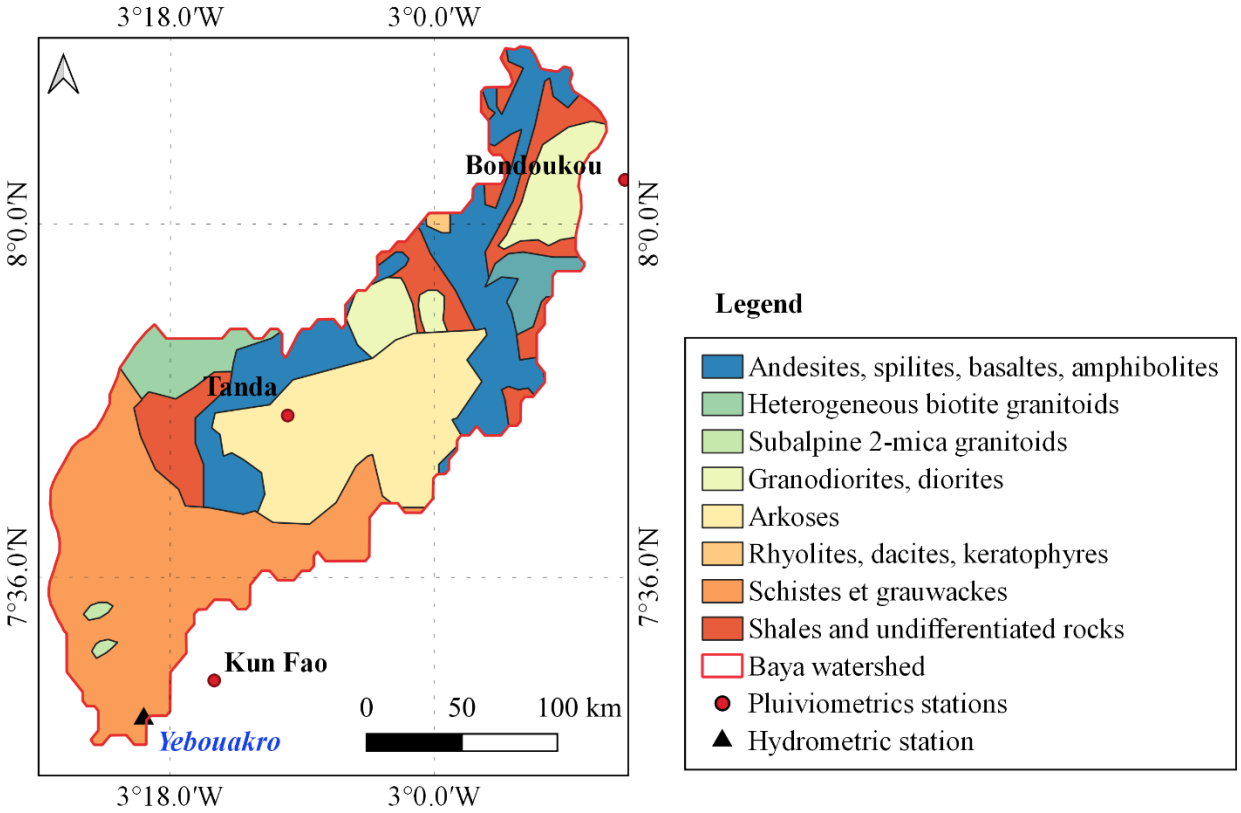

Figure 5: Geology of Baya watershed

d. Lobo watershed

Lobo watershed lies between 6°05' and 6°55' west longitude and 6°02' and 7°55' north latitude, in the center-west of Côte d'Ivoire. It is one of the major left-bank tributaries of the Sassandra River. Its elevation varies from 163 m to 617 m (Yao et al., 2016). The plateaus, which make up the majority of the basin, range in height from 240 to 320 meters, with a crescent-shaped greenstone massif rising to a height of 617 meters in the basin's far north. The Precambrian basement (Middle Precambrian) is where most of the geological formations in the Lobo catchment (Figure 6) area are located, and they can be divided into two main categories: the granitoids, which are essentially found in most of the basin, and the magmatic rocks, which are of the plutonic and volcanic types. Moreover, the banded, leucomigmatized, and ancient migmatites and schistous metamorphic rocks make up the riverbed (Bonnot et al., 1989).

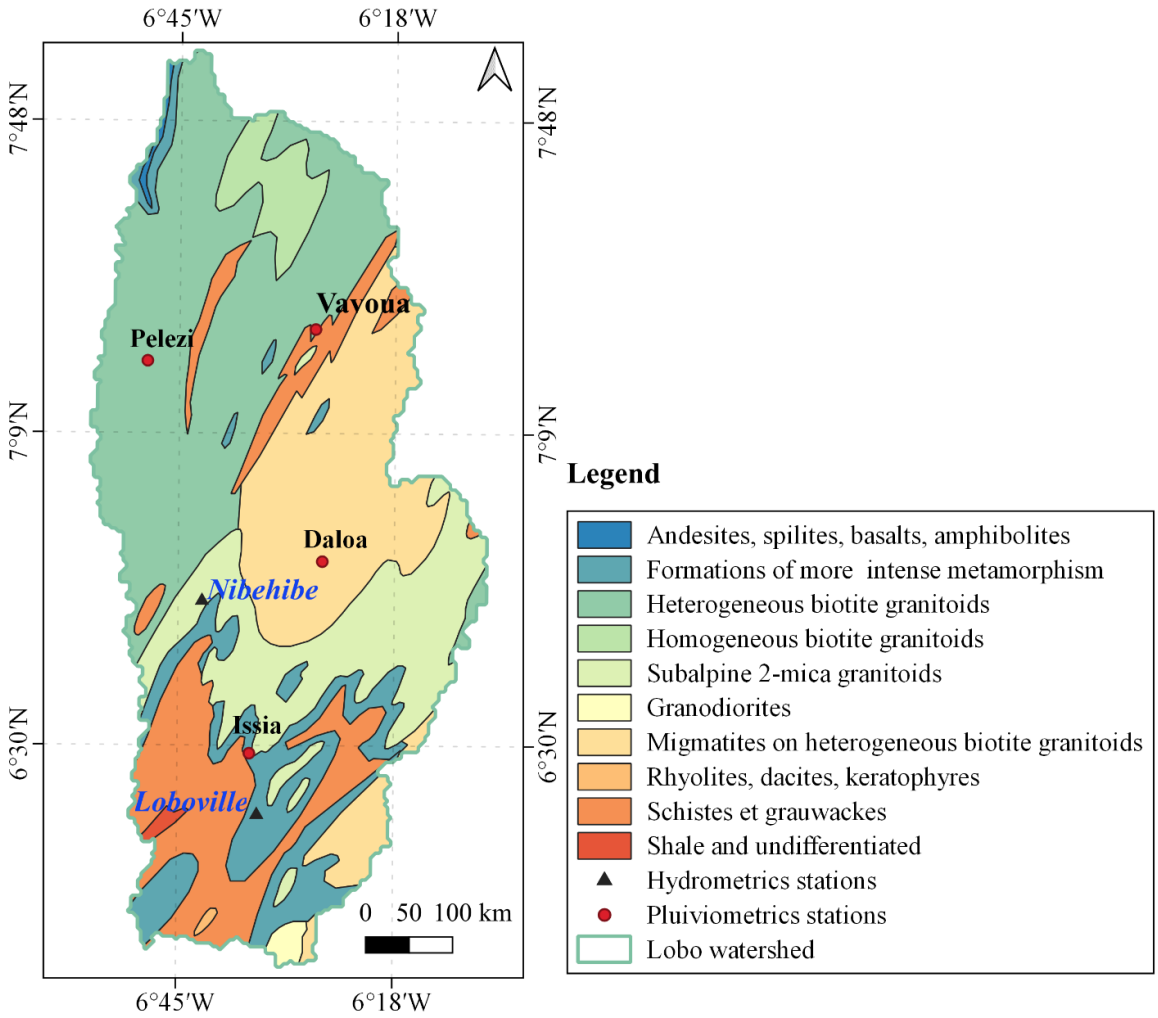

Figure 6: Geology of Lobo watershed

e. N’zo watershed

The N'zo at Kahin catchment region is located between longitudes 7°15' and 8°05' west and latitudes 7°50' and 6°50' north Goula et al., 2006). There are notable points in these regions, such as the DAN Mountains and Mount Tonkpi, which peak between 1100 and 1180 m in Côte d'Ivoire (Anouman, 2020), whereas the center and south of N'zo to Kahin are at elevations of less than 453 m. The geology of the Man is integrated by two primary geological entities: magmatic rocks and metamorphic rocks. Granitoids, such as the heterogeneous granites found in the eastern section of the N'zo sub-catchment (Figure 7), are the most common magmatic rocks discovered. Migmatite, mylonite, gneiss, and schist dominate the metamorphic rocks found in the basin's south-west, south, and south-east (Sodemi, 1972).

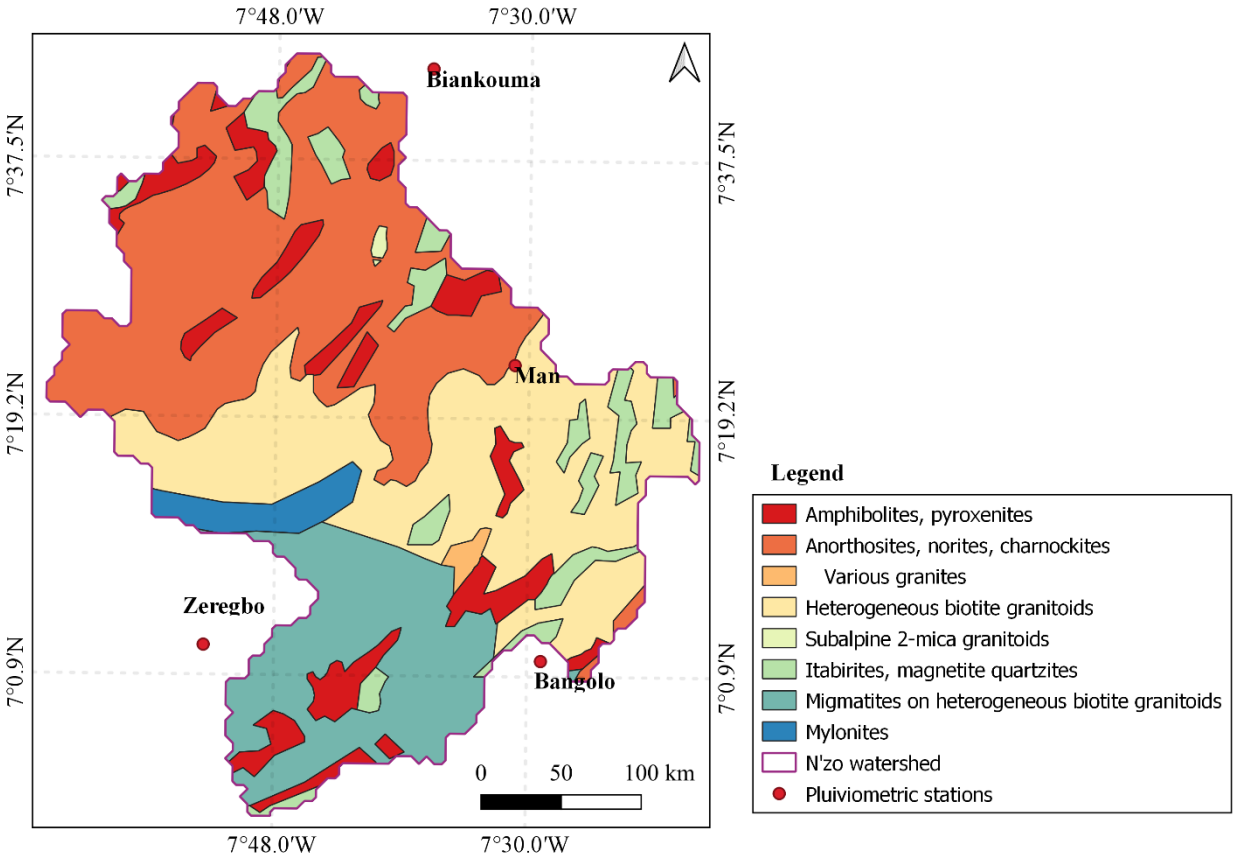

Figure 7: Geology of N'zo watershed

2.4. Climate

Both a humid equatorial climate and a tropical climate can be found in the south of Côte d'Ivoire. The southern region of the nation experiences an equatorial climate with two wet and two dry seasons. One wet season and one dry season define the tropical climate, which is prevalent in the north and center of the planet. Although rainfall in the tiny western mountainous area can reach 2,000 mm, rainfall is more frequent in the interior, ranging between 1,200 and 1,500 mm per year, while it is sparser towards the coast, averaging between 1,500 and 2,500 mm per year. The country's regular rainy season lasts from June to October, and the average annual temperature ranges between 24 and 28 ^{o}C.

a. Agneby

Agneby's coastal basin experiences a sub-equatorial climate with four distinct seasons: two dry (December–March) and two wets (April–July, which is more significant, and September–November, which is quite irregular), with the wet seasons centered in June and October. The average annual temperature is 26.8 °C, and the usual southern rainfall ranges from 1,400 to 2,500 mm/year (Koudou et al., 2018).

b. Bagoue

The Kouto sub-catchment is located in the Sudan climatic zone and has a transitional tropical climate with a single rainy season from April-May to October. This is followed by the dry season from October to April, which is characterised by long dry spells, large daily thermal contrasts, and the harmattan haze. The area is marked by high insolation, with an average ambient temperature of around 26.5 °C (Miessan et al., 2019).

c. Baya

The Baya Basin has two distinct seasons: a protracted dry season and a protracted wet season with an average annual rainfall of 1200 mm. The quantity of rainfall received during this time ranges between 867 mm and 1217 mm, according to observations of daily rainfall data at the Bondoukou synoptic station during the years 2000 to 2010. The hydrometric station between Tanda and Agnibilekrou has recorded average monthly temperatures between 22 and 27 °C for the years 1960 to 2010; this corresponds to a thermal amplitude of 5 °C annually (N'guettia, 2021).

d. Lobo

The Lobo watershed has an equatorial transitional climate, with the rainy season lasting from March to October and the dry season lasting from November to February. The basin has a sub-equatorial climate with four distinct seasons, including two dry ones (December through March and July through September) and two wet ones (April-July, which is more important, and September-November, which is very irregular). Over the years 1990 to 2015, 1,238.2 mm of rain fell annually on average. With a thermal amplitude of 4°C, the trend in the average monthly temperature varies generally between 24°C and 28°C (Koffi et al., 2020)**.**

e. N'zo

The N'zo is characterized by a unique alpine environment with two distinct seasons that last for uneven amounts of time: the dry season from November to February and the rainy season from March to October (Saley, 2003). The Sassandra watershed's western region is home to this regime. It includes the areas from N'zo to Kahin as well as the southwest region from Sassandra to Semien. About 1600 and 2000 mm of rainfall per year. Being near the western extremity of the Guinean ridge, the region's orographic characteristics have a significant impact on the mountain regime. It is a transitional area between sub-equatorial, humid tropical, and tropical climates (Soro, 2011)**.**

2.5 Hydrology

Côte d'Ivoire has four major rivers (Cavally, Sassandra, Bandama and Comoé) running in a general north-south direction, coastal rivers (San-Pédro, Agnéby, la Mé, Bia…) in the south of the country and coastal lagoon systems (Aby, Ehy, Ébrié, Grand-Lahou…).

a. Agneby

The largest coastal basin in Côte d'Ivoire, the Agneby River rises in a little community at Angoua in the department of Bongouanou at an elevation of 260 m and runs from north to south. The entire woodland zone is traversed by the river's course (Figure 8). The Ebrié Lagoon, which is close to Dabou, is where it empties in its lower stages after flowing over marshes (Koudou et al., 2018).

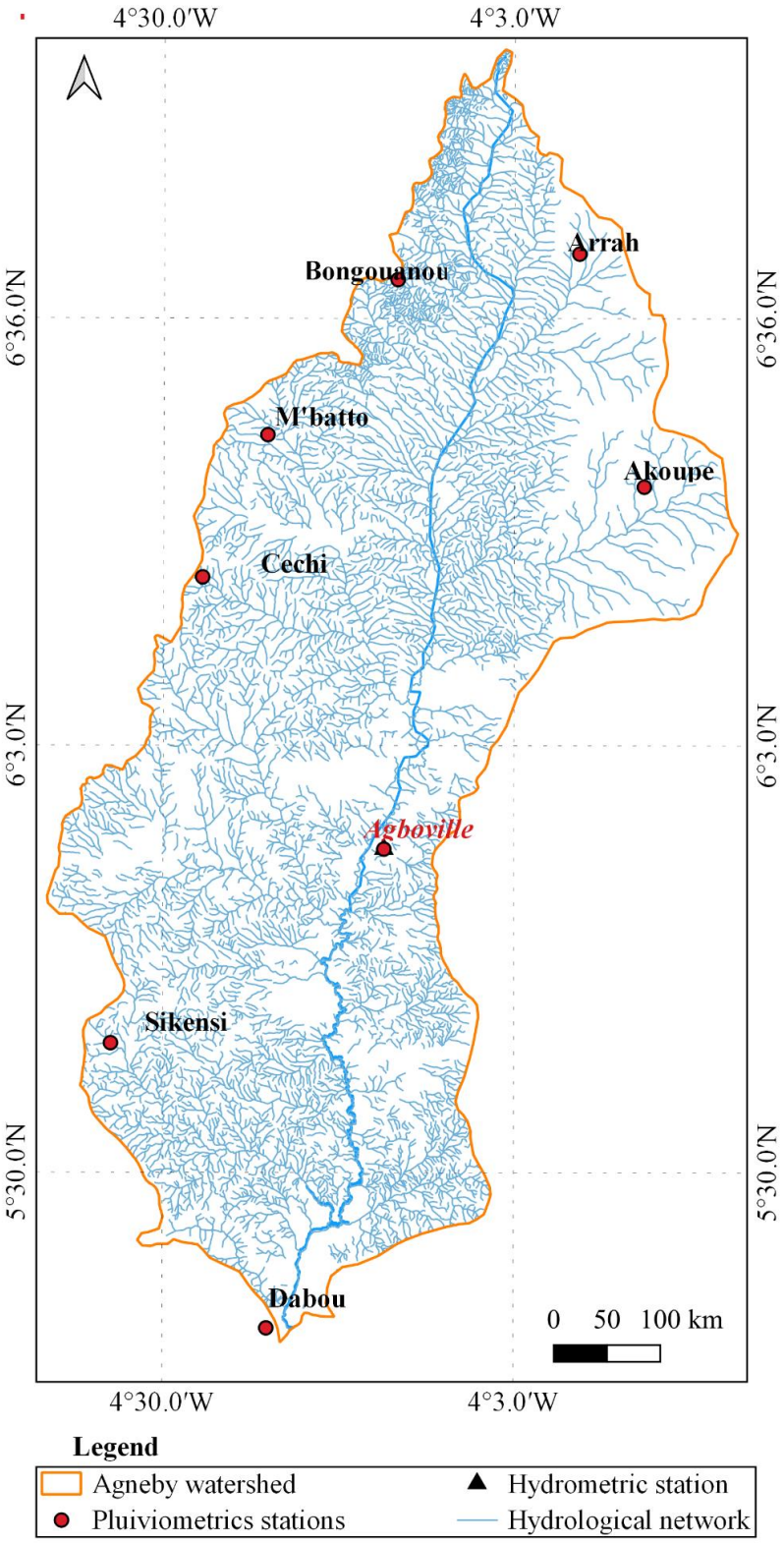

Figure 8: Hydrology of Agneby watershed

b. Bagoue

The hydrographic network has a drainage density of 0.84 km/km² and is characterised by a main watercourse, which is the Bagoé river, and its main tributaries (Gbanani, Palé, Sougoumon, Gnangbé, and Katiananka). This hydrographic network (Figure 9), has favoured the construction of dams for drinking water supply (AEP), which are currently influenced by the effects of climatic variability (Miessan et al., 2019).

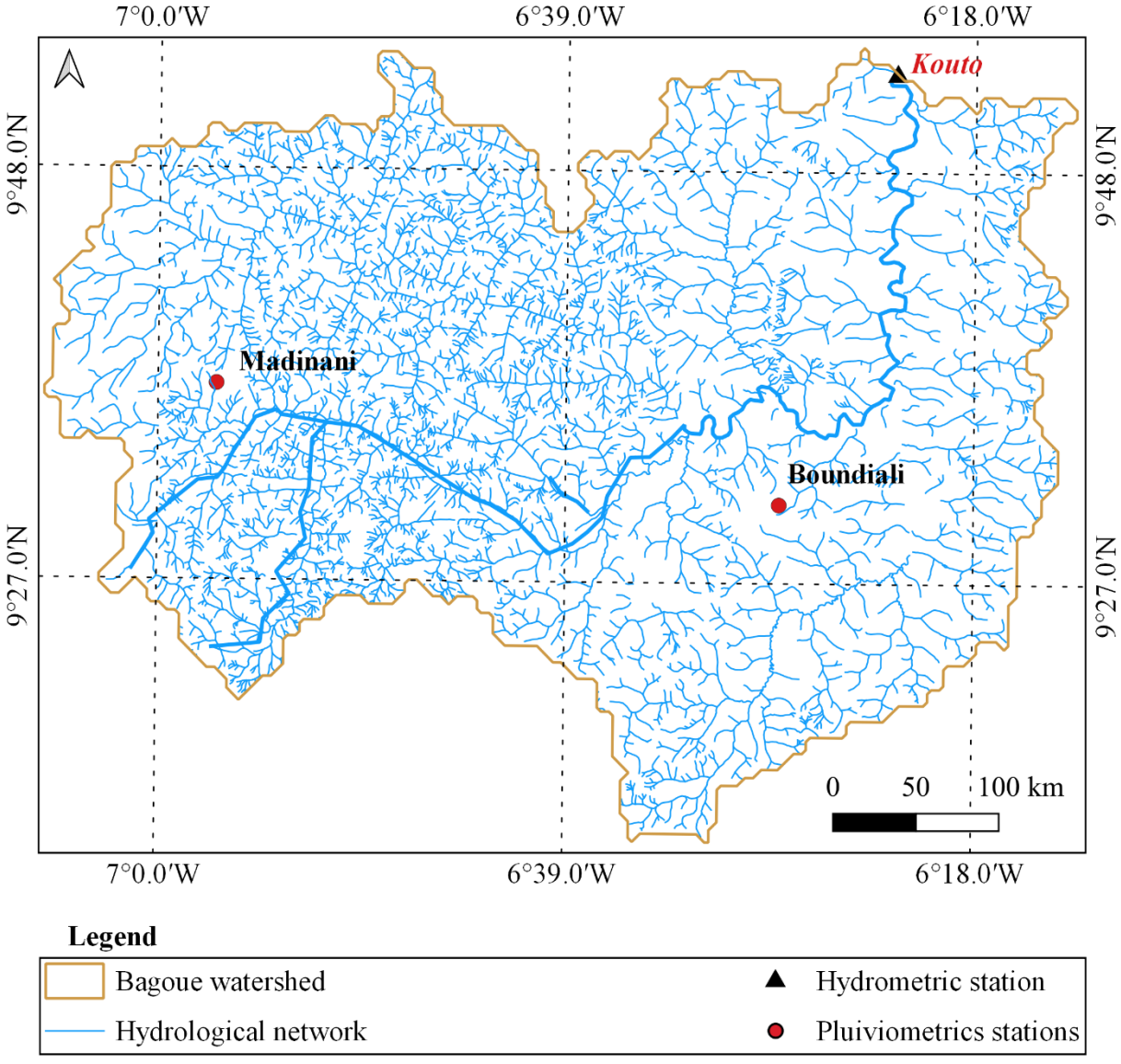

Figure 9: Hydrology of Bagoue watershed

c. Baya

The hydrology of the basin is quite diversified. It is made up of permanent and temporary streams that originate in the hills and flow towards the natural outlet before joining the main stream of the Comoé River (Figure 10). It is subdivided into two branches: The Babilé, which rises in the Kinkua mountain, north of Assueffry, and the Bayakokoré, which rises north of Tabagne and flows southward. In addition to the main rivers, there are secondary rivers: The Seinou, which rises on the southern side of the pass between Batié and Kiendi; and the Djéré, which rises between Mount Bowé and the village of Siminimi, flows southwards and into the Baya (N'guettia, 2021).

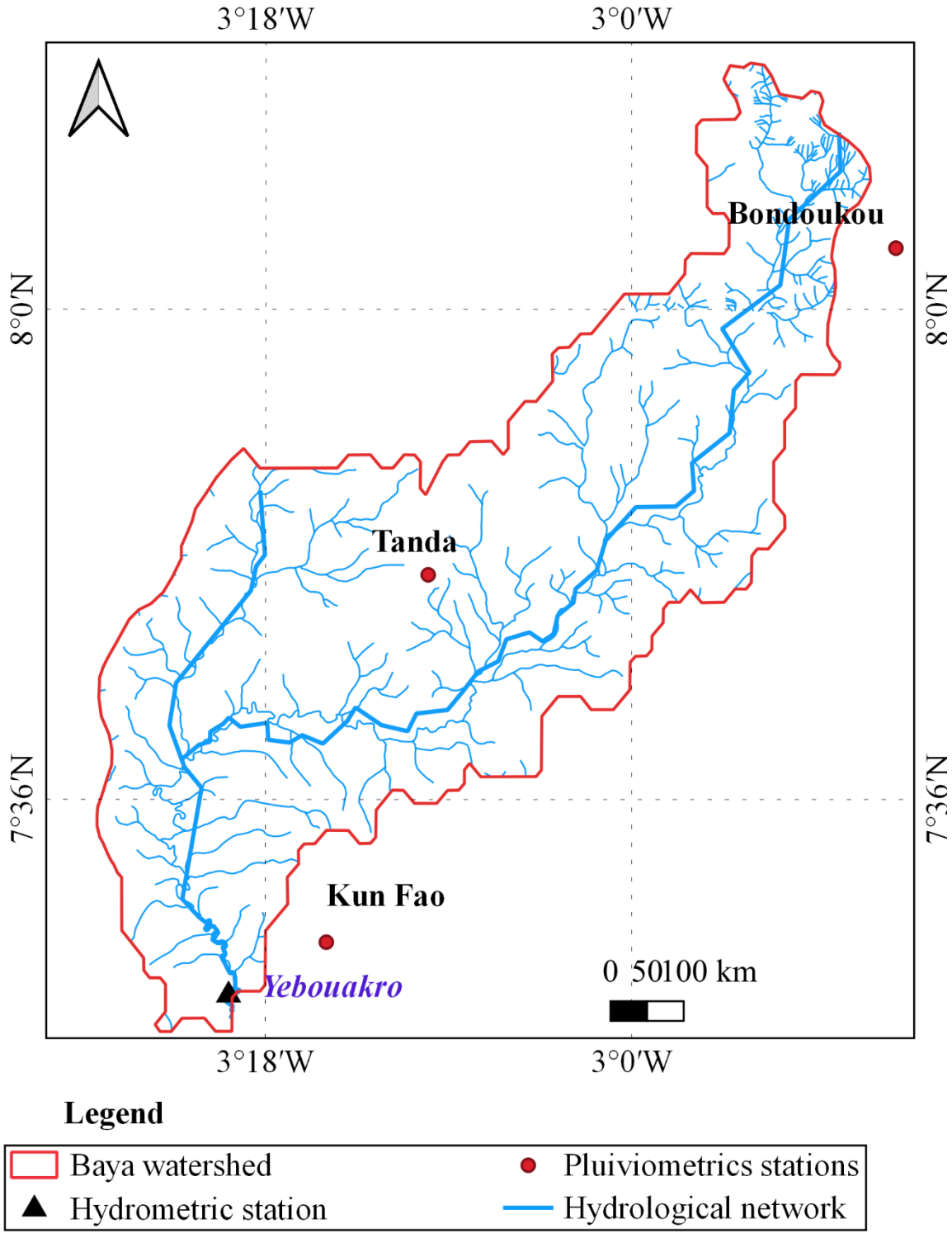

Figure 10: Hydrology of Baya watershed

d. Lobo

One of the major left-bank tributaries of the Sassandra River, the Lobo River has a length of 355 km and drains an area of 12,722 km^2. South of Séguéla, the Lobo River rises at a height of 400 meters, and it empties into the Sassandra River not far from the village of Loboville. The hydrographic network of the Lobo catchment area is more developed on its extreme left than on its extreme right, and these main tributaries have a permanent regime (Figure 11). The waters of the Lobo flow in a north-south direction, and the beginning of the year is when the water levels are at their lowest (January and February) (Deguy, 2021). It is an extremely valuable resource, especially as a supply of drinking water for Daloa, the third-largest city in Côte d'Ivoire. Sometimes during rainy periods, floods are observed.

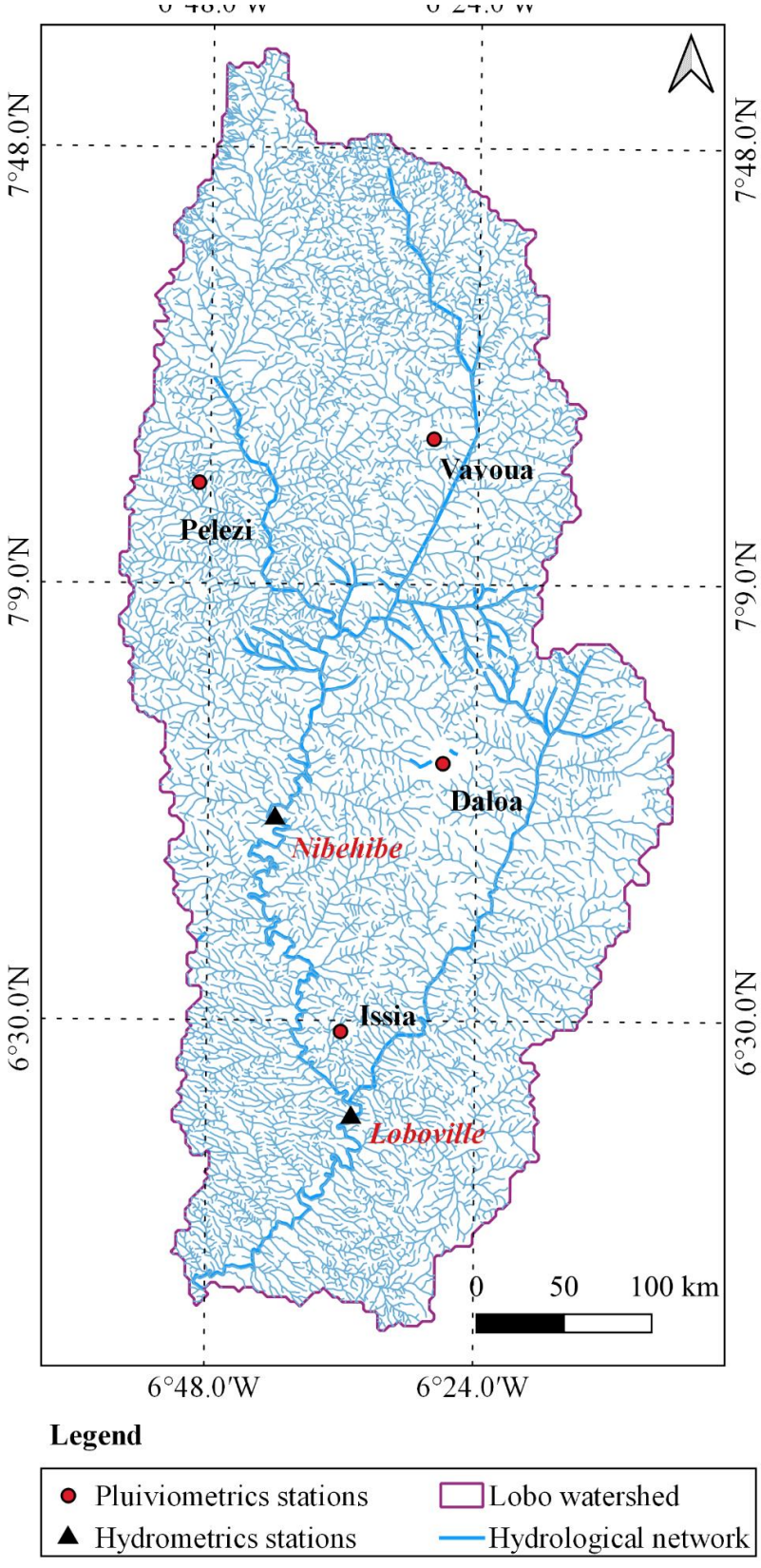

Figure 11: Hydrology of Lobo watershed

e. N’zo

The Sassandra River originates in the Beyla region of Guinea, under the name of Feredougouba. Its basin covers an area of about 75,038 km^2, of which 8,000 km^2 are outside the territory of Côte d'Ivoire. The Sassandra is 650 km long and has two major tributaries on its right bank: The Bafing and the N'Zo. After Guessabo, the Sassandra receives, on the right bank, the N'Zo, whose catchment area at Guiglo is about 7,000 km^2 (Figure 12).

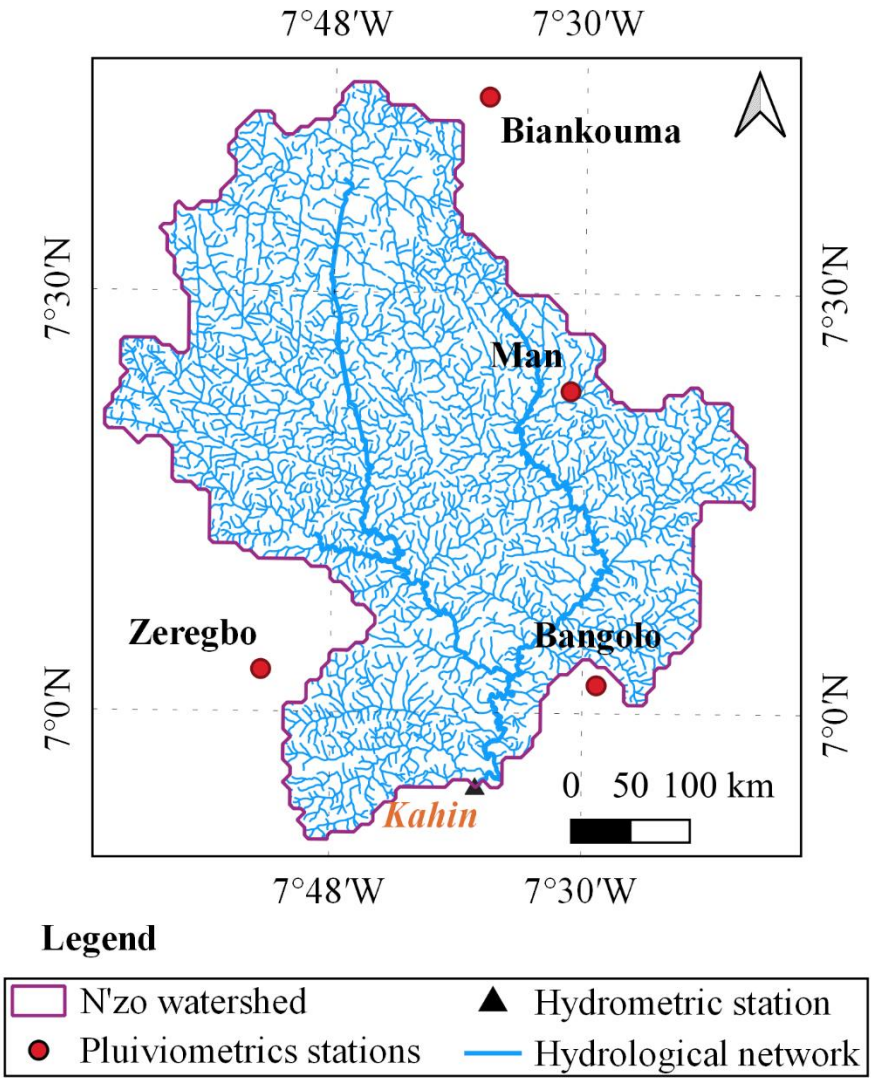

Figure 12: Hydrology of N'zo watershed

2.6 Land use and cover

a. Agneby

The Agnéby watershed is composed of dense rainforest, cleared forest, perennial crops, swamp forest, and very rarely savannah (Koné et al., 2019). The species *Mapania spp. and Diospyros spp.*, whose foliage is perpetually renewed, are the constituents of the climate, and highly sought-after species such as *Bassam mahogany, Khaya ivorensis, Azobé, Lophira alata, Niangon, and Terrietia utilise* the characteristics of this forest zone (Sankare et al., 1999). These formations are in retreat because of soil impoverishment or degradation caused by man during the establishment of plantations. In this basin, perennial crops, cereal and food crops (tubers, roots, plantains, etc.), as well as fruit and vegetable crops are often grown in association (Konin et al., 2022).

b. Bagoue

The study area belongs to the Savannah and Denguélé districts of north-western Côte d'Ivoire, more precisely to the Bagoué region. It is the west Sudanian savannah type, with trees 8 to 12 m tall and scattered shrubs, and a canopy density of 25 to 35%. This region is home to four classified forests: Niangboué, with a surface area of 14,800 ha; Palée, with a surface area of 200,000 ha; Fengolo, located between Kolia and Madinani, with a surface area of 188 ha; and Nyangbou, with a surface area of 62 ha. But there are also cash crops such as cotton, cashew nuts, and mango orchards, especially the Kent variety (N'guessan et al., 2015).

c. Baya

The Baya catchment area is characterised by dense forest in the south of the catchment area, in the Tanda region. Over time, this primary vegetation has been progressively transformed by human activities into degraded forests, coffee and cocoa orchards, fallow land, and wooded savannah. The savannah occupies the northern part of the basin and is made up of grassy savannah and wooded savannah. The palm tree (Borassus aethiopium), characteristic of this type of savannah, appears from Tanda to the north (Mangoua et al., 2019). This vegetation is degraded by human activity and bush fires, particularly in areas of high population density.

d. Lobo

The mesophilic sector of the Guinean domain includes the forest sections of the Lobo watershed, which are ideal for agricultural use. The samba Triplochiton scleroxylon, the ako Antiaris africana, and the bété Mansonia altissima are just a few of the many species found in this woodland (Avenard, 1971). However, due to intense agricultural pressure that has altered its floristic composition, it is currently made up of forest remnants connected with annual or perennial crop plantations (rice, cassava, yams, and market gardens) or perennial crop plantations (rubber trees, cashew nuts, coffee, and cocoa) (Koffie-Bikpo et al., 2013). This agriculture is widespread, unorganized, rain-fed, and labor-intensive, and it makes up for its flaws by systematically annexing more land (Noufou, 1998).

e. N'zo

The N'zo basin offers a range of agricultural potential. Over time, plantation agriculture has replaced a naturally imposed gathering economy, especially with the dominance of dense, cleared forest. The gathering economy then evolved into a plantation economy, first through the modernization of rubber cultivation, then with the cultivation of cocoa and coffee, and finally with the exploitation of wood. About the latter, the mahogany, avodire, azobe, and framire varieties are also the basis for the relative economic development of modern Côte d'Ivoire. The N'zo watershed is currently made up of forest relics associated with perennial crop plantations (rubber trees, cashew nuts, coffee, and cocoa) or annuals (rice, cassava yams, and market gardens).

2.7 Population and socio-economic aspect

a. Agneby

The Agneby basin is home to several ethnic groups and has been populated in successive waves thanks to the presence of forests favorable to agriculture, with an estimated population of 767,398 inhabitants in 2021 (RGPH, 2022). Socio-economic activity is based on agriculture, which is a predominant sector with extensive practices, including shifting cultivation, except some agro-industrial units using intensive methods. In this south forest zone, agriculture is strongly centred on cash crops, particularly the coffee-cocoa binomial, oil palm, rubber, coconut, and fruit products (sweet banana, pineapple, papaya, cashew, etc.), as well as food crops (rice, yam, plantain, cassava, maize, fresh vegetables, etc.) (Assoma et al., 2016).

b. Bagoue

The population of the study area is essentially rural and includes people whose socio-economic lives are dominated by agricultural and pastoral activities. It covers the regional capital of Boundiali and the departments of Kouto and Madinani, with an estimated population of 296,986 inhabitants (INS, 2014). Agriculture and livestock are the main socio-economic activities in the Bagoué Region. The crops grown are generally food crops: rice, maize, groundnuts, millet, fonio, cassava, potatoes, and yams (Miessan et al., 2019).

c. Baya

The population of the Baya catchment region is made up of non-native Sénoufos and Malinkés as well as citizens of ECOWAS nations, including Burkinabe, Malians, Ghanaians, Mauritanians, Togolese, Beninese, Nigerians, and other Africans, primarily traders, farmers, and craftspeople. According to the most recent population census, this population's size is predicted to be 667185 people, with an urbanization rate of 51.6% and a growth rate of 2.8%. (INS, 2014). The main source of income for the inhabitants of the basin is agriculture, and the crops grown there include citrus fruits, starchy crops, and cereals (yams, sweet potatoes, and cassava) (Minagra, 2001).

d. Lobo

The population of the Lobo watershed is essentially rural compared to 26% in urban areas and is unevenly distributed over the three main departments of the basin: 41% for the department of Daloa, compared to 28% for Vavoua, 22.9% for Issia, and 8.1%, which is estimated at 1,430,960 inhabitants in 2014 (INS, 2014). Economic activities are not very diversified in the Lobo basin. Agriculture is large, anarchic, rain-fed, and manual, and it makes up for its flaws by perpetually encroaching on new territory (Noufou, 1998). The production system is dominated by the coffee-cocoa binomial. Since its habitation and agricultural growth began in 1970, this area has become Côte d'Ivoire's second "cocoa loop" (Ibo, 2007). The timber industry, although in decline, remains an important activity in the region. The operators are either companies or individuals who, for the most part, have no representation in the basin. Livestock farming is one of the economic activities of the agricultural sector in the basin and is mainly cattle and sheep farming (Deguy, 2021).

e. N’zo

The population is estimated at 600,000 inhabitants (INS, 2001), with an average demographic density of 48 inhabitants per km^2 and an estimated growth rate of 4.06%. Economic activities are very diversified, with activities such as fishing, agro-pastoral, and agriculture. The latter is the main income-generating activity of the population, and it is extensive, anarchic, rain-fed, and manual agriculture (Noufou, 1998). Agricultural activities are dominated by the cultivation of coffee, cocoa, oil palm, cashew nuts, and cotton. These crops are grown by both indigenous and non-indigenous people. There is therefore strong agricultural pressure on the land in the catchment area, leading to a significant degradation of natural resources.

Conclusion

Location, geology, climate, hydrology, land use and cover, population, and socioeconomic factors were the foundation for this chapter. These factors have all been detailed and covered in the document as a whole. Specifically, between latitudes 4°30' and 10°30' North and longitudes 8°30' and 2°30' West, Côte d'Ivoire is situated in West Africa in the intertropical zone between the equator and the Tropic of Cancer. In the mountainous area, the N'zo watershed has two distinct seasons: a long-wet season (8 months) and a short dry season (4 months), with two main seasons of varying duration, between 1,600 and 2,000 mm of rainfall per year. Its geology is identical to that of the town of Man, which is made up of two primary geological entities: magmatic rocks and metamorphic rocks. Lobo watershed in the sub-equatorial climate is represented by transitional equatorial with a dry season from November to February and a rainy season from March to October, the average annual rainfall is 1238.2 mm. The plateaus, which make up the majority of the basin, range in height from 240 to 320 meters, with a crescent-shaped greenstone massif rising to a height of 617 meters in the basin's far north. The Kouto sub-catchment is located in the Sudan climatic zone and has a transitional tropical climate with a single rainy season from April-May to October. The hydrographic network has a drainage density of 0.84 km/km^2 and is characterised by a main watercourse, which is the Bagoé river, and its main tributaries (Gbanani, Palé, Sougoumon, Gnangbé, and Katiananka). The geology of the area consists of solitary domes of granitic, metamorphosed, or granitic intrusive and metasomatized rocks. The Baya watershed is located in a humid tropical climate characterised by a maximum annual rainfall of 1,200 m; seasons divided into three parts: a major rainy season

(April-June), a short dry season, and a mainly dry season (November-March) (July-August). The hydrology of the basin is highly diversified. It is made up of permanent and temporary watercourses that originate in the hills and flow towards the natural outlet before joining the main course of the River Comoé. The Tarkwaan volcanic formations are found almost throughout the catchment area, from south to north, deposited in a sedimentation basin subject to major compressive deformations. Agneby's coastal basin experiences a sub-equatorial climate with four distinct seasons: two dry (December–March) and two wet (April–July, which is more significant, and September–November, which is quite irregular), with the wet seasons centered in June and October. The annual precipitation of 1400 to 2500 mm. The basin belongs to a group formed by two geological units: the sedimentary basin in the south and the crystalline and crystallophyllous basement in the north, made up of volcano-sedimentary rocks.

CHAPTER 3: DATA, MATERIALS AND METHODS

This chapter outlines the different types of data gathered, the supplies and methods used to gather and analyze them, as well as the tools and materials employed. It is divided into three sections. The first section deals with the data collection, pre-processing, and extraction of extreme indices. The second section deals with the materials and model description. The last section describes the analysis of trends in hydrological time series, the detection of breakpoints, and climate change impact methods.

3.1 Data

3.1.1 Observed data

Daily rainfall from 21 rainfall stations dispersed across the watersheds and discharge hydrometric measurements from six hydrometric stations were the observed data used in this investigation. We had good spatial representativeness because all stations were chosen based on the number of years of observations. The Airport, Aeronautical and Meteorological Exploitation and Development Corporation (SODEXAM) of Côte d'Ivoire's database has rainfall information for the years 1970 to 2017 and 1980 to 2017 for select stations (Table 2). The hydraulics control provided the flow statistics. According to figure 12 and table 3, these daily discharges cover the time periods 1970–2017 for the Agneby watershed, 1980–2017 for the N'zo watershed, 1980–2018 for the Bagoue watershed, 1980–2004 for the Baya watershed, and 1988-2015 for the Lobo watershed with two differents stations: Loboville and Nibehibe. They also cover the time periods 1980–2018 for the Bagoue watershed.

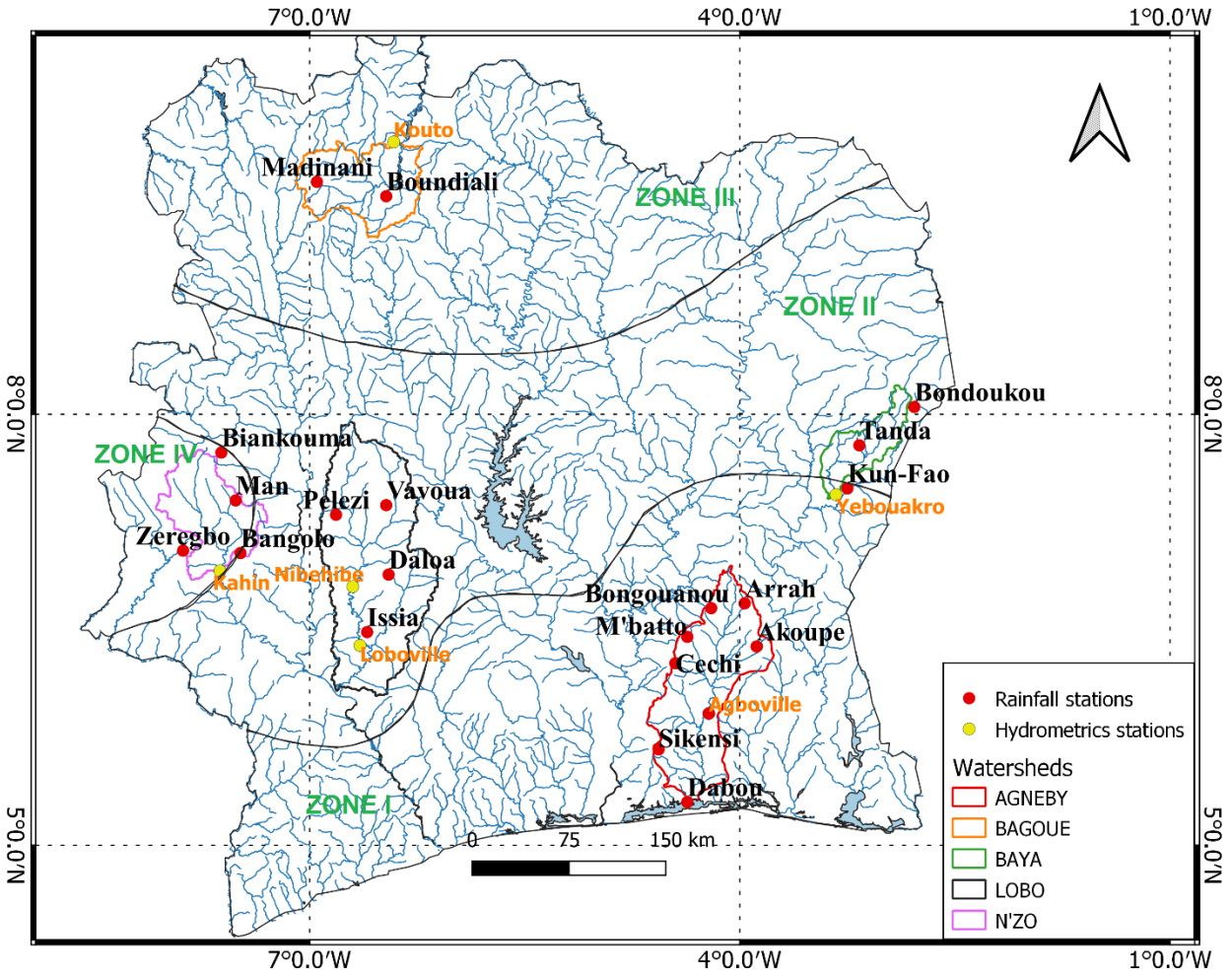

Figure 13: Rainfall and hydrometrics stations used in this study

Table 2: Rainfall stations used in this study

Watersheds	Stations	Latitude(°)	Longitude(°)	Data Range
Agneby	Agboville	5.9	-4.2	1976-2017
	Akoupe	6.3	-3.8	
	Arrah	6.6	-3.9	
	Bongouanou	6.6	-4.2	
	Cechi	6.2	-4.4	
	Dabou	5.3	-4.3	
	M'batto	6.4	-4.3	

	Sikensi	5.6	-4.5	
Bagoue	Boundiali	9.5	-6.4	1980-2017
	Madinani	9.6	-6.9	
Baya	Bondoukou	8.1	-2.7	1976-2017
	Kun Fao	7.4	-3.2	
	Tanda	7.7	-3.1	
Lobo	Daloa	6.8	-6.4	1983-2017
	Issia	6.5	-6.6	
	Pelezi	7.3	-6.8	
	Vavoua	7.3	-6.4	
N'zo	Bangolo	7.03	-7.4	1983-2017
	Biankouma	7.7	-7.6	
	Man	7.4	-7.5	
	Zeregbo	7.05	-7.8	

3.1.2 Data pre-processing

3.1.2.1 Rainfall data

The data were visually pre-processed before the extraction of the variables to be studied. Indeed, data visualization is an essential procedure in statistical analysis because it helps to decide on the nature of the data we have in terms of its quality. The data pre-processing first consisted of studying the spatialization between the rainfall stations in order to know the relationship between the stations for a possible filling of the missing data. To complete the missing data, missing values were filled by using rainfall data from Africa Rainfall Climatology 2.0 (ARC2™) estimated by the Climatology 2.0 (ARC2™) rainfall data estimated by the National Oceanic and Atmospheric Administration, or NOAA (P. Xie and P. A. Arkin, 1996, p. 843; N. S. Novella and W. M. Thiaw, 2013, p. 590). and before using the Africa Rainfall Climatology 2.0 (ARC2™) data to fill in the missing data from the ground stations

(SODEXAM), correlation tests between the different datasets were performed using Pearson's correlation coefficient (r) (Coulibaly et al., 2020).

3.1.2.2 Discharge data

The runoff signal from a watershed basin is calculated using mathematical formulas based on the rainfall signal received by the basin (Larbi, 2019). As a result, hydrologic models are shortened, conceptual explanations of a certain phase of the hydrologic cycle. They are also commonly used to generate stream flow data to: fill blanks in existing records; evaluate current and/or natural flows and yields for ungauged catchment regions; generate long-term data to develop statistics and estimates of yield reliability; and input information for other research projects such as environmental flow, creating scenarios, or forecast prediction (Table 3). Following the calibration and validation procedures, the output of rainfall-runoff modeling using the GR4J was utilized to first substitute missing discharge data in our case study.

Table 3: Stations and missing data

Stations	Data types	Periods	Periods of missing data	Percentage of missing data (%)
Agboville	Rainfall	1970-2017	2015-2017	4. 25
Akoupe	Rainfall	1970-2017	2015-2017	4. 25
Arrah	Rainfall	1976-2017	2015-2017	4. 25
Bangolo	Rainfall	1983-2017	1983-1994;1998-2014	79.41
Biankouma	Rainfall	1983-2017	1993-1994;1996	5.88
Bondoukou	Rainfall	1970-2017	None	0
Bongouanou	Rainfall	1970-2017	2015-2017	4. 25
Boundiali	Rainfall	1980-2017	1993;1994	0.0541
Cechi	Rainfall	1970-2017	None	0
Dabou	Rainfall	1970-2017	1983-1984;2015-2017	6.38
Daloa	Rainfall	1970-2017	none	0
Issia	Rainfall	1983-2017	1981-1982	2.9

Kun-Fao	Rainfall	1976-2017	1993	2.43
M'abatto	Rainfall	1970-2017	2015-2017	4. 25
Madinani	Rainfall	1970-2017	1993;1994;1996	0.0638
Man	Rainfall	1970-2017	none	0
Pelezi	Rainfall	1976-2017	1976-1977;1981-1982	4.87
Sikensi	Rainfall	1976-2017	2013-2017	9.75
Tanda	Rainfall	1976-2017	1993-1994	2.44
Vavoua	Rainfall	1970-2017	1977;1994	4.25
Zeregbo	Rainfall	1983-2017	1996-2017	61.76
Agboville	Discharge	1970-2017	2006-2017	23.4
Kahin	Discharge	1980-2017	2015-2017	5.4
Kouto	Discharge	1970-2017	none	0
Loboville	Discharge	1988-2015	2012-2014	7.41
Nibehibe	Discharge	1971-2018	1989-1991;1998;2003	8.51
Yebouakro	Discharge	1980-2004		

3.1.3 Regional climate models' datasets

A high-resolution regional climate model (RCM) with a typical horizontal resolution of 50 km is used to downscale daily rainfall data from a range of scenarios. The Swedish Meteorological and Hydrological Institute's RCA4 Rossby Center regional atmospheric model, the fourth iteration of the RCM, was employed (SMHI). Three global climate models (GCMs) were downscaled using the RCA4 as part of the Coordinated Regional Climate Downscaling Experiment: CNRM-CERFACS-CNRM-CM5 at a resolution of 1.4° 1.4°, IPSL-IPSL-CM5A-MR at a resolution of 1.25° x 2.5°, and MPI-M-MPI-ESM-LR at a resolution of 1.9° 1.9°. (CORDEX-Africa). Two sets of representative concentration pathways (RCPs) scenarios were examined in this study, but only for the 2020–2050-time frame. These scenarios were RCPs 4.5, the average scenario, which presupposes that strategies to reduce greenhouse gas emissions will cause radiative forcing to stabilize at 4.5 W/m2, and RCPs 8.5, the pessimistic scenarios, which

assume that increased greenhouse gas emissions will cause radiative forcing to reach 8.5 W/m2 by the year 2100. In numerous studies on the effects, variability, and extreme events of climate change, these Representative Concentration Pathways (RCP 4.5 and RCP 8.5) have been widely used in West Africa (Sylla et al., 2016). They have also provided information about the future changes under various RCPs and levels of global warming. The RCMs used were chosen based on their performance over West Africa, and in particular, their capacity to accurately reproduce West African rainfall regimes (Akinsanola et al., 2017); (Kwawuvi et al., 2022). The data were extracted for each of the following stations at grid cell level.

Table 4: Selected stations and watershed

Watersheds	**Stations**	**Latitude(°)**	**Longitude(°)**
Agneby	Agboville	5.9	-4.2
	Akoupe	6.3	-3.8
	Arrah	6.6	-3.9
	Bongouanou	6.6	-4.2
	Cechi	6.2	-4.4
	Dabou	5.3	-4.3
	M'batto	6.4	-4.3
	Sikensi	5.6	-4.5
Bagoue	Boundiali	9.5	-6.4
	Madinani	9.6	-6.9
Baya	Bondoukou	8.1	-2.7
	Kun Fao	7.4	-3.2
	Tanda	7.7	-3.1
	Daloa	6.8	-6.4
	Issia	6.5	-6.6

Lobo	Pelezi	7.3	-6.8
	Vavoua	7.3	-6.4
N'zo	Bangolo	7.03	-7.4
	Biankouma	7.7	-7.6
	Man	7.4	-7.5
	Zeregbo	7.05	-7.8

3.1.4 Normalized Difference Vegetation Index (NDVI) datase

Due to its simplicity and effectiveness as a proxy measure for vegetation condition (i.e., vegetation health, cover, and phenology), the NDVI has been widely employed to investigate vegetation dynamics. This can be accomplished with the use of remote sensing methods, which offer the capacity to record the vegetation dynamics in response to climatic changes at high temporal resolutions over extensive time series. Utilizing multiple residual regression analysis, NDVI time series data have been widely employed to evaluate the spatiotemporal dynamics of local vegetation in response to local climatic conditions as well as human activity.

The Landsat/5/7/8 satellite remote sensing dataset, which was made available by climate engine.org (https://app.climateengine.org/climateEngine#), was utilized to generate the daily NDVI data used in this work.

3.1.5 Extraction of extreme rainfall and flow indices

To better comprehend and sense future changes, conducted climate change research in hydrology often uses long-term climatic indices. This helps researchers test the impact of the phenomenon and enhance early warning systems, risk management, and adaptation. As a result, the World Meteorological Organization (WMO), through the Commission for Climatology (CCl) Expert Team on Climate Risk and Sector-Specific Indices (ETCRSCI), makes the rainfall data available at http://www.wmo.int/pages/prog/wcp/ccl/opace/opace4/expertteam.php. Thirty-four (34) extreme rainfall and temperature indices, along with nine extra ones, offer a thorough grasp of climate change. In our study on the analysis of hydro-climatological extremes, eleven (11) indices out of twenty-seven (27) rainfall extreme indices were used. There were four rainfall extremes (Pmaxan, R95p, Rx5 days, and CDD), three flood indices (Qmaxan, 5-day, and

VCX30), and four low water levels (Qminan, QMNA, VN7, and WFD) e.g., (Yao et al., 2018) **;(**Okafor et al., 2021)**;** (Kouassi et al., 2020) **;** (UlMoazzam et al., 2022).

3.1.5.1 Extreme rainfall indices

The extreme climate indices are based on indicators adopted by the expert team on climate change detection and monitoring (ETCCDM) and have been used in numerous research around the world e.g., (Yao et al., 2021); (Okafor et al., 2021a). To characterize the extreme flows, four indices were chosen, including the maximum rainfall index (Pmaxan), which was extracted annually, and the consecutive dry day index (CDDI), which was extracted from the database by taking into account the maximum number of consecutive days with daily rainfall of less than 1 mm (1mm). To evaluate the effects of rainfall during the high-water period on flood events in each climatic zone, we concentrated more on extremely wet days (R95p) and maximum 5-day rainfall (Rx5days). The Agneby, Lobo, and N'zo watersheds started in March to October, when there is a substantial amount of rainfall, for climatic zones I, II, and IV, respectively. Extraction in the Bagoue watershed, which is located in climatic zone III, began in May and continued until October, but extraction in the Baya watershed began in April and ran until October. The maximum 5-day rainfall (Rx5days), the very wet day (R95p), and the average daily discharges over five (5) consecutive days were utilized to construct their yearly extractions using moving averages. Table 5 provides detailed explanations of the four indices (Pmaxan, R95p, Rx5 days, and CDD) related to excessive rainfall that were selected.

Table 5: Rainfall extremes indexes used in this study

Index	**Name**	**Definition**
Pmaxan	Maximum rainfall	Maximum annual rainfall
R95p	Very wet day	Annual total rainfall when RR > 95 percentiles
Rx5 days	Maximum 5-days rainfall	Maximum 5-days rainfall
CDD	Consecutive dry days	Maximum number of consecutive days with daily rainfall <1mm

3.1.5.2 Extreme discharge indices

To describe the extreme flows, seven (7) indices were chosen, including the maximum flow over five days (QX5days), the peak flow over one month (Qmaxan), the maximum monthly flow (VCX30), the minimum annual flow (Qminan), the mean monthly flow (QMNA), the daily flow (VCN7), and the low-water feature (WFD). These indices, which are indicative of flood and drought features (Yao et al., 2021); (Assoko et al., 2020); (Kouassi et al., 2020); (Garcia et al., 2017), have been widely employed in numerous research with positive findings. All the indices are shown in Table 6.

- **Maximum annual discharge (Qmaxan)**: Qmaxan was obtained by selecting the highest annual discharge.
- **Mean monthly discharge (VCX30):** The greatest average flow over 30 consecutive days was used to calculate the VCX30, and it was noted that for each year, the data may be divided into three categories: below normal when below the first quartile, above normal when above the third quartile, and normal when in between.
- **5-day maximum flow (QX5days):** The average daily maximum discharges over five (5) consecutive days were used to generate the moving averages on which the QX5days was derived annually.

  Annual minimum flows (Qminan): Low water is referred to as the time of the year when a river has a low flow; in this instance, we will refer to low water as the time of the year with the lowest flow or the time with the lowest annual minimum daily flow. The minimum annual discharge was chosen in order to extract Qminan.
- **QMNA, average monthly debit:** The lowest average monthly flow for the year, the QMNA, is used to distinguish between low water flows from the monthly scale and low water flows determined by daily moving averages. The lowest mean monthly flow of the year was chosen, together with the low water flows derived from the daily moving averages (Anouman et al., 2019); (Assoko et al., 2020).
- **Flow rate VCN7day**: The VCN7day is an average flow rate that is normal over seven days in a season. These values are yearly averages derived from the average daily discharges over seven (7) consecutive days (Kouassi et al., 2020); Gailliez,2013; (Anouman et al., 2019); (Piniewski et al., 2018).

- **Characteristic low flow Q(WFD):** A flow rate of no more than 10 days per year falls under the definition of the characteristic low flow rate (CFR). It is a term usually used to describe how low the water is in a stream. Using values that exceeded 90, 75, and 50% of the year, for example, characteristic flows can also be given as a percentage. The minimum monthly flows that were less than or equal to the 0.03 quantile were used to calculate the WFD for a given year Lang,2011.

Table 6: High and Low flow extreme indices

Index	Name	Definition
	High flow index	
QX5-days	5-day maximum flow	Moving average of maximum discharge rate over five days.
Qmaxan	Peak discharge	Annual maximum discharge
VCX30	Mean monthly discharge	maximum average discharge over 30 consecutive days
	Low flow index	
Qminan	Annual minimum discharges	The lowest discharge value of the year
QMNA	Average monthly discharges	The lowest average monthly discharge for the year
VCN7	Daily discharge rate	Moving average discharge rate over seven days.
WFD	Characteristic of low discharge	The discharge rate equals or does not exceed 10 days per year.

3.1.6 Land used data

The data used in this study are optical images collected from the website http://earthexplorer.usgs.gov/, which is a free website for downloading images for various purposes. These images are from the Landsat 4 and 5 generations with the TM (Thematic Mapper) sensor in 1986, Landsat 7 with the ETM+ (Enhanced Thematic Mapper) sensor in 2000, and Landsat 8 with the OLI (Operational Land Imager) sensor in 2017. The choice of these images is justified by their spectral characteristics, i.e., images taken at different wavelengths;

their high resolution, i.e., 30 m resolution; and their good repeatability, allowing for good mapping of land cover at a large scale with a download period between November and April to avoid cloud cover and atmospheric humidity, and a 15- to 14-year gap to better observe the changes between the selected classes (Table 7).

Table 7: Dates and scenes used in this study

Watersheds	**Images**	**Scene**	**Periods**
Agneby	Landsat_4	*Path:196*	1987-12-24
	Landsat_8	*Row: 55-56*	2020-04-20
Bagoue	Landsat 5	*Path:198*	Apr 13, 1986
	Landsat_7	*Row:53-54*	Jan 06 2000
	Landsat_8		2017-01-12
Baya	Landsat 5	*Path:195*	Nov 02, 1986
	Landsat 7	*Row:54-55*	Feb 02, 2000
	Landsat_8		2017-12-25
Lobo	Landsat 5	*Path:197/198*	Jan 16, 1986
	Landsat_8	*Row:55-56/55*	2017-12-23
N'zo	Landsat 5	*Path:198*	Jan 16, 1986
	Landsat_7	*Row:55*	Feb 07, 2000
	Landsat 7		Feb. 13, 2017

3.2 Materials

3.2.1 Rstudio: *R Package "qmap"*

R Package "*qmap*" program performs a bias reduction technique. It is a tool used to extract data from regional and global climate models and bias-correct that data. The adjustment parameters for the future period for the RCP4.5 and RCP8.5 scenarios are calculated by the R Package "*qmap*" using the overlapping technique using the observed and simulated rainfall data (i.e., the historical and future scenarios). The difference between simulated and observed climate

variables is minimized, and the adjusted data should roughly match the observed ones. The flexibility provided by R Package "*qmap*" flexibility makes it easier to analyze climate model data and improve observational replication.

3.2.2 Hydrological model

3.2.2.1 Hydrological model (GR4J) 's parameters

The GR4J model (4-parameter daily model) is a conceptual rainfall-runoff model with reservoirs. It was developed by Cemagref (Makhlouf and Michel, 1992) for applications at the catchment scale (global mode). The GR4J conceptual model is composed of several components, the most important of which is a precipitation interception module expressed as a water level, a portion of which can be evapotranspired and the remainder is reconvened to the transfer module. A performance function manages the emptying of the production tank, whose maximum capacity is determined by a first free parameter X1 expressed in mm. The emptying can be done by two distinct paths: evapotranspiration and percolation. The percolating water then passes through a transfer module materialized by two-unit hydrographs (UH1 and UH2), whose base time is governed by the free parameter X4 expressed in days. UH1 returns 90% of the water to the routing reservoir, which has a maximum capacity of X3 in mm, and UH2 manages the transfer of the remaining 10% of water to the outlet. The water transferred, either to the routing tank or directly to the outlet, is also subject to an exchange function with the subsoil, thanks to an exchange coefficient expressed in mm (Amoussou, 2015). These different parameters are summarised in Table 8 and Figure 14, which provide a complete description of the model.

Table 8: GR4J parameters

Parameters	Definitions	Units
X1	The capacity of the production reservoir: this reservoir controls the production of effective rainfall from precipitation inputs	mm
X2	the groundwater exchange coefficient, which can be either positive or negative depending on whether there is groundwater inflow or loss, or zero if there is no exchange.	mm
X3	the day-ahead capacity of the routing tank: this tank controls the recession phases.	mm

X4	The unit hydrographs' respective base times (UH1, UH2): The effective precipitation is dispersed throughout time, and they imitate the intervals between rainfall episodes. The identical time parameter, X4, stated in days, is required for both unit hydrographs.	Day

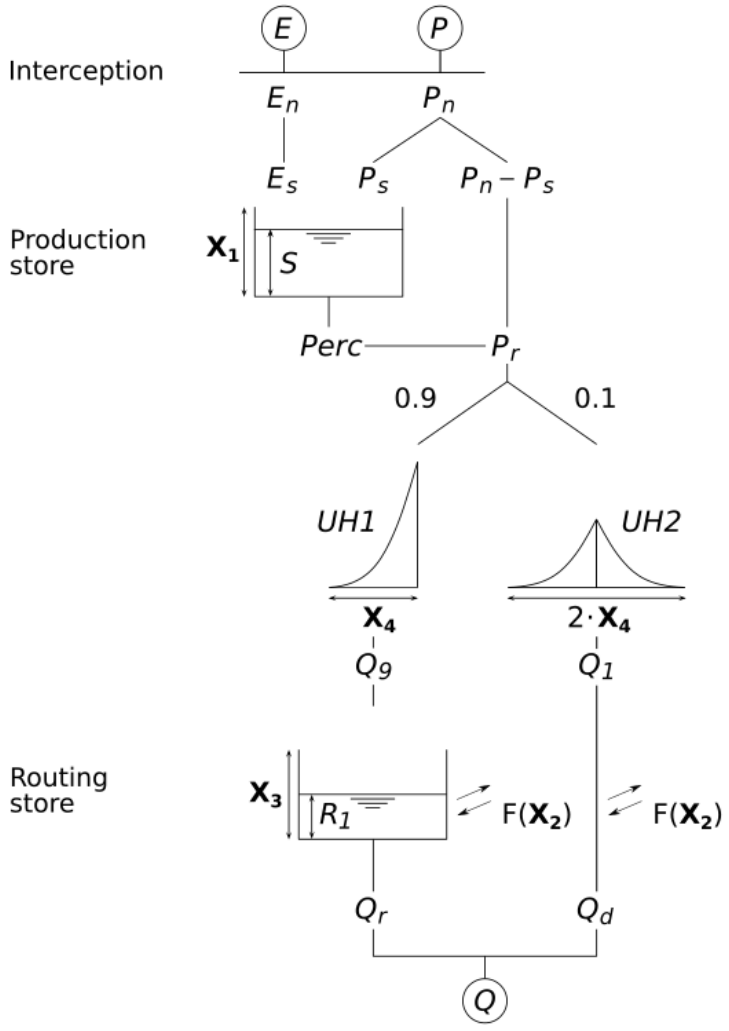

Figure 14: GR4J rainfall–runoff model diagram (Perrin,2003)

3.2.2.2 Hydrological model (GR5J) 's parameters

The GR5J model is a version of the GR4J model and is a rainfall-runoff model that focuses on soil moisture partitioning (Le Moine, 2008); (De Lavenne et al., 2016). This modification incorporated an additional parameter to consider the exchange of groundwater

between more complex catchments, which can take positive or negative (dimensionless) values. The latter parameter, X5, is a threshold for the exchange between precipitation catchment (dimensionless) and groundwater (Le Moine, 2008). The maximum production capacity, X1, and a maximum capacity conveyance shop, X3, are the two shop compartments fed by the time base of a unit hydrograph, X4, respectively. These various parameters are made up of five model parameters that can be calibrated (days). X4 unit hydrograph (days). The other two parameters, which measure the exchange capacity of the basins, are the inter-basin exchange threshold, X5, and the inter-basin exchange coefficient, X2 (mm/d). The balance of water is connected to X1 and X2 Table 8 and Figure 14. This study does not activate the snow degree day module (Valéry et al., 2014) because there is no snow in the application. Real positive values X1 and X3 are involved, as are positive and negative numbers for X2, and X4 is always greater than 0.5 (Perrin et al., 2003).

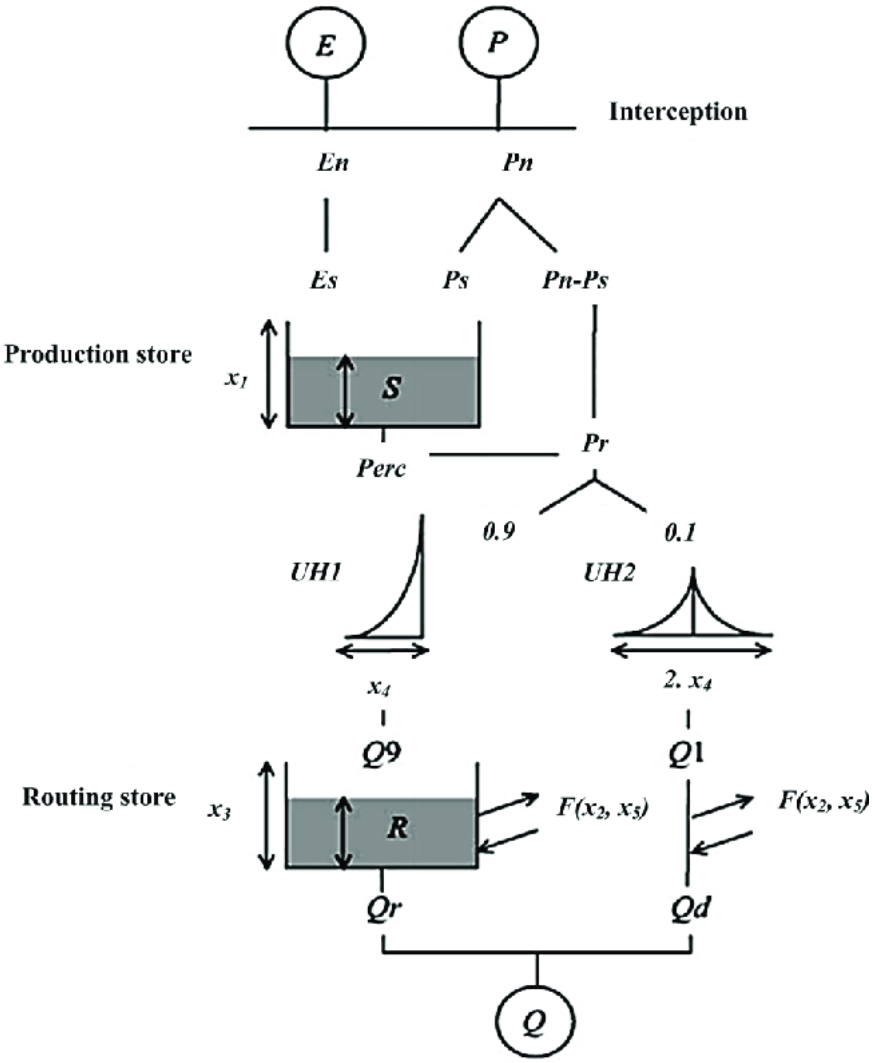

Figure 15: GR5J rainfall–runoff model diagram *(Le Moine, 2008)*

3.2.2.3 HEC HMS model

a. Description of the model

The Hydrologic Modeling System (HEC-HMS) is a hydrologic modeling software (Figure 16) that provides an integrated modeling tool for all hydrologic processes in dendritic watershed systems. It was created by the US Army Corps of Engineers Hydrologic Engineering Center (HEC). The HEC-HMS model is a physically based and theoretically semi-distributed model created to simulate rainfall-runoff processes in a wide range of geographic locations, from tiny urban and natural watershed runoffs to huge river basin water supply and flood hydrology. Huge activities related to hydrological research, such as losses, runoff transformation, open channel routing, analysis of meteorological data, rainfall-runoff simulation, and parameter estimate, are

simply handled by the system. It has gained popularity and been used in many hydrological studies due to its ability to reproduce runoff in both short- and long-term events, simplicity of operation, and use of well accepted methods. It is made up of various component processes for rainfall loss, direct runoff, and routing. It has been used to anticipate flooding, model hydrologic events, and evaluate runoff in many locations throughout the world (Knebl et al., 2005). The Attanagalu Oya River in Sri Lanka was calibrated by Halwatura and Najim (2013) using the HECHMS model. In the Chinese regions of Misai and Wan'an, HEC-HMS has also been used to predict flood disasters (Oleyiblo and Li, 2010). The HEC-HMS model was used by (Yusop et al., 2007) to simulate stormflow hydrographs for an oil palm watershed in Malaysia.

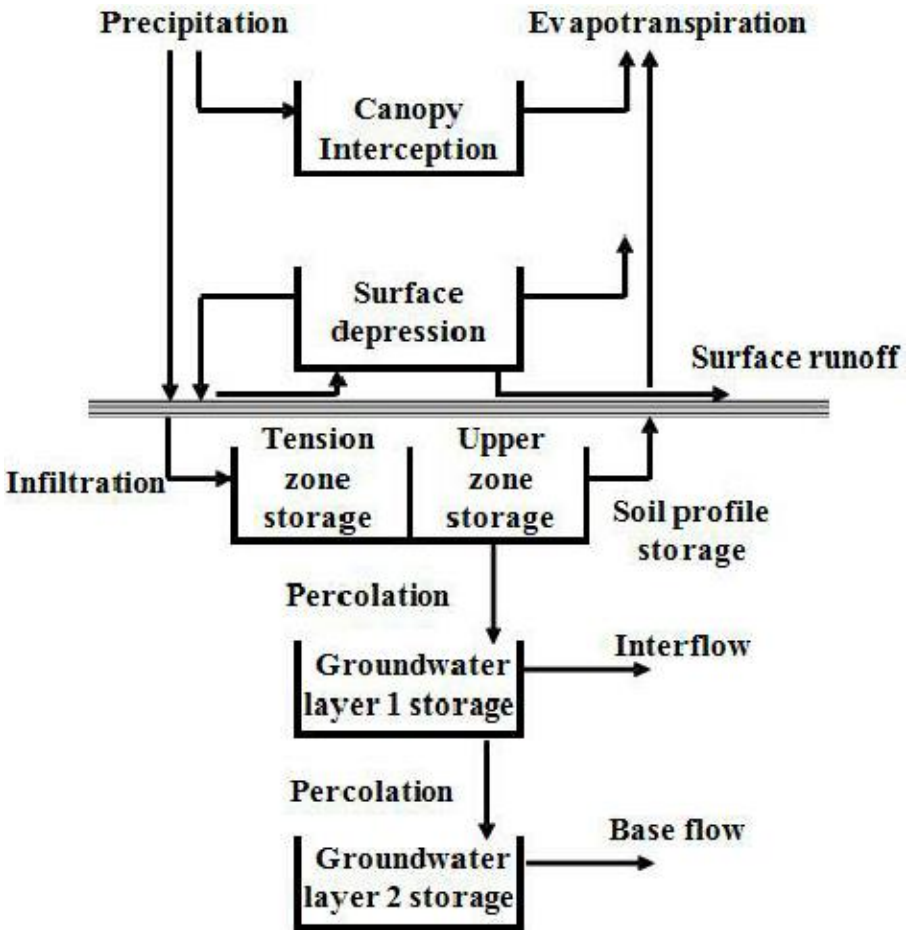

Figure 16:HEC-HMS model diagram

b. Curve number

The loss technique or the Soil Conservation Service-curve number (SCS-CN) approach is chosen to estimate the direct runoff from a specified or design rainfall, soil cover, land use, and antecedent moisture (Table 9). It is frequently employed in various settings and offers superior outcomes than the initial and continuous loss rate procedures (Sardoii et al., 2012). Its calculation is simplified by the fact that only a few variables need to be approximated using the following equation based on hydrologic soil types, land use, and slope maps:

$$S = \frac{25400 - 254.CN}{CN} \quad \textbf{(1)}$$

The curve number, or CN for short, is a transitional parameter that connects the maximum retention to watershed features. Based on the SCS tables and knowledge of the research area's soil type and land use, the CN values which ranged from 30 to 100 were approximated. The SCS Curve Number method is used to calculate precipitation losses that result from runoff and infiltration. Based on an empirically developed link between location, soil type, land use, antecedent moisture conditions, and runoff, the approach determines the effective precipitation of a hydrological event (Sardoii et al., 2012).

$$P_e = \frac{(P - 0,2.S)^2}{P + 0,8.S} \quad \textbf{(2)}$$

where P_e stands for the excess of accumulated precipitation at time t, P for the depth of accumulated precipitation at time t, and S for the possible maximum retention. The Technical Reference Handbook advises estimating the initial abstraction (Ia) at a fixed 20% of the maximum potential retention (S).

c. Transform method

The SCS Unit Hydrograph, which calculates peak discharge and peak time, is used to mimic the process of direct runoff of excess precipitation on the watershed:

$$U_p = C\frac{A}{T_p} \quad (3)$$

$$T_p = \frac{\Delta t}{2} + t_{lag}$$

where: T_P = time of peak; t = duration of excess precipitation; t_{lag} = the basin lag, equal to 60% of the time of concentration; U_P = UH peak; A = watershed area; C = conversion constant (2.08 in SI); t = excess precipitation duration (Tc).

Table 9: Parameters used for calibration and validation of HEC HMS model

Elements	**Components**	**Data / method**
Model type	Basin model	DEM for watershed delineation
Hydrological process	Precipitation (specified hyetograph)	Averaged precipitation using kriging method
	Potential evaporation	Mean temperature using Hamon method
	Direct runoff	Soil Conservation Service Unit
	Base flow	Hydrograph (SCS-UH)
		Recession constant
	Loss rate	Soil Conservation Service method using Curve Number (SCS-CN)
		Soil moisture accounting method (SMA
	Canopy interception Surface method	Simple canopy
		Simple surface

3.3 Methods

3.3.1 Analysis of trends in hydrological time series

Trend analysis is computed at annual and monthly scales on each of the eleven (11) indices as well as the four (4) rainfall indices and seven (7) discharge indices for the observed and future data. Interannual fluctuations, and seasonal variations are eliminated by using a non-recurrent low-pass Hanning filter of order 2. Trends are detected using the Modified Mann–Kendall Test (MMK), and homogeneity detection is carried out by the Standard Normal Homogeneity Test (SNHT) at a 0.05 level of confidence.

3.3.1.1 Inter-annual variation on historical data

According to Dorsouma et al. 2008, climate variability refers to the natural intra- and inter-annual variation in climate that significantly modifies the climate. Historical data is influenced by this variability, which often compromises the results of some studies. Thus, for a good inventory of time series and a better observation of interannual fluctuations, seasonal variations are often eliminated by using a non-recurrent low-pass Hanning filter of order 2 (weighted moving average). This method consists in filtering the data to perform data averaging seasonal variations in order to better visualise the periods of deficit and surplus on an interannual scale. This exercise was performed using the equations recommended by (Tyson et al., 1975) and used by (Anouma et al., 2021); (Yao, 2015); (Amichiatchi et al., 2023) with good results. According to this method, each term in the series is calculated by the equation:

$$X_t = 0.06x_{t-2} + 0.25x_{t-1} + 0.38x_t + 0.25x_{t+1} + 0.06x_{t+2} \quad (4)$$

With:

x_{t-2} and x_{t-1} totals of the observed discharges of two terms immediately preceding the term x_t; x_{t+2} and x_{t+1} totals of the observed discharges of two terms immediately following the term x_t.

The weighted discharge totals of the first two (X_1 and X_2) and the last two (X_{n-1} and X_{n-2}) terms of the series are calculated using equations 3, 4, 5,6 (n being the size from the series):

$$\boldsymbol{X_1 = 0.54x_1 + 0.46x_2} \quad \textbf{(5)}$$

$$X_2 = 0.25x_1 + 0.50x_2 + 0.25x_3 \quad (6)$$

$$X_{n-1} = 0.25x_{n-2} + 0.50x_{n-1} + 0.25x_n \quad (7)$$

$$X_n = 0.54x_n + 0.46x_{n-1} \quad (8)$$

$$\boldsymbol{Y_t = \frac{(X_t - m)}{\sigma}} \quad \textbf{(9)}$$

Y_t : The average discharge
X_t: total annual weighted flows
m: is the mean of the series of weighted means and σ the standard deviation of the series of weighted moving averages.

3.3.1.2 Modified Mann-Kendall Test

The trends in the hydrometric data series were evaluated using the modified Mann–Kendall test (Hamed et al., 1998), which is a non-parametric test used in several studies. The choice of this test was justified by the fact that it takes into account the effect of autocorrelation in the data. Indeed, the presence of autocorrelation in the data affects the power of the classical Mann–Kendall statistical test by introducing outliers, and the effect of positive autocorrelation increases the risk of rejecting the type 1 error (overestimated trends), while the effect of negative autocorrelation modifies the risk of rejecting the type 1 error (underestimated trends). Therefore, an additional contribution to the Mann–Kendall (MK) test was made to take into account this autocorrelation phenomenon. The principle is based on a modification of the *(S)* statistic in the MK test. Based on this principle, a modified version of the original MK test was proposed (Hamed et al., 1998), in which the variance of the test statistic is modified to account for autocorrelation in the series and the statistics are adjusted to adjust the variance as follows:

$$Var(S) = \frac{1}{18}(n(n-1)(2n+5))\frac{n}{ns^*} \quad (10)$$

where *ns** is the effective number of observations to account for autocorrelation in the data.

$$\frac{n}{ns^*} = 1 + \frac{2}{n(n-1)(n-2)}\sum_{s=1}^{m}(n-s) \quad (11)$$

The modified Mann–Kendall trend test was implemented using the package “modifiedmk” (Sandeep et al.,2021) on R software, with the null hypothesis (Ho) corresponding to "no trend" and the alternative hypothesis ($H1$) corresponding to the presence of a trend in the series at a significance level of 5%.

3.3.2 Standard Normal Homogeneity Test (SNHT)

The detection of breakpoints was performed by applying the standard normal homogeneity test (SNHT), which is a non-parametric test used by several authors (Ilori et al., 2020); (Jenifer et al., 2021). This test is sensitive to the detection of breaks at the beginning and end of the series ; it is also insensitive to possible missing values and is simple with good relative performance compared to the other tests, which explains the choice of this method for the detection of breaks. The application of the SNHT test is based on the following equation:

$$Q_i = Y_i - \frac{\sum_{j=1}^{k} \rho_j^2 x_{ij}\, \bar{y}/\bar{x}}{\sum_{j=1}^{k} \rho_j^2} \qquad (12)$$

$$1 \leq i \leq n \;\; et \; 1 \leq j \leq k$$

The value of year i in the base series is represented by Y_i, whereas X_{ij} denotes the observation *i* in the reference series *j*. The correlation coefficient between the base series and the reference series j is denoted by ρ_j. This test was computed on R software using the package trend Thorsten,2020 "*snh.test*" under the null hypothesis $H_{0,}$ "no change point", while the alternative hypothesis H1 is the "presence of a change point" defined at a significance level of 5%.

3.3.3 Assessment of the performance of the hydrological model.

3.3.3.1 Simulation process

a. Calibration

Because some parameters are often impossible to measure or evaluate, calibration in modeling is vital for achieving excellent findings and understanding hydrological behavior. Thus, this exercise aims to find the values that best imitate a set of reference data based on a predetermined criterion without affecting the previously calibrated parameters (Robinson et al., 2002). This approach involves optimizing model parameters using an iterative numerical algorithm based on

several model quality criteria while underestimating the error between simulated and observed flows. This calibration can be automatic for better automatic parameter adjustment or manual using estimated parameters to obtain a good match between the simulated and observed data, with observation periods ranging from 2 years to 10 years depending on the objective, and a start-up period of 12 months or 1 year for the quantification of the error in the form of a numerical criterion. For example, concerning the GR4J and GR5J, the calibration period was Agneby (1980-1990), Bagoue (1981-1989); Baya (1986-1992); Lobo (2006-2010) and N'zo (1983-1988). Calibration was done differently for each basin in our analysis, with various calibration years from one station to the next.

b. Validation

Validation is the process of proving the model's accuracy. It verifies that the calibrated model perfectly reproduces the reference data that were not used during calibration, allowing us to assess the calibration's robustness and test the simulated flows with the calibration parameters over a validation period independent of the calibration period (Kleme, 1986). This validation is performed utilizing observation data from the same time period but from different decades. The model parameters for each calibration time step are evaluated using data from the same time step but from a different decade to check changes in the basin's characteristics based on a hydrological model. Validation was performed specifically for each basin in our study, with validation years varying from station to station.

3.3.3.2 Performance evaluation

Hydrological models are numerical tools that simulate the relationship between rainfall and flow at the catchment size in a laboratory, typically taking into account the field's hydrogeological realities. They provide a set of equations or rules that can be used to describe or explain an event in a reproducible and simulable manner. As a result, it is critical to assess the performance of these models in order to detect any incorrect predictions, biases, or increasing inconsistencies in the data. And the majority of measurements of model success are based on comparing model predictions to known values of the dependent variable in a data set. Model performance evaluation is a critical stage in both calibration and validation. This step evaluates the model's performance using objective evaluation functions. As a result, the quality of the calibration or validation during the reference period is often assessed using the value of an

objective function as a criterion. It gives a global measure of the difference between a sequence of measured and simulated values for a set of preset parameters. The Nash-Sutcliffe criterion (Nash, Sutcliffe, 1970) is the most often used criterion, with values ranging from 0 to 1 (very good 0.75<NSE<1.00; good 0.65<NSE<0.75; satisfactory 0.50<NSE<0.65; and poor NSE>0.50) (Aye et al., 2017). The formula used to calculate this criterion is:

$$NSE = 1 - \frac{\sum_{i=1}^{n}(OBS_i - SIM_i)^2}{\sum_{i=1}^{n}(OBS_i - \overline{OBS})^2} \quad (13)$$

where OBSi is the observation value and SIMi is the forecast value and OBSbar is average of observation values. Kling Gupta Efficiency (KGE), an alternate approach derived from the breakdown of the Nash-Sutcliffe efficiency (NSE), is used to avoid issues such as high sensitivity to extreme values. And The values range from -Inf to 1, with the one closest to 1 being the best. The formula used to calculate this criterion is:

$$KEG = 1 - \sqrt{(r-1)^2 + (\frac{\sigma sim}{\sigma obs} - 1)^2 + (\frac{\mu sim}{\mu obs} - 1)^2} \quad (14)$$

where σobs is the standard deviation in observations, σsim the standard deviation in simulations, μsim the simulation mean, and μobs the observation mean.

The percentage of bias (PBIAS) can be used to assess bias by measuring the average tendency of the simulated data to be bigger or smaller than their observed counterparts. PBIAS should be set to 0 for a precise model simulation, and low magnitude values suggest this. Negative numbers represent overestimation bias, and positive numbers represent underestimating

$$\text{Percent of bias (PBIAS)} = \frac{\sum_{i=1}^{n}[s_i - o_i]}{\sum_{i=1}^{n} o_i} * 100 \quad (15)$$

bias (Golmohammadi et al., 2014). The formula used to calculate this criterion is:

3.3.3.3- Estimation du bilan hydrologiques

The balance allows precipitated water to be distributed over the hydrological cycle's several terms. It focuses on the four major components of the water cycle : rainfall (P), actual

evapotranspiration (ETR), runoff (Q), and infiltration (I). This balance conforms to the equation below:

$$P = Q + ETR + I \quad (16)$$

The infiltrated water level (I) is deduced from equation 16

$$I = P - (ETR + I) \quad (17)$$

And AET is obtained by this follow equation:

$$ETR = (EPT - E_n) + E_s \quad (18)$$

With En: net evapotranspiration and Es: the amount of evaporation removed from the production reservoir.

3.3.4 Assessing climate change impact

3.3.4.1 Impact of land use change on extreme

Satellite image pre-processing, which consists of the two primary sub-operations of radiometric correction and geometric correction, allowing the quality of the image to be improved before the information is recovered, was one of the many activities necessary to process the gathered images. In our investigation, the different photos were merely subjected to the radiometric and atmospheric corrections by Envi 5.3, the mosaic, and then the extraction of the study region using the Envi 4.7 programs. Comparing satellite photos to reality on the ground is made possible through the identification of land cover classes, which is a well-structured intellectual endeavor. Thus, a group of surfaces on an image that shares similar properties (spectral, morphological, and textural) highlight a physical or biological cover of the land surface and distinguish between a so-called "artificial" land cover like buildings or ground cover and a natural land cover like trees, shrubs, or grassland. These observations led us to establish five categories of land use in our situation, which are Forest type: dense containing large areas of dense forest or natural reserves; Less dense, degraded forests make up the light forest class. Fallow land class, which includes perennial crops represented by shrubby plantations; Settlements, rocky outcrops, and barren soil are examples of the habitat class. Investigation of land cover dynamics was carried out in this exercise using the most widely used method

worldwide (Näschen et al., 2019):the pixel-based maximum likelihood integer classification method in Envi software. Then, a confusion matrix of the statistical relationship was created based on the training sites, allowing for the evaluation of the satellite pictures' ability to distinguish between the various classes of retained jobs. This matrix enables the determination of the overall accuracy and offers a quantitative indication of the sample quality and class reparability. Lastly, the reliability of the classification findings about the reference data is assessed by the Kappa coefficient, which ranges from 0 to 1.

3.3.4.2 Investigation of dynamics occupation

a. Determination of rate of change

Following the examination of the dynamics of occupation, a comparison exercise was conducted with the goal of statistically quantifying the changes acquired using the rate of change, which is a factor allowing to analyze the modifications that have occurred. So, a rate of change of positive values suggests a "progression" of the class, a rate of change of negative values shows a "regression" of the class, and values near zero indicate that the class is generally "stable". Using the following equation, this rate is calculated:

$$T_c = \frac{(S_2 - S_1)}{S_1} * 100 \quad (16)$$

With S_1 the area of an area unit class at date t_1; S_2 the area of the same area unit class at date t_2

b. Relationship between extreme indices and vegetation indices

Vegetation indices are widely used to identify and monitor vegetation dynamics, but also to estimate certain biophysical parameters characteristic of plant cover, such as biomass, leaf area index, fraction of photo synthetically active radiation, etc. (Checkcheck et al., 2019). Normalized Difference Vegetation Index NDVI (Rouse and Haas, 1973; Tucker, 1979) is a standard vegetation index in the study of vegetation. This index is calculated using the red (R) and near infrared (NIR) electromagnetic bands (Table 10). The result is normalized between -1 (other than vegetation such as water) and 1 (dynamic vegetation). The formula is as follows:

(17)

$$NDVI = \frac{Nir - R}{\text{Nir} + \text{R}}$$

This formula varies according to the type of Landsat used. For the purposes of our study, our images come from Landsat 8,7,5 (8 for 2018, 7 for 2000, 5 for 1985). Depending on the type of Landsat, near infrared (NIR) and red (R) correspond to.

Table 10: Characteristics of the images used

	NIR	R
LANDSAT 8	BANDS 5	BANDS 4
LANDSAT 7	BANDS 4	BANDS 3
LANDSAT 5	BANDS 4	BANDS 3

Pearson correlation analysis was used to assess the connections between the vegetation and extreme hydro-climate indices. A correlation coefficient above zero denotes a positive association, whereas one below zero denotes a negative correlation. A higher absolute value of the correlation coefficient denotes a closer association between the two variables. The significance of the correlation coefficient between the two variables was tested using the *P-value< 0.05* indicates a significant correlation coefficient at the 95% confidence level (Chang et al., 2022).

The formula for calculating this correlation coefficient is:

$$r_p = \frac{\sum_{i=1}^{N}(x_i - x) * (y_i - y)}{\sqrt{\sum_{i=1}^{N}(x_i - x)^2} * \sqrt{\sum_{i=1}^{N}(y_i - y)^2}} \quad (18)$$

Where: xi and yi are the respective data for the rainfall and NDVI variables;

X is the mean rainfall and is equal to : $\frac{1}{N} * \sum_{i=1}^{N} x_i$

Y Is the mean NDVI and is equal to: $\frac{1}{N} * \sum_{i=1}^{N} y_i$

c. Dynamics of vegetation cover on runoff

The water retention capacity index for each land use class is calculated to assess the impact of vegetation cover dynamics on runoff (Cecchi et al., 2009; Soro et al., 2014). High values (>100) correspond to 'wild' (uncontrolled) basins with high vegetation cover and high water retention capacity, and therefore not conducive to increased runoff, while low values correspond to entropized or even degraded basins with low retention capacity, and therefore, unlike the above, conducive to high runoff (Seydou et al., 2018). The formula for calculating this water retention capacity index and the weighting coefficient (Table 11) are:

$$C_r = \sum_i P_i * a_i \quad (19)$$

With P_i: percentage of the surface area of the study area occupied by land use class *i* land use class *i*;

a_i: weighting coefficient indicating the effective water retention capacity of land use class *i*

Table 11: Values of the weighting coefficient

Land use classes	**ai**
Water body	1
Habitat/Bare	1
Primary forest	2
Sparse forest	2
Crops land	1

3.3.4.2 Impact on hydro-climate extreme

a. Climate model bias correction and performance evaluation

Climate projection data are corrected using the distribution mapping bias-correction technique, which helps to adjust the simulated RCMs' climate values to fall in line with the

observed (Switanek et al., 2017); (McGinnis et al.,2015). This method has been widely used in the bias correction of RCMs (Dobler et al., 2008); (Piani et al., 2010) and is capable of correcting other statistical properties with a better outcome compared to other bias correction methods such as the delta change method, linear scaling, and empirical quantile mapping technique. The bias-correction method adjusts for errors in the shape of the distribution of the modelled data with reference to the observed distribution, and the change factor is calculated to be used for the modelled values adjustment. A statistical method for evaluation of model performance that includes the mean absolute error (MAE) and percent of bias (PBIAS) was used to assess the effectiveness of the RCM using the following equations:

$$MAE = \frac{\sum_{i=1}^{n} |y_{i-x_i}|}{n} \quad (20)$$

Where MAE=Mean Absolute Error, y_i is prediction; x_i is the true value and n the total number of the data.

$$\text{Percent of bias (PBIAS)} = \frac{\sum_{i=1}^{n} [s_i - o_i]}{\sum_{i=1}^{n} o_i} x100 \quad (21)$$

A PBIAS value of 0 indicates that there is no systematic difference between the amounts simulated and observed, whereas a large PBIAS value indicates that the RCM rainfall amount is significantly different from the one that was observed. Overestimation of the observed variables is indicated by a positive PBIAS, while underestimation is indicated by a negative PBIAS. The range for the statistical measures MAE = 0 to ∞, with lower values showing better performance, showed how well the RCM simulates the observed rainfall.

3.3.4.3 Impact on discharge simulation for future period

After evaluating the performance of the hydrological models, the hydrological model with the best performance will be used for the simulation of future flows. After correcting for biases in the data from the future climate models, these will be used as input data for the hydrological model chosen for the simulation of future flows. Thus, the ensemble mean of the

different climate models will be used as input against these input parameters for calibration and validation under the two study scenarios and the changes in simulated discharge over the period 2020-2050 will be analysed with the modified Mann-Kendall test to understand the behavior of hydrological extremes over the different study basins (Larbi et al.,2023).

Conclusion

The aim of this chapter was to construct a methodological framework. First, it was necessary to establish the data that would be used throughout this study, namely flow and evapotranspiration, which are daily data for the periods 1970-2017 from six hydrometric stations, and rainfall, with daily rainfall from 21 rain gauge stations spread across the catchment areas, obtained from the database of the Airport, Aeronautical and Meteorological Exploitation and Development Corporation (SODEXAM) of Côte d'Ivoire for the years 1970 to 2017, satellite images collected on the website http : //earthexplorer. usgs.gov/, and NDVI data from the Landsat/5/7/8 satellite remote sensing dataset, which were made available by climate engine.org (https://app.climateengine.org/climateEngine#). Secondly, the hardware used in this study includes the R package "qmap" to perform a bias reduction technique and the hydrological models (GR4J, GR5J, and HEC-HMS) that will be used for the modeling part. Finally, the methodologies that will be used for this work include the extraction of extreme indices with four precipitation extremes (Pmaxan, R95p, Rx5 days, and CDD), three flood indices (Qmaxan, 5 days, and VCX30), and four low-water levels (Qminan, QMNA, VN7, and WFD), the application of homogeneity (SNHT) and trend (MMK) tests, hydrological simulation, and the methods used to assess the effect of climate.

CHAPTER 4 : CHANGE IN HYDRO-CLIMATE EXTREMES

For the observed data, chapter 4 presents the results of inter-annual variation, break point, and trend analysis on the extreme indices over the climatic zone on discharge and rainfall. The inter-annual fluctuation result for discharge and rainfall data can be found in Section 4.1. Section 4.2 summarized the break point result on extreme discharge and rainfall, and Section 4.3 featured the trend analysis result. The extreme discharge indices on monthly and annual scales, as well as the rainfall over each climatic zone, are computed in this chapter.

4.1 Inter-annual variation

The results of applying Hanning's second-order low-pass filter to the recorded rainfall and discharge are shown in Figure 17. It demonstrates a significant inter-annual variation in rainfall and discharges across the country's climatic zones. All of the stations analysed (rainfall or discharge) showed an alternating of wet (surplus zone) and dry (deficit zone) seasons. Watersheds in N'zo since 1993 and Bagoue since 1990 are more vulnerable to deficit years, whereas watersheds in Baya, Agneby, Lobo, and N'zo are more vulnerable to surplus years. Rainfall data in the Lobo and Baya watersheds fluctuates over time. In terms of discharge data, the Lobo at Nibehibe and Baya watersheds are more vulnerable to deficiency years, whilst the Bagoue and N'zo watersheds are more vulnerable to surplus years. Data from the Agneby watershed and the Lobo at the Loboville station show alternate variations throughout time.

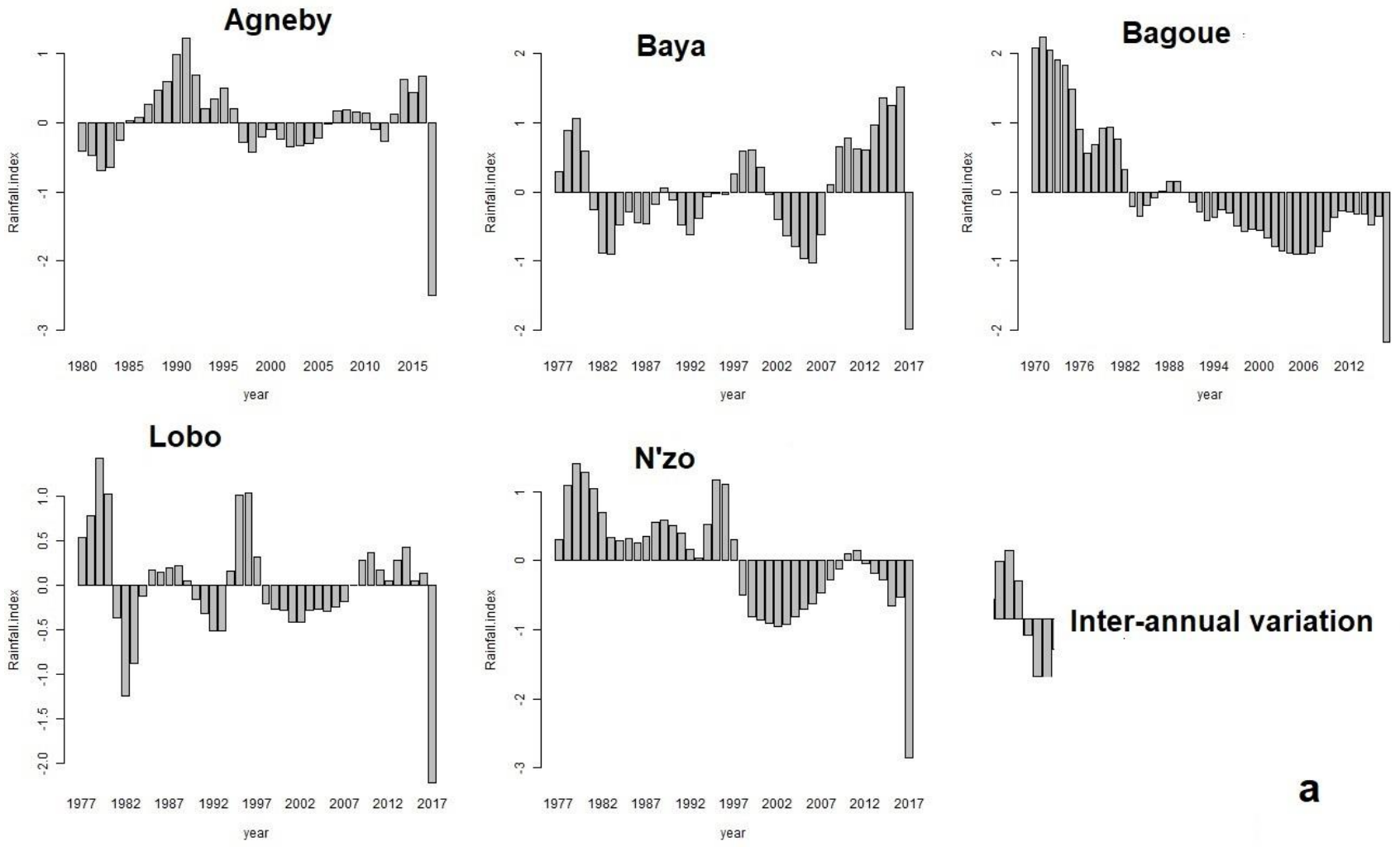
Agneby
Baya
Bagoue
Lobo
N'zo
Inter-annual variation
Rainfall.index
year
a

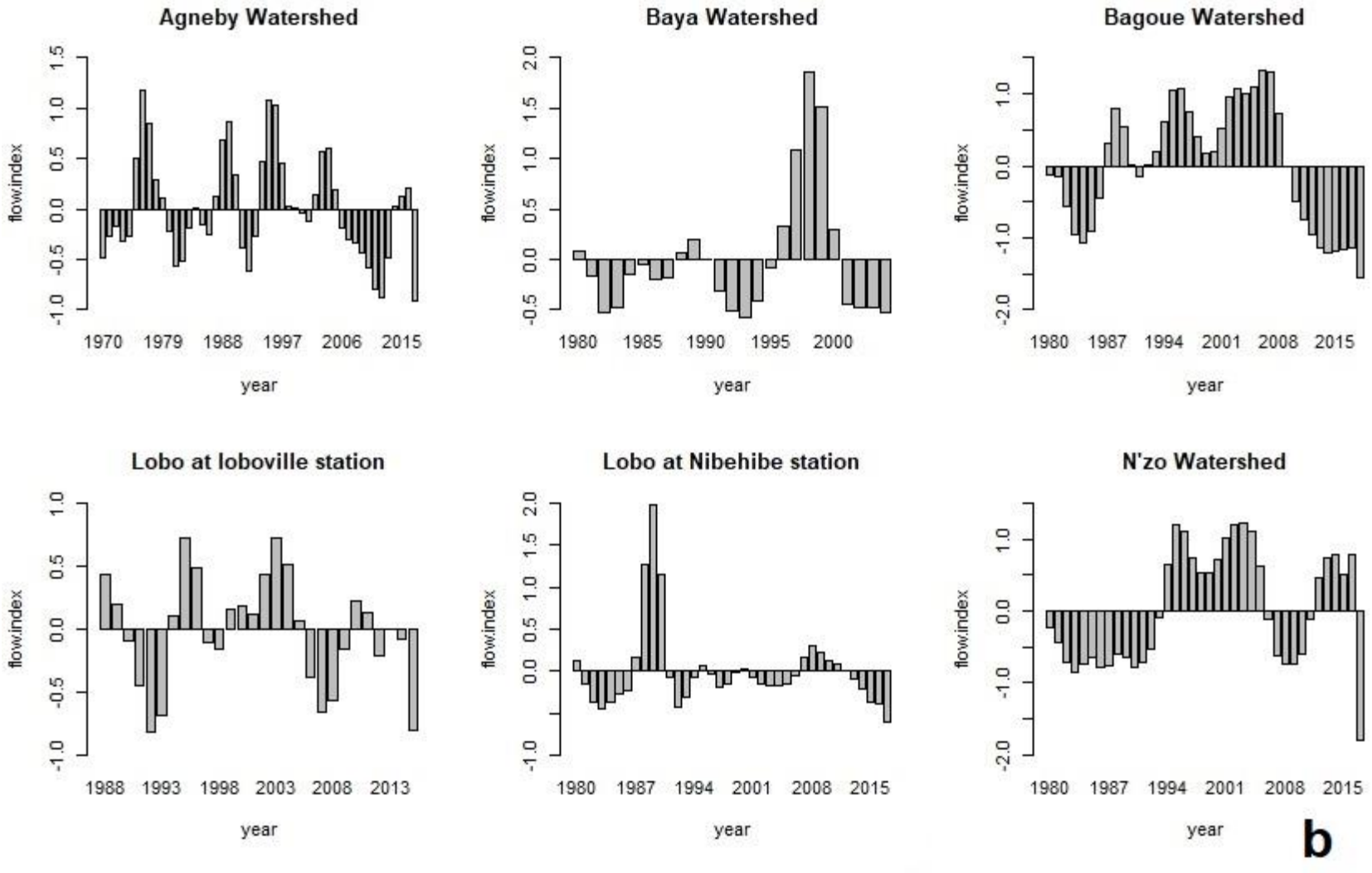

Figure 17 : Interannual variations in rainfall (a) and discharge (b) data in each watershed using the non-recursive low-pass Hanning filter of order

4.2 Break point

The results of the break point analysis of recorded rainfall and discharge are coupled with other extreme indices at a level of 0.05 in this section. Regarding the rainfall data, the maximum annual rainfall (Pmaxan), consecutive dry days (CDD), maximum 5-day rainfall (Rx5days), and very wet day (R95p) may be viewed for all watersheds. There will be seven (7) discharge indices : 5-day maximum flow (QX5-days), peak discharge (Qmaxan), maximum monthly discharge (VCX30), minimum annual discharges (Qminan), average monthly discharges (QMNA), daily discharge rate (VCN7), and low water characteristic (WFD). Whether it was rainfall or outflow, all of the indices show a significant break period across each climatic zone for each watershed.

4.2.1 Break point on rainfall data

4.2.1.1 Climatic zone I

The results of the break point study for extreme rainfall are shown in Table 12 and Figure 18. Figure 18 shows the breaking year of each indices, and it can be seen that the CDD indice has a substantial breakpoint period with the majority of the stations, with the break year between 1973 and 1983. Four stations are affected by distinct breaking durations for R95p indices. Pmaxan and Rx5days exhibited one station per indie, which was influenced by Akoupe in 1982 and M'batto in 1978, respectively. The outcome of the important breakpoint period is shown in Figure below.

Table 12: Break point detection related rainfall indices in climatic zone I for the period 1980-2017. * indicates a significant break while '–'indicate non a significant break.

			Rainfall indices			
Watersheds	**Stations**	**Periods**	**Pmaxan**	**Rx5days**	**CDD**	**R95p**
Agneby	Agboville	1972-2017	-	-	1975*	-
	Akoupe	1980-2017	1982*	-	1983*	1983*
	Arrah	1976-2017	-	-	1979*	1978*
	Bongouanou	1970-2017	-	-	1973*	1973*
	Cechi	1970-2017	-	-	1973*	1972*
	Dabou	1970-2017	-	-	1973*	-

	Mbatto	1976-2017	-	1978*	1979*	-
	Sikensi	1976-2017	-	-	1979*	-

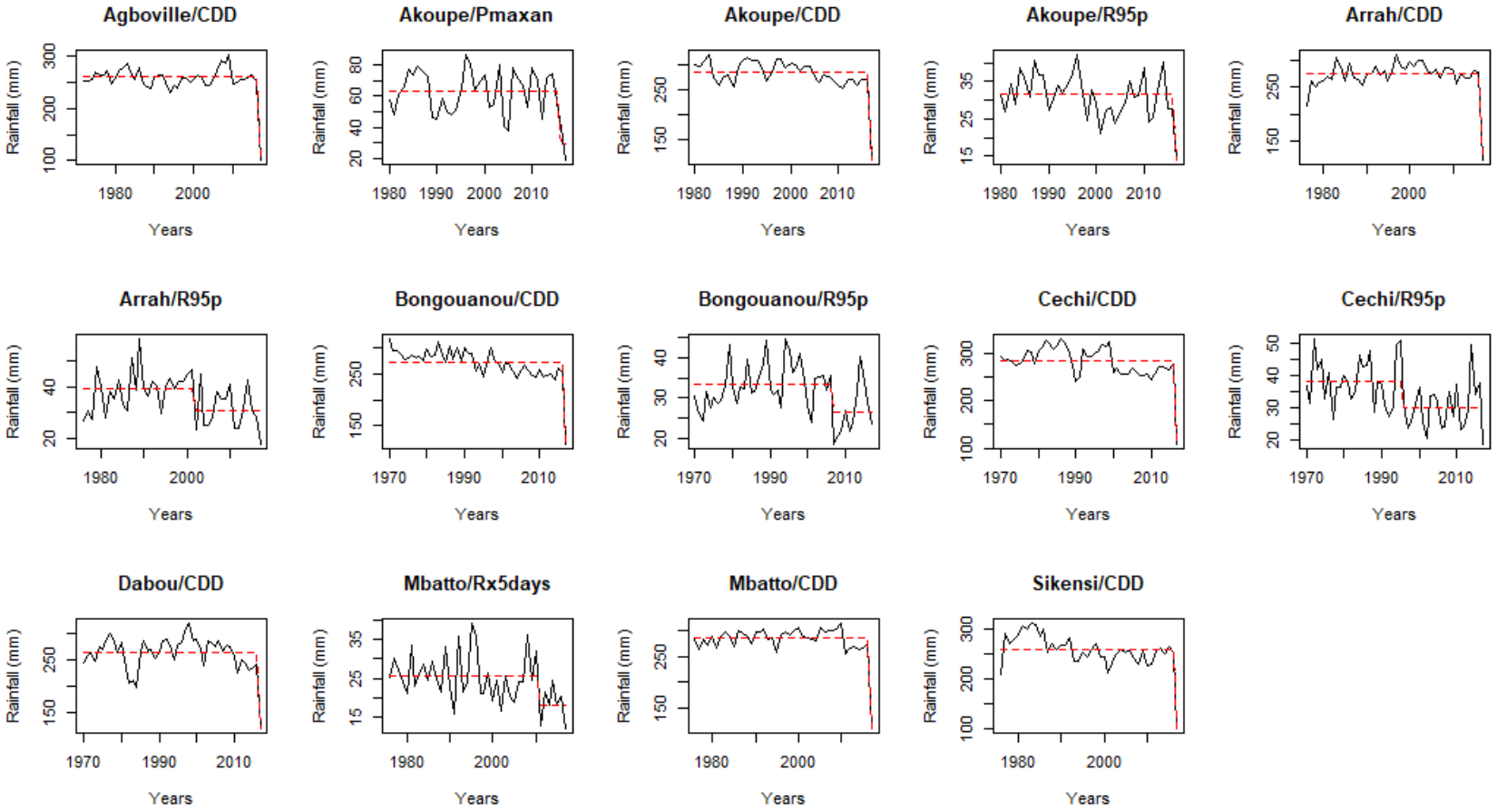

Figure 18: Evolution inter-annual of Pmaxan, Rx5days, CDD and R95p indices under climatic zone I

4.2.1.2 Climatic zone II

The results of the break point period study on extreme rainfall indices are shown in Table 13 and Figure 19. During the examined period, all indices, as well as Pmaxan Rx5 days, CDD, and R95p, were influenced, and the mean break period for all stations was between 1970 and 1980.Figure depicts the results of the significant breakpoint periods.

Table 13: Break point detection related to rainfall indices in climatic zone II for the period 1980-2017. * indicates a significant break while '–'indicate no significant break.

			Rainfall indices			
Watersheds	**Stations**	**Periods**	**Pmaxan**	**Rx5days**	**CDD**	**R95p**
Baya	Bondoukou	1970-2017	1972*	1972*	1972*	1972*
	Kun-Fao	1977-2017	-	-	-	-
	Tanda	1976-2017	-	1978*	1977*	1978*
Lobo	Daloa	1920-2017	1926*	1926*	1928*	1926*
	Issia	1977-2017	-	-	1980*	1977*
	Pelezi	1976-2017	1976*	1976*	1979*	1976*
	Vavoua	1953-2017	1956*	1956*	1958*	1956*

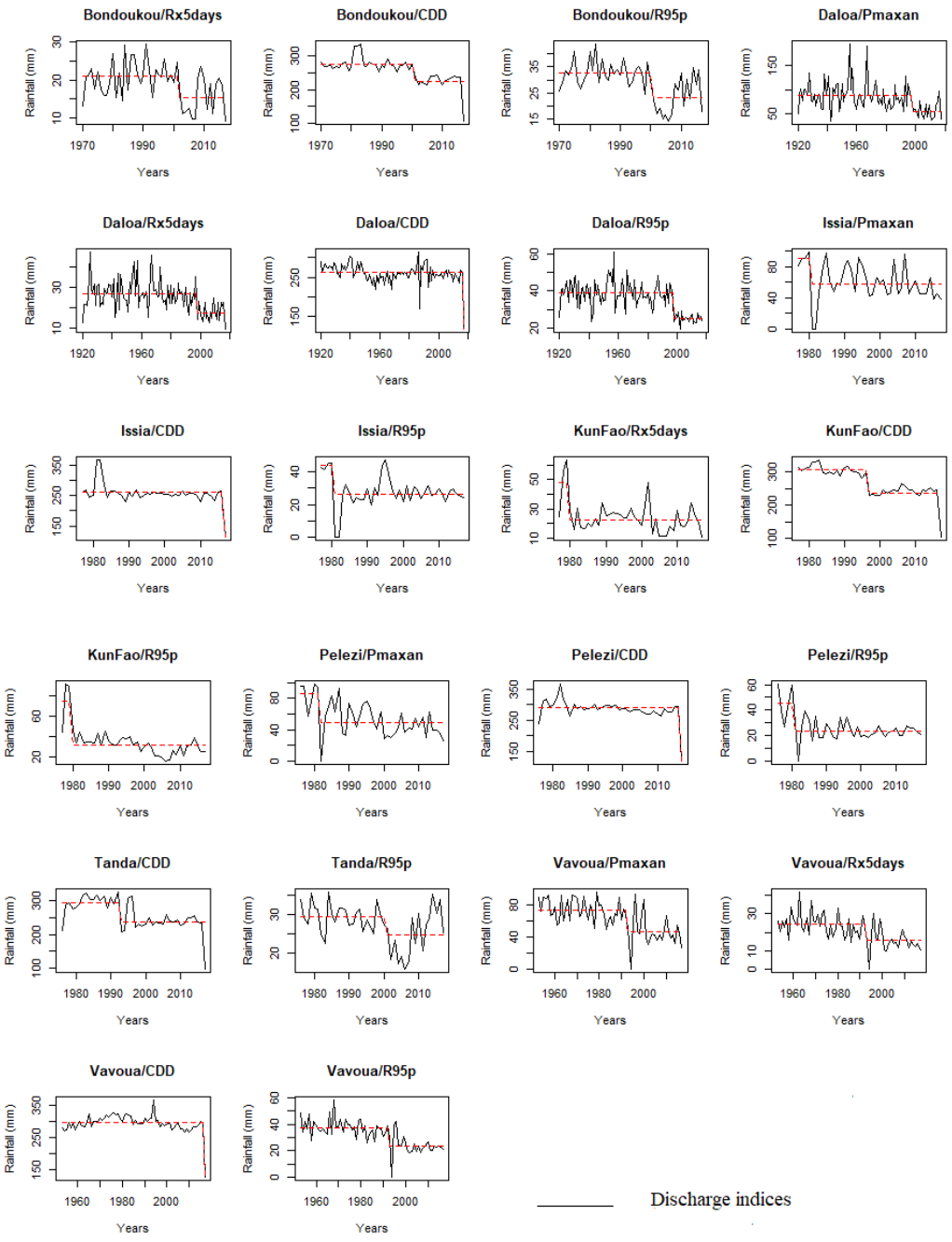

Figure 19: Evolution inter-annual of Pmaxan, Rx5days, CDD and R95p indices under climatic zone II

4.2.1.3 Climatic zone III

Table 14 and Figure 20 show the results of the break point analysis on extreme rainfall indices. For the results, except for the CDD indices, all the indices were impacted during the study period. The breaking period for the stations Boundiali and Madinani was found between the years 1985 and 1998, and the significant break point period is plotted in Figure .

Table 14: Break point detection related to rainfall indices in climatic zone III for the period 1980-2017. * indicates a significant break while '–'indicate no significant break.

		Rainfall indices				
Watersheds	**Stations**	**Periods**	**Pmaxan**	**Rx5days**	**CDD**	**R95p**
Bagoue	Boundiali	1922-2017	-	1995*	-	1998*
	Madinani	1962-2017	1985*	1983*	-	1983*

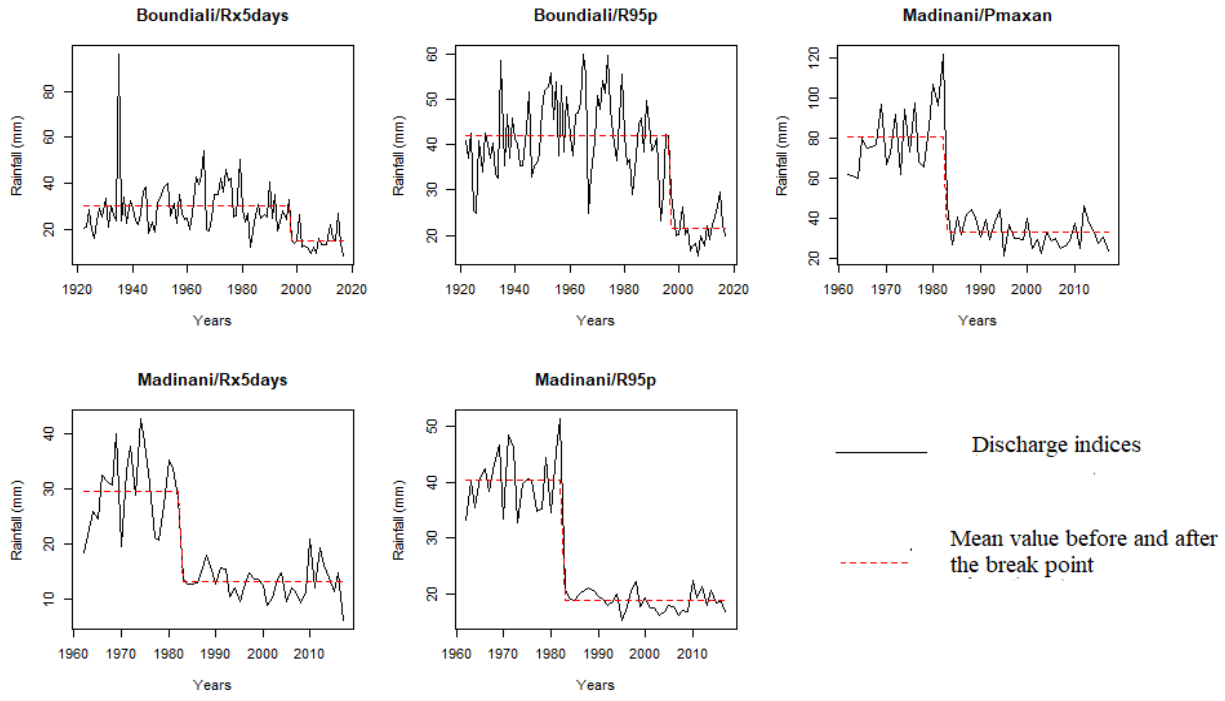

Figure 20: Evolution inter-annual of Pmaxan, Rx5days, CDD and R95p indices under climatic zone III

4.2.1.4 Climatic zone IV

Table 15 and Figure 21 show the results of the break point analysis on extreme rainfall indices, with a great break point period for most of the indices on three important stations affected, such as Bangolo, Biankouma, and Man (Table 15). It is showing that only one station, Zeregbo, did not show a break point. For these other stations, the breaking point period was found between 1976 and 2016 under each index, and the result of the significant break point analysis is summarized in Figure 21 below.

Table 15: Break point detection related to rainfall indices in climatic zone IV for the period 1980-2017. * indicates an significant break while '–'indicate not significant break.

			Rainfall indices			
Watersheds	**Stations**	**Periods**	**Pmaxan**	**Rx5days**	**CDD**	**R95p**
N'zo	Bangolo	1976-2017	1976*	1976*	1979*	1976*
	Biankouma	1976-2017	1998*	1983*	2015*	1998*
	Man	1923-2017	1997*	1996*	2016*	1996*
	Zeregbo	1977-2017	-	-	-	-

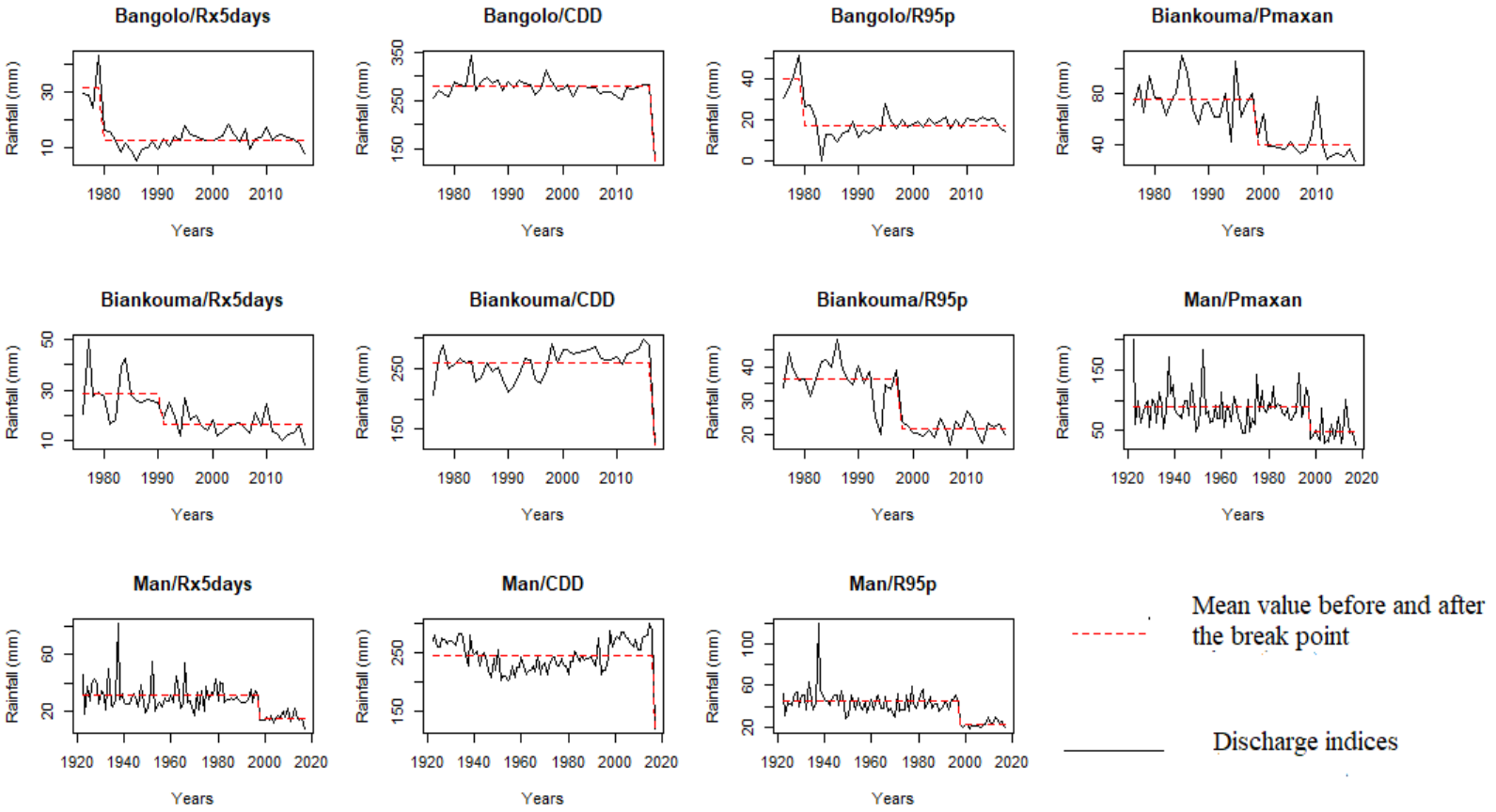

Figure 21: Evolution inter-annual of Pmaxan, Rx5days, CDD and R95p indices under climatic zone IV

4.2.2 Break point on discharge data

4.2.2.1 Climatic zone I

Table 16 and Figure 22 summarize the SNHT test result for the changing point in the extreme discharge data. Change points in the flood indices at the Agneby watershed for the Qmaxan and VCX30 indices were found in 2013 and 2014. Only Qminan and WDF demonstrated a considerable break phase in the low discharge indices in 2006 and 2003, respectively.

Table 16: Break point detection related to flood and low discharge indices in some watersheds in climatic zone I for the period 1980-2017.

			Flood indices			**Low discharge indices**			
Watersh	**Period**	Stations	Qmaxan	VCX30	QX5-days	Qminan	QMNA	VCN7	WDF
Agneby	1980-2017	Agboville	2013*	2014*	-	2006*	-	2003*	-

* *indicates a* significant break while '–'indicate not significant break.

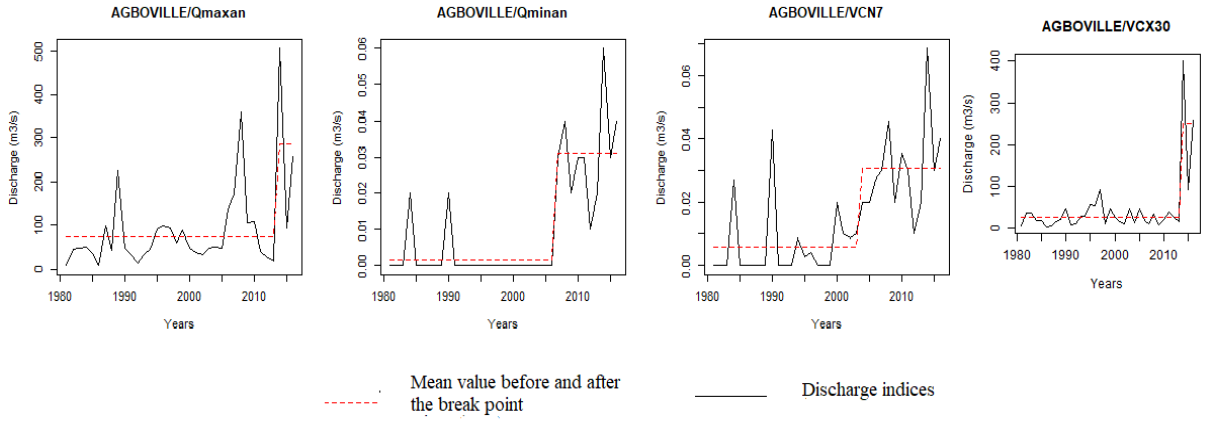

Figure 22: Stations and indices indicating significant break point detection related to flood and low discharge indices under climatic zone I

4.2.2.2 Climatic zone II

Table 17 summarizes the result of the ne change point computed with the SNHT test in the extreme discharge data under climatic zone II. The change points were detected in 2008 and 1980 at the Lobo and Baya watersheds for only the low discharge indices. The flood indices have not shown any significant break periods.

Table 17: Break point detection related to flood and low discharge indices in some watersheds in climatic zone II for the period 1980-2017. * indicates a significant break while '–'indicate no significant break

		Flood indices				Low discharge indices			
Watershed	**Period**	Stations	Qmaxan	VCX30	QX5-days	Qminan	QMNA	VCN7	WDF
Lobo	1988-2015	Nibehibe	-	-	-	2008*	2008*	2008*	2008*
	1980-2017	Loboville	-	-	-	2008*	2008*	2008*	2008*
Baya	1980-2004	Yebouakro	-	-	-	1980*	1980*	-	-

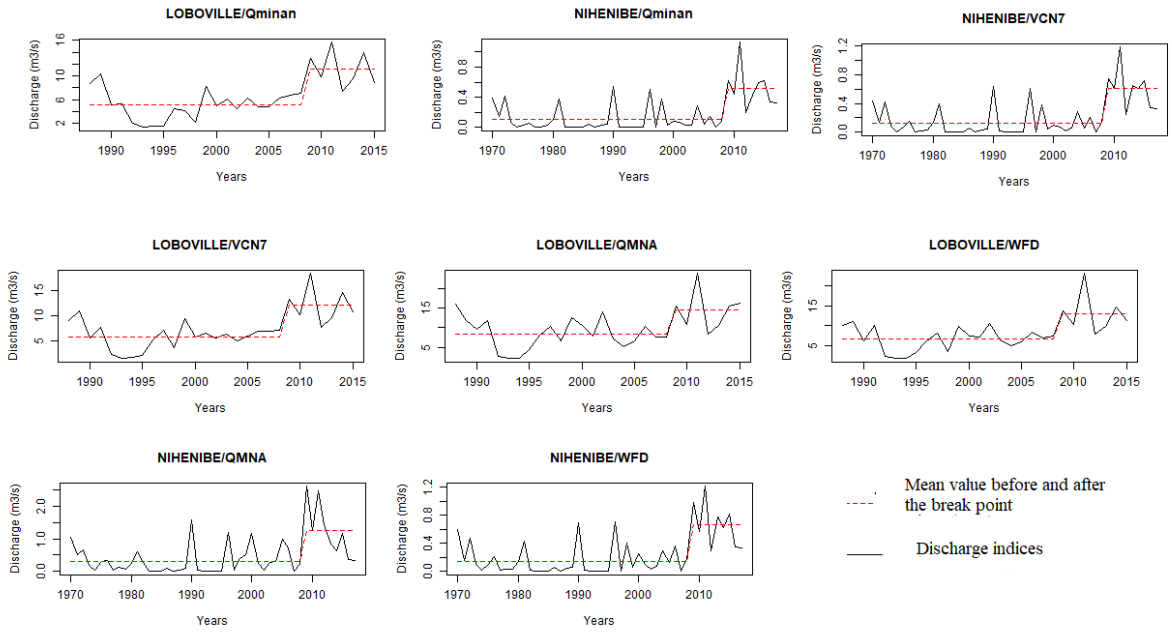

Figure 22: Stations and indices indicating significant break point detection related to flood and low discharge indices under climatic zone II

4.2.2.3 Climatic zone III

With the SNHT test, the Bagoue watershed in climatic zone III has seen significant alteration. All of the indices have a major breakpoint period, with 1984 for all of the low discharge indices and 2012, 2008, and 1970 for the flood indices, respectively.Table 18 and Figure show the outcome.

Table 18: Break point detection related to flood and low discharge indices in some watersheds in climatic zone III for the period 1980-2017. * indicates a significant break while '–'indicate no significant break

		Flood indices			Low discharge indices				
Watershed	**Period**	Stations	Qmaxan	VCX30	QX5-days	Qminan	QMNA	VCN7	WDF
Bagoue	1970-2017	Kouto	2012*	2008*	1970*	1984*	1984*	1984*	1984*

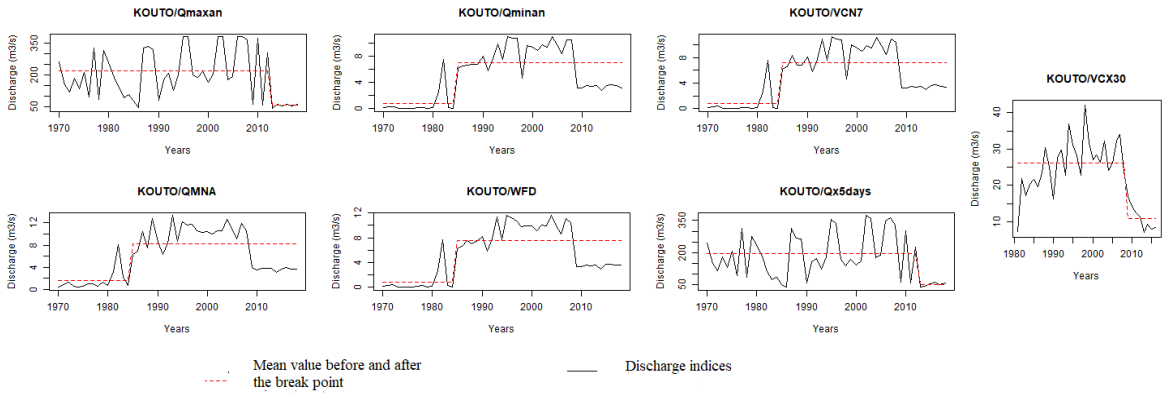

Figure 23: Stations and indices indicating significant break point detection related to flood and low discharge indices under climatic zone III

4.2.2.4 Climatic zone IV

The N'zo watershed under climatic zone IV showed one great breakpoint period with the VCX30 index for the flood discharge in 1994. Regarding the other indices, a non-significant result was found, and the summary is shown in Table 19 and Figure below.

Table 19: Break point detection related to flood and low discharge indices in some watersheds in climatic zone IV for the period 1980-2017.

		Flood indices			Low discharge indices				
Watershed	**Period**	Stations	Qmaxan	VCX30	QX5-days	Qminan	QMNA	VCN7	WDF
N'zo	1980-2018	Kahin	-	1994*	-	-	-	-	-

* indicates a significant break while '–'indicate no significant break

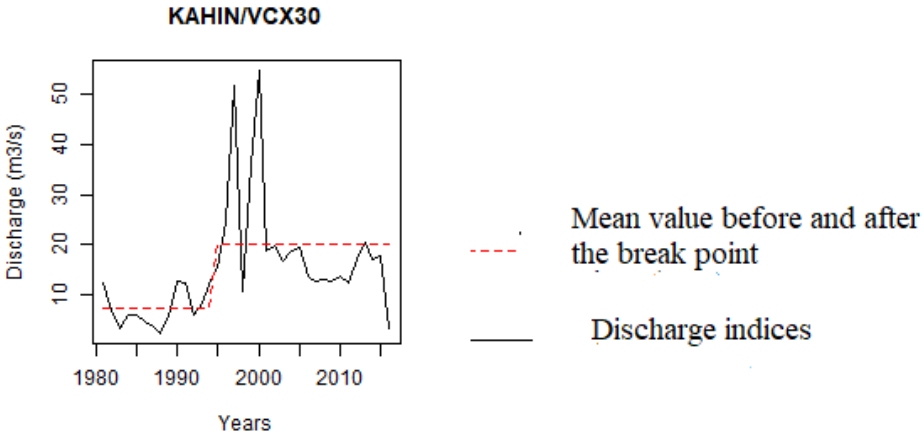

Figure 24 : Stations and indices indicating significant break point detection related to flood and low discharge indices under climatic zone IV

At a level of 0.05 confidence, all of the indices, whether rainfall or discharge, have presented a break point. The break point period for the rainfall extreme indices differed from station to station and from watershed to watershed; no one date of break could be found with a consistent range between 1970 and 1990. Concerning the extreme discharge indices, the 2008 break point period was noted under climatic zones II and III as a significant year for low and high discharge indices, and the break point period was divided into two periods for most of the indices : 1970-1990 and 2005-2015. In climatic zones I and IV, all indices indicated a break time in terms of high or low discharge indices, but only the low discharge flow showed a significant break point period.

4.3 Trend analysis

The findings of the trend analysis of observed rainfall and discharge are coupled with different extreme indicators at a level of 0.05 in this section. For each watershed, the maximum annual rainfall (Pmaxan), consecutive dry days (CDD), maximum rainfall over five days (Rx5days), and very wet day (R95p) can be viewed. There are seven (7) discharge indices : QX5-days, peak discharge (Qmaxan), maximum monthly discharge (VCX30), minimum yearly discharges (Qminan), average monthly discharges (QMNA), daily discharge rate (VCN7), and low water characteristic (WFD). The overall result depicts a change for each selected indicator over each watershed. Over each climatic zone, all of the indices show a substantial drop trend in most of the rainfall data, a significant increase trend in the low discharge indices, and a non-significant trend in the high discharge indices.

4.3.1 Rainfall trend

4.3.1.1 Climatic zone I: Agneby watershed

The results of the trend analysis on extreme rainfall are shown in Table 21, Table 21 and Figure . Table 20 displays the statistical results of the trend analysis on the extreme indices utilizing Zc, Pvalue, and the Sen Slope value, with a significant trend in bold regarding the Pvalue. Table 21 further shows that the majority of the stations show a significant reduction trend, with the CDD index being the most important. Pmaxan, Rx5days, and R95p indices showed a trend for Agboville, Akoupe, Cechi, Sikensi, and M'batto stations. Figure shows the outcome of this strong trend.

Table 20: Statistics of trend analysis of observed data in climatic zone I.

	Pmaxan			**Rx5days**			**CDD**			**R95p**		
Stations	**Zc**	**P value**	**Sen slope**	**Zc**	**P value**	**Sen slope**	**Zc**	**P value**	**Sen slope**	**Zc**	**P value**	**Sen slope**
Agboville	-0.66	0.51	-0.09	-0.46	0.64	-0.04	-0.64	0.52	-0.10	-0.06	0.95	0.00
Akoupe	-1.99	**0.05**	-0.16	-1.66	0.10	-0.10	-2.47	**0.01**	-1.09	-1.86	0.06	-0.19
Arrah	-1.06	0.29	-0.41	-1.21	0.22	-0.11	1.13	0.26	0.34	-1.06	0.29	-0.13
Bongouanou	-1.08	0.28	-0.20	-0.59	0.55	-0.05	-6.72	**0.00**	-1.17	-0.26	0.79	-0.03
Cechi	-1.81	0.07	-0.63	-2.56	**0.01**	-0.11	-1.96	**0.05**	-0.91	-7.73	**0.00**	-0.26
Dabou	0.42	0.68	0.18	0.92	0.36	0.16	-0.53	0.60	-0.27	-0.47	0.64	-0.08
Mbatto	-1.85	0.06	-0.52	-2.51	**0.01**	-0.18	0.14	0.89	0.00	-2.77	**0.01**	-0.25
Sikensi	-1.37	0.17	-0.16	2.43	**0.02**	0.05	-2.97	**0.00**	-1.29	-1.58	0.11	-0.17

Bold=significant trend

Table 21: Trend analysis of observed data in climatic zone I.

			Rainfall indices			
Watersheds	**Stations**	**Periods**	**Pmaxan**	**Rx5days**	**CDD**	**R95p**
Agneby	Agboville	1972-2017	*	-	*	-
	Akoupe	1980-2017	*	-	*	-
	Arrah	1976-2017	-	-	-	-
	Bongouanou	1970-2017	-	-	*	-

	Cechi	1970-2017	-	*	*	*
	Dabou	1970-2017	-	-	-	-
	Mbatto	1976-2017	-	*	-	*
	Sikensi	1976-2017	-	*	*	-

* And ** indicate a decreasing and Increasing trend respectively while – indicates a non-significant trend.

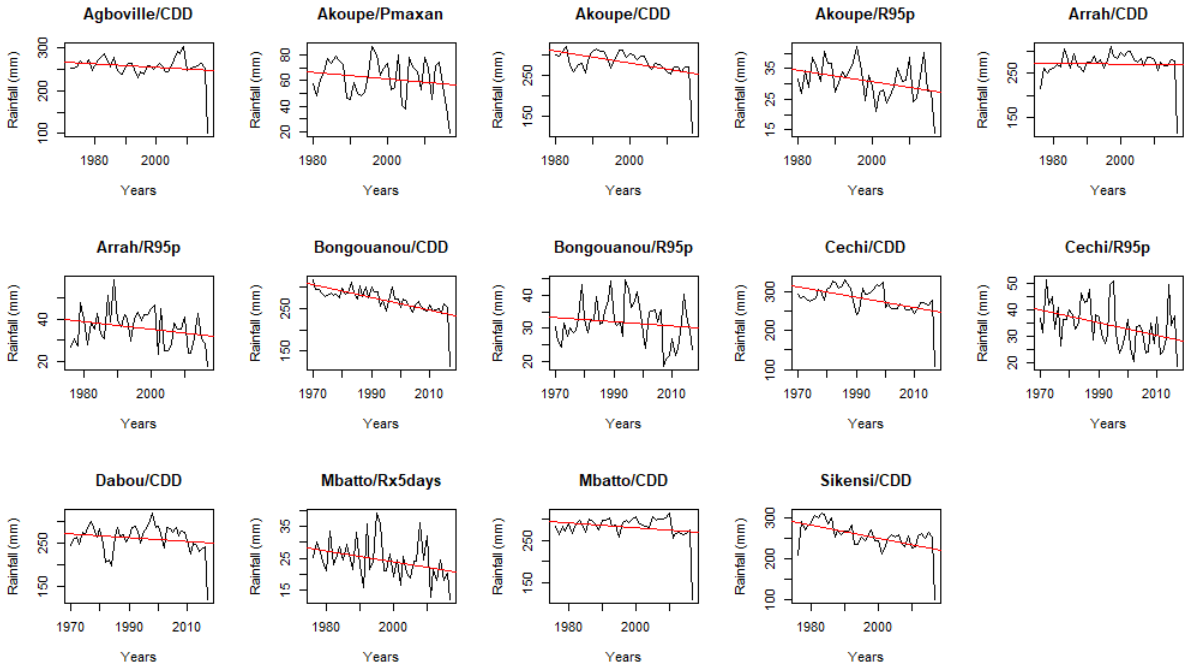

Figure 25: Significant trend analysis result of observed data from 1976 to 2017 under climatic zone I

4.3.1.2 Climatic zone II: Baya and Lobo watersheds

Table 22, Table 23 and Figure show the results of the trend analysis on extreme rainfall indices. The statistics Zc, the Pvalue, and the Sen slope are shown in Table 22, with a significant trend in bold regarding the Pvalue. In Table 23, it can be seen that most of the stations showed a significant decrease trend for all the different indices, as well as the Pmaxan Rx5days, CDD, and R95p indices. Pmaxan and CDD recorded 71.43% and Rx5days and R95p 57.14% at the stations. And all the results of this significant trend are presented in Figure below.

Table 22: Statistics of trend analysis of observed data in climatic zone II.

	Pmaxan			Rx5days			CDD			R95p		
Stations	**Zc**	**P value**	**Sen slope**	**Zc**	**P value**	**Sen slope**	**Zc**	**P value**	**Sen slope**	**Zc**	**P value**	**Sen slope**
Bondoukou	-1.30	0.19	-0.09	-2.18	**0.03**	-0.04	-3.00	**0.00**	-0.10	-2.07	**0.04**	0.00
Daloa	-3.68	**0.00**	-0.16	-3.39	**0.00**	-0.10	-1.94	**0.05**	-1.09	-3.00	**0.00**	-0.19
Issia	-2.57	**0.01**	-0.41	-1.35	0.18	-0.11	-2.37	**0.02**	0.34	-0.65	0.51	-0.13
KunFao	-1.74	0.08	-0.20	-1.78	0.07	-0.05	-2.98	**0.00**	-1.17	-3.33	**0.00**	-0.03
Pelezi	-3.92	**0.00**	-0.63	-2.34	**0.02**	-0.11	-4.92	**0.00**	-0.91	-1.86	0.06	-0.26
Tanda	-1.84	0.07	0.18	-0.48	0.63	0.16	-1.94	0.05	-0.27	-2.36	**0.02**	-0.08
Vavoua	-5.51	**0.00**	-0.52	-4.70	**0.00**	-0.18	-0.86	0.39	0.00	-9.27	**0.00**	-0.25

Bold=significant trend

Table 23: Trend analysis of observed data in climatic zone II

			Rainfall indices			
Watersheds	**Stations**	**Periods**	**Pmaxan**	**Rx5days**	**CDD**	**R95p**
Baya	Bondoukou	1970-2017	-	*	*	*
	Kun-Fao	1977-2017	-	-	-	-
	Tanda	1976-2017	*	-	*	*
Lobo	Daloa	1920-2017	*	*	*	*
	Issia	1977-2017	*	-	*	-
	Pelezi	1976-2017	*	*	*	-
	Vavoua	1953-2017	*	*	-	*

* And ** indicate a decreasing and Increasing trend respectively while - indicates a non-significant trend.

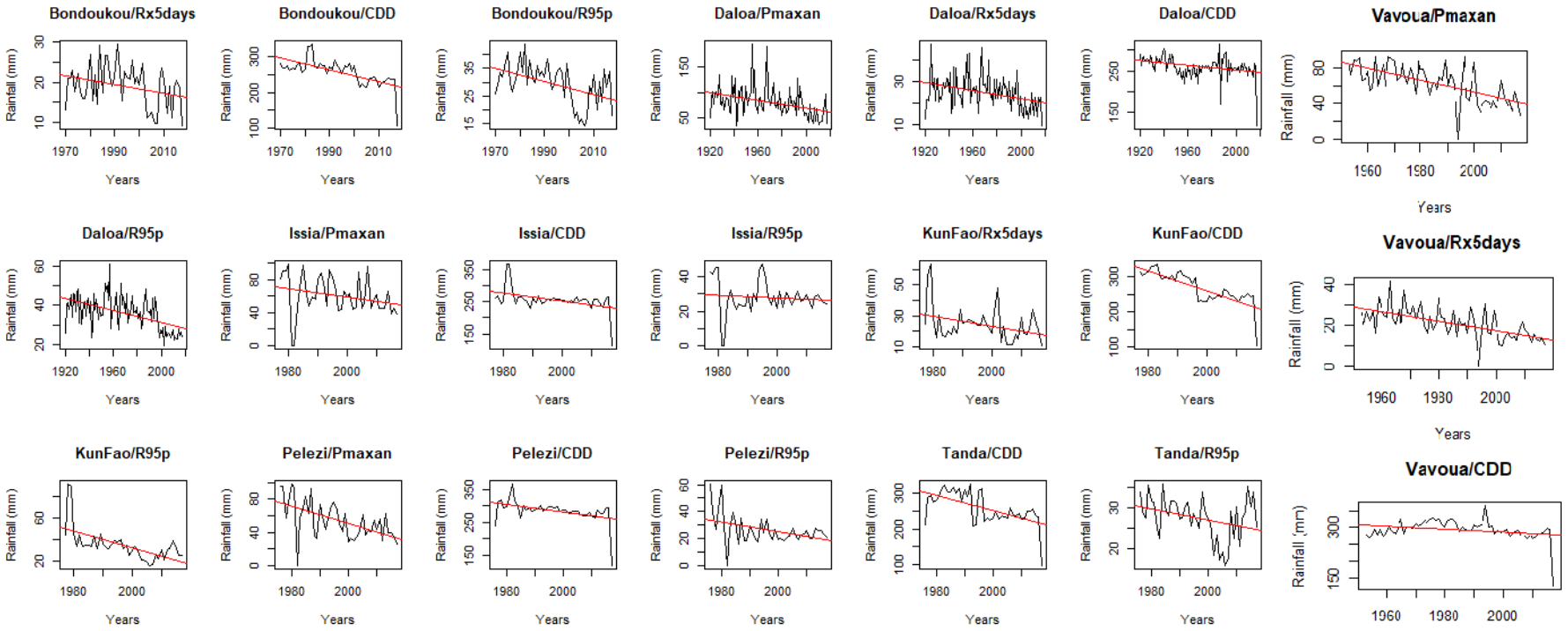

Figure 26: Significant trend analysis result of observed data from 1976 to 2017 under climatic zone II

4.3.1.3 Climatic zone III: Bagoue watershed

The trend analysis of extreme rainfall indices is shown in Table 24, Table 25 and Figure . Table 24 displays the statistical results using the statistic, the Pvalue, and the Sen slope, with a significant trend in bold for the Pvalue. Table 25 shows that the Madinani station is suffering a significant reduction in all observed data, with 100% of the indices disrupted. For the Boundiali station, the Rx5days and R95p indices reveal a significant drop. Figure 26 depicts all of the significant trend data.

Table 24: Statistics of trend analysis of observed data in climatic zone III.

	Pmaxan			**Rx5days**			**CDD**			**R95p**		
Stations	Zc	P value	Sen slope	Zc	P value	Sen slope	Zc	P value	Sen slope	Zc	P value	Sen slope
Boundiali	-1.85	0.06	-0.43	-1.78	0.08	-0.13	-1.85	0.06	-0.18	-1.65	0.10	-0.20
Madinani	-3.16	**0.00**	-0.96	-3.08	**0.00**	-0.33	-2.94	**0.00**	-0.33	-2.83	**0.00**	-0.44

Table 25: Trend analysis of observed data in climatic zone III.

			Rainfall indices			
Watersheds	**Stations**	**Periods**	**Pmaxan**	**Rx5days**	**CDD**	**R95p**
Bagoue	Boundiali	1922-2017	-	*	-	*
	Madinani	1962-2017	*	*	*	*

* and ** indicate a decreasing and increasing trend respectively while - indicates non-significant trend

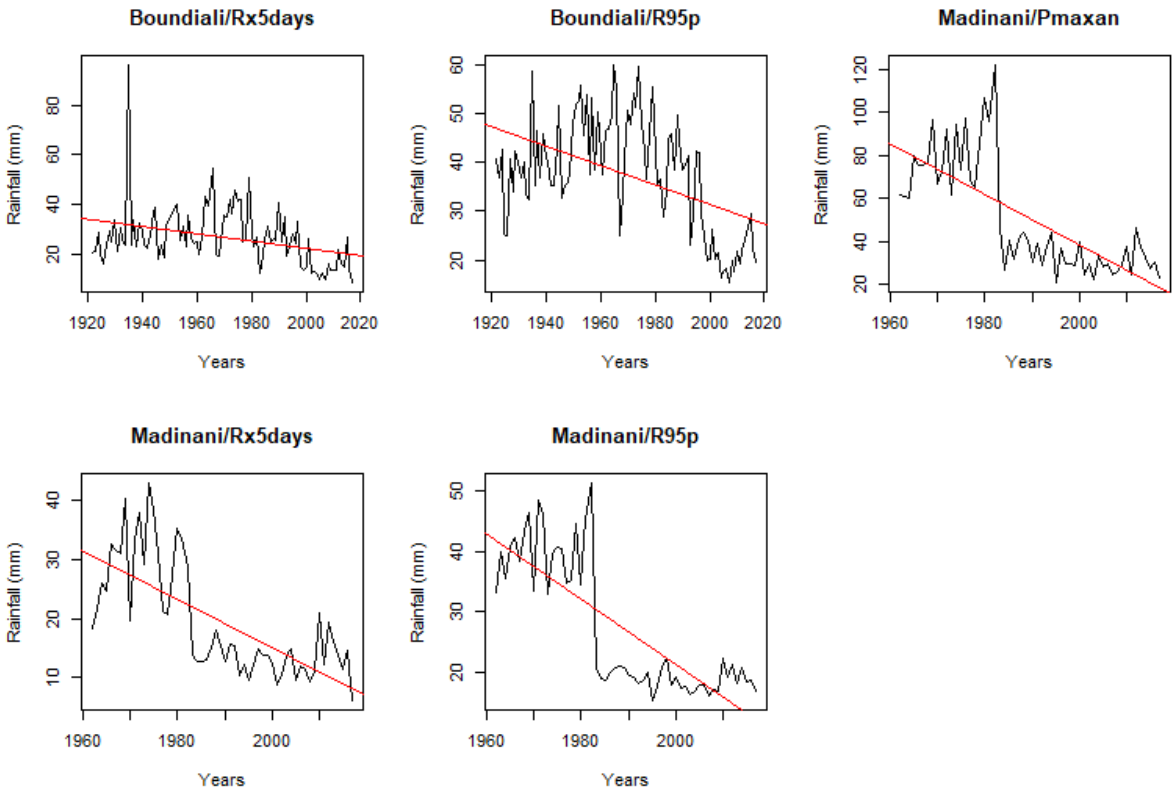

Figure 27: Significant trend analysis result of observed data from 1976 to 2017 under climatic zone III

4.3.1.4 Climatic zone IV: N'zo watershed

The results of the trend analysis of extreme rainfall indices are shown in Table 26 and Table 27, as well as Figure, with a significant decline in the majority of the indicators. Bangolo, Biankouma, and Man all show substantial trends (Table 26). With the CDD indices, all of the stations showed falling trends. Three stations for Rxdays, Bangolo, Biankouma, and Man, and two stations for the R95p index, Man and Biankouma, show a rising trend. Table 26 and Figure summarize the important trend analysis findings.

Table 26: Statistics of trend analysis of observed data in climatic zone IV

	Pmaxan			**Rx5days**			**CDD**			**R95p**		
Stations	**Zc**	**P value**	**Sen slope**	**Zc**	**P value**	**Sen slope**	**Zc**	**P value**	**Sen slope**	**Zc**	**P value**	**Sen slope**
Bangolo	-0.71	0.48	-0.16	-0.18	0.86	-0.02	-1.80	0.07	-0.35	0.30	0.77	0.03
Biankouma	-5.54	**0.00**		-5.97	**0.00**		2.12	**0.03**		-4.05	**0.00**	

Man	-3.40	**0.00**	-4.14	**0.00**	0.52	0.61	-2.94	**0.00**
Zeregbo	-1.31	0.19	-0.60	0.55	-2.44	**0.01**	0.09	0.93

Bold=significant trend

Table 27: Trend analysis of observed data in climatic zone IV. * and ** indicate a decreasing and increasing trend respectively while - indicates non-significant trend

			Rainfall indices			
Watersheds	**Stations**	**Periods**	**Pmaxan**	**Rx5days**	**CDD**	**R95p**
N'zo	Bangolo	1976-2017	-	*	*	-
	Biankouma	1976-2017	*	*	*	*
	Man	1923-2017	*	*	*	*
	Zeregbo	1977-2017	-	-	*	-

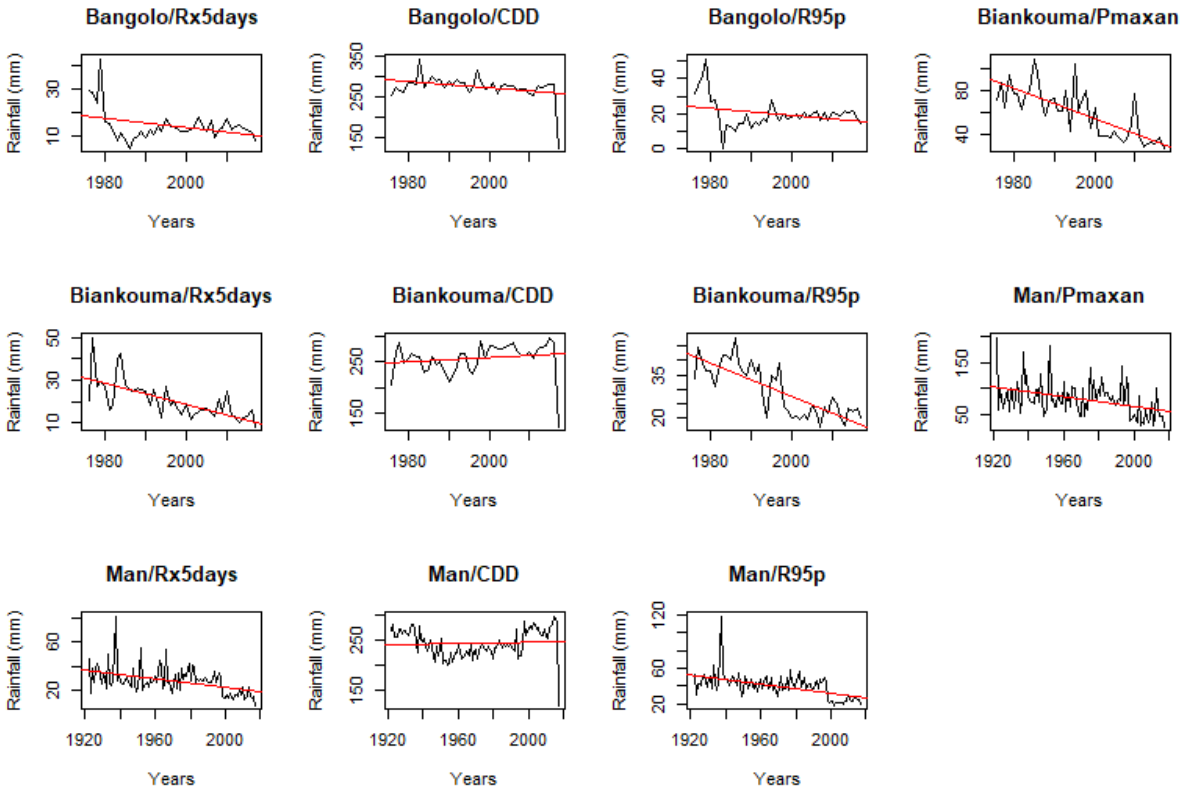

Figure 28: Significant trend analysis result of observed data from 1976 to 2017 under climatic zone IV

4.3.2 Discharge trend analysis

4.3.2.1 Climatic zone I: Agneby watershed

The trend test findings for the climatic zone I generated from observed discharge data These results were analysed using the modified Mann-Kendall test on flood indices such as (QX5-days), peak discharge (Qmaxan), maximum monthly discharge (VCX30), drought indices, minimum annual discharge (Qminan), mean monthly discharge (QMNA), daily discharge (VCN7), and low discharge characteristic (WFD). The trend analysis revealed a non-significant trend for the Agboville outlet across all flood and drought indices.

Table 28: Statistics of trend analysis of observed discharge data

	High discharge indices									**Low discharge indices**									
	Qmaxan			VCX30			QX5-days			Qminan			QMNA			VCN7			WDF		
Stations	**Zc**	**P value**	**Sen slope**	**Zc**	**P value**	**Sen slope**	**Zc**	**P value**	**Sen slope**	**Zc**	**P value**	**Sen slope**	**Zc**	**P value**	**Sen slope**	**Zc**	**P value**	**Sen slope**	**Zc**	**P value**	**Sen slope**
Agboville	0.91	0.36	0.25	-0.55	0.02	-0.01	-0.57	0.56	-0.15	0.04	0.96	-0.00	-0.62	0.53	-0.00	0.23	0.81	0	0.06	0.95	0

Table 29: Trend analysis of flood and low discharge indices in climatic zone I.

		Trend (MMK test)							
		High discharge indices				Low discharge indices			
Watersheds	**Period of analysis**	**Stations**	Qmaxan	VCX30	QX5-days	Qminan	QMNA	VCN7	WDF
Agneby	1970-2017	Agboville	-	-	-	-	-	-	-

4.3.2.2 Climatic zone II: Baya and Lobo watershed

The results of the trend test obtained from the observed discharge data for climatic zone II on flood and drought indices are presented in Table 30, Table 31, Table 32, and Figure . It was observed that only Loboville station showed an increasing trend on minimum annual discharge (Qminan), daily discharge (VCN7), and low discharge characteristic (WFD).

Table 30: Statistics of trend analysis of observed high discharge indices

	High discharge indices								
	Qmaxan			VCX30			QX5-days		
Stations	**Zc**	**P value**	**Sen slope**	**Zc**	**P value**	**Sen slope**	**Zc**	**P value**	**Sen slope**
Yebouakro	-0.07	0.94	-0.04	-0.36	0.71	-0.01	-0.03	0.97	-0.03
Loboville	-1.89	0.057	-3.09	0.87	0.37	0.11	-2.07	0.03	-2.77
Nibehibe	-0.51	0.61	-0.17	1.04	0.29	0.01	-0.43	0.66	-0.18

Table 30: Statistics of trend analysis of observed low discharge indices

	Low discharge indices											
	Qminan			QMNA			VCN7			WDF		
Stations	**Zc**	**P value**	**Sen slope**	**Zc**	**P value**	**Sen slope**	**Zc**	**P value**	**Sen slope**	**Zc**	**P value**	**Sen slope**
Yebouakro	0.59	0.55	0	1.42	0.15	0.002	1.02	0.30	0	1.07	0.28	0
Loboville	3.43	0.00	0.29	1.79	0.07	0.21	3.18	0.00	0.30	2.5	0.01	0.26
Nibehibe	1.78	0.07	0.00	1.76	0.07	0.01	1.66	0.09	0.004	1.82	0.06	0.004

Table 31: Trend analysis of flood and low discharge indices in climatic zone II. * and ** indicate decreasing and increasing trend respectively, while - indicate non-significant trend.

		Trend (MMK test)							
		High discharge indices				Low discharge indices			
Watersheds	**Period of analysis**	**Stations**	Qmaxan	VCX30	QX5-days	Qminan	QMNA	VCN7	WDF
Lobo	1988-2015	Loboville	-	-	*	**	-	**	**
	1980-2017	Nibehibe	-	-	-	-	-	-	-
Baya	1980-2004	Yebouakro	-	-	-	-	-	-	-

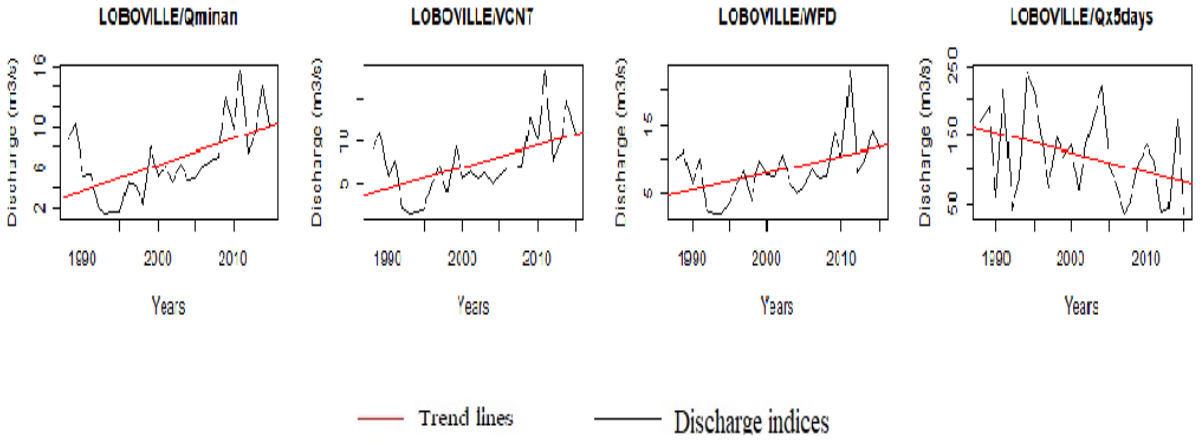

Figure 29: Significant trend analysis of flood and low discharge indices in climatic zone II

4.3.2.3 Climatic zone III: Bagoue watershed

The trend test findings for the climatic zone I generated from observed discharge data. These findings were based on flood indices such as (QX5-days), peak discharge (Qmaxan), maximum monthly discharge (VCX30), drought indices, minimum annual discharge (Qminan), mean monthly discharge (QMNA), daily discharge (VCN7), and low discharge characteristic (WFD). The trend study revealed a non-significant trend for the Kouto outlet across all flood and drought indices.

Table 32: Statistics of trend analysis of observed high discharge indices of climatic zone III

	High discharge indices								
	Qmaxan			VCX30			QX5-days		
Stations	**Zc**	**P value**	**Sen slope**	**Zc**	**P value**	**Sen slope**	**Zc**	**P value**	**Sen slope**
Kouto	-0.52	0.60	-0.64	0.11	0.91	0.01	-0.52	0.60	-0.78

Table 33: Statistics of trend analysis of observed low discharge indices of climatic zone III

	Low discharge indices											
	Qminan			QMNA			VCN7			WDF		
Stations	**Zc**	**P value**	**Sen slope**	**Zc**	**P value**	**Sen slope**	**Zc**	**P value**	**Sen slope**	**Zc**	**P value**	**Sen slope**
Kouto	1.60	0.11	0.09	1.34	0.17	0.09	1.46	0.14	0.09	1.67	0.09	0.1

Table 34: Trend analysis of flood and low discharge indices in climatic zone III. * and ** indicate decreasing and increasing trend respectively, while - indicate non-significant trend.

		Trend (MMK test)							
		High discharge indices				Low discharge indices			
Watersheds	**Period of analysis**	**Stations**	Qmaxan	VCX30	QX5-days	Qminan	QMNA	VCN7	WDF
Bagoue	1980-2018	Kouto	-	-	-	-	-	-	-

4.3.2.4 Climatic zone IV: N’zo watershed

Table 36, Table 37 and Figure 30 show the results on flood and drought indices in the IV climatic zone. For the high discharge indices, only maximum monthly discharge (VCX30) presented a significant increase trend. The low discharge indices showed increasing trend in all of the variables, namely, minimum annual discharge (Qminan), mean monthly discharge (QMNA), daily discharge (VCN7), and low discharge characteristic (WFD) at the outlet of the N'Zo watershed.

Table 35: Statistics of trend analysis of observed discharge data of climatic zone IV

	High discharge indices									Low discharge indices											
	Qmaxan			VCX30			QX5-days			Qminan			QMNA			VCN7			WDF		
Stations	Zc	P value	Sen slope	Zc	P value	Sen slope	Zc	P value	Sen slope	Zc	P value	Sen slope	Zc	P value	Sen slope	Zc	P value	Sen slope	Zc	P value	Sen slope
Kahin	1.01	0.30	1.41	1.13	0.25	0.14	1.39	0.16	1.296	4.31	0.00	0.083	3.52	0.000	0.123	4.72	0.00	0.099	4.55	0.000	0.109

Table 36: Trend analysis of flood and low discharge indices in climatic zone IV. * and ** indicate decreasing and increasing trend respectively, while - indicate non-significant trend.

		Trend (MMK test)							
		High discharge indices				Low discharge indices			
Watersheds	**Period of analysis**	**Stations**	Qmaxan	VCX30	QX5-days	Qminan	QMNA	VCN7	WDF
N'zo	1980-2017	Kahin	-	**	-	**	**	**	**

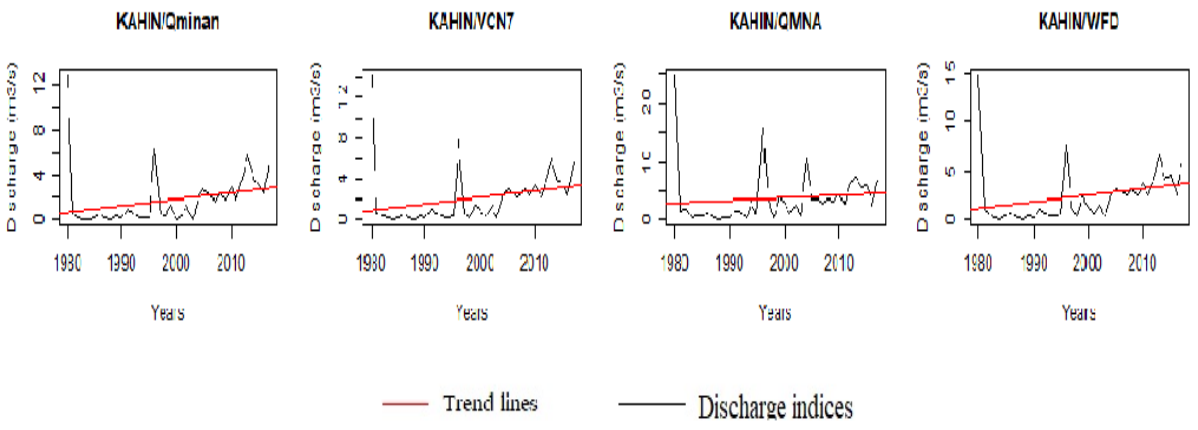

Figure 30: Significant trend analysis of flood and low discharge indices in climatic zone IV

In general, all the indices presented a significant trend at the level of 0.05. For the extreme rainfall indices, most of the stations showed a significant decrease trend under each climatic zone. However, concerning the extreme discharge indices, the Mann-Kendall modified test indicated a non-significant trend for most outlet stations. Under climatic zones II and IV, respectively at Loboville and Kahin stations, the MMK test presented a significant increasing trend for the high (Qx5 days) and low discharge indices.

4.4 Discussion

The objective of this study was to assess the historical (1970–2017) hydro-climatic (rainfall and discharge) trends and the impact of rainfall variability on low and high flows in some selected river basins using Hanning's second-order low-pass filter, the Standard Normal Homogeneity Test (SNHT), and the modified Mann-Kendall test (MMK). The analysis was done on the extreme rainfall and discharge (flood and drought-related) indices in each of the climatic zones of Côte d'Ivoire at a level of 0.05 for the SNHT and MMK tests. The analysis was used for the rainfall extremes indices on maximum annual rainfall (Pmaxan), consecutive dry days (CDD), maximum 5-day rainfall (Rx5days), and the very wet day (R95p), and for the extreme discharge indices on 5-day maximum flow (QX5-days), the peak discharge (Qmaxan), the maximum monthly discharge (VCX30), the minimum annual discharges (Qminan), the average monthly discharges (QMNA), the daily discharge rate (VCN7), and the low water characteristic (WFD).

- *Extreme rainfall indices*

The drought index (CDD), which is defined by the length of the dry season, has changed in each climatic zone. With the observed data, the CDD index demonstrated a strong negative trend at the Bagoue watershed in the north, Baya in the east, Agneby in the south, and Lobo and N'zo in the southwest over the entire country. The significant downward trend in this drought index could be explained by the fact that the climate has been marked by a long period of variation dominated by either a long rainy season or a long moderate season, which has significantly reduced the length of the dry period, particularly in West Africa after the severe drought period of the 1970s. This shift in the drought index trend is consistent with the findings of Agyekum et al. (2022), who discovered a drop in the trend of dry continuous days over the Volta watershed from 1985 to 2014. This conclusion could be explained by the fact that the climatic variability of the country's climatic zones is not uniform.

With observed data, three extreme indices (Pmaxan, R95p, and Rx5days) were used to examine the flooding phenomenon. The indices describing flooding all exhibited a broad multiform trend with downward tendencies over the observed time under each climatic zone after trend analysis of these data. The large downward trend seen could be attributed to the fact that the early and late recovery of rainfall after catastrophic droughts was insufficient to influence these extreme indicators across the whole research area. As a result, typical rainfall in each climatic zone and the country's significant rainfall variability dominated these extreme rainfall indices. This observation is consistent with the findings of Coulibaly (2021), who found a statistically significant drop in yearly rainfall in Cote d'Ivoire from 1951 to 2017. Furthermore, Balliet et al. (2016) discovered a substantial mixed trend (increase and decrease) in the Rx5days index in Gagnoa's Goh region between 1961 and 2010.

The large increased trend in extreme rainfall reported in the N'Zo watershed could be attributed to the watershed's geographical location. Indeed, in a forested and mountainous region of the country, there is sufficient rainfall, a resumption of rainfall, and support for an upward trend in extreme rainfall indices. As a result, the frequency of flooding in this location may exacerbate the phenomena of soil erosion caused by runoff. Yao et al. (2023) discovered an increased trend in the R95p index in their study in Côte d'Ivoire's south-west, which is consistent with our funding.

- *High discharges*

These different analyses gave a non-significant trend for most of the flood indices in the period analysed, with the exception of the VCX30 index at Kahin, which showed a significant upward trend, and QX5 days, which showed a decrease trend at Loboville. These results could be due to the high interannual variability observed in the data, as shown by the Hanning test, and the daily impacts of climate change observed across the country, even influencing precipitation. All the study watersheds were affected in the same way due to the influence of local climates. Furthermore, this predominance of non-significant changes in the flood variables (i.e., 5-day maximum flow (QX5days), peak discharge (Qmaxan), and maximum monthly discharge (VCX30)) could be due to the method used. Indeed, the method used is powerful to detect trends but does not seem to be very robust on the extreme variables because a non-significance does not translate the absence of a trend but the incapacity of the detection. (Ago et al., 2005), in their study in Togo-Benin, found no trend. The significant breaks in the annual maximum discharge (Qmaxan) and monthly maximum discharge (VCX30) confirm the results obtained concerning the decrease in the maximum discharge of rivers in Côte d'Ivoire. Indeed, a sudden decrease in the series of extreme maximum discharges could be explained by climatic factors and the variability experienced by these different watersheds, as shown by the result of the Hanning test. Rainfall in Côte d'Ivoire is decreasing in all climatic zones, which affects river discharges even with the recovery predicted by Nicholson et al. (2000). These flood variables also show a decreasing trend after their break period, reflecting the general decrease in rainfall recorded in Côte d'Ivoire. These rainfall deficits have been notable in some regions of the country. For example, a 66.5% hydrological deficit in the Bandama discharges at Tortiya was recorded by Kamagaté et al. (2019). A decrease in rainfall with a deficit of 22% on Agneby was noted by Assoma et al. (2016), and irregularities in rainfall with a direct impact on the hydrological evolution of the river and on the flood discharges were found on Kahin by Anouman (2020).

- *Low discharge rates*

The results show a general upward trend with the MMK test for the low flow series in all cases considered, especially in the four climatic zones (Zone I, Zone II, and Zone IV), where local climate and high intervariability are of great importance. This could be explained by the fact that the return of rainfall after the great drought predicted by Nicholson et al. (2000) is felt more from the south to the north. This is because the inter-variability influenced

by the local climate allows for constant rainfall over the whole territory and at any time of the year, thus inducing significant trends towards increased river flow in the different catchment areas. (Nouaceur, 2020) concluded in his work that the analysis of rainfall trend evolution shows that, following a long Sahelian drought, rains returned to this part of West Africa. Also, the work of Ago et al. (2005) concluded that the evolution of the flow of the Mono River remains dependent on climatic factors. These results agree with the work of Amogu et al. (2010).

- *Relationship between rainfall and the discharge*

The statistics show significant climate change from south to north through the west of the country, with many climatic periods recorded. These climate periods are higher above normal in the flow data than in the rainfall data, indicating a poor correlation between the variables. This inter-variability has resulted in a considerable break in the extreme indices evaluated. In addition to these findings, it was discovered that there was a considerable break in almost all of the analysed stations due to abnormalities in each climatic zone.

Conclusion

Using observed rainfall from 1976 to 2017, we used the modified Mann-Kendall statistical test to examine trends in four extreme rainfall and seven extreme discharge indicators on an annual and monthly basis. The trend analysis of rainfall indices revealed that all of the indices describing flooding and dry season length (CDD index) indicate general decreasing trends in the observed data from 1976 to 2017. We obtained non-significant trends for the flood variables in general and substantial upward trends for the low-flow variables for the discharge indices. The Standard Normal Homogeneity Test (SNHT) detected a substantial break for most of the variables evaluated in general across all of our study basins. Furthermore, the results obtained by applying Hanning's second-order low-pass filter to the observed data show a significant inter-annual irregularity of the data in each of the country's climatic zones. The various methodologies utilized yield solid results throughout this study, but it would be interesting to extend this analysis to a seasonal scale and to other confidence intervals for improved monitoring and visibility of the influence of climate change. It has also provided a good understanding of the progression of past rainfall, drought, and flood indices in each of the country's climatic zones. It is crucial to emphasize that changes in climate extremes are of more relevance to local decision-makers since they imply changes in the types of dangers that are frequently of greatest concern to communities. Thus, future research

should include a good database of available extremes from observing stations, as well as different trend analysis techniques at different time steps (e.g., monthly and decadal), as well as different time series techniques to predict extremes at monthly and seasonal scales, which would be useful for farmers while also boosting the Ivorian economy. Furthermore, the understanding will enable policy planning and strategies to prepare for possible issues resulting from the effects of climate change in the research area.

CHAPTER 5 : ABILITY OF THE MODELS TO REPRODUCE HYDROLOGICAL EXTERMES

In Chapter 5, the results of GR4J, GR5J, and HEC-HMS modeling for each watershed in each climatic zone are shown. The calibration and validation times, as well as the model performance, are plotted for each hydrological model. Section 5.1 presents the GR4J and GR5J results for each outlet in relation to each watershed. In addition, the results of the HEC-HMS modeling may be retrieved in Part 5.2. The focus on hydrological modeling in this chapter helps us understand how each model functions in each climatic zone.

5.1 Hydrological modeling with GR4J and GR5J

5.1.1 Calibration

The calibration process for each model was carried out using the same periods for each output point and for each GR4J and GR5J models. The periods where the models showed a good result of the objective function (NASH and KGE) with values reaching 0.65 overall were considered a good calibration period for each model, and it can be seen that for each model, the calibration period is rather 5 or 10 years for the considered watershed. Only the Agneby watershed was underestimated by the GR4J model, with the lowest Nash value (0.05). The annual water balance was calculated at the calibration and validation levels, summarizing the annual sums of the balance parameters for each watershed. The calibration of the GR4J and GR5J models evolved in the same order, and the balance showed a higher value for the ETR for all the GR models in all the watershed areas studied. For the Agneby watershed, the mean annual rainfall over the calibration period is 1033.56mm, the ETR is 950.08mm, the runoff is 28.75 mm, and the infiltration is 54.73mm. The Bagoue watershed shows rather relative values, with a constant increase in the ETR value of 660.15 mm, precipitation of 763.38mm, infiltration of less than 92.9 mm, and runoff of 196.13mm. In the Baya watershed, the mean rainfall during calibration is 962.90mm, providing an ETR of 797.44mm, runoff of 36.99 mm, and infiltration of 136.47 mm. The mean annual rainfall during calibration is 954.59mm over the Lobo watershed at the Nibehibe station, with a value of 896.61mm for the ETR, 21.36mm for the runoff, and 36.62mm for the underground infiltration. At the Loboville station, the mean annual precipitation was 970.91mm, the ETR was 889.71mm, the runoff was 69.98 mm, and the infiltration was 11.22mm. Finally, in the N'zo watershed, the mean annual precipitation was 956.45mm, the ETR was 727.45mm, the runoff was 279.88mm, and the infiltration was less than 50.88mm. These different values of the water balance parameters are approximately equal to those of the GR5J model in the study

watersheds. And the result for each model is shown from Table 37 to Table 39 and Figure and Figure below. And also, the graphical result of the simulation (Figure 31) shows a fairly good representation between the calculated and observed flows, which evolve together. Low flows and high flows are correctly reproduced in most cases. However, the simulated hydrographs are underestimated at the Agboville station in the Agneby basin and overestimated in places at the Kahin station in the N'zo basin.

Table 37: Objectives functions after calibration of GR4J and GR5J models

Watersheds	**Stations**	**GR4J**			**GR5J**		
	Calibration	Years	NSE	KGE	Years	NSE	KGE
Agneby	Agboville	1980-1990	0.05	-0.08	1980-1990	0.70	0.781
Bagoue	Kouto	1981-1989	0.58	0.63	1981-1989	0.56	0.649
Baya	Yebouakro	1986-1992	0.72	0.79	1986-1992	0.732	0.792
Lobo	Nibehibe	1983-1988	0.67	0.64	1983-1988	0.75	0.793
	Loboville	2006-2010	0.91	0.94	2006-2010	0.904	0.922
N'Zo	Kahin	1983-1988	0.64	0.73	1983-1988	0.63	0.674

Table 38: Parameters of water balance for GR4J model

Calibration	**Parameters of water balance for GR4J model**				
Watersheds	Stations	Annual rainfall (mm)	ETR Annual (mm)	Runoff (mm)	Infiltration (mm)
Agneby	Agboville	1033.56	950.08	28.75	54.73
Bagoue	Kouto	763.38	660.15	196.13	-92.9
Baya	Yebouakro	962.90	797.44	36.99	136.47
Lobo	Nibehibe	954.59	896.61	21.36	36.62
	Loboville	970.91	889.71	69.98	11.22
N'Zo	Kahin	956.45	727.45	279.88	-50.88

Table 39: Parameters of water balance for GR5J model

Calibration	**Parameters of water balance for GR5J model**				
Watersheds	Stations	Annual rainfall (mm)	ETR Annual (mm)	Runoff (mm)	Infiltration (mm)
Agneby	Agboville	1033.56	948.55	29.21	55.8
Bagoue	Kouto	763.38	622.21	191.36	-77.19
Baya	Yebouakro	962.90	804.01	38.17	120.72
Lobo	Nibehibe	954.59	901.43	17.96	35.2
	Loboville	970.91	888.59	70.18	12.14
N'Zo	Kahin	956.45	714.92	281.45	-39.92

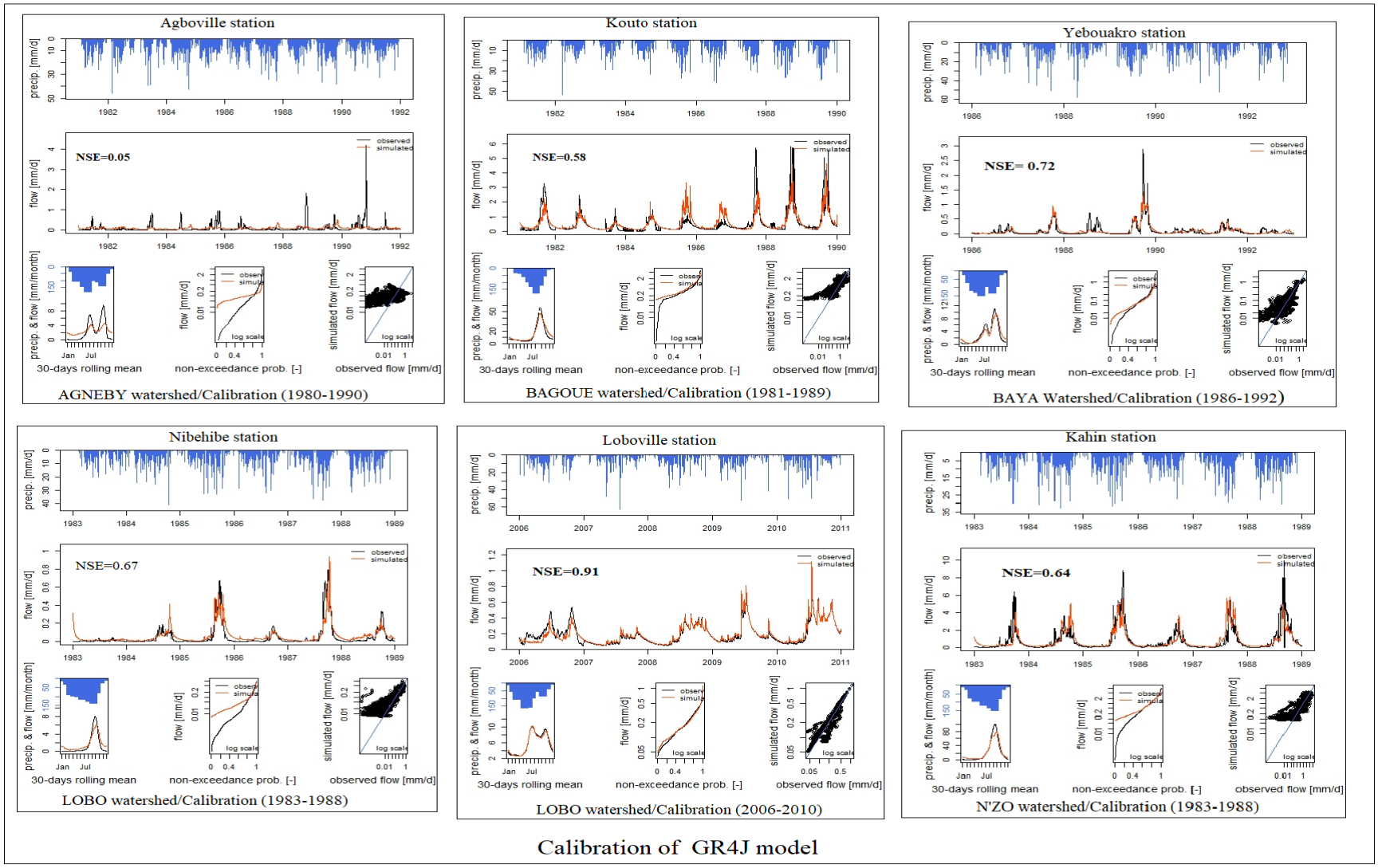

Figure 31 : Calibration period of GR4J model

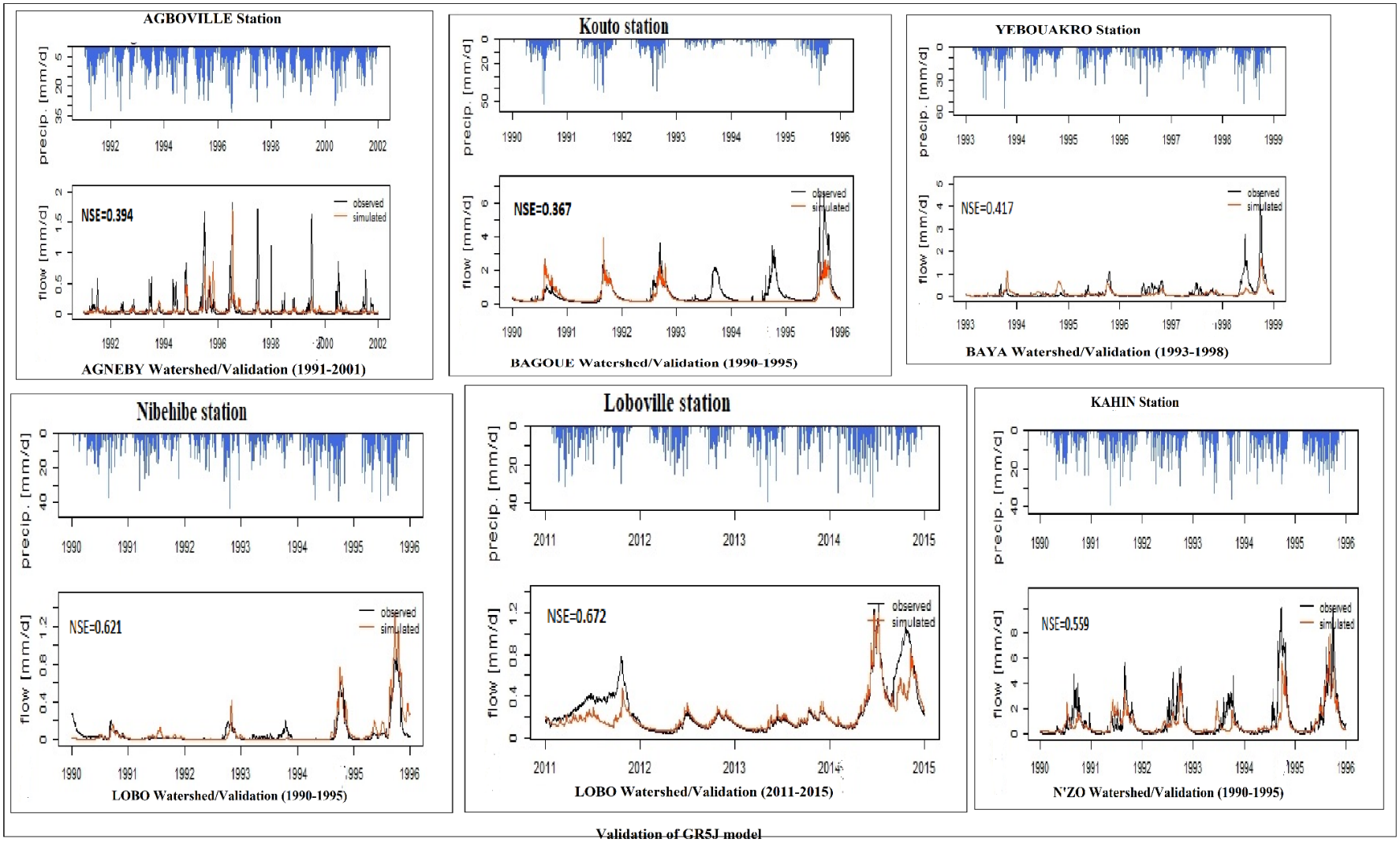

Figure 32: Calibration period of GR5J model

5.1.2 Validation

The validation process for each model was carried out using similar periods for each model The validation process for each model was carried out using similar time periods for each model, GR4J and GR5J, and based on each model parameter, four and five, respectively. Validation with the GR4J model gave unsatisfactory results for Agneby, Baya, Bagoue and Lobo at Nibehibe watersheds. The Lobo at Loboville and N'zo at Kahin watersheds provided satisfactory findings, with Nash values ranging from 0.90 to 0.58, respectively. For GR5J, Nash values were generally acceptable compared with GR4J. Better values were obtained for the Lobo and N'zo watersheds, with values of around 0.7 for the Lobo watershed and 0.6 for the N'zo watershed. The annual water balance was calculated at the validation level by summarizing the annual sum of the balance parameters for each watershed. Using the GR4J model, the mean annual rainfall over the validation period is 978.97 mm, the ETR is 789.35 mm, the discharge is 224.19 mm, and infiltration is less than 34.57 mm in the Agneby watershed. Bagoue watershed shows fairly relative values, with an increase in the ETR of 429.19mm, rainfall of 608.11mm, infiltration of less than 35.81 mm, and runoff of 214.73mm. In the Baya basin, average rainfall is 978.73 mm, providing a ETR of 758.66 mm, runoff of 256.85 mm, and infiltration of less than 57.64 mm. The mean annual rainfall at validation is 978.73 mm in the Lobo basin at the Nibehibe station, with a value of 758.66 mm for the ETR, 256.85 mm for runoff, and less than 36.78 mm for underground infiltration. And finally, in the N'Zo basin, the average annual rainfall is 1033.119 mm, the ETR is 772.38 mm, the flow is 305.44 mm, and the infiltration is less than 44.7 mm. The graphic results of the simulation (Figure 32) show that low water and high water are not correctly reproduced in most cases during the validation period. The simulated hydrographs are underestimated at all the study stations. These different values for the hydrological balance parameters are more or less equal to those of the GR5J model for the N'zo basin (Table 37 to Table 40). The results for each model are shown from Table 41 to 44 and Figure 33 and 34 below:

Table 40:GR4J parameters

Watersheds	**Stations**	**GR4J**					
	Validation	Years	X1	X2	X3	X4	NSE
Agneby	Agboville	1991-2001	9701.15	-4.45	32.78	20.0	0.09

Bagoue	Kouto	1990-1995	817.94	1.977	52.12	15.86	0.20
Baya	Yebouakro	1993-1998	915.549	-16.5	83.812	15.86	0.38
Lobo	Nibehibe	1990-1995	1436.55	-2.38	20.68	2.384	0.25
	Loboville	2011-2015	1239.815	0.567	95.387	3.563	**0.90**
N'Zo	Kahin	1990-1995	95.9	1.2	147.3	5.1	**0.58**

Table 41: Parameters of water balance for GR4J model for GR4J validation

Validation	**Parameters of water balance for GR4J model**				
Watersheds	Stations	Annual rainfall (mm)	ETR Annual (mm)	Runoff (mm)	Infiltration (mm)
Agneby	Agboville	978.97	789.35	224.19	-34.57
Bagoue	Kouto	608.11	429.19	214.73	-35.81
Baya	Yebouakro	1110.52	730.77	437.39	-57.64
Lobo	Nibehibe	978.73	758.66	256.85	-36.78
N'Zo	Kahin (1990-1995)	1033.12	772.38	305.44	-44.7

Table 42: Parameters of water balance for GR4J model for GR5J validation

Validation	**Parameters of water balance for GR5J model**				
Watersheds	Stations	Annual rainfall (mm)	ETR Annual (mm)	Runoff (mm)	Infiltration (mm)
Agneby	Agboville	978.97	922.78	21.55	34.64
Bagoue	Kouto	608.11	513.88	155.73	-61.5
Baya	Yebouakro	1110.52	868.39	46.89	

	Nibehibe	978.73	878.36	26.01	74.36
Lobo					
	Loboville	999.45	919.15	80.60	-0.3
N'Zo	Kahin	1033.12	758.57	305.46	-30.91

Table 43: GR5J parameters

Watersheds	**Stations**	**GR5J**						
	Validation	Years	X1	X2	X3	X4	X5	NSE
Agneby	Agboville	1991-2001	1099.182	-1.867	3.463	10.450	0.475	0.39
Bagoue	Kouto	1990-1995	428.762	-0.156	100.080	0.923	0.875	0.36
Baya	Yebouakro	1993-1998	1201.009	-4.274	54.124	11.993	0.270	0.41
Lobo	Nibehibe	1990-1995	2296.029	-0.295	15.405	8.236	0.030	**0.62**
	Loboville	2011-2015	983.104	-0.085	102.536	3.249	0.482	**0.67**
N'Zo	Kahin	1990-1995	70.395	-0.073	160.046	4.031	1.000	**0.56**

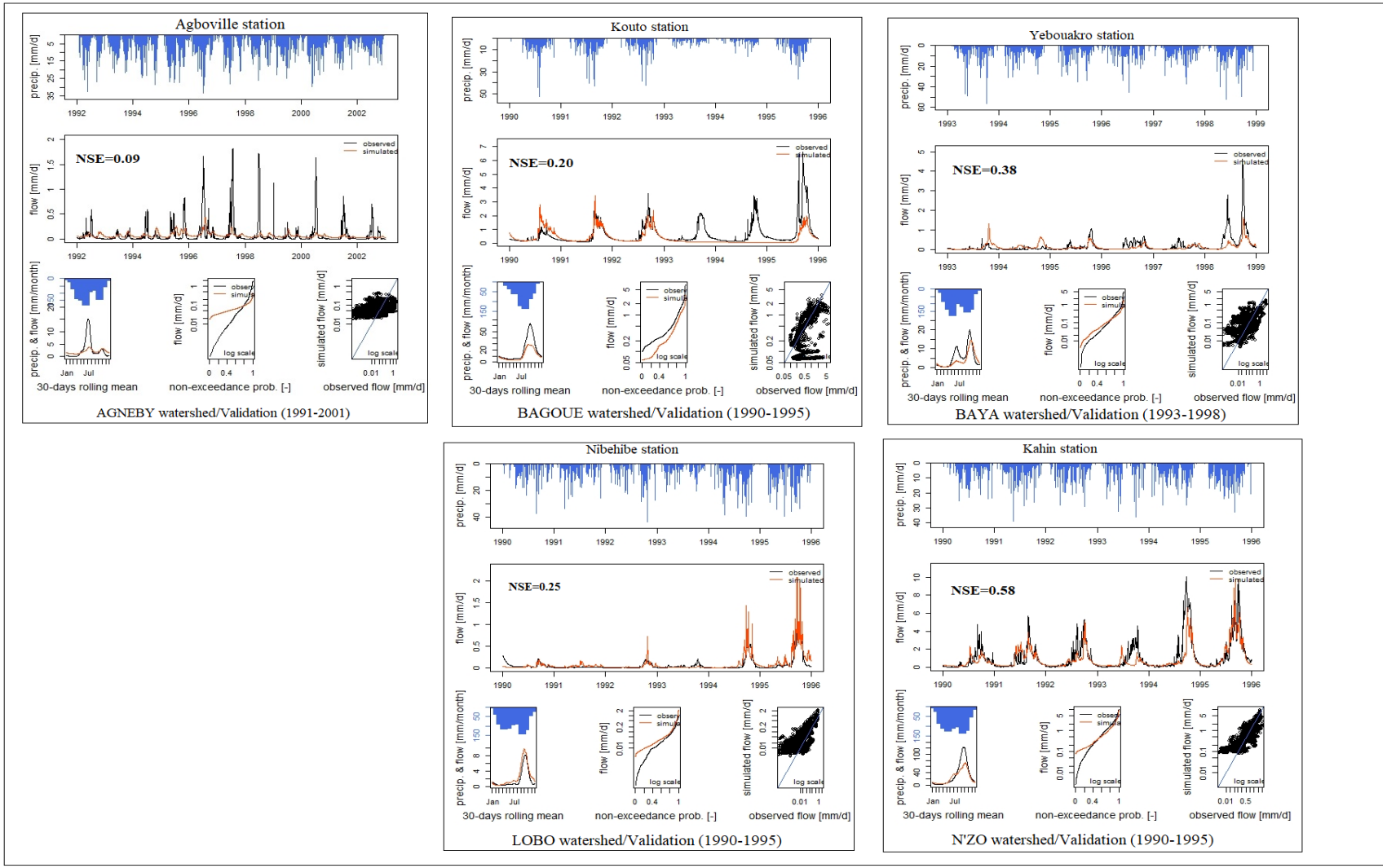

Validation of GR4J model

Figure 33: Validation period of GR4J

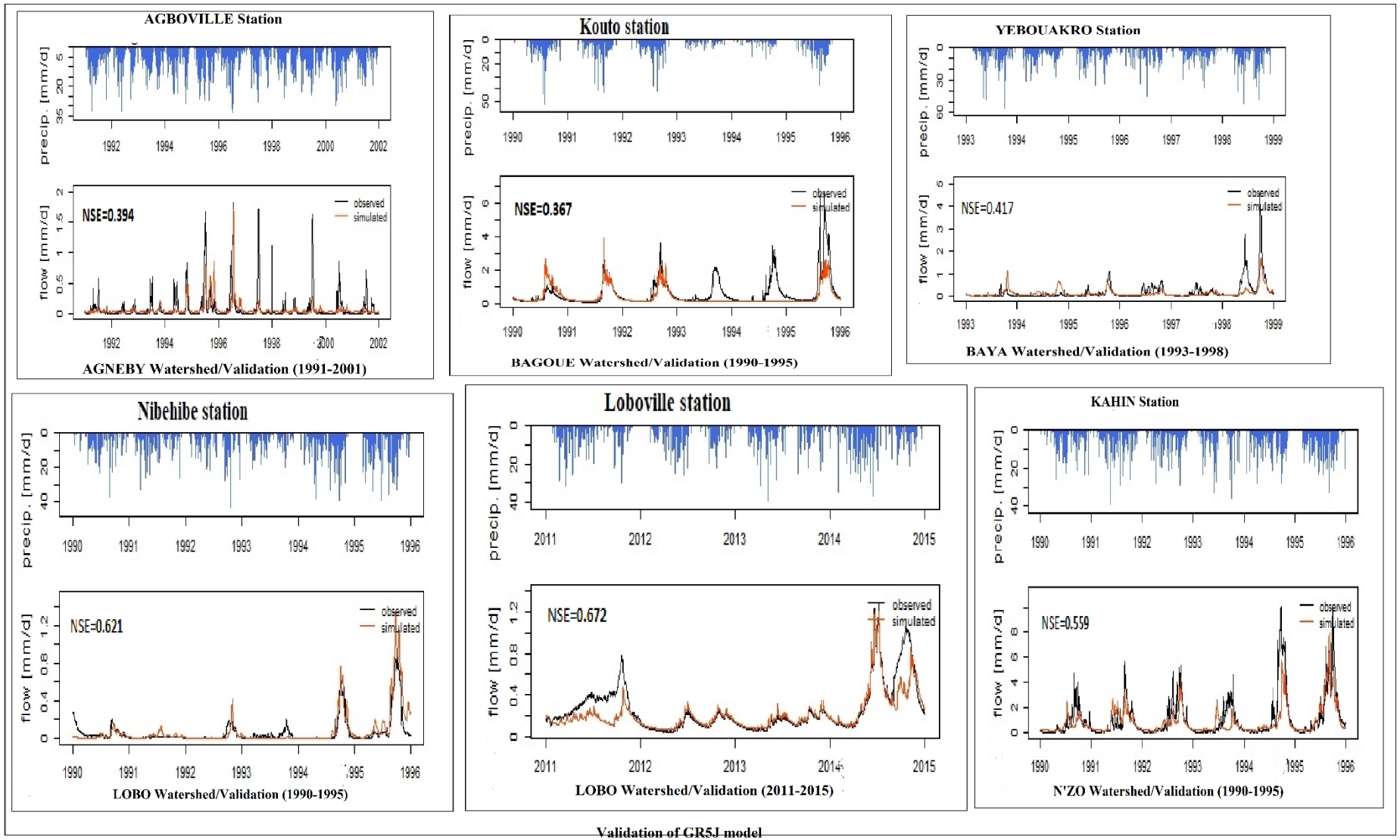

Figure 34 : Validation period of GR5J

5.2 Hydrological modeling with HEC-HMS

Calibration is the most important part of hydrological modeling, and its success guarantees a good outcome for the whole modeling process. As far as HEC HMS is concerned, this part was done according to each individual basin while respecting the normal procedure. It was done manually using the estimated parameters to obtain a good match between the simulated and observed data. Self-calibration through optimization trials available in the HEC-HMS model was used to optimize the model parameters, which differ from one basin to another. According to each river basin and each available piece of data, one half was used for the calibration, either 5 or 10 years depending on the study basins, and the other half for the optimization of the parameters using a systematic search procedure that gives the best match between the observed and calculated runoff. For the validation, the parameters obtained during the calibration with a good objective function are maintained and used with the rest of the basin data. The results obtained from each watershed are presented for each studied catchment.

5.2.1 Agneby watershed

For the Agneby watershed, the HEC-HMS model is calibrated based on the curve number loss method, and the calibration period was done using daily data from 1995–2000 with a good optimization parameter, while the validation was done from 2005–2010. Each parameter in HEC-HMS represents a distinct hydrologic condition. As a result, the sensitivity analysis in this study is performed on a number of distinct parameters. The model parameter optimization result, simulated result, baseflow, and observed flow hydrograms are detailed below:

Table 44: Optimization parameters of HEC HMS model for Agneby watershed

	Agneby/Parameters	**Optimized value**	**Unit**
1	Initial Abstraction	174.85	mm
2	Recession - Initial Discharge	4.42	m3/s
3	Recession - Threshold Discharge	0.14	m3/s
4	Simple Canopy - Initial Storage	29.56	%
5	Simple Canopy - Max Storage	11.83	mm
6	Lag time	10815.26	min
7	Curve number	98.86	

5.2.2 Baya watershed

The Baya watershed model is calibrated using the curve number loss approach. The calibration period employed daily data from 1995 to 1999 with a decent optimization parameter, and the validation period was from 2000 to 2003. The sensitivity analysis in this study is performed on a variety of separate parameters because each parameter in HEC-HMS reflects a distinct hydrologic state. The baseflow and observed flow hydrograms, optimization outcomes for model parameters, and simulated results are all reported in Table 46.

Table 45: Optimization parameters of HEC HMS model for Baya watershed

	Baya/Parameters	**Optimized value**	**Unit**
1	Initial Abstraction	2.84	mm
2	Recession -Threshold Discharge	64.82	m3/s
3	Simple Canopy - Initial Storage	11.52	%
4	Simple Canopy - Max Storage	66.39	mm
5	Lag time	28999.15	min
6	Curve number	95	

5.2.3 Bagoue watershed

With a good optimization parameter, the calibration period from 1982 to 1992 and the validation period from 1995 to 2005 were done using daily data for the Bagoue watershed. Because each parameter represents a distinct hydrologic condition, the sensitivity analysis in this study is carried out on a number of distinct parameters. The baseflow and observed flow hydrograms, model parameter optimization results, and simulated results are all detailed below in Table 47.

Table 46: Optimization parameters of HEC HMS model for Bagoue watershed

	Bagoue/Parameters	**Optimized value**	**Unit**
1	Initial Abstraction	307.50	mm
2	Recession - Initial Discharge	11.967	m3/s
3	Recession - Threshold Discharge	8.63	m3/s

4	Simple Canopy - Initial Storage	74.40	%
5	Simple Canopy - Max Storage	65.9	mm
6	Lag time	29000	min
7	Curve number	39	

5.2.4 Lobo watershed

The calibration period from 1990 to 1995 and the validation period from 1995 to 2005 were done using daily data for the Lobo watershed. The baseflow and observed flow hydrograms, model parameter optimization results, and simulated results are all detailed below (Table 48):

Table 47: Optimization parameters of HEC HMS model for Lobo watershed

	N'zo/Parameters	**Optimized value**	**Unit**
1	Initial Abstraction	32.41	mm
2	Recession - Initial Discharge	6.81	m3/s
3	Simple Canopy - Initial Storage	17.42	%
4	Simple Canopy - Max Storage	35.61	mm
5	Lag time	29335.83	min
6	Curve number	32.14	

5.2.5 N'zo watershed

The calibration period was from 1990 to 1995, and the validation period was from 2000 to 2010. The model parameter values were carefully adjusted until the results matched the observed data Table 49 summarizes the baseflow and observed flow hydrograms, model parameter optimization outcomes, and simulated results.

Table 48: Optimization parameters of HEC HMS model for N'zo watershed

	N'zo/Parameters	**Optimized value**	**Unit**
1	Initial Abstraction	331.59	mm
2	Recession - Initial Discharge	0.14	m3/s

3	Simple Canopy - Initial Storage	78.05	%
4	Simple Canopy - Max Storage	62.11	mm
5	Lag time	20573.83	min
6	Curve number	98.95	

5.3 Performance evaluation

In calibration simulated, a good performance was noted in the representation between the observed and simulated daily data for most of the models, with a value below 0.6 for the Nash. In the validation section, only the GR5J model showed a good performance with two watersheds (Lobo and N'zo); most of the others presented an underestimated performance. With the KGE function, the function indicated very good performance with the GR5J model with 0.6–0.7 regarding the calibration and validation parts, respectively. The PBIAS value has shown some negative values, highlighting how the HEC-HMS overestimated the value in both calibration and validation. The positive one shows the underestimation, while the value close to zero shows the great performance of the model. The different results are detailed in the different tables (Table 50 and Table 51) below.

Table 49: Performance evaluation for calibration period of GR4J, GR5J and HEC-HMS hydrological models

Watersheds	**Stations**	**GR4J**			**GR5J**			**HEC-HMS**		
	Calibration	Years	NSE	KGE	Years	NSE	KGE	Years	NSE	PBAIS (%)
Agneby	Agboville	1980 - 1990	0.05	-0.08	1980-1990	0.70	0.78	1980-1990	-0.86	7.64
Bagoue	Kouto	1981 - 1989	0.58	0.63	1981-1989	0.56	0.65	1981-1989	0.54	-2.47
Baya	Yebouakro	1986 - 1992	0.72	0.79	1986-1992	0.73	0.79	1986-1992	0.48	-10.18
	Nibehibe	1983 -	0.67	0.64	1983-1988	0.75	0.79			

Lobo		1988								
	Loboville	2006 - 2010	0.91	0.94	2006-2010	0.90	0.92	2006-2010	-1.53	20.82
N'Zo	Kahin	1983 - 1988	0.64	0.73	1983-1988	0.63	0.67	1983-1988	0.57	1.28

Table 50: Performance evaluation for validation period of GR4J, GR5J and HEC-HMS hydrological models

Watersheds	**Stations**	**GR4J**			**GR5J**			**HEC-HMS**		
	Validation	Years	NSE	KGE	Years	NSE	KGE	Years	NSE	PBAIS (%)
Agneby	Agboville	1991-2001	0.09	0.8	1991-2001	0.39	0.78	1991-2001	-3.9	33.68
Bagoue	Kouto	1990-1995	0.20	0.25	1990-1995	0.37	0.65	1995-2005	0.49	0.45
Baya	Yebouakro	1993-1998	0.38	0.42	1993-1998	0.42	0.79	1993-1998	0.15	14.97
Lobo	Nibehibe	1990-1995	0.25	0.20	1990-1995	0.62	0.79			
	Loboville	2011-2015	0.90	0.89	2011-2015	0.67	0.92	2011-2015	-1.9	57.72
N'Zo	Kahin	1995-2000	0.26	0.3	1990-1995	0.56	0.67	1990-1995	0.48	-30.41

5.4 Discussions

This section's objective was to assess how well the hydrological models GR4J, GR5J, and HEC-HMS perform in simulating floods and low flows. During the calibration process, the different models all showed a good overall result with the evaluation of the performance criteria. With the Nash and KGE criteria, the models showed a good calibration over the

different watersheds, showing that the models are acceptable and capable of reproducing extreme flows over all the climatic zones of the country, especially with the GR models. This result is in line with the work of Flores et al. (2021), who obtained remarkable values during the calibration of their models. With the HEC HMS model, the Nash showed an unsatisfactory result with often negative values and PBIAS values that indicate an overestimation or underestimation of the model in the simulation of hydrological extremes over the different study basins. In modeling, the process of validation is as crucial as that of calibration. Using different periods than those used for calibration, validation is performed after a successful calibration of the model's parameters. In our circumstance, the GR4J model was able to provide an acceptable outcome for the Lobo watershed with Nash values above 0.5; the GR5J model showed good validation with two watersheds (Lobo and N'zo), but overall, the HEC-HMS model provided Nash values below 0.5. Some watersheds have shown very good performance, which may be explained by the values of the various parameters selected are adequate for the data used during the various validation periods without frequently considering the significant climatic variability and the actual physical characteristics of the terrain. The low Nash values observed during validation on the other basins may be because the GR4J, GR5J, and HEC-HMS models either underestimate or overestimate the data observed on these basins due to either the high climatic variability of the area or the physical conditions of the terrain, and also due to the fact that a good calibration of the model parameters does not always guarantee a good validation. Because a successful fit does not always mean that a correct set of parameter values has been obtained, calibrations may frequently have been performed entirely by numerical curve fitting without considering whether the resulting parameter values are physically feasible. The studies by Brulebois et al. (2018) showed good performance during calibration and poor performance during validation of the GR4J model used. Hydrological balances were performed by GR models during the calibration and validation periods of the various basins. The results showed a dominance of the real evapotranspiration cycle, with a rise in temperature observed in the study basins. In both the calibration and validation processes, runoff showed lower values overall, which could be due to the lower rainfall observed or to the extent of land use in all the study basins. Infiltration had low values among the components of the water balance parameters, with values that were often negative, which could be due to strong runoff or soil type.

Conclusion

The goal of this part was to evaluate how effectively the hydrological models GR4J, GR5J, and HEC-HMS simulate floods and low flows. The hydrological simulation period was different in each basin with the three hydrological models. The evaluation of the performance of these different models was studied by three different functions, namely an objective function common to all three models (Nash), an objective function common to the GR models, which is the KGE, and an objective function specific to the HEC-HMS model, which is the PBAIS. These different functions allowed us to evaluate the two fundamental processes of hydrological simulation, which are calibration and validation. During the calibration process, all the performance evaluation criteria showed good performance, with values reaching 0.7, indicating a good optimization of the different key parameters. At validation, these criteria showed shortcomings in the appreciative validation values, which either underestimated or overestimated the study data. This study showed that under conditions of high climate variability, it would be preferable to model with the GR5J, which performed well under each climatic zone considered in the high and low flow simulation. It also showed that it is difficult to identify watershed-specific parameters with the HEC-HMS model, which performs badly with limitations in the simulation of high flows. In the context of climate change and the management of flood and drought flows, the GR5J model would be one of the most effective models in an African context where data is often lacking.

CHAPTER 6 : FUTURE PATTERNS AND TRENDS IN HYDRO-CLIMATIC EXTREMES UNDER RCP 4.5 AND RCP 8.5 SCENARIOS FROM 2020-2050

The results of the influence of land use change on extremes for each watershed in each climatic zone, as well as future trend analyses under RCP scenarios 4.5 and 8.5 on rainfall and discharge, are shown in Chapter 6. The impact of land use change on extremes is discussed in Section 6.1. The rainfall outcomes and future trend analyses for RCP scenarios 4.5 and 8.5 will be reported in Part 6.2. Future trend analysis for RCP scenarios 4.5 and 8.5 is presented in Section 6.3. This chapter focuses on the effects of climate change on patterns in each climatic zone.

6.1 Dynamic of land use change

6.1.1 Agneby watershed

The results of the change detection in land cover classes examined using the confusion matrices of multiple years selected, respectively 1987 and 2020 from Landsat 5 and 8 images, are shown in Table 51. The Kappa coefficients show a reasonably good degree of classification accuracy, with values ranging from 0.97 to 0.96 and low levels of confusion ranging from 8.33% to 13.33% amongst numerous classifications, including sparse forest, savannah, and agriculture. Figure 34 shows the decline in surface area over the years. This figure shows that the proportions vary from 1986 to 2017. And with the land use map, it is easy to see how each class is distributed across the study area (figure 35).

Table 51: Confusion matrix of Landsat 4 and 8 images from 1987 and 2020 for Agneby watershed

Agneby 1987	Water body	Primary forest	Sparse forest	Habitat/Bare	Crops land
Water body	**100.00**	0.00	0.00	0.00	0.00
Primary forest	0.00	**100.00**	8.33	0.00	0.00
Sparse forest	0.00	0.00	**91.67**		0.00
Habitat/Bare	0.00	0.00	0.00	**100.00**	0.00
Crops land	0.00	0.00	0.00	0.00	**100.00**
Total	100.00	100.00	100.00	100.00	100.00
Kappa Coefficient = 0.97					

Agneby 2020	Water body	Primary forest	Sparse forest	Habitat/Bare	Crops land
Water body	100.00	0.00	0.00	0.00	0.00
Primary forest	0.00	100.00	0.00	0.00	0.00
Sparse forest	0.00	0.00	86.67	0.00	0.00
Habitat/Bare	0.00	0.00	0.00	100.00	0.00
Crops land	0.00	0.00	13.33	0.00	100.00
Total	100.00	100.00	100.00	100.00	100.00
Kappa Coefficient = 0.96					

The spatial distribution map of land use classes for the years 1987 and 2020 derived from Landsat 4 and 8 pictures of the Agneby basin is used to evaluate categorization findings (Figure 36).

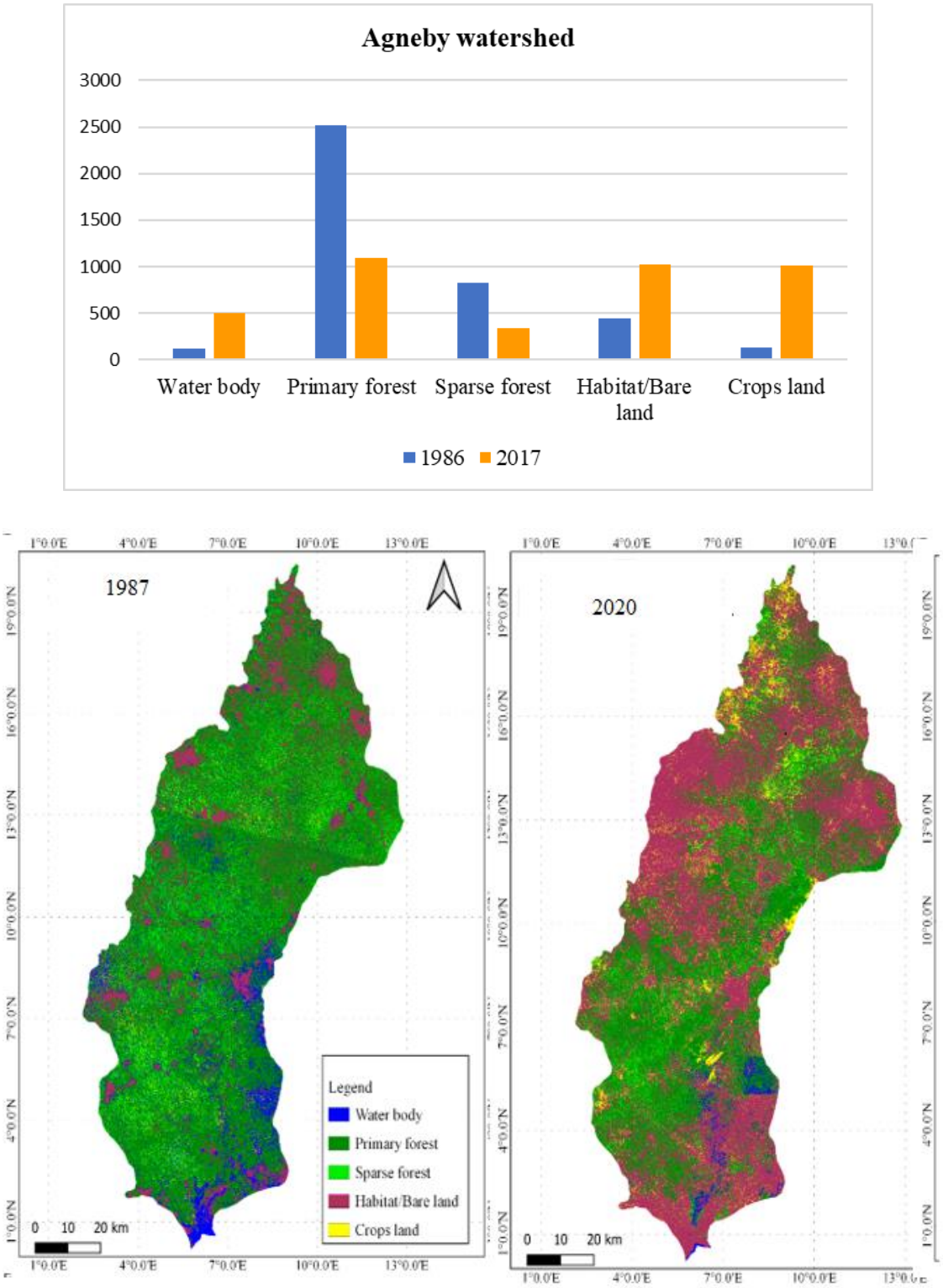

Figure 36: Distribution of land use classes in 1987 and 2020 for Agneby watershed

6.1.2 Bagoue watershed

The classification results from the confusion matrices for 1986, 2000, and 2017, respectively, and the Kappa coefficients (0.97, 0.97, and 0.98 for 1987, 2000, and 2017, respectively) reported in Table 52 indicate that the classifications are of good quality, with some low confusion between some classes such as the sparse forest, savannah, and crop land classes observed. Figure 37 shows the decline in surface area over the years. This figure shows that the proportions vary from 1986 to 2017.

Table 52: Confusion matrix of Landsat 5, 7 and 8 images from 1986, 2000 and 2017

Bagoue1986	**Water body**	**Sparse forest**	**Savannah**	**Habitat/Bare**	**Crops land**
Water body	**100.00**	0.00	0.00	0.00	0.00
Sparse forest	0.00	**100.00**	4.76	0.00	0.00
Savannah	0.00	0.00	**95.24**	0.00	10.00
Habitat/Bare	0.00	0.00	0.00	**100.00**	0.00
Crops land	0.00	0.00	0.00	0.00	**90.00**
Total	100.00	100.00	100.00	100.00	100.00
Kappa Coefficient = 0.97					
Bagoue 2000	**Water body**	**Sparse forest**	**Savannah**	**Habitat/Bare**	**Crops land**
Water body	**100.00**	0.00	0.00	0.00	0.00
Sparse forest	0.00	**95.83**	0.00	0.00	0.00
Savannah	0.00	4.17	**100.00**	4.35	0.00
Habitat/Bare	0.00	0.00	0.00	**95.65**	0.00
Crops land	0.00	0.00	0.00	0.00	**100.00**
Total	100.00	100.00	100.00	100.00	100.00
Kappa Coefficient = 0.97					
Bagoue 2017	**Water body**	**Sparse forest**	**Savannah**	**Habitat/Bare**	**Crops land**

Water body	**100.00**	0.00	0.00	0.00	0.00
Sparse forest	0.00	**100.00**	0.00	0.00	3.70
Savannah	0.00	0.00	**96.43**	0.00	0.00
Habitat/Bare	0.00	0.00	0.00	**100.00**	0.00
Crops land	0.00	0.00	3.70	0.00	**96.43**
Total	100.00	100.00	100.00	100.00	100.00
Kappa Coefficient = 0.98					

Evaluation of classification results from the spatial distribution map of land use classes of selected years 1986, 2000 and 2017 of Landsat 5, 7 and 8 images of the Bagoue river basin respectively (Figure 37).

Figure 37: Distribution of land use classes in 1986, 2000 and 2017

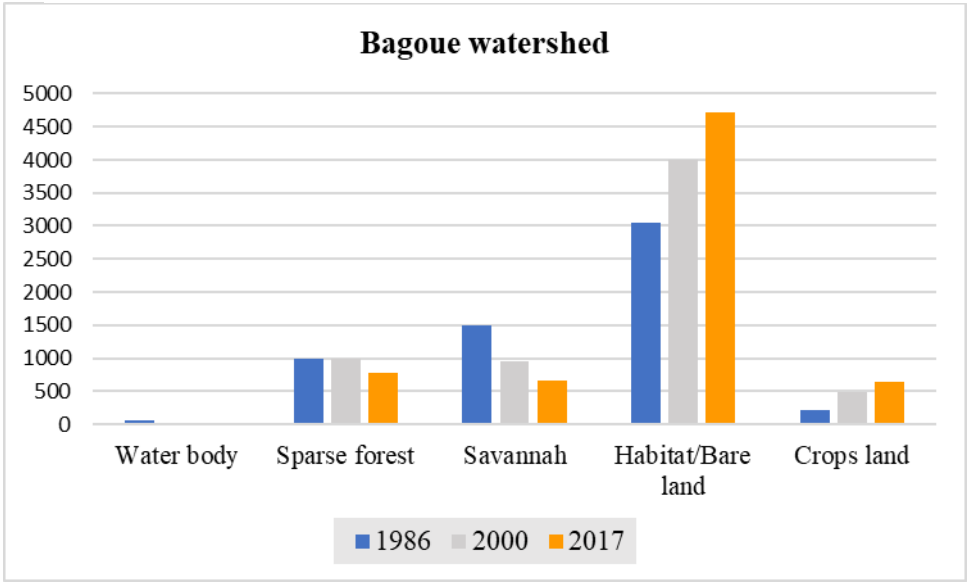

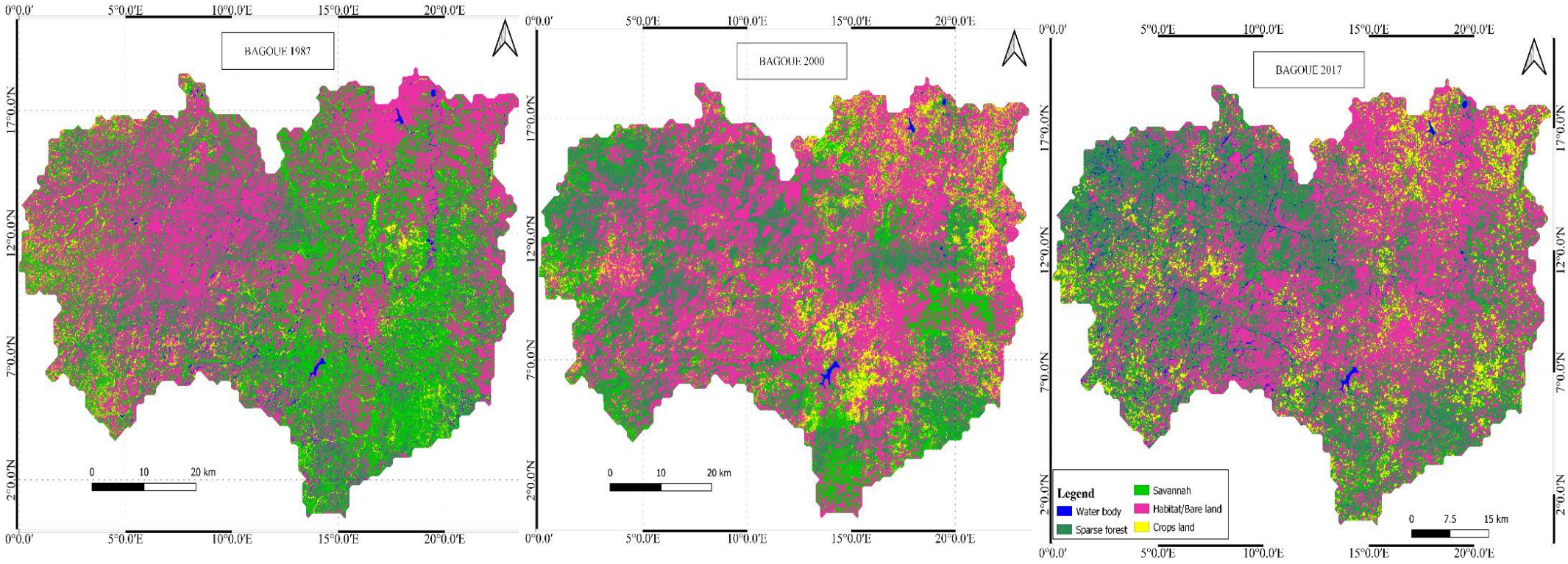

Figure 38: Land use maps of Bagoue watershed in 1987,2020 and 2017

6.1.3 Baya watershed

Table 53 displays the outcomes of the evaluation of the Landsat 5, 7, and 8 images data from the years 1986, 2000, and 2017 for the land cover class change detection. The values of the Kappa coefficients, which range from 0.96 to 0.98, indicate a rather high level of classification accuracy. There is little overlap between some classes, such as sparse woodland, savannah, and cropland, which are all seen. Figure 39 shows the decline in surface area over the years. This figure shows that the proportions vary from 1986 to 2017.

Table 53: Confusion matrix of Landsat 5, 7 and 8 images from 1986, 2000 and 2017

Baya1986	**Water body**	**Sparse forest**	**Savannah**	**Habitat/Bare**	**Crops land**
Water body	**100.00**	0.00	0.00	0.00	0.00
Sparse forest	0.00	**92.31**	7.14	0.00	0.00
Savannah	0.00	7.69	**92.86**	0.00	0.00
Habitat/Bare	0.00	0.00	0.00	**100.00**	0.00
Crops land	0.00	0.00	0.00	0.00	**100.00**
Total	100.00	100.00	100.00	100.00	100.00
Kappa Coefficient = 0.96					

Baya 2000	**Water body**	**Sparse forest**	**Savannah**	**Habitat/Bare**	**Crops land**
Water body	**100.00**	0.00	0.00	0.00	0.00
Sparse forest	0.00	**86.25**	0.00	0.00	0.00
Savannah	0.00	8.75	**96.72**	0.00	2.28
Habitat/Bare	0.00	0.00	0.00	**100.00**	0.00

Crops land	0.00	5.00	3.28		**97.72**
Total	100.00	100.00	100.00	100.00	100.00
Kappa Coefficient = 0.89					

Baya 2017	**Water body**	**Sparse forest**	**Savannah**	**Habitat/Bare**	**Crops land**
Water body	**100**	0.00	0.00	0.00	0.00
Sparse forest	0.00	**92.86**	0.00	0.00	0.00
Savannah	0.00	7.14	**100**	0.00	0.00
Habitat/Bare	0.00	0.00	0.00	**100**	0.00
Crops land	0.00	0.00	0.00	0.00	**100**
Total	100	100	100	100	100
Kappa Coefficient = 0.98					

Landsat 5, 7, and 8 pictures from the years 1986, 2000, and 2017 were used to evaluate the classification results from the geographic distribution map of the land cover classes, accordingly (Figure 39).

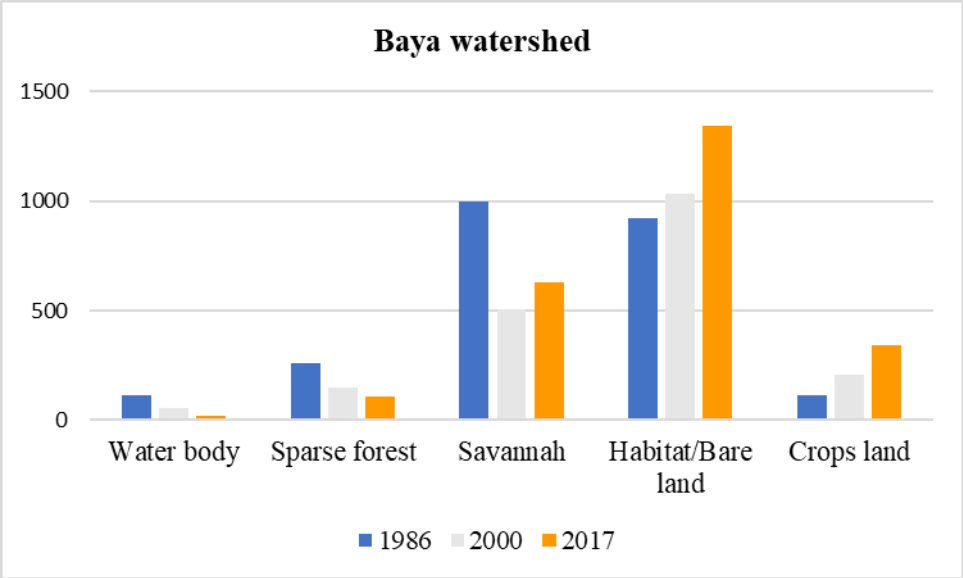

Figure 39: Distribution of land use classes in 1986, 2000 and 2017

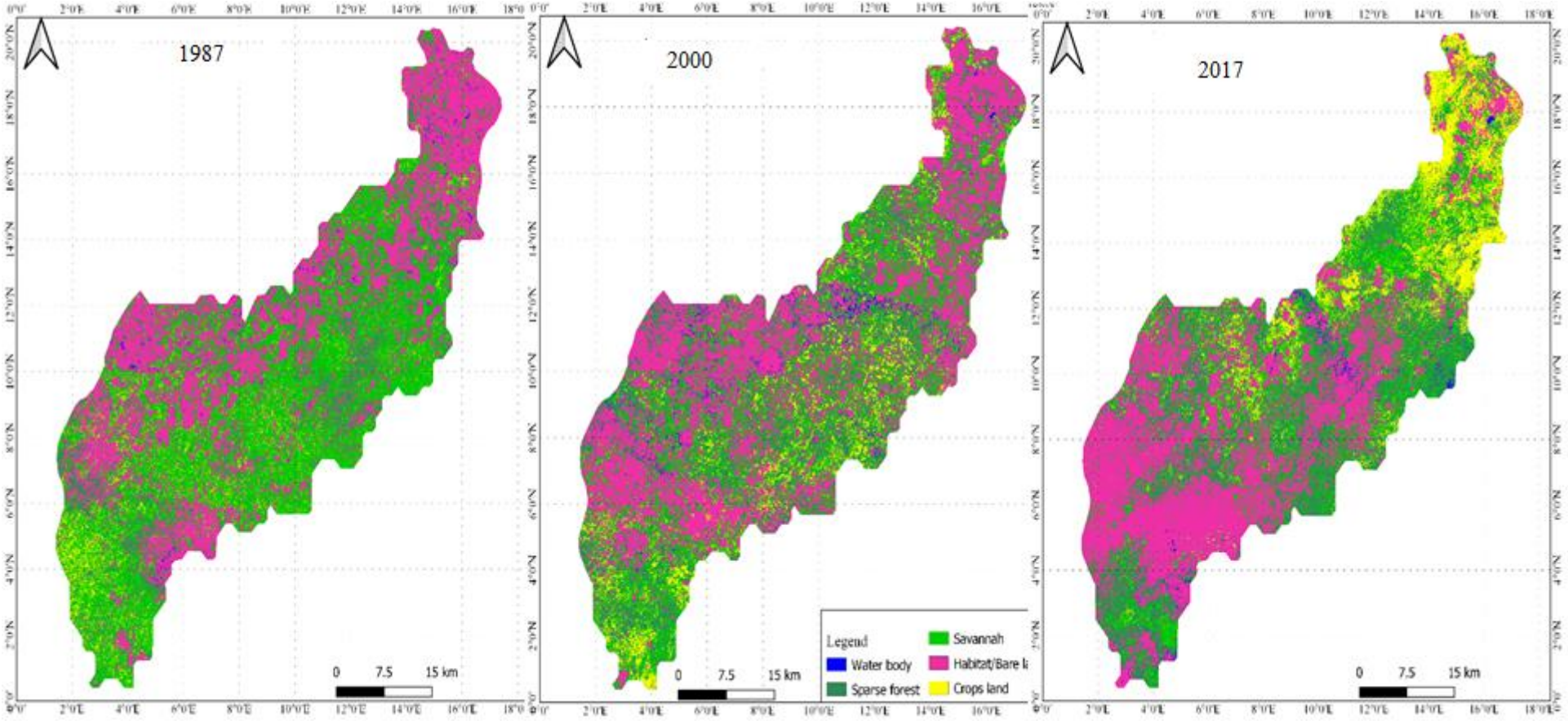

Figure 40: Land use maps of Baya watershed in 1987,2000 and 2017

6.1.3 Lobo watershed

Table 54 shows the results of the evaluation of the land cover class change detection using the confusion matrices of the different years chosen, respectively, 1986 and 2017, using Landsat 5 and 8 images. With values ranging between 0.95 and 0.96, the Kappa coefficients show a rather good level of classification accuracy, with some little misunderstanding between some classifications, such as the sparse woodland, savannah, and crop land types mentioned. Figure 41 shows the decline in surface area over the years. This figure shows that the proportions vary from 1986 to 2017.

Table 54 : Confusion matrix of Landsat 5and 8 images from 1986 and 2017 for Lobo watershed

Lobo 1986	**Water body**	**Primary forest**	**Sparse forest**	**Habitat/Bare**	**Crops land**
Water body	**100.00**	0.00	0.00	0.00	0.00
Primary forest	0.00	**90.48**	0.00	0.00	0.00
Sparse forest	0.00	9.52	**100.00**		7.14
Habitat/Bare	0.00	0.00	0.00	**100.00**	0.00
Crops land	0.00	0.00	0.00	0.00	**92.86**
Total	100.00	100.00	100.00	100.00	100.00
Kappa Coefficient = 0.95					

Lobo 2017	Water body	Primary forest	Sparse forest	Habitat/Bare land	Crops land
Water body	100.00	0.00	0.00	0.00	0.00
Primary forest	0.00	95.65	5.56	0.00	0.00
Sparse forest	0.00	4.35	88.89	0.00	0.00
Habitat/Bare	0.00	0.00		100.00	0.00
Crops land	0.00	0.00	5.56	0.00	100.00
Total	100.00	100.00	100.00	100.00	100.00
Kappa Coefficient = 0.96					

Analysis of the categorization outcomes from the spatial distribution map of the chosen land cover classes from the chosen Landsat 5 and 8 images years of 1986 and 2017, respectively (Figure 41).

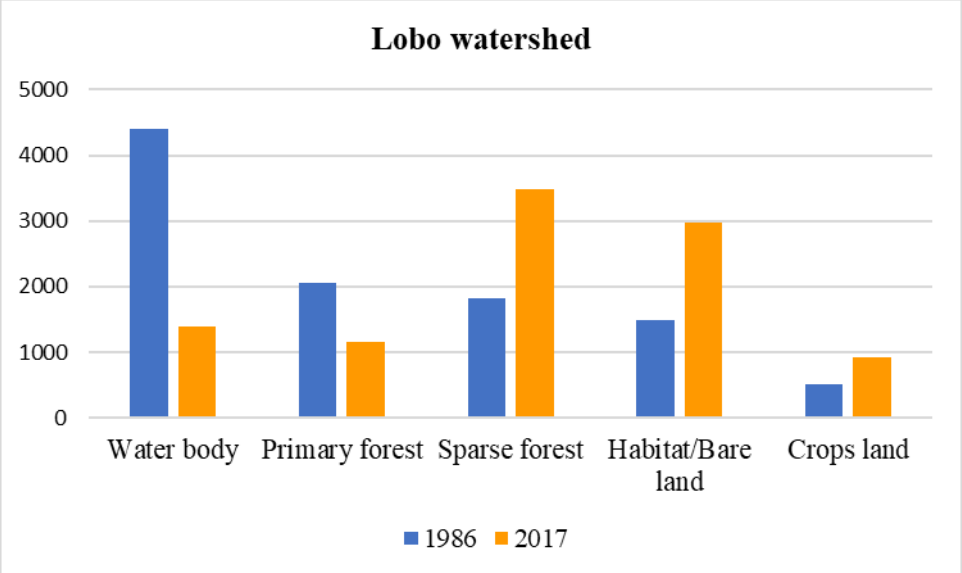

Figure 41: Distribution of land use classes in 1986 and 2017 for Lobo watershed

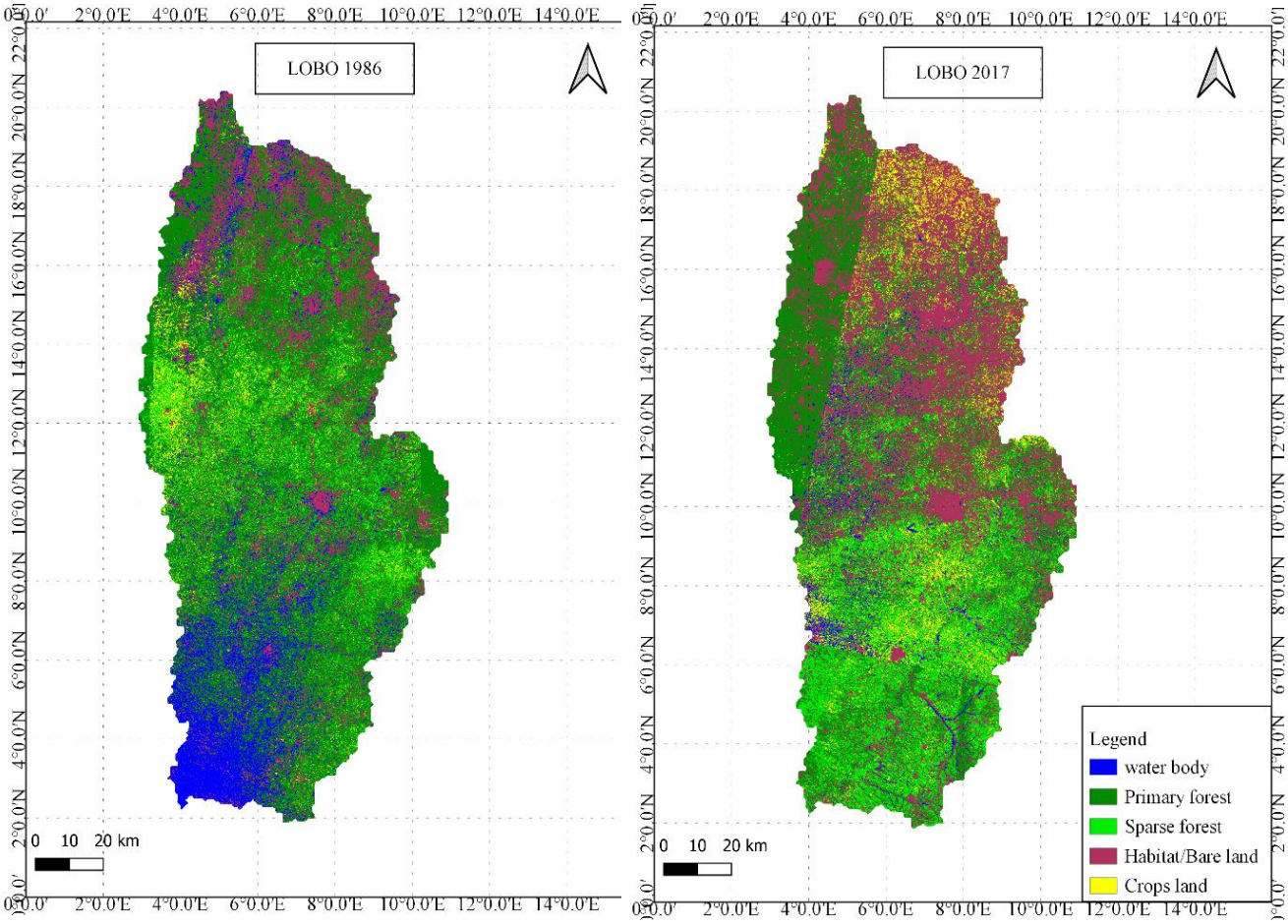

Figure 42: Land use maps of Lobo watershed in 1986 and 2017

6.1.4 N'zo watershed

The Kappa coefficient and the confusion matrices for the three different years of Landsat 5, 7, and 8 pictures, respectively, 1985, 2000, and 2017, are shown in Table 55. While there is some low confusion between some classes, such as the sparse forest and savannah classes observed, the results of the detection of changes in the land cover classes evaluated as well as the Kappa coefficients indicate a fairly good quality of the classifications performed, with values between 0.97, 0.98, and 0.96, respectively. Figure 43 shows the decline in surface area over the years. This figure shows that the proportions vary from 1986 to 2017.

Table 54: Confusion matrix of Landsat 5, 7 and 8 images from 1986, 2000 and 2017 for N'zo

N'zo 1985	**Water body**	**Primary forest**	**Sparse forest**	**Habitat/Bare**	**Crops land**
Water body	**100.00**	0.00	0.00	0.00	0.00
Primary forest	0.00	**93.75**	0.00	0.00	0.00
Sparse forest	0.00	6.25	**100.00**	0.00	0.00
Habitat/Bare	0.00	0.00	0.00	**100.00**	0.00
Crops land	0.00	0.00	0.00	0.00	**100.00**
Total	100.00	100.00	100.00	100.00	100.00
Kappa Coefficient = 0.98					

N'zo 2000	Water body	Primary forest	Sparse forest	Habitat/Bare	Crops land
Water body	**100.00**	0.00	0.00	0.00	0.00
Primary forest	0.00	**97.44**	0.00	0.00	0.00
Sparse forest	0.00	2.56	**100.00**	0.00	0.00
Habitat/Bare	0.00	0.00	0.00	**100.00**	0.00
Crops land	0.00	0.00	0.00	0.00	**100.00**
Total	100.00	100.00	100.00	100.00	100.00
Kappa Coefficient = 0.98					

N'zo 2017	Water body	Primary forest	Sparse forest	Habitat/Bare	Crops land
Water body	**100.00**	0.00	0.00	0.00	0.00
Primary forest	0.00	**94.12**	5.00	0.00	0.00
Sparse forest	0.00	5.88	**95.00**	0.00	0.00
Habitat/Bare	0.00	0.00	0.00	**100.00**	0.00
Crops land	0.00	0.00	0.00	0.00	**100.00**
Total	100.00	100.00	100.00	100.00	100.00
Kappa Coefficient = 0.96					

Figure 44 shows the spatial distribution map of the several selected classes from the chosen Landsat 5, 7, and 8 images years of 1986, 2000, and 2017, respectively, provides the results of the classification evaluation.

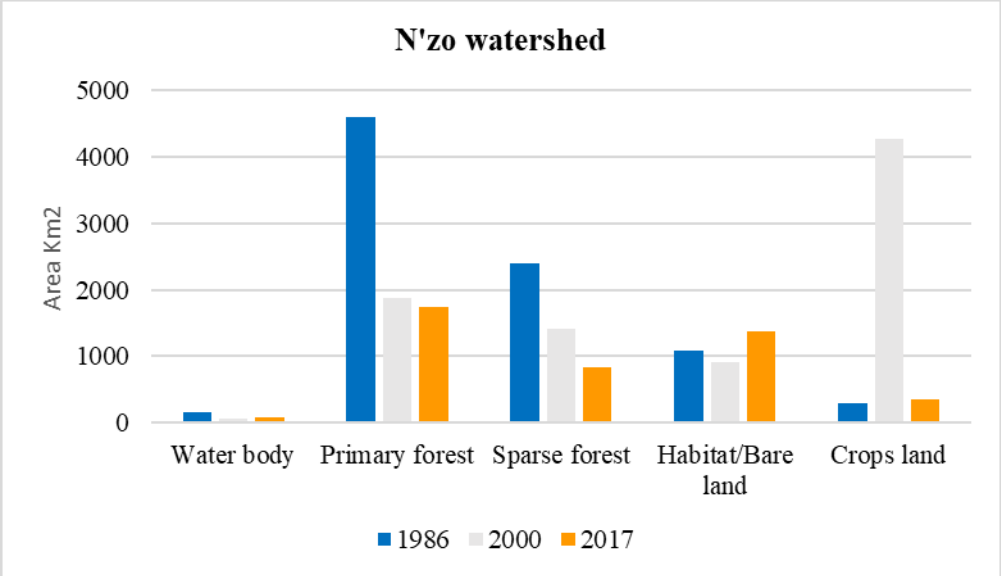

Figure 43: Distribution of land use classes in 1986, 2000 and 2017 for N'zo watershed

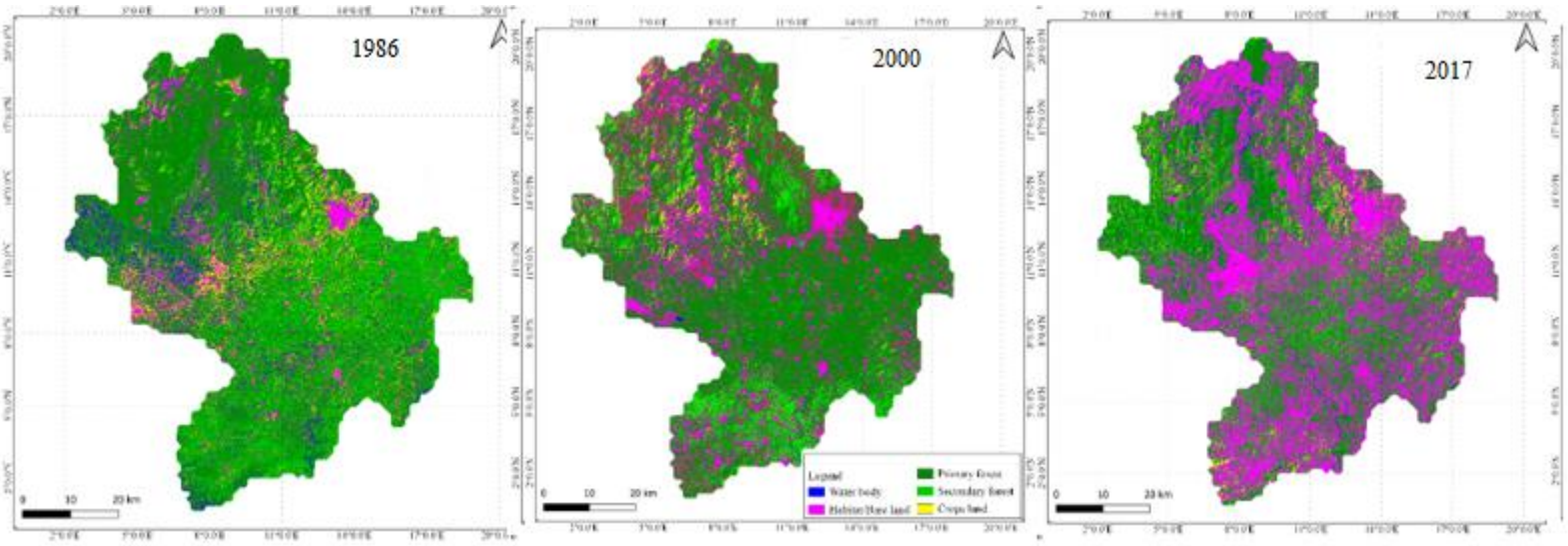

Figure 44: Land use maps of N’zo watershed in 1986, 2000 and 2017

6.2 Investigation of occupation dynamics

6.2.1 Determination of rate of change

a. Agneby watershed

The watershed in the south of Cote d'Ivoire is shown in Table 56 as the result of the land cover class change detection evaluated from the area of the various classes selected from the Landsat 4 and 8 pictures taken in 1987 and 2020, respectively. Between 1987 and 2020, we can see a decrease in the classes of water body, main forest, and sparse forest of 52.44%, 94.89%, and 62.12%, respectively. Between 1987 and 2020, the areas of the habitat/bare land and crop land classifications increased by 91.01% and 51.46%, respectively.

Table 55: Distribution of land use classes in 1987 and 2020 and annual rate of change for Agneby watershed

Agneby	**Area Km²**		**Annual rate of change (%)**
Classes	**1987**	**2020**	**1987-2020**
Water body	123.72	502.48	306.14
Primary forest	2519.72	1097	**-56.46**
Sparse forest	828.51	334.2	**-59.66**
Habitat/Bare land	445.68	1018	128.41
Crops land	125.74	1012	704.83

b. Bagoue watershed

The evaluation of the classification results based on the area of the different selected classes and the annual rate of change of the occupancy units in the selected years 1986, 2000, and 2017, respectively, is shown in the table below. We can observe that from one year to another, the area of the classes differs. The different classes have undergone quite significant regressions in their evolution. Thus, from 1986 to 2017, we observed a regression of 70% of the water body class, 5.7% of the habitat/bare land class, and 30.37% of the crop land class. The sparse forest and savannah classes increased by 25.77% and 11.96%, respectively.

Table 56: Distribution of land use classes in 1986, 2000 and 2017 and Annual rate of change

Bagoue	**Area Km²**			**Annual rate of change (%)**		
Classes	**1986**	**2000**	**2017**	**1986-2000**	**2000-2017**	**1986-2017**
Water body	65.61	8.06	19.06	**-87.71**	136.47	**-70.94**
Sparse forest	991.65	882.73	781.33	**-12.33**	**-12.97**	**-21.209**
Savannah	1500	952.31	670.71	**-57.51**	**-41.98**	**-55.28**
Habitat/Bare land	4239.4	4001.04	4709.26	**-5.95**	15.03	11.08
Crops land	212.45	491.74	647.89	95.67	24.10	204.96

c. Baya watershed

Table 58 shows the results of an examination of changes in land cover classes based on the area of the various classes selected using Landsat 5, 7, and 8 images from 1986, 2000, and 2017, respectively. With a progression of 167.15% from 1986 to 2017, we can notice a progression of the water body class with each passing year of observation. Furthermore, the habitat/bare land class has risen by 424.34%. With the exception of the Savannah class, which saw a 36.68% regression from 1986 to 2017, we see a rise in all of the classes from 1986 to 2017.

Table 57: Distribution of land use classes in 1986, 2000 and 2017 and Annual rate of change

Baya	**Area Km^2**			**Annual rate of change Tc (%)**		
Classes	**1986**	**2000**	**2017**	**1986-2000**	**2000-2017**	**1986-2017**
Water body	110	57.14	19.38	**-48.05**	**-66.08**	**-82.38**
Sparse forest	258.1	150.2	106.45	**-71.83**	**-41.09**	**-58.75**
Savannah	995.97	504.12	630.61	**-97.56**	20.05	**-36.68**
Habitat/Bare land	923.41	1031.1	1341.91	10.44	23.16	45.32
Crops land	112.54	205	339.42	45.10	39.602	201.59

d. Lobo watershed

The Lobo watershed in central western Cote d'Ivoire is illustrated in Table 59 as a result of land cover class change identification using Landsat 5 and 8 data from 1988 and 2017, respectively. From 1987 to 2017, the percentages for, sparse forest, habitat/bare land, and crop land were 90.90%, 19.53%, and 76.36%, respectively. Between 1985 and 2017, the area of the water body and primary forest class dropped by 95.24% and 91.05%.

Table 58: Distribution of land use classes in 1986 and 2017 and Annual rate of change for Lobo watershed

Lobo	**Area Km^2**		**Annual rate of change (%)**
Classes	**1986**	**2017**	**1987-2017**
Water body	4412.06	1399.78	**-68.27**
Primary forest	2056.74	1157.6	**-43.71**
Sparse forest	1826.78	3487.36	90.90
Habitat/Bare land	1490.07	2976.82	99.77
Crops land	520.21	917.46	76.36

e. N'zo watershed

The N'Zo watershed in western Cote d'Ivoire is covered by Landsat 5, 7, and 8 images. Table 60 displays the results of the land cover class change detection evaluation for the regions of the different classes selected with the years 1987, 2000, and 2018, respectively. From 1987 to 2017, there was a progression in the habitat/bare land and crop land classifications, with percentages of 25.36% and 21.61%, respectively. Between 1985 and 2017, there was a 45.06%, 62.03%, and 65.38% regression in the area for the water body, main forest, and sparse forest classes, respectively.

Table 59: Distribution of land use classes in 1986, 2000 and 2017 and Annual rate of change for N'zo watershed

N'zo	**Area Km^2**			**Annual rate of change Tc(%)**		
Classes	**1987**	**2000**	**2017**	**1987-2000**	**2000-2017**	**1987-2017**
Water body	158.675	66.651	87.174	**-58**	30.79	**-45.06**
Primary forest	4598.210	1884.545	1745.532	**-14.39**	**-7.96**	**-62.04**
Sparse forest	2396.588	1405.127	829.672	**-70.56**	**-69.36**	**-65.38**
Habitat/Bare land	1095.406	907.125	1373.210	**-20.76**	33.94	25.36
Crops land	294.282	4279.714	357.906	93.12	**-10.95**	21.62

6.2.2 Relationships between extremes rainfall indices and vegetation dynamic

The relationship between changes in the NDVI indices and extreme rainfall indices was very weak overall, with a negative correlation on most of the extreme indices. The Pearson correlation test showed no significant correlation between the rainfall extremes indices except at the N'Zo catchment, where the test showed a significant correlation between the NDVI indices and the Rx5days and R95p extremes indices.

Table 60: Relationships between extremes rainfall indices and vegetation dynamic

	Pmaxan			**R95p**			**Rx5days**			**CDD**		
Watersheds	t	p-value	cor	t	p-value	cor	t	p-value	cor	t	p-value	cor
Agneby	1.185	0.25	0.245	-0.34	0.73	-0.07	-0.40	0.69	-0.08	0.18	0.85	0.04

Bagoue	-0.65	0.52	-0.12	-0.584	0.56	-0.10	-0.61	0.54	-0.11	-0.88	0.38	-0.16
Baya	-1.20	0.23	-0.222	-1.39	0.17	-0.25	-1.25	0.22	-0.23	-1.42	0.16	-0.25
Lobo	-0.01	0.99	-0.001	-0.203	0.84	-0.04	-1.99	0.058	-0.39	-1.48	0.15	-0.30
N'zo	-1.74	0.092	-0.31	**-3.022**	**0.005**	**-0.49**	-2.72	**0.010**	**-0.45**	0.82	0.41	0.15

Bold= significant correlation

6.2.3 Relationships between extremes discharge indices and vegetation indices

Table 62 below shows the relationship between changes in the vegetation index and discharge extreme indices. It can be seen that most of the extreme indices were positively correlated to the NDVI indices, even though they were not significant. The Pearson correlation test showed a not significant correlation with the NDVI indices for the high discharge indices and some of the low discharge indices except at the N'zo catchment, where the test showed a significant correlation between the NDVI indices and the QMNA low discharge indices.

Table 61: Relationships between extremes discharge indices and vegetation indices Bold= significant correlation

	High discharge indices									**Low discharge indices**										
	Qmaxan			VCX30			QX5-days			Qminan			QMNA			VCN7			WDF		
Watersheds	t	p-value	cor	t	p-value	cor	t	p-value	cor	t	p-value	cor	t	p-value	cor	t	p-value	cor	t	p-value	cor
AGNEBY	1.31	0.20	0.27	0.53	0.59	0.11	1.54	0.14	0.31	1.27	0.22	0.26	-0.39	0.69	-0.085	-0.38	0.70	-0.08	0.95	0.35	0.20
BAGOUE	0.77	0.44	0.142	0.46	0.6441	0.086	0.33	0.74	0.06	-0.75	0.45	-0.139	-0.60	0.548	-0.11	-0.18	0.85	-0.034	-0.88	0.382	-0.162
BAYA	-1.13	0.27	-0.28	-0.79	0.43	-0.202	-0.79	0.43	-0.202	-0.31	0.75	-0.081	-0.08	0.93	-0.021	-0.81	0.43	-0.205	-0.36	0.72	-0.094
LOBO	-0.13	0.89	-0.029	-0.087	0.930	-0.018	-0.133	0.89	-0.028	1.03	0.31	0.215	0.214	0.83	0.045	-0.087	0.93	-0.018	1.13	0.26	0.23
NZO	0.56	0.57	0.106	1.01	0.31	0.188	0.821	0.41	0.153	1.96	0.059	0.347	**2.06**	**0.047**	**0.364**	1.197	0.241	0.22	0.74	0.46	0.139

6.2.4 Water retention capacity for each watershed

Figure 45 depicts the results of each watershed's water retention capacity over the several years of land use map observations. It is clear that all of the selected land use classifications have seen their water retention capacity decline over time in all of our study basins. This demonstrates that these basins are very dynamic, with little vegetation cover, and thus more susceptible to runoff intensification, including flooding in some areas.

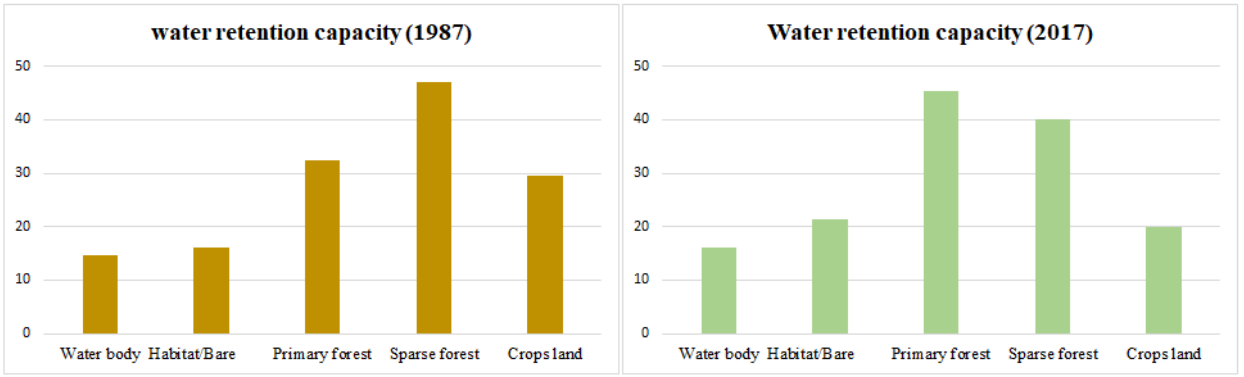

Agneby watershed

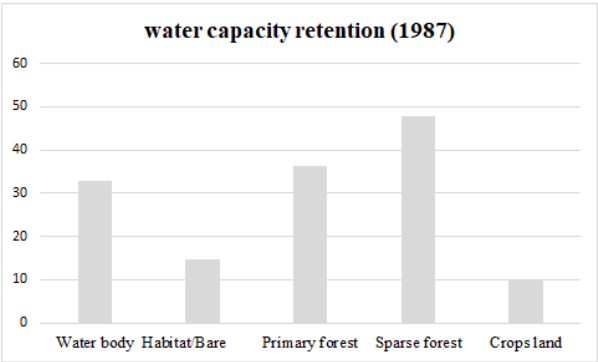

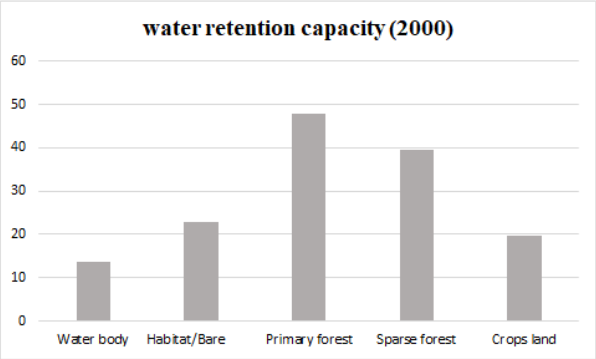

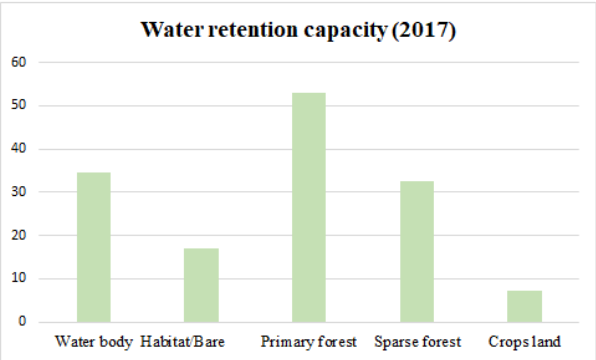

Bagoue watershed

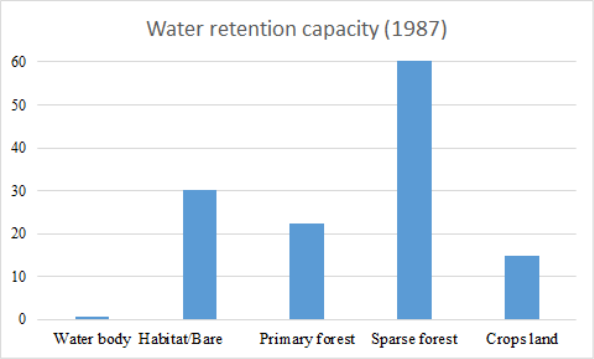

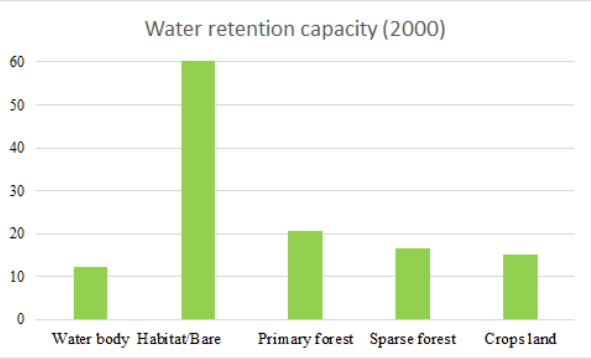

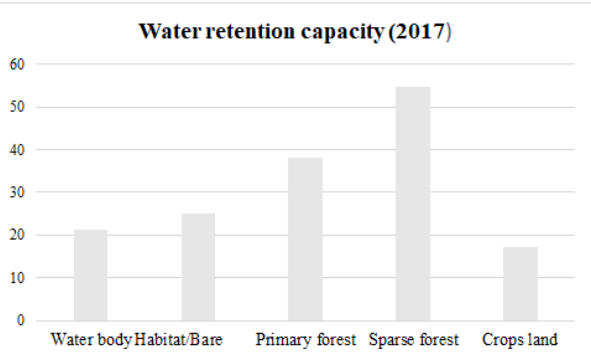

Baya watershed

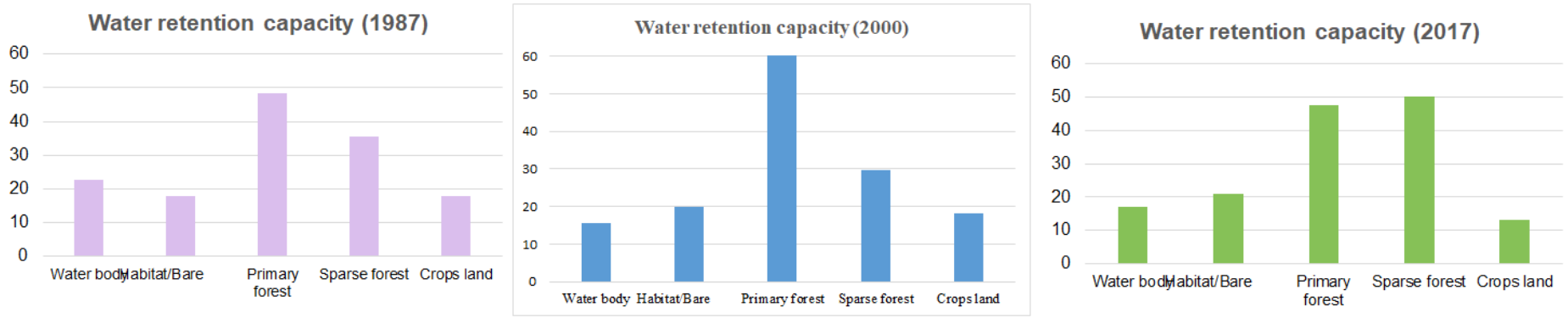

N'zo watershed

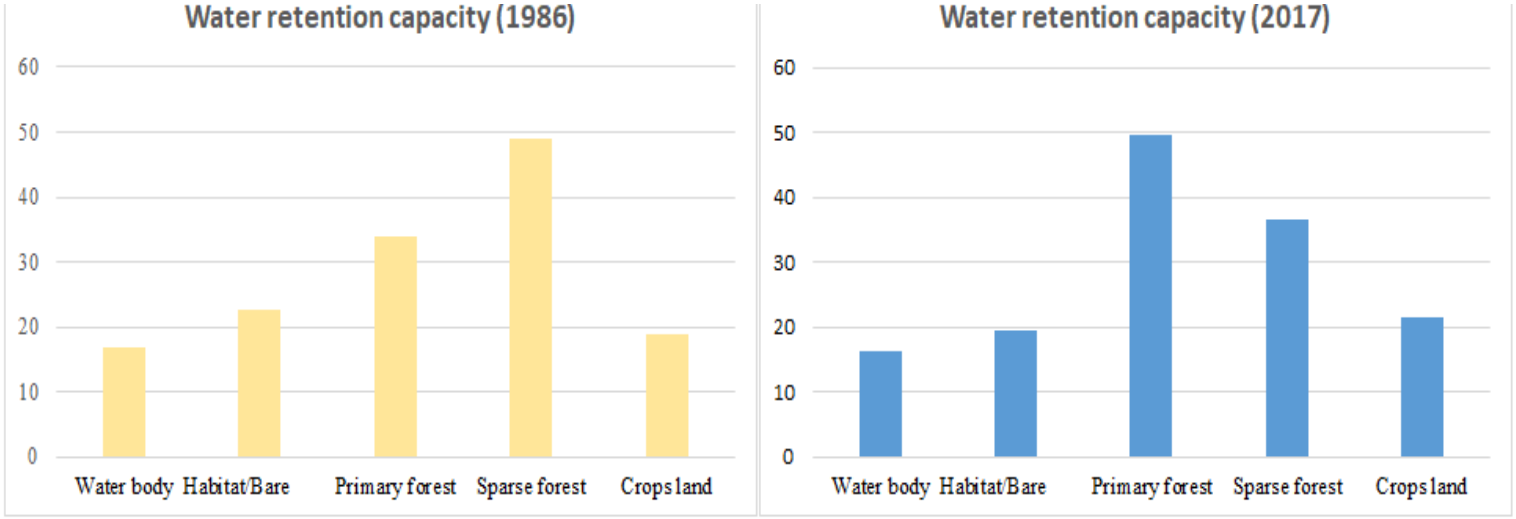

Lobo watershed

Figure 45 : Water retention capacity for each watershed

In general, all the selected classes have changed either downwards or upwards. In the Agneby basin (1987–2017) in climatic zone I, habitat/bare land and crop land experienced decreases, while the other classes each experienced gains in area. From 1986 to 2017, the Baya basin in climatic zone II in the east saw a significant increase in the area of nearly all of the selected classes, with the exception of the savannah class, which saw a decrease. In the Lobo basin in the center-west, still in the same climatic zone, from 1987–2017, only the water resources class experienced a decrease in its area; the other classes had gains in their different areas. In the Bagoue basin, climatic zone III, during 1986–2017, the sparse forest and savannah classes have witnessed a rise. Although the water body, habitat/barren land, and crop land classes suffered a large reduction in their separate surplus areas by 71%, 6%, and 30%, respectively, In the N'zo catchment in climatic zone IV, the surplus areas of the water body, primary forest, and sparse forest classes have significantly decreased between 1987 and 2017, while those of habitat/bare land and cropland have increased marginally. And also, for the investigation of the dynamics, it can be noticed that all the watersheds are somewhat more dynamic, as evidenced by the change in rate, the relationship between extreme indices and vegetation dynamics (NDVI), and the water retention capacity for each catchment area.

6.3 Future pattern and trend in the extreme rainfall RCP scenario

6.3.1 Evaluation of the performance RCMs data

Figure showed the results of the evaluation of the performance of the RCMs data. It can see that after bias correction, statistics are the best one. The mean absolute error (MAE) before was comprised between [0-1600] depending of each model and after bias correction showed a value between [0-600] depending of each model. The percent bias (PBAIS), before the bias correction indicated at some stations an overestimation or underestimation of the values but after bias almost of the values indicated “0” meaning no systematic difference between simulated and observed amounts.

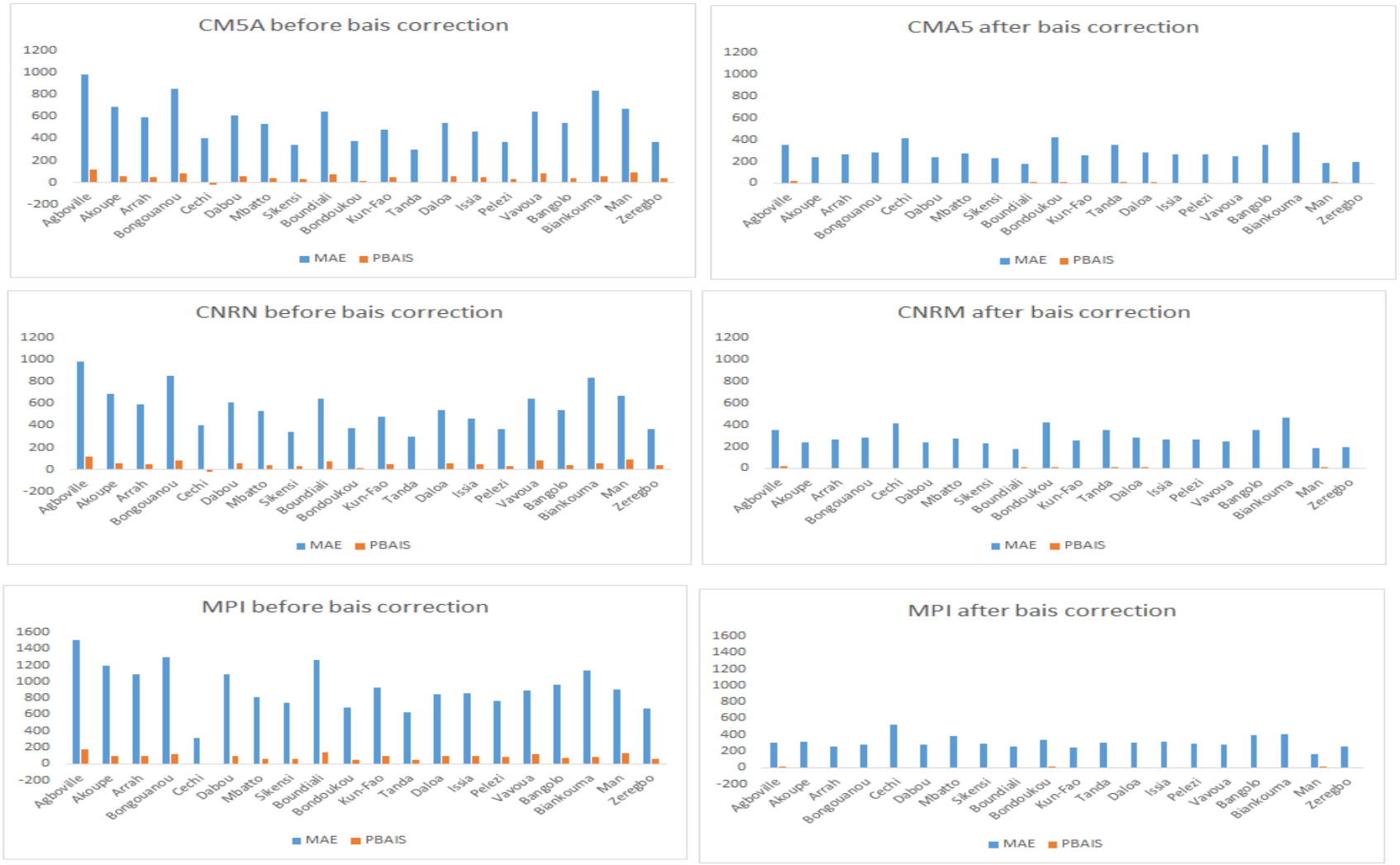

Figure 46: Evaluation of the performance RCMs data

6.3.2 Change in climate patterns under RCP 4.5 and RCP 8.5 scenarios

6.3.2.1 Rainfall pattern

Table 63 predictions are different from one catchment to another, with either a decrease or an increase in the studied parameters. For the Agneby catchment, the scenarios predicted an increase value of 0.92% for the RCP 4.5 scenario with 1828.76mm/year. In the same way, the RCP 8.5 shows 1892.30mm/year, i.e., an increase of 4.25% regarding the historical period (1976–2005). For the Bagoue basin, the scenarios predicted a decrease in rainfall over the period 2021–2050 for the scenario RCP4.5 of 1294.72 mm/year and an increase for the scenario RCP8.5 of 0.64% with an annual rainfall of 1381.88 mm/year. The Baya watershed will experience an overall decrease in precipitation over the period 2021–2050 for the RCP4.5 and RCP8.5 scenarios, from 1622.70 mm/year to 1535.92 mm/year, respectively. The projections for the Lobo River basin are increasing. The annual rainfall will increase by 11.81% with 1750.28 mm/year under RCP4.5 and by 15.77% with 1832.48 mm/year under RCP8.5. The N'Zo basin in the western part of the country will also be exposed to the effects of climate change. It will experience a decrease in annual rainfall over the period 2021–2050. The RCP4.5 scenario predicts an annual rainfall of 1633.03 mm/year, or -12.55% rate of change, and the RCP8.5 scenario predicts an annual rainfall of 1557.14 mm/year, or -18.04 rate of change.

Table 62: Annual rainfall pattern under RCP scenario

Annual Rainfall (mm)					
Watersheds	Historical (1976-2005)	RCP4.5 (2020-2050)	Rate change%	RCP 8.5 (2020-2050)	Rate change%
Agneby	1811.93	1892.30	4.25	1828.76	0.92
Bagoue	1373.04	1294.72	**-6.05**	1381.88	0.64
Baya	1633.93	1622.70	**-0.69**	1535.92	**-6.38**
Lobo	1543.41	1750.28	11.81	1832.48	15.77
N’zo	1838.06	1633.03	**-12.55**	1557.14	**-18.04**

6.3.2.2 Temperature pattern

The future predictions are different from one catchment to another, with either a slight increase or a great increase in the temperature with reference (1976–2005). For the Agneby catchment, the scenarios predicted an increase in the pattern of temperature. It will be 30.55°C under RCP4.5 scenarios and 32.18°C under RCP8.5. For the Bagoue watershed, it will also increase from 30.86°C under RCP4.5 to 33.46°C under RCP8.5 scenarios. In the same way, under the Baya watershed, the forecast will move from 31.89°C under RCP4.5 to 32.05°C under RCP8.5. The Lobo and N'Zo watersheds will also follow the same pattern, with an increase in their different temperatures. For Lobo, we will see an increase from 31.39°C under RCP4.5 to 34.72°C under RCP8.5; N'zo, in the same way, will expect an increase from 29.41°C under RCP4.5 to 33°C under RCP8.5.

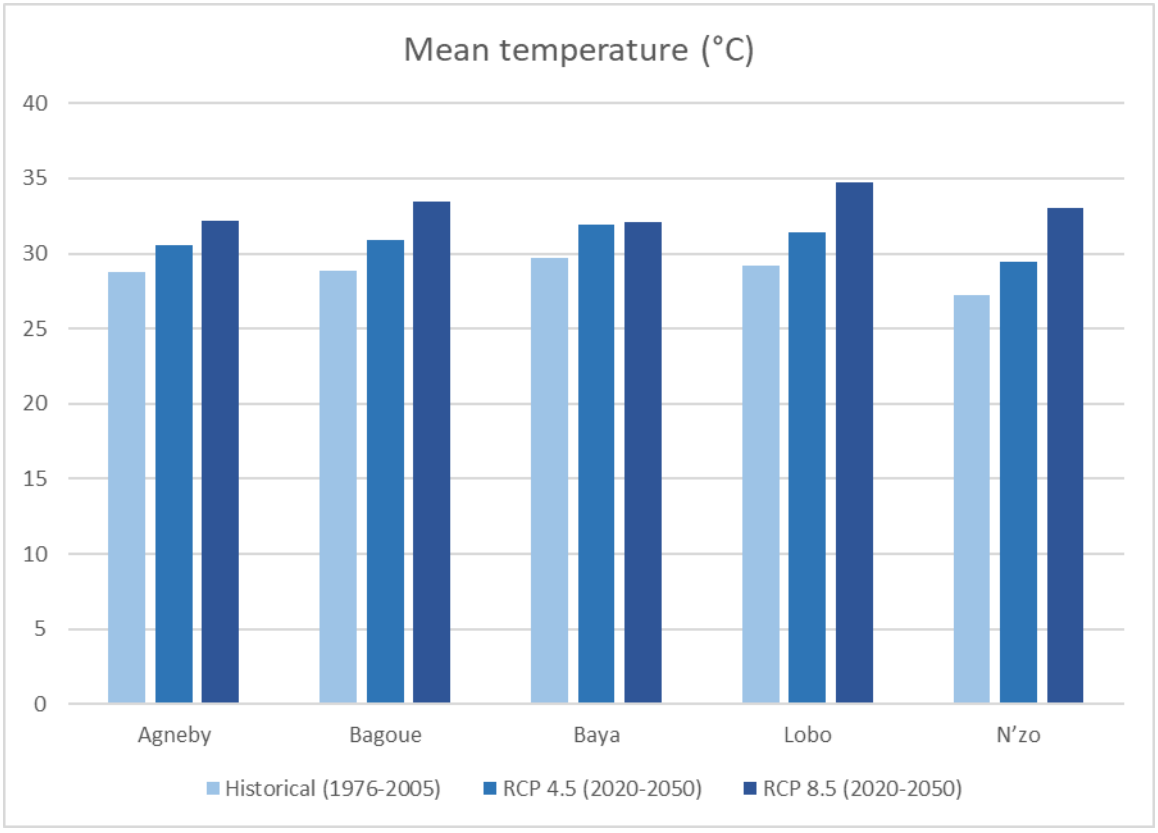

Figure 47: Mean temperature pattern under RCP scenario

6.3.2.3 Evapotranspiration pattern

The projections on evapotranspiration in each watershed are presented below. Agneby watershed will increase from 1580.97mm/year to 1691.80mm/year for RCP 4.5 and RCP 8.5, respectively. In the Bagoue basin, the scenarios predicted an increase in rainfall over the

period 2021–2050 of 6.15% for RCP4.5 and 9.32% for RCP8.5. Over the same period, evapotranspiration is projected to increase in all scenarios, by 1209.59 mm/year for the RCP4.5 scenarios and by 1275.17 mm/year for the RCP 8.5 scenario in Baya. With the Lobo watershed, the predicted evapotranspiration will increase for the scenarios with 1535.09 mm/year and 1591.08 mm/year, respectively, for RCP4.5 and RCP8.5. N'zo Watershed will expect a decrease in the evapotranspiration value under RCP4.5, which will show 1347.04 mm/year, or -0.93% decreasing, and under RCP8.5, it will have expected 1329.57 mm/year, or -2.25% decreasing.

Table 63: Evapotranspiration pattern under RCP scenario

Evapotranspiration (mm)					
Watersheds	Historical	RCP 4.5	Rate change %	RCP 8.5	Rate change %
Agneby	1543.28	1580.97	2.38	1691.80	8.78
Bagoue	1112.73	1185.69	6.15	1227.14	9.32
Baya	1149.75	1209.59	4.94	1275.17	9.83
Lobo	1459.10	1535.09	4.95	1591.08	8.29
N'zo	1359.57	1347.04	**-0.93**	1329.57	**-2.25**

6.3.3 Future trend analysis on rainfall extreme indices under the RCP 4.5 scenario

Table 65, Figure 48, and Figure 49 below show the results of the trend analysis on RCP 4.5 data of Pmaxan, Rx5day, CDD, and R95p extreme rainfall index of the study area under each climatic zone, with a non-significant trend for CNRM out of the three models (CM5A, CNRM, and MPI). The climatic zone I with the Agneby watershed can expect a significant upward trend with CM5A and MPI at Akoupe, Arrah, Agboville, Dabou, and Sikensi stations concerning the indexes (Rx5days, Pmaxan, and R95p). At the climatic zone II, Lobo and Baya watersheds, the model CM5A showed a significant upward trend at Bondoukou, Kun-Fao and Tanda at Baya watershed, and Issia at Lobo watershed regarding Pmaxan indices and a non-significant trend for the MPI model. It can be noticed at Bagoue

watershed for the climatic zone III a significant upward trend at Boundiali and Madinani stations concerning Pmaxan, Rx5days, and R95p indices for only the CM5A model. CNRM and MPI showed a non-significant trend. N'zo watershed at climatic zone IV in the western part of the country also showed a significant upward trend for Pmaxan and R95p and a significant downward trend for CDD indices at Zeregbo and Man stations for the climate models CM5A and MPI. The ensemble model showed a significant result at Lobo and N'zo watersheds concerning Pmaxan, Rx5 days, and CDD indices at Issia, Daloa, and Zeregbo stations.

Table 64: Trend analysis results of rainfall indices for RCP 4.5 data (CMA5, CNRM, MPI, ENSEMBLE)

		Rainfall indices for RCP 4.5 data															
		CM5A				**CNRM**				**MPI**				**ENSEMBLE**			
Watersheds	**Stations**	**Pmaxan**	**Rx5days**	**CDD**	**R95p**	**Pmaxan**	**Rx5days**	**CDD**	**R95p**	**Pmaxan**	**Rx5days**	**CDD**	**R95p**	**Pmaxan**	**Rx5days**	**CDD**	**R95p**
Agneby	Agboville	-		-	-	-	-	-	-	**	-	-	-	-	-	-	-
	Akoupe	-	**	-	-	-	-	-	-	-	-	-	-	-	-	-	-
	Arrah	-	*	-	-	-	-	-	-	-	-	-	-	-	-	-	-
	Bongouanou	-	-	-	-	-	-	-	-	-	-	-	-	-	-	-	-
	Cechi	-	-	-	-	-	-	-	-	-	-	-	-	-	-	-	-
	Dabou	-	-	-	-	-	-	-	-	-	**	-	-	-	-	-	-
	Mbatto	-	-	-	-	-	-	-	-	-	-	-	-	-	-	-	-
	Sikensi	-	-	-	-	-	-	-	-	**	-	-	**	-	-	-	-
Bagoue	Boundiali	**	**	-	-	-	-	-	-	-	-	-	-	-	-	-	-
	Madinani	**	-	-	**	-	-	-	-	-	-	-	-	-	-	-	-
Baya	Bondoukou	**	-	-	-	-	-	-	-	-	-	-	-	-	-	-	-
	Kun-Fao	**	-	-	-	-	-	-	-	-	-	-	-	-	-	-	-
	Tanda	**	-	-	-	-	-	-	-	-	-	-	-	-	-	-	-
Lobo	Daloa		-	-	-	-	-	-	-	-	-	-	-	-	**	-	-

	Issia	**	-	-	-	-	-	-	-	-	-	-	-	**	**	-	-
	Pelezi	-	-	-	-	-	-	-	-	-	-	-	-	-	-	-	-
	Vavoua	-	-	-	-	-	-	-	-	-	-	-	-	-	-	-	-
N'zo	Bangolo	-	-	-	-	-	-	-	-	-	-	-	-	-	-	-	-
	Biankouma	-	-	-	-	-	-	-	-	-	-	-	-	-	-	-	-
	Man	-	-	-	-	-	-	-	-	-	-	*	-	-	-	-	-
	Zeregbo	**	-	-	**	-	-	-	-	-	-	-	-	-	-	**	-

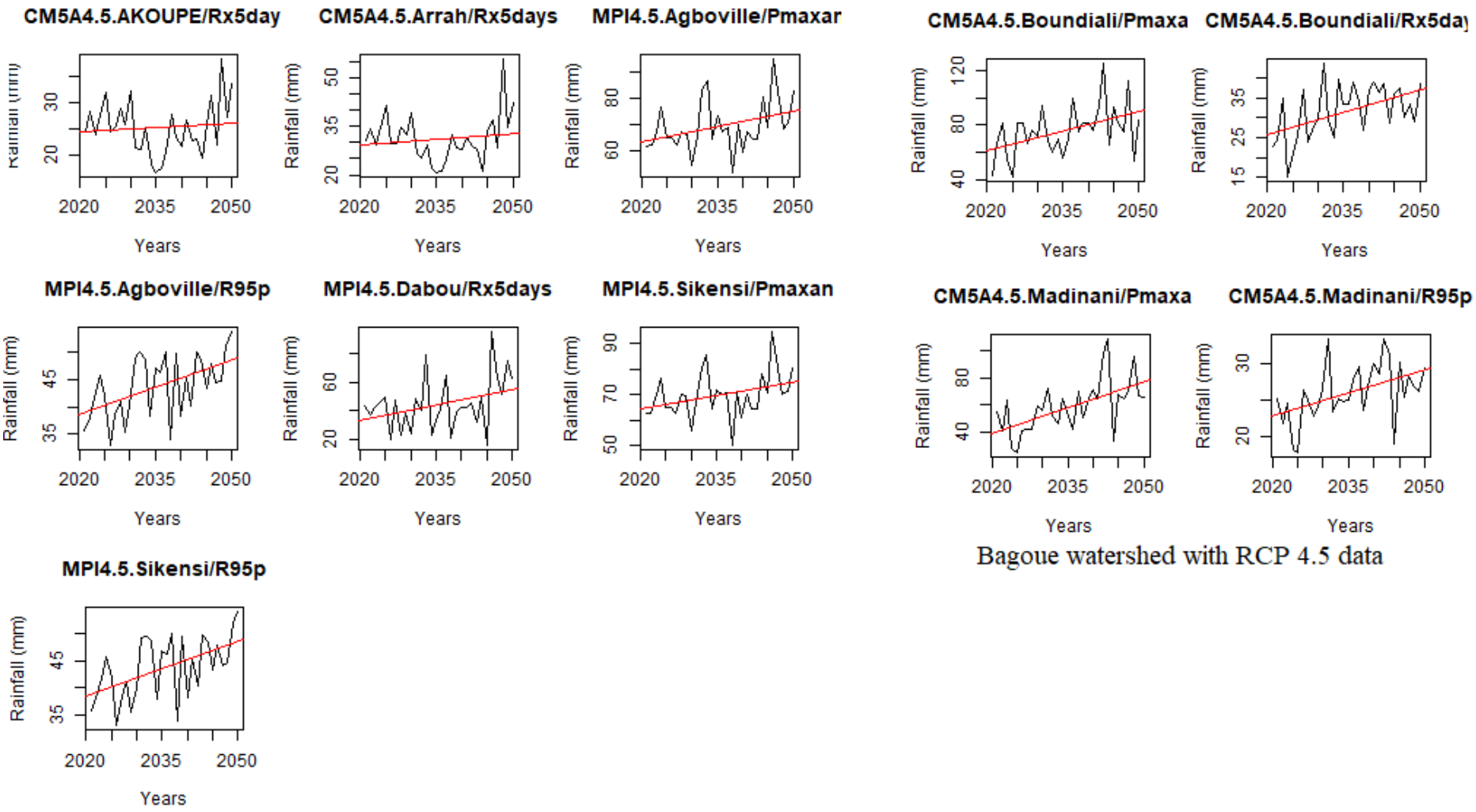

Agneby watershed with RCP 4.5 data

Bagoue watershed with RCP 4.5 data

Figure 48: Trend analysis results of rainfall indices for RCP 4.5 data (CMA5, CNRM, MPI, ENSEMBLE)

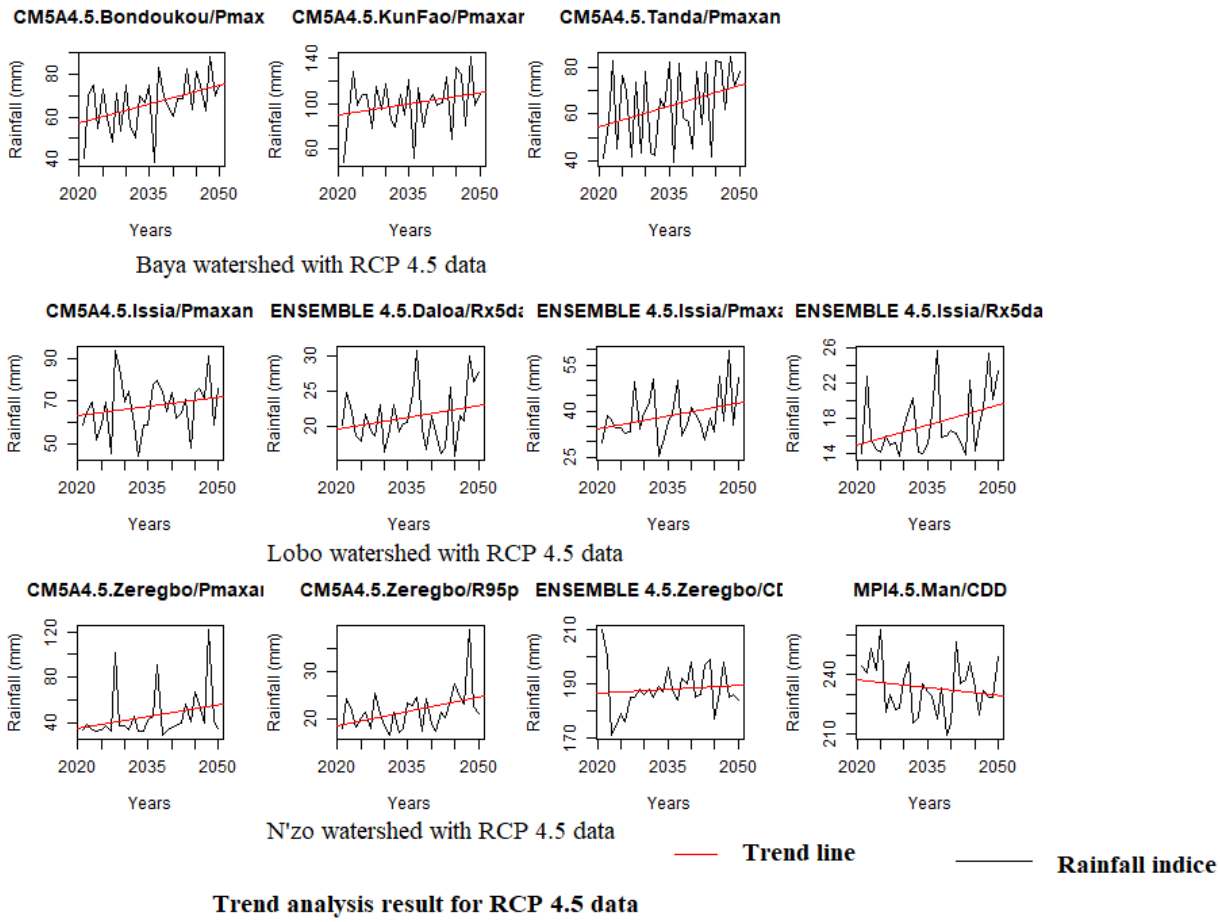

Figure 49: Trend analysis results of rainfall indices for RCP 4.5 data (CMA5, CNRM, MPI, ENSEMBLE)

6.3.4 Future trend analysis on rainfall extreme indices under the RCP 8.5 scenario

Tables 66 and Figure 50 below show the results of the trend analysis on the RCP 8.5 data of Pmaxan, Rx5day, CDD, and R95p extreme rainfall index of the study area under each climatic zone with three models (CM5A, CNRM, and MPI). The climatic zone I with the Agneby watershed can greatly experience a significant upward trend with CM5A and CNRM at Akoupe, Arrah, Agboville, Cechi, and Sikensi stations, respetively concerning the Rx5days indices. At the climatic zone II, Lobo, and Baya watersheds, the models showed a significant upward and downward trend. The CM5A presented a significant upward trend at Bondoukou, Kun-Fao, Tanda, and Issia for the Baya and Lobo watersheds regarding the Pmaxan indices. CNRM allowed us to see at Kun-Fao, Daloa, and Issia a mixed trend (decrease and increase

trend) for CDD indices at Lobo watershed and an increasing trend for Pmaxan at Kun-Fao station for Pmaxan at Baya watershed. For the MPI model, only Kun-Fao station presented a significant upward trend for the Baya watershed; other stations presented a non-significant trend. It can be noticed at Bagoue watershed for the climatic zone III, a significant upward trend for only the CM5A model regarding Pmaxan, R5days, and R95p indices at Madinani and Boundiali stations CNRM and MPI showed a non-significant trend. N'zo watershed at climatic zone IV in the western part of the country also showed a significant upward trend for Pmaxan, Rx5days, and R95p at Zeregbo and Man stations for the climate models CM5A and CNRM. The ensemble model generally showed a significant result at Lobo and N'zo watersheds concerning Pmaxan, Rx5days, R95p, and CDD indices.

Table 65: Trend analysis results of rainfall indices for RCP 8.5 data (CMA5, CNRM, MPI, ENSEMBLE)

		Rainfall indices for RCP 8.5 data															
		CM5A				**CNRM**				**MPI**				**ENSEMBLE**			
Watersheds	**Stations**	**Pmaxan**	**Rx5days**	**CDD**	**R95p**	**Pmaxan**	**Rx5days**	**CDD**	**R95p**	**Pmaxan**	**Rx5days**	**CDD**	**R95p**	**Pmaxan**	**Rx5days**	**CDD**	**R95p**
Agneby	Agboville	-	-	-	-	-	**	-	-	-	-	-	-	-	-	-	-
	Akoupe	-	**	-	-	-	-	-	-	-	-	-	-	-	-	-	-
	Arrah	-	**	-	-	-	-	-	-	-	-	-	-	-	-	-	-
	Bongouanou	-	-	-	-	-	-	-	-	-	-	-	-	-	-	-	-
	Cechi	-	-	-	-	-	**	-	-	-	-	-	-	-	-	-	-
	Dabou	-	-	-	-	-	-	-	-	-	-	-	-	-	-	-	-
	Mbatto	-	-	-	-	-	-	-	-	-	-	-	-	-	-	-	-
	Sikensi	-	-	-	-	-	**	-	-	-	-	-	-	-	-	-	-
Bagoue	Boundiali	**	**	-	-	-	-	-	-	-	-	-	-	-	-	-	-
	Madinani	**	-	-	**	-	-	-	-	-	-	-	-	-	-	-	-
Baya	Bondoukou	**	-	-	-	-	-	-	-	-	-	-	-	-	-	-	-
	Kun-Fao	**	-	-	-	**	-	-	-	-	-	*		-	-	-	-
	Tanda	**	-	-	-	-	-	**	-	-	-	-	-	-	-	-	-
Lobo	Daloa		-	-	-	-	-	**	-	-	-	-	-	-	**	-	-

	Issia	**	-	-	-	-	-	**	-	-	-	-	-	**	**	-	-
	Pelezi	-	-	-	-	-	-	-	-	-	-	-	-	-	-	-	-
	Vavoua	-	-	-	-	-	-	-	-	-	-	-	-	-	-	-	-
N'zo	Bangolo	-	-	-	-	-	-	-	-	-	-	-	-	-	-	-	-
	Biankouma	-	-	-	-	-	-	-	-	-	-	-	-	-	-	-	-
	Man	-	-	-	-	-	**	-	-	-	-	-	-	-	-	-	-
	Zeregbo	**	-	-	**	-	-	-	-	-	-	-	-	-	-	**	-

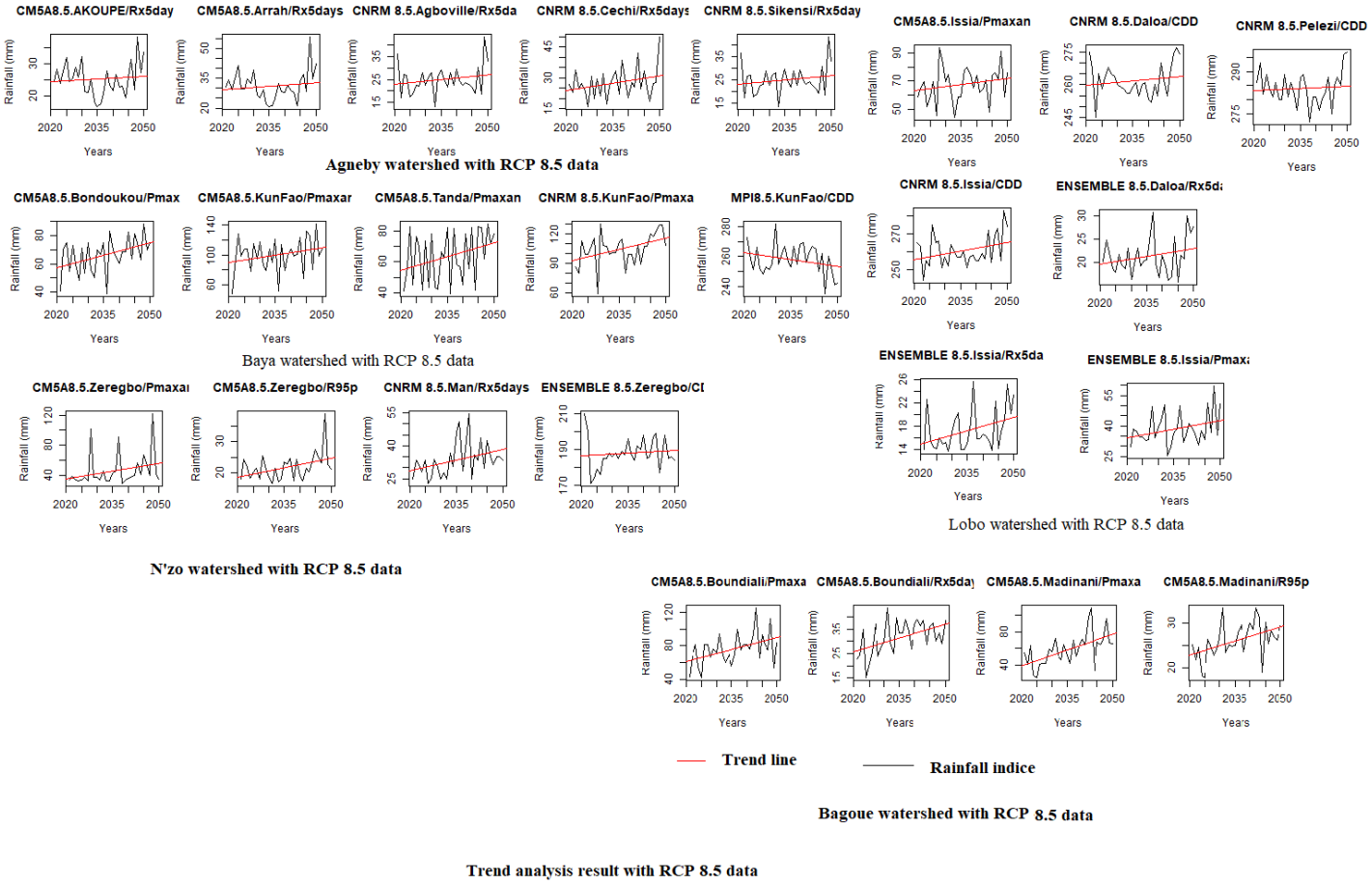

Figure 50: Significant trend result of RCP 8.5 data (CM45,CNRM,MPI,ENSEMBLE)

From the above, whether it is the drought index CDD or the flood indices Pmaxan, Rx5days and R95p chosen and under one climatic zone to another, we note in general that the future projections show either a significant upward trend or a non-significant trend under each scenario.

6.4 Future pattern and trend in discharge extreme RCP scenario

After the result of the performance evaluation of the hydrological models, the GR5J model was selected for the simulation of future flows because of its very good performance on all basins at the same time in both calibration and validation. Also, with the result of the bias correction, the ensemble model was used as input in the future simulation process. Overall, under the scenarios RCP4.5 and RCP8.5, the future means of daily flows will decrease significantly compared to the observed mean flows. Under RCP4.5, the decrease will be less pronounced than under RCP8.5. Thus, the Agneby catchment will have a mean daily flow of 0.54 m3/s/year compared to 0.86 m3/s/year under RCP4.5 and RCP8.5, respectively. In climatic zone II, the mean daily flow values vary from station to station. The Baya will see its mean daily flow value decrease from 3.43 m3/s/year to 0.404 m3/s/year under RCP4.5 and 0.52 m3/s/year under RCP8.5. The average mean daily flow of the Lobo River will also be influenced, whether the station is in Nibehibe or Loboville, from 0.69 m3/s/yr to 0.96 m3/s/yr and from 0.97 m3/s/year to 1.29 m3/s/year, respectively. The N'zo catchment area will also be confronted with this general decrease in mean daily flow values from 1.87 m3/s/year to 1.96 m3/s/year under the RCP4.5 and RCP8.5 scenarios, respectively.

Table 66: Mean Daily discharge under RCP scenario

	Mean Daily discharge (m3/s/Years)		
Watersheds	Observed	RCP 4.5	RCP 8.5
AGNEBY	4.55	0.54	0.86
BAGOUE	32.75	1.47	1.62
BAYA	3.43	0.404	0.52
LOBO at LOBOVILLE	34.88	0.97	1.29
LOBO at NIBEHIBE	14.01	0.69	0.96
NZO	60.35	1.87	1.96

6.4.1 Future trend analysis on discharge extreme indices under RCP 4.5 scenario

Under the RCP4.5 scenarios, the different watersheds of the four main climatic zones of the country showed a non-significant trend with the flood and low flow indices. Except for the Bagoue river basin in climatic zone III in the north of the country, it will experience a significant upward trend in the maximum annual flow Qmaxan over the period 2020–2050.

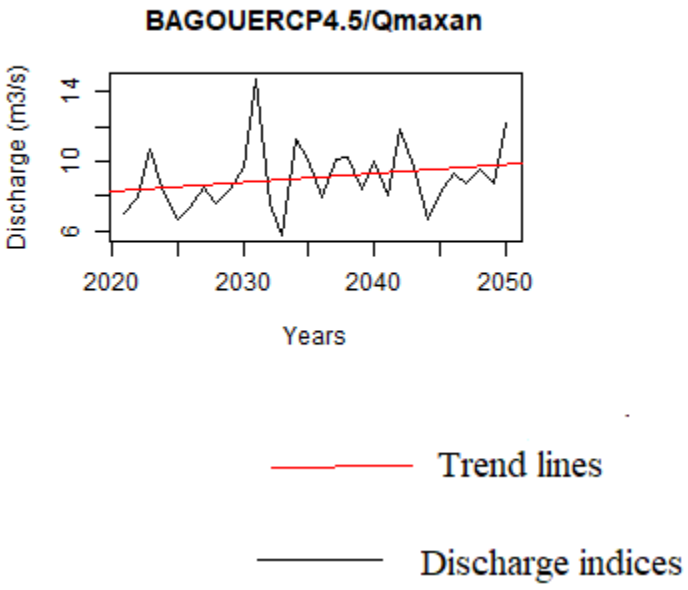

Figure 51: Trend analysis of significant results on discharge extreme indices under RCP 4.5

Table 67: Statistical trend analysis result on discharge extremes indices under RCP4.5

	High discharge indices						Low discharge indices											
RCP4.5	Qmaxan			VCX30			QX5-days			Qminan			QMNA			VCN7			WDF		
Watersheds	**Zc**	**P value**	**Sen slope**	**Zc**	**P value**	**Sen slope**	**Zc**	**P value**	**Sen slope**	**Zc**	**P value**	**Sen Slope**	**Zc**	**P value**	**Sen slope**	**Zc**	**P value**	**Sen slope**	**Zc**	**P value**	**Sen slope**
AGNEBY	-0.37	0.70	-0.00	-0.21	0.83	-0.003	-0.60	0.54	-0.003	-0.28	0.77	-0.00	0	1	0.00	-0.42	0.66	0.00	-0.46	0.64	-0.00
BAGOUE	2.52	**0.01**	0.05	-0.67	0.49	-0.011	2.88	0.00	0.054	-0.28	0.77	-0.00	-0.10	0.91	-0.00	-0.82	0.41	-0.01	-0.42	0.66	-0.00
BAYA	-0.37	0.70	-0.00	-0.21	0.83	-0.003	-0.60	0.54	-0.003	-0.28	0.77	-0.00	0	1	0.00	-0.42	0.66	0.00	-0.46	0.64	-0.00
LOBO	0	1	0.00	0.38	0.69	-0.0037	0.10	0.91	0.000	-0.10	0.91	-0.00	-0.31	0.75	-0.00	-0.13	0.89	-0.00	-0.31	0.75	-0.00
NZO	-0.7	0.43	0.00	-0.53	0.59	-0.002	-0.7	0.47	0.0002	-0.9	0.33	0.00	-0.64	0.52	0.00	-1.8	0.06	0.003	-0.87	0.38	0.00

Bold value= significant trend

6.4.2 Future trend analysis of discharge extreme indices under RCP 8.5 scenario

Under the RCP 8.5 scenario, the extreme flow indices will change in the near future (2020–2050). Specifically, the flood indices QMAXAN and QXR5-days will show a significant downward trend in climatic zone II and in the Lobo watershed at Loboville and Nibehibe. Regarding the low flow indices, all indices will be subject to disturbances in the near future, with decreasing trends overall. On the Agneby basin in zone I and Baya in zone II, the indices (Qminan, QMNA, VCN7, and WDF) will experience disturbances. On the Bagoue basin in zone III and N'zo in zone IV, only the QMNA and WDF indices, respectively, will be affected. In the Lobo basin, only the QMNA, VCN7, and WDF indices will be modified.

Table 68: Statistical trend analysis result on discharge extreme indices under RCP 8.5

	High discharge indices									Low discharge indices									
RCP8.5	Qmaxan			VCX30			QX5-days			Qminan			QMNA			VCN7			WDF		
Watersheds	**Zc**	**P value**	**Sen slope**	**Zc**	**P value**	**Sen slope**	**Zc**	**P value**	**Sen slope**	**Zc**	**P value**	**Sen slope**	**Zc**	**P value**	**Sen slope**	**Zc**	**P value**	**Sen slope**	**Zc**	**P value**	**Sen slope**
AGNEBY	-1.4	0.14	-0.02	-0.7	0.37	-0.00	-1.31	0.19	-0.02	-2.07	**0.03**	-0.00	-2.1	**0.03**	-0.00	-2.1	**0.03**	-0.00	-2.2	**0.02**	-0.00
BAGOUE	0.82	0.41	0.02	-1.7	0.69	-0.00	0.89	0.37	0.02	-1.28	0.19	-0.00	-2.2	**0.02**	-0.00	-1.2	0.2	-0.00	-1.0	0.3	-0.00
BAYA	-1.7	0.08	-0.01	-1.9	0.33	-0.00	-1.78	0.07	-0.02	-3.25	**0.001**	-0.00	-3.7	**0.00**	-0.00	-3.2	**0.001**	-0.00	-3.4	**0.00**	-0.00
LOBO at LOBOVILLE	-1.6	0.10	-0.023	-2.4	0.09	-0.00	-2.03	**0.04**	-0.03	-3.46	0.00	-0.002	-3.3	**0.00**	-0.00	-3.5	**0.00**	-0.00	-3.6	**0.00**	-0.00
LOBO at NIBEHIBE	-2.1	**0.03**	-0.01	-1.8	0.09	-0.00	-2.25	**0.02**	-0.019	-3.10	0.00	-0.004	-3.1	**0.002**	-0.00	-3.1	**0.00**	-0.00	-3.4	**0.0**	-0.00
NZO	1.10	0.26	0.02	-0.6	0.47	-0.00	1.43	0.15	0.02	-1.86	0.06	-0.00	-1.8	0.07	-0.00	-1.7	0.08	-0.00	-2.2	**0.02**	-0.00

Bold value= significant trend

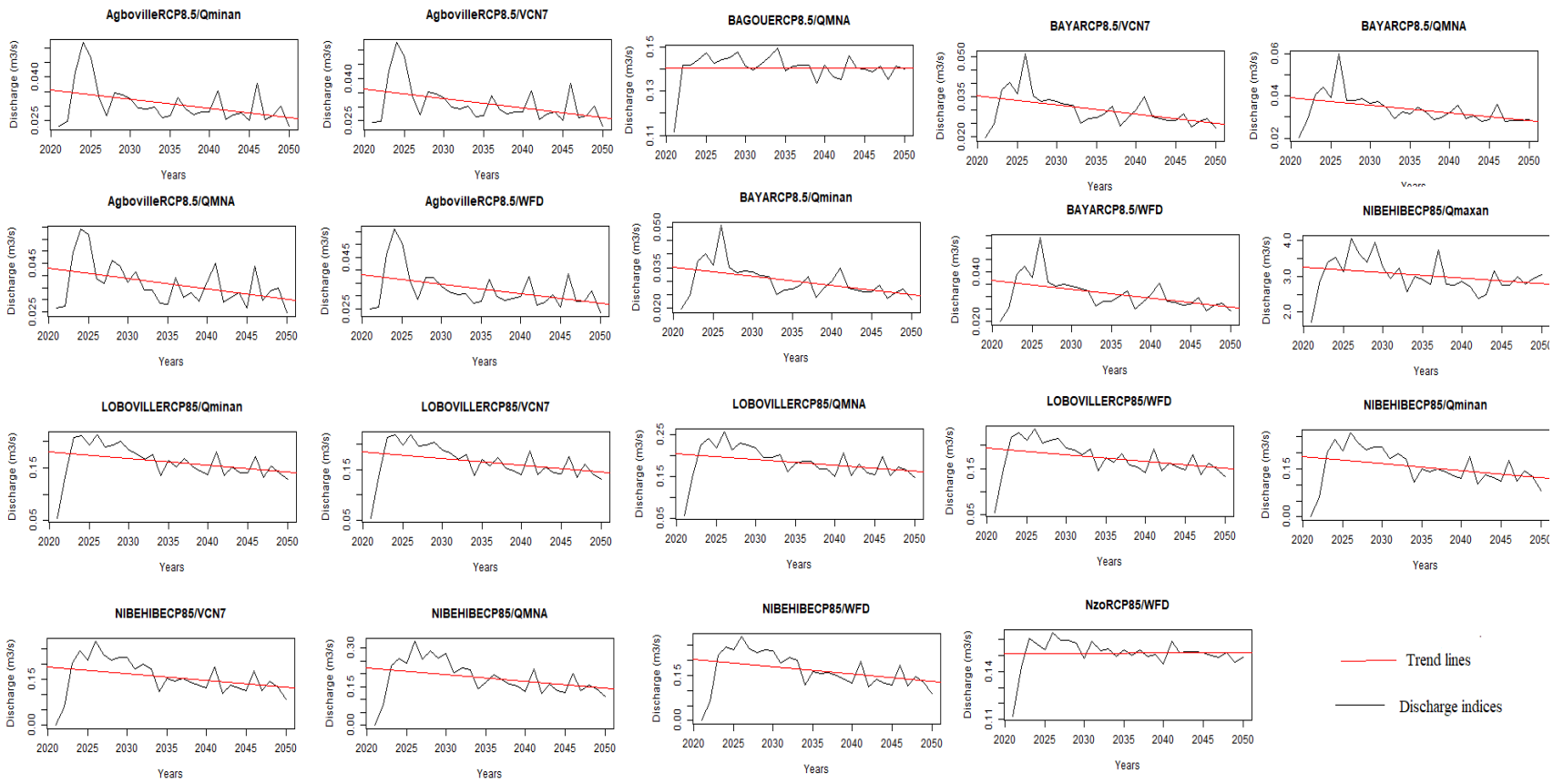

Figure 52: Trend analysis significant results on discharge extreme indices under RCP 8.5

6.5 Discussion

- *Dynamic of land use change*

Several methods were used to evaluate the dynamics of land use at the extremes, showing that all our study basins have been dynamically affected, either positively or negatively. It revealed that from the south to the north and from the west to the east of Côte d'Ivoire, there has been a significant regression of forest or savannah, of water resources, and an increase or regression of habitat and cultivated areas from one place to another, indicating that the country's land use is dynamic. These land-use dynamics in Côte d'Ivoire have mainly had an impact on extreme water flows, which have shown an upward trend, even though extreme rainfall has decreased significantly due to the major silting-up of rivers caused by erosion and soil loss. Research by Hu et al. (2019) in Europe shows significant changes in climate extremes after land cover change. (Alexis et al., 2018) showed that strong land use dynamics led to strong erosion and soil loss in the Sassandra catchment. Also, the relationship between changes in the vegetation index (NDVI) and extreme rainfall indices showed a non-significant negative correlation overall in the study catchments, which would indicate that the recurrence of flooding or drought in Côte d'Ivoire is linked to the loss of vegetation cover. Similarly, this analysis revealed a positive correlation between vegetation indices (NDVI) and extreme flow indices as a whole. This could, in fact, be explained by the fact that a loss or gain of vegetation cover has a greater impact on runoff with a faster time of concentration to cause flooding in the study basins. This is because land use plays an important role in the climatic system of a catchment as well as in the production of runoff and the infiltration rate of rainwater. The water retention capacity studied in the various catchment areas gave values greater than 100 overall. This result can be explained by the fact that our study basins are still uncontrolled, with significant plant cover and a high-water retention capacity, but are subject to uncontrolled land use dynamics. This is because constant, uncontrolled changes in land use influence the climate system, which affects extremes by increasing peak flood flows with an upward trend and by reducing or increasing low flows in certain areas with an upward or downward trend. This result is consistent with research by Soro et al. (2014), who reached the same conclusion on how changes in land use have affected the hydrological behavior of the upper Bandama catchment.

- *Future pattern and trend in rainfall extreme RCP scenario*

The mean annual rainfall has all decreased in the different basins and under each climatic zone under the RCP 4.5 and RCP 8.5 scenarios. The Agneby and Lobo basins will experience an increase in the value of their mean annual rainfall from 4.25% to 0.92% and from 11.81% to 15.77%, respectively, under RCP 4.5 and RCP 8.5. This result is in line with those obtained by Larbi et al. (2022), who found a slight increase in annual rainfall in the Tano basin in Ghana. At the same time, the Bagoue basin will see an alternating decrease in the mean annual rainfall of 6.05% under RCP 4.5 and an increase of 0.64% under the RCP 8.5 scenario. This alternating result was observed in Benin by the work of Yèkambèssoun et al. (2017) and Bodian et al. (2018) in Senegal. The Baya and N'zo basins will experience a significant decrease in the near future, from 0.69% to 6.38% and from 12.55% to 18.04%, respectively, under the RCP 4.5 and RCP 8.5 scenarios. This significant decrease was found in the research of Berenger Koffi et al. (2021) on the Lobo River in Cote d'Ivoire, where precipitation will also experience a significant mean annual decrease of about 6.51% over the period 2021–2040. Also, the Koua et al. (2014) study on the Buyo found a decrease in rainfall of about 10.3% in the 2050s. In the same way, under the RCP 4.5 and RCP 8.5 scenarios, the CDD index shows a significant downward trend at Man station in the N'Zo watershed, and under the RCP 8.5 scenario, the number of consecutive dry days will decrease at Kun-Fao station at Baya watershed in the eastern region, reflecting a rather uncertain climate model in the near future. The long duration of the consecutive dry days predicted by both scenarios (RCP 4.5 and RCP 8.5) will greatly impact Ivorian agriculture, the source of the national economy, with a great delay in the agricultural calendar, and crops that need water, such as rice, cassava, yams, etc., will be greatly disrupted. The development of new cropping strategies with an insufficiency and sufficiency in water use will be needed because of the great uncertainty of the index, which could threaten the supply of pasture and animal feed. And some regions will experience longer and more intense droughts due to rising temperatures and decreasing rainfall. Therefore, in an uncertain climate, it is more than urgent that adaptation strategies are known to all sections of the population. Also, the different flood indices used (Pmaxan, R95p, and Rx5days) have generally shown a projected mix trend (upward and downward trend), with the most important trend not being significant under the two scenarios (RCP 4.5 and 8.5) in each of the study areas in the near future (2021–2050). Thus, under both scenarios, the Bagoue watershed in the north, the Agneby watershed in the south, the N'zo watershed in the mountainous west, and the Baya watershed in the east are

expected to experience a significant upward trend in flooding in the near future. This could be explained by the expected impact of climate change on rainfall due to the severe climatic variability experienced in these climatic zones. This result has been reported by several recent works in other parts of Africa, such as Teshome et al. (2022) over Africa, Okafor et al. (2021b) in the Dano catchment, Burkina Faso, and Adeyeri et al. (2019) over the Komadugu-Yobe watershed, Lake Chad region. (Okafor et al., 2021b) observed increasing trends in Rx5day under both RCPs 4.5 and 8.5 scenarios in their study. The inhabitants of the Bagoue watershed are maize and rice farmers whose livelihoods could be damaged by the expected floods, thus directly impacting the socio-economic activities of the riparian population. The Baya watershed is marked by yam cultivation, the Agneby by cassava, and the N'zo by rain-fed rice, all of which are the main economic activities of the riparian population and could be affected by floods with environmental and socio-economic damaging effects resulting from the impact of climate change in these areas.

The future mean maximum temperature will increase slightly or strongly in our different river basins with the reference years 1976–2005. For the Agneby watershed, the scenarios predict an increase in temperature. It will reach 1.82°C for the RCP4.5 scenarios and 3.45°C for the RCP8.5 scenarios. For the Bagoue watershed, the temperature will also increase from 2.03°C under the RCP4.5 scenarios to 4.63°C under the RCP8.5 scenarios. Similarly, for the Baya watershed, the temperature will increase from 2.2°C under RCP4.5 to 2.35°C under RCP8.5. The Lobo and N'zo watersheds will also follow the same pattern with an increase in their different temperatures. For Lobo, we will see an increase from 2.2°C under RCP4.5 to 5.52°C under RCP8.5; N'zo, in the same way, will expect an increase from 2.2°C under RCP4.5 to 5.8°C under RCP8.5. These increases in temperature in each study area follow the global order of temperature increases due to climate change effects under all scenarios. Thus, these results are in agreement with the studies by Koffi et al. (2021) on the Lobo River, Cote d'Ivoire, where the predictions are for an increase of 1.27°C to 2.58°C by 2021–2040. Also, in Ghana, in the Tano basin, Larbi et al. (2022) found that the mean annual temperature has increased (2.1°C and 2.6°C), and according to Patchali et al. (2020), this temperature will increase in Togo, whatever the scenario chosen (0.1–2.0 °C or 0.5–7.3%) in all the stations studied. Like the other climate parameters studied in this research, evapotranspiration will also be affected by climate change in our different study areas. Thus, the watersheds of Agneby, Bagoue, Baya, and Lobo will experience an increase in the mean annual evapotranspiration value under both study scenarios. This increase was also obtained in the

Batablinlè et al. (2021) study in Mono, Benin; Kofi et al. (2015) in Togo; and Serdeczny et al. (2017) in Sub-Saharan Africa. This parameter will decrease slightly in the N'zo watershed in the west of the country, i.e., by -0.93% for the RCP4.5 scenarios and by -2.25% for the RCP 8.5scenario.

Like rainfall, temperature, and evapotranspiration, flow will also be affected by climate change and will decrease significantly by 2020–2050 in all study basins. Under RCP4.5, the decrease will be less pronounced than under RCP8.5. Thus, the Agneby catchment will have a mean flow of 0.54 m3/s/year compared to 0.86 m3/s/year under RCP4.5 and RCP8.5, respectively. In climatic zone II, the mean flow values vary from station to station. The Baya will see its mean flow value decrease from 3.43 m3/s/year to 0.404 m3/s/year under RCP4.5 and 0.52 m3/s/year under RCP8.5. The average mean flow of the Lobo River will also be influenced, whether the station is in Nibehibe or Loboville, from 0.69 m3/s/yr to 0.96 m3/s/yr and from 0.97 m3/s/year to 1.29 m3/s/year, respectively. The N'zo catchment area will also be confronted with this general decrease in average flow values from 1.87 m3/s/year to 1.96 m3/s/year under the RCP4.5 and RCP8.5 scenarios, respectively. These different results are in line with some works in Cote d'Ivoire, notably those of Michel et al. (2021) on the Sasandra basin in N'zo and N'Dri et al. (2019) on the Aghien basin, who found that a decrease in the annual flow of nearly 10% on average under RCP 4.5 and under RCP 8.5, the average annual flow should decrease by more than 17%. Larbi et al. (2022) in Ghana found that the average annual flow would decrease and that the decrease would be more pronounced under RCP8.5 (37.5%) than under RCP4.5 (19.9%).

- *Future pattern and trend in discharge extreme RCP scenario*

In addition, the MMK test on extreme flood and low water indices showed a non-significant result overall under both scenarios. The test showed a significant trend in the QMAXAN index at Bagoue watershed under the RCP 4.5 scenario with respect to flood debits indices. Under RCP 8.5 scenario, trends will alternate. The extreme flood indices will experience a downward trend of the QMAXAN and QX5days indices in the north of the country. For the low water flow indices, the results also show a significant downward trend in almost all study basins.

Conclusion

The study of the impact of climate change was done by first analyzing the dynamics of land use in the different study areas. The results showed that the Ivorian vegetation cover from north to south and west to east is subject to a great dynamism that has severely impacted the hydrological extremes. This dynamic has seen the forest, savannah, and water classes strongly reduced or slightly increased in the study areas. Crop and wetland classes have increased throughout the study area. And also, for the investigation of the dynamics, it can be noticed that all the watersheds are somewhat more dynamic, as evidenced by the change in rate, the relationship between extreme indices and vegetation dynamics (NDVI), and the water retention capacity for each catchment area. Secondly, the analysis of the impacts on some climate parameters, namely rainfall, temperature, and evapotranspiration, these parameters will be subject to a major change in their usual evolution by 2020–2050. The mean annual rainfall will decrease over all study basins under the study scenarios (RCP 4.5 and RCP 8.5) in the near future. Mean temperatures and mean annual evapotranspiration will generally increase in all study basins in the near future. In addition, the analysis showed that extreme rainfall through the study of extreme rainfall indices showed a significant decrease in all study basins overall. However, the flood indices showed either significant upward or downward trends in some areas, notably climatic zone I with the Agneby catchment and climatic zone II with the Lobo and Baya watersheds, where the CM5A and MPI climate models showed a significant increase in the indices (Rx5days, Pmaxan, and R95p) under the RCP 4.5 scenario. Under RCP 8.5, climatic zones I and II will see an alternating decrease or increase in these indices with the CM5A and CNRM climate models. The drought index, CDD, will undergo a mixed trend with the CNRM model over the Baya watershed in particular. Finally, this analysis revealed that the overall flow and extreme flow indices will be affected by a significant downward trend in the different watersheds under both study scenarios. Under the RCP 4.5 scenario, the extreme flood index QMAXAN will show a slight increase in the Bagoue basin, and the low flow indices will show a non-significant trend. Under RCP 8.5, the flood indices will show a non-significant trend overall except for the QMAXAN and QXR5 days, which will show a significant downward trend in climatic zone II and in the Lobo to Loboville and Nibehibe catchments. The water level indices as a whole will show a significant downward trend in all the study basins. These results allow us to have a good knowledge of the behavior of hydrological extremes in the near future for the good planning of adaptation and mitigation measures.

CHAPTER 7 : GENERAL CONCLUSION AND PERSPECTIVES

Sections 7.1 and 7.2 of the thesis provide a general conclusion and perspectives

7.1 Conclusion

Water is an indispensable source of life in any area. Unfortunately, it has become a source of destruction in recent decades, mostly due to the effects of climate change. Thus, the goal of this study was to evaluate the effects of climate change on severe flows through the climatic zone in Côte d'Ivoire. It is structured into three different parts. The first section was to analyze historical hydro-climatic (rainfall and discharge) patterns from 1970 to 2017 and the effect of rainfall variability on low and high flows in a few selected river basins. By doing so, inter-annual variation, break point, and trend analysis using the modified Mann-Kendall statistical test at a 95% confidence level with observed data over the period 1976–2017 were carried out by different methods. The results of the trend analysis regarding the rainfall indices showed that all the indices characterizing flooding and the dry season duration (CDD index) depict general downward trends in the observed data from 1976–2017. For the discharge indices, we obtained non-significant trends for the flood variables in general and significant upward trends for the low-flow variables. The detection of breaks by the Standard Normal Homogeneity Test (SNHT) indicated a significant break for most of the variables studied in general in all our different study basins. And also, the results obtained by applying Hanning's second-order low-pass filter to the observed data indicate a great inter-annual irregularity of the data in each climatic zone of the country. The outcome of this study provided a good understanding of the evolution of past rainfall, droughts, and flood indices in each climatic zone of the country. It is important to note, then, that changes in climate extremes are of greater interest to decision-makers at the local scale as they imply changes in the types of hazards that are often of greatest concern to communities. The second part was to analyze the effectiveness of several hydrological models in simulating low flows and floods in a few chosen river basins. The goal of this part was to evaluate how effectively the hydrological models GR4J, GR5J, and HEC-HMS simulate floods and low flows. The hydrological simulation period was different in each basin with the three hydrological models. The evaluation of the performance of these different models was studied by three different functions, namely an objective function common to all three models (Nash), an objective function common to the GR models, which is the KGE, and an objective function specific to

the HEC-HMS model, which is the PBAIS. These different functions allowed us to evaluate the two fundamental processes of hydrological simulation, which are calibration and validation. During the calibration process, all the performance evaluation criteria showed good performance, with values reaching 0.9, indicating a good optimization of the different key parameters. At validation, these criteria showed shortcomings in the appreciative validation values, which either underestimated or overestimated the study data. This study showed that under conditions of high climate variability, it would be preferable to model with the GR5J, which performed well under each climatic zone considered in the high and low flow simulation. It also showed that it is difficult to identify watershed-specific parameters with the HEC-HMS model, which performs well but has limitations in the simulation of high flows. In the context of climate change and flood and drought flow management, the GR5J model was the most efficient. And the last part was to examine the impact of climate change by following the patterns and trends in hydro-climatic extremes under the RCP4.5 and RCP8.5 climate scenarios for the period 2020–2050. The study of the impact of climate change was done by first analyzing the dynamics of land use in the different study areas. The results showed that the Ivorian vegetation cover from north to south and west to east is subject to a great dynamism that has severely impacted the hydrological extremes. This dynamic has seen the forest, savannah, and water classes strongly reduced or slightly increased in the study areas. Crop and wetland classes have increased throughout the study area. And also, for the investigation of the dynamics, it can be noticed that all the watersheds are somewhat more dynamic, as evidenced by the change in rate, the relationship between extreme indices and vegetation dynamics (NDVI), and the water retention capacity for each catchment area. Secondly, the analysis of the impacts on some climate parameters, namely rainfall, temperature, and evapotranspiration, these parameters will be subject to a major change in their usual evolution by 2020–2050. The mean annual rainfall will decrease overall study basins under the study scenarios (RCP 4.5 and RCP 8.5) in the near future. Mean temperatures and mean annual evapotranspiration will generally increase in all study basins in the near future. In addition, the analysis showed that extreme rainfall through the study of extreme rainfall indices showed a significant decrease in all study basins overall. However, the flood indices showed either significant upward or downward trends in some areas, notably climatic zone I with the Agneby catchment and climatic zone II with the Lobo and Baya watersheds, where the CM5A and MPI climate models showed a significant increase in the indices (Rx5days, Pmaxan, and R95p) under the RCP 4.5 scenario. Under RCP 8.5, climatic

zones I and II will see an alternating decrease or increase in these indices with the CM5A and CNRM climate models. The drought index, CDD, will undergo a mixed trend with the CNRM model over the Baya watershed in particular. Finally, this analysis revealed that the overall flow and extreme flow indices will be affected by a significant downward trend in the different watersheds under both study scenarios. Under the RCP 4.5 scenario, the extreme flood index QMAXAN will show a slight increase in the Bagoue basin, and the low flow indices will show a non-significant trend. Under RCP 8.5, the flood indices will show a non-significant trend overall except for the QMAXAN and QXR5 days, which will show a significant downward trend in climatic zone II and in the Lobo to Loboville and Nibehibe catchments. The water level indices as a whole will show a significant downward trend in all the study basins. At the end of this work, it appears that the various catchment areas are confronted with the phenomenon of hydrological extremes, which have evolved in the past and will continue to do so in the near future, with a definite climatic impact. It has also enabled us to understand hydrological behavior through the study and evaluation of the performance of certain hydrological models in simulation. This knowledge will be used to plan policies and strategies to prepare for the potential challenges that will result from climate change impacts in each study area.

7.2 Perspectives

This study assessed the impacts of climate change on hydrological extremes in different watersheds in a comprehensive manner. In the near future, the perspectives of this study are that: -more detailed studies on each study watershed using a distributed model to better assess the water balance for the implementation of a water use efficiency system as part of effective water resources management. -A detailed study of each watershed area for the analysis of future climate change by integrating socio-economic and human data (population density, technology, and politics) could improve decision-making performance. -More detailed studies on each study watershed on calibration and validation of land use scenarios in the near future will link with the evolution of extreme events over each watershed.

REFERENCES

Adeyeri, O. E., Lawin, A. E., Laux, P., Ishola, K. A., & Ige, S. O. (2019). Analysis of climate extreme indices over the Komadugu-Yobe basin, Lake Chad region: Past and future occurrences. *Weather and Climate Extremes*, *23*(January), 100194. https://doi.org/10.1016/j.wace.2019.100194

Abiodun, B. J., Adegoke, J., Abatan, A. A., Ibe, C. A., Egbebiyi, T. S., Engelbrecht, F., and Pinto I. Potential impacts of climate change on extreme precipitation over four African coastal cities. Climatic Change, 2017, 143(3), 399-413.

Ago, E. E., Petit, F., & Ozer, P. (2005). Analyse des inondations en aval du barrage de Nangbeto sur le fleuve mono (Togo et Bénin). *Geo-Eco-Trop*, *29*(1–2), 1–14.

Aguilar, E., Barry, A. A., Brunet, M., Ekang, L., Fernandes, A., Massoukina, M., … Zhang, X. (2009). Changes in temperature and precipitation extremes in western central Africa, Guinea Conakry, and Zimbabwe, 1955-2006. *Journal of Geophysical Research Atmospheres*, *114*(2), 1–11. https://doi.org/10.1029/2008JD011010

Agyekum, J., Annor, T., Quansah, E., Lamptey, B., & Okafor, G. (2022). Extreme precipitation indices over the Volta Basin: CMIP6 model evaluation. *Scientific African*, *16*(May), e01181. https://doi.org/10.1016/j.sciaf.2022.e01181

Ahoussi, K., Koffi, Y., Kouassi, A., Soro, G., & Biemi, J. (2013). Étude hydrochimique et microbiologique des eaux de source de l'ouest montagneux de la Côte d'Ivoire : Cas du village de Mangouin-Yrongouin (souspréfecture de Biankouman). *Journal of Applied Biosciences*, *63*(1), 4703. https://doi.org/10.4314/jab.v63i1.87245

Akinsanola, A. A., & Ogunjobi, K. O. (2017). Recent homogeneity analysis and long-term spatio-temporal rainfall trends in Nigeria. *Theoretical and Applied Climatology*, *128*(1), 275–289. https://doi.org/10.1007/s00704-015-1701-x

Allechy, F. B., Youan Ta, M., N'Guessan Bi, V. H., Yapi, F. A., Koné, A. B., & Kouadio, A. (2020). Trend of Extreme Precipitations Indices in West-central Côte d'Ivoire: Case of the Lobo Watershed. *European Journal of Engineering Research and Science*, *5*(10), 1281–1287. https://doi.org/10.24018/ejers.2020.5.10.2195

Amichiatchi, N. J. M. C., Soro, G. E., Hounkpè, J., Goula Bi, T. A., & Lawin, A. E. (2023).

Evaluation of Potential Changes in Extreme Discharges over Some Watersheds in Côte d'Ivoire. *Hydrology*, *10*(1). https://doi.org/10.3390/hydrology10010006

Amogu, O., Descroix, L., Yéro, K. S., Breton, E. Le, Mamadou, I., Ali, A., … Belleudy, P. (2010). Increasing river flows in the Sahel? *Water (Switzerland)*, *2*(2), 170–199. https://doi.org/10.3390/w2020170

Amoussou, E. (2015). *Analyse hydrométéorologique des crues dans le bassin-versant du Mono en Afrique de l ' Ouest avec un modèle conceptuel pluie-débit To cite this version : HAL Id : halshs-01143318 Bourses Fernand Braudel*.

Anouma Fhorest Yao, B., & Gneneyougo Soro, E. (2021). Detection of Hydrologic Trends and Variability in Transboundary Cavally Basin (West Africa). *American Journal of Water Resources*, *9*(2), 92–102. https://doi.org/10.12691/ajwr-9-2-6

Anouman, D. G.-L., N'go, Y. A., Soro, G. E., & Bi, T. A. G. (2019). Spatial and Temporal Evolution of Low Water Flows in the Sassandra River Catchment Area in Cote d'Ivoire. *Journal of Geoscience and Environment Protection*, *07*(06), 184–202. https://doi.org/10.4236/gep.2019.76015

Anouman Djoro Gauthier-Lopez. (2020). Etude hydroclimatique et morphostructurale du bassin versant du sassandra : influence sur les aleas crue et tarissement des cours d'eau. Abidjan: Université Nangui Abrogoua.

Assoko A.V.S., Kouassi A.M., N. R. A. . (2020). Modélisation statistique des débits d'étiages et détermination de seuils d'étiages dans le bassin versant de la marahoué (bandama, côte d'ivoire) statistical. *Larhyss Journal, ISSN 1112-3680, N°41, n°41*, 121–147.

Assoma, V. T., Adiaffi, B., & Koudou, A. (2016). Influence de la Variabilité Climatique sur les Réserves en eau du sol et dans les Systèmes Agricoles du Bassin Côtier de l'Agnéby (Côte d'Ivoire). *European Journal of Scientific Research*, *143*(2), 186–202. Retrieved from http://www.europeanjournalofscientificresearch.com/issues/EJSR_143_2.html

Atcheremi K.N.D Jourda J. P. R., Saley M. B., Kouame K. J., B. R. . (2018). Etude de l'evolution des extremes pluviometriques et de temperature dans le bassin versant de riviere davo (sud-ouest de la cote d'ivoire) a partir de certains indices du logiciel rclimdex. *Larhyss Journal, ISSN 1112-3680, N°41, n°36*(6), 99–117.

Avenard, J.-M. (1971). Aspects de la Résistance. *Annales. Histoire, Sciences Sociales*, *20*(2), 405–405. https://doi.org/10.1017/s0395264900114301

Ávila, L., Silveira, R., Campos, A., Rogiski, N., Gonçalves, J., Scortegagna, A., … Fan, F. (2022). Comparative Evaluation of Five Hydrological Models in a Large-Scale and Tropical River Basin. Water (Switzerland), 14(19), 1–21. https://doi.org/10.3390/w14193013

Awotwi, A., Annor, T., Anornu, G. K., Quaye-Ballard, J. A., Agyekum, J., Ampadu, B., … Boakye, E. (2021). Climate change impact on streamflow in a tropical basin of Ghana, West Africa. *Journal of Hydrology: Regional Studies*, *34*(February), 100805. https://doi.org/10.1016/j.ejrh.2021.100805

Aye, P. P., Koontanakulvong, S., & Long, T. T. (2017). Estimation of Groundwater Flow Budget in the Upper Central Plain, Thailand from Regional Groundwater Model. *Internet Journal of Society for Social Management Systems*, *11*(April), 17–3216.

Balliet, R., Saley, M. B., Anowa Eba, E. L., Sorokoby, M. V., N'Guessan Bi, H. V., N'Dri, A. O., … Biémi, J. (2016). Évolution Des Extrêmes Pluviométriques Dans La Région Du Gôh (Centre-Ouest De La Côte d'Ivoire). *European Scientific Journal, ESJ*, *12*(23), 74. https://doi.org/10.19044/esj.2016.v12n23p74

Batablinlè, L., Agnidé, L. E., Japhet, K. D., Ernest, A., & Expédit, V. (2021). Future changes in precipitation, evapotranspiration and streamflows in the Mono Basin of West Africa. *Proceedings of the International Association of Hydrological Sciences*, *384*, 283–288. https://doi.org/10.5194/piahs-384-283-2021

Bigi, V., Pezzoli, A., & Rosso, M. (2018). Past and future precipitation trend analysis for the city of Niamey (Niger): An overview. *Climate*, *6*(3). https://doi.org/10.3390/cli6030073

Bodian, A., Dezetter, A., Diop, L., Deme, A., Djaman, K., & Diop, A. (2018). Future climate change impacts on streamflows of Two Main West Africa River Basins: Senegal and Gambia. *Hydrology*, *5*(1). https://doi.org/10.3390/hydrology5010021

Bonnot-Courtois, C., & Flicoteaux, R. (1989). Distribution of rare-earth and some trace elements in Tertiary phosphorites from the Senegal Basin and their weathering products. *Chemical Geology*, *75*(4), 311–328. https://doi.org/https://doi.org/10.1016/0009-

2541(89)90004-1

Brulebois, E., Ubertosi, M., Castel, T., Richard, Y., Sauvage, S., Sanchez-Perez, J.-M., … Amiotte-Suchet, P. (2018). Robustness and performance of semi-distributed (SWAT) and global (GR4J) hydrological models throughout an observed climatic shift over contrasted French watersheds. *Open Water Journal*, *5*(1), 41–56. Retrieved from https://hal.archives-ouvertes.fr/hal-02368907%0Ahttps://hal.archives-ouvertes.fr/hal-02368907/document

Bundock, K., Callan, G. L., Longhurst, D., Rolf, K. R., Benney, C. M., & McClain, M. B. (2021). Mathematics Intervention for College Students with Learning Disabilities: A Pilot Study Targeting Rate of Change. Insights into Learning Disabilities, 18(1), 1–28. Retrieved from https://search.ebscohost.com/login.aspx?direct=true&db=eric&AN=EJ1295246&amp%0Alang=hr&site=eds-live&authtype=shib&custid=s4162699

Carroget, A., Perrin, C., Sauquet, É., Vidal, J.-P., Chazot, S., Rouchy, N., & Chauveau, M. (2017). Explore 2070 : quelle utilisation d'un exercice prospectif sur les impacts des changements climatiques à l'échelle nationale pour définir des stratégies d'adaptation ? *Sciences Eaux & Territoires*, *Numéro 22*(1), 4–11. https://doi.org/10.3917/set.022.0004

Cecchi J.-P., F. Gourdin, S. Koné, D. Corbin, A. Etienne, et Casenave, (2009). Les petits barrages du nord de la Côte d'Ivoire : inventaire et potentialités hydrologiques. Sécheresse, vol. 20, No. 1, pp. 112–122.

Chang, J., Liu, Q., Wang, S., & Huang, C. (2022). Vegetation Dynamics and Their Influencing Factors in China from 1998 to 2019. *Remote Sensing*, *14*(14). https://doi.org/10.3390/rs14143390

Change, C., & Basis, T. S. (2001). *C Limate C Hange 2001 :*

Coulibaly Kolotioloma Alama. (2021). Impacts de la variabilité récente de la pluviométrie sur les paramètres agroclimatiques majeurs et les calendriers agricoles pour une corrélation avec le système couplé océan-atmosphère en côte d'ivoire (Université). Abidjan.

Chekchek Amira &Fennouh Zeyneb, 2019. Détection et extraction des surfaces d'eau a partie des données spatiales : cas du bassin versant côtier constantinois ouest, 91p

Dacharry, M. (1996). Les grandes crues historiques de la Loire. *Houille Blanche*, *51*(6–7), 47–53. https://doi.org/10.1051/lhb/1996067

David, K., Ephrem, M., Nestor, N. G., Roland, B., Kossonou, K., & Pria, J. (2022). Pétrographie et Origine des Granitoides du Secteur Bondoukou – Tanda (Nord- Est de la Côte d ' Ivoire , *Craton Ouest Africain)*. *11*(5), 10–21. https://doi.org/10.35629/6734-1105011021

De Lavenne, A., Thirel, G., Andréassian, V., Perrin, C., & Ramos, M. H. (2016). Spatial variability of the parameters of a semi-distributed hydrological model. *IAHS-AISH* Proceedings and Reports, 373(2011), 87–94. https://doi.org/10.5194/piahs-373-87-2016

Décamps, H. (2010). *Événements climatiques extrêmes Réduire les vulnérabilités* (RAPPORT SU).

Deguy Attoungbré Jean-Philippe. (2021). Evaluation de la vulnérabilité à l'érosion hydrique des sols du bassin versant de la Lobo (Côte d'Ivoire) : Approche par modélisations (THESE UNIQ; Université NANGUI ABROGOUA, ed.). Abidjan.

Dibi-Anoh, P. A., Koné, M., Gerdener, H., Kusche, J., & N'Da, C. K. (2023). Hydrometeorological Extreme Events in West Africa: Droughts. *Surveys in Geophysics*, *44*(1), 173–195. https://doi.org/10.1007/s10712-022-09748-7

Dimri, T., Ahmad, S., & Sharif, M. (2022). Hydrological modelling of Bhagirathi River basin using HEC-HMS. Journal of Applied Water Engineering and Research, (July). https://doi.org/10.1080/23249676.2022.2099471

Djellouli, F., Bouanani, A., & Baba-Hamed, K. (2016). Efficiency of some meteorological drought indices in different time scales, case study: Wadi Louza basin (NW-Algeria). *Journal of Water and Land Development*, *31*(1), 33–41. https://doi.org/10.1515/jwld-2016-0034

Dobler, A., & Ahrens, B. (2008). Precipitation by a regional climate model and bias correction in Europe and South Asia. *Meteorologische Zeitschrift*, *17*(4), 499–509. https://doi.org/10.1127/0941-2948/2008/0306

Donat, M. G., Peterson, T. C., Brunet, M., King, A. D., Almazroui, M., Kolli, R. K., … Al Shekaili, M. N. (2014). Changes in extreme temperature and precipitation in the Arab region: Long-term trends and variability related to ENSO and NAO. *International Journal of Climatology*, *34*(3), 581–592. https://doi.org/10.1002/joc.3707

Dorsouma Al Hamndou et Mélanie Requier-Desjardins (2008). « Variabilité climatique, désertification et biodiversité en afrique: s'adapter, une approche intégrée », VertigO - la revue électronique en sciences de l'environnement [En ligne], Volume 8 Numéro 1 | avril, URL: http://journals.openedition.org/vertigo/5356 ; DOI : https://doi.org/10.4000/vertigo.5356

Draman-donou, E. N., Fofié, Y., Adjambri, E., France, M., & Sawadogo, D. (2015). Caractérisation et évaluation in vitro de l ' effet antifalcimiant des graines de Cajanus cajan (Fabacées) sur les drépanocytes à Abidjan - Côte d ' Ivoire Characterization and in vitro evaluation of the antisickling effect of the seeds of Cajanus cajan. 9(October), 2300–2308.

Ehuitché, B. T. (2015). An analysis of dynamics of deforestation and agricultural productivity in Côte d'Ivoire. *International Research Journal of Agricultural Science and Soil Science*, *5*(4), 103–111.

Fabrice, T. F., & Brice, K. A. (2022). Spatial Analysis of Access to Drinking Water for the Populations of the Lobo Watershed in Nibéhibé (Central-Western Côte d'Ivoire). *Advances in Image and Video Processing*, *10*(3). https://doi.org/10.14738/aivp.103.12375

Fabrice, Y. A., Hermann, N. B. V., Solange, O. Y. M., Gautier, K. O. J., Blanchard, A. F., & Jean, B. (2020). Modélisation Des Extrêmes Climlatiques De La Région De La Marahoué À Partir D'un Générateur Stochastique De Temps Mono-Site (Weagets). *European Scientific Journal ESJ*, *16*(36), 70–91. https://doi.org/10.19044/esj.2020.v16n36p70

Faye, C. (2014). Étude des tendances de la distribution régionale des débits et de l'intensité de l'écoulement dans le bassin du fleuve Sénégal à l'exutoire du haut bassin (Bakel). ResearchGate, Climat,(January), 20p.

Flores, N., Rodríguez, R., Yépez, S., Osores, V., Rau, P., Rivera, D., & Balocchi, F. (2021).

Comparison of three daily rainfall-runoff hydrological models using four evapotranspiration models in four small forested watersheds with different land cover in south-central Chile. Water (Switzerland), 13(22), 1–28. https://doi.org/10.3390/w13223191

Fofana, M., Adounkpe, J., Larbi, I., Hounkpe, J., Djan'na Koubodana, H., Toure, A., … Limantol, A. M. (2022). Urban flash flood and extreme rainfall events trend analysis in Bamako, Mali. *Environmental Challenges*, *6*, 100449. https://doi.org/https://doi.org/10.1016/j.envc.2022.100449

Gailliez S. Low Discharge Discharge Estimation at Ungauged Sites. Application in Walloon Region. Ph.D. Thesis, Liège: Université of Liège, 2013, pp 272.

Garcia, F., Folton, N., & Oudin, L. (2017). Which objective function to calibrate rainfall–runoff models for low-flow index simulations? *Hydrological Sciences Journal*, *62*(7), 1149–1166. https://doi.org/10.1080/02626667.2017.1308511

Gauze, T. K. M., Morton, K. Y., Hermann, M. N., Largaton, S. G., & Emile, S. G. (2018). Impacts des changements de l'occupation du sol et des changements climatiques sur le bassin versant de la rivière Davo, Côte d'Ivoire. *European Scientific Journal, ESJ*, *14*(33), 408. https://doi.org/10.19044/esj.2018.v14n33p408

Golmohammadi, G., Prasher, S., Madani, A., & Rudra, R. (2014). Evaluating three hydrological distributed watershed models: MIKE-SHE, APEX, SWAT. *Hydrology*, *1*(1), 20–39. https://doi.org/10.3390/hydrology1010020

Goubanova, K., & Li, L. (2007). Extremes in temperature and precipitation around the Mediterranean basin in an ensemble of future climate scenario simulations. *Global and Planetary Change*, *57*(1), 27–42. https://doi.org/https://doi.org/10.1016/j.gloplacha.2006.11.012

Goula, B., Kouassi, V., & Savane, L. (2009). Impacts du changement climatique sur les ressources en eau en zone tropicale humide : cas du bassin versant du Bandama en Côte d\'Ivoire. *Agronomie Africaine*, *18*(1), 1–11. https://doi.org/10.4314/aga.v18i1.1674

Goula, B. T. A., Savane, I., Konan, B., Fadika, V., & Kouadio, G. B. (2006). Impact de la variabilité climatique sur les ressources hydriques des bassins de N'Zo et N'Zi en Côte

d'Ivoire (Afrique tropicale humide). *VertigO*, *7*(Volume 7 Numéro 1), 1–12. https://doi.org/10.4000/vertigo.2038

Guillaumet, J. L., & Adjanohoun, E. (1971). La végétation de la Côte d'Ivoire. Le milieu naturel de la Côte d'Ivoire, 50, 166-262.

Halwatura, D., & Najim, M. M. M. (2013). Application of the HEC-HMS model for runoff simulation in a tropical catchment. *Environmental Modelling and Software*, *46*, 155–162. https://doi.org/10.1016/j.envsoft.2013.03.006

Hamed, K. H., & Ramachandra Rao, A. (1998). A modified Mann-Kendall trend test for autocorrelated data. *Journal of Hydrology*, *204*(1–4), 182–196. https://doi.org/10.1016/S0022-1694(97)00125-X

Hu, X., Huang, B., & Cherubini, F. (2019). Impacts of idealized land cover changes on climate extremes in Europe. Ecological Indicators, 104(May), 626–635. https://doi.org/10.1016/j.ecolind.2019.05.037

Ilori, O. W., & Ajayi, V. O. (2020). Change Detection and Trend Analysis of Future Temperature and Rainfall over West Africa. *Earth Systems and Environment*, *4*(3), 493–512. https://doi.org/10.1007/s41748-020-00174-6

Ibo G. J. (2007). Fronts pionniers et retraits de terres: points de vue sur la sécurisation du foncier en Côte d'Ivoire. Revue de l'Institut de Géographie, (1) : 3-19.

Moatti Boubou Cisse, S. L. (2006). To cite this version : *Revue Teledetection*, *8*(1), 17–34.

Jenifer, M. A., & Jha, M. K. (2021). Assessment of precipitation trends and its implications in the semi-arid region of Southern India. *Environmental Challenges*, *5*, 100269. https://doi.org/https://doi.org/10.1016/j.envc.2021.100269

Kamagaté, A., Koffi, Y. B., Kouassi, A. M., Kouakou, B. D., & Seydou, D. (2019). Impact des Évolutions Climatiques sur les Ressources en eau des Petits Bassins en Afrique Sub-Saharienne: Application au Bassin Versant du Bandama à Tortiya (Nord Côte d'Ivoire). *European Scientific Journal ESJ*, *15*(9), 84–105. https://doi.org/10.19044/esj.2019.v15n9p84

Kamenan, Y. M., Mangoua, O. M. J., Dibi, B., Georges, S. E., Kouassi, K. L., & Kouassi, K.

A. (2020). Assessment of Vulnerability to Groundwater Pollution in the Lobo Watershed at Nibéhibé (Central-West, Côte d'Ivoire). Journal of Water Resource and Protection, 12(08), 657–671. https://doi.org/10.4236/jwarp.2020.128040

KlemeŠ, V. (1986). Operational testing of hydrological simulation models. Hydrological Sciences Journal, 31(1), 13–24. https://doi.org/10.1080/02626668609491024

Knebl, M. R., Yang, Z. L., Hutchison, K., & Maidment, D. R. (2005). Regional scale flood modeling using NEXRAD rainfall, GIS, and HEC-HMS/ RAS: A case study for the San Antonio River Basin Summer 2002 storm event. *Journal of Environmental Management*, *75*(4 SPEC. ISS.), 325–336. https://doi.org/10.1016/j.jenvman.2004.11.024

Kodja, D. J., Mahé, G., Amoussou, E., Boko, M., & Paturel, J.-E. (2018). Assessment of the Performance of Rainfall-Runoff Model GR4J to Simulate Streamflow in Ouémé Watershed at Bonou's outlet (West Africa). *Preprint*, (March), 18. https://doi.org/10.20944/preprints201803.0090.v1

Koffi, B., Kouadio, Z. A., Kouassi, K. H., Yao, A. B., Sanchez, M., & Kouassi, K. L. (2020). Impact of Meteorological Drought on Streamflows in the Lobo River Catchment at Nibéhibé, Côte d'Ivoire. *Journal of Water Resource and Protection*, *12*(06), 495–511. https://doi.org/10.4236/jwarp.2020.126030

Koffi, D., & Komla, G. (2015). Trend analysis in reference evapotranspiration and aridity index in the context of climate change in Togo. *Journal of Water and Climate Change*, *6*(4), 848–864. https://doi.org/10.2166/wcc.2015.111

Koffi, Zilé Alex Kouadio, Affoué Berthe Yao, Kouakou Hervé Kouassi, Martin Sanchez Angulo, and K. L. K. (2021). *Evaluation of the impacts of climate change and land-use dynamics on water resources : The case of the Lobo River watershed : Central- Western Côte d ' Ivoire Evaluation of the impacts of climate change and land-use dynamics on water resources : The case* . (April). https://doi.org/10.5194/egusphere-egu21-506

Koffie-Bikpo, C. Y., & Kra, K. S. (2013). La Région du Haut-Sassandra dans la distribution des produits vivriers agricoles en Côte d'Ivoire. *Revue de Géographie Tropicale et d'Environnement*, *2*, 95–103.

Koné, B., Dao, A., Fadika, V., Noufé, D., & Kamagaté, B. (2019). Effet de la Variabilité Pluviométrique sur les Écoulements de Surface dans le Bassin Versant de l'Agnéby au Sud-Est de la Côte d'Ivoire. *European Scientific Journal ESJ*, *15*(27), 383–401. https://doi.org/10.19044/esj.2019.v15n27p383

Konin, N. J. C., N'go, Y. A., Soro, G. E., & Goula, B. T. A. (2022). Impact of rainfall trends on flood in Agnéby watershed. *Journal of Water and Land Development*, *52*, 9–20. https://doi.org/10.24425/jwld.2021.139938

Koua, T. J., Jourda, J. P., Kouame, K. J., Anoh, K. A., Balin, D., & Lane, S. N. (2014). Potential climate change impacts on water resources in the Buyo Lake Basin (Southwest of Ivory Coast). *International Journal of Innovation and Applied Studies*, *8*(3), 1094–1111.

Kouadio Z.A., Soro G.E., Kouakou K.E.3, Goula Bi T.A., S. I. . . (2018). Inondations Frequentes À Agboville (Côte D'Ivoire): Quelles Origines? *Larhyss Journal*, *n°33*(1112–3680), 189–207.

Kouakou, A. B. P., Lawin, E. A., Kamagaté, B., Dao, A., Savané, I., & Srohourou, B. (2016). Rainfall variability across the agneby watershed at the Agboville outlet in Côte d'Ivoire, West Africa. *Hydrology*, *3*(4), 1–11. https://doi.org/10.3390/hydrology3040043

Kouamelan, A. N., Delor, C., & Peucat, J.-J. (1997). Geochronological evidence for reworking of Archean terrains during the Early Proterozoic (2.1 Ga) in the western Coˆte d'Ivoire (Man Rise-West African Craton). *Precambrian Research*, *86*(3), 177–199. https://doi.org/https://doi.org/10.1016/S0301-9268(97)00043-0

Kouassi, A M, Nassa, R. A., Bi, T. M. N., Kouame, K. F., & Biemi, J. (2018). Caractérisation des débits d'étiage dans un contexe de changements climatiques : Cas du bassin versant du N'zi (Côte d'Ivoire). *Agronomie Africaine*, *30*(3), 215–223.

Kouassi, Amani Michel, Yahot, A., & Gnangouin, J. (2021). Prospective impact study of flood flows in a context of climate change in West Africa : Case of the N ' zo watershed (Sassandra , West of Ivory Coast) Etude d ' impact prospective des débits de crues dans un contexte de changements climatiques en Afriqu. (November).

Kouassi, K. H., Kouadio, Z. A., N'go, Y. A., Koffi, B., & Ouédé, G. B. (2021). Modeling the

Propagation of Flood Waves at the Mouth of the Comoé River in Grand-Bassam (South East of Côte d'Ivoire). *International Journal of Environment and Climate Change*, (February), 33–42. https://doi.org/10.9734/ijecc/2021/v11i130328

Kouassi, K. M., Yao, K. B., Kouassi, K. L., Biemi, J., & Soro, N. (2020). Extreme flow variability analysis at the Bianouan hydrometric station on the Bia River watershed in Côte d'Ivoire. *Proceedings of the International Association of Hydrological Sciences*, *383*, 319–325. https://doi.org/10.5194/piahs-383-319-2020

Koudou, A., Assoma, T. V., Niamke, K. H., & Anoh, K. A. (2018). Caractérisation et quantification de la relation entre le réseau hydrographique et la fracturation du bassin versant côtier de l'Agnéby en Côte d'Ivoire. *Afrique SCIENCE*, *14*(5), 311–324.

Kouman, K. D., Kabo-Bah, A. T., Kouadio, B. H., & Akpoti, K. (2022). Spatio-Temporal Trends of Precipitation and Temperature Extremes across the North-East Region of Côte d'Ivoire over the Period 1981–2020. *Climate*, *10*(5). https://doi.org/10.3390/cli10050074

Kwawuvi, D., Mama, D., Agodzo, S. K., Hartmann, A., Larbi, I., Bessah, E., … Yangouliba, G. I. (2022). Spatiotemporal variability and change in rainfall in the Oti River Basin, West Africa. *Journal of Water and Climate Change*, *13*(3), 1151–1169. https://doi.org/10.2166/wcc.2022.368

Lang C. Les étiages : Définitions hydrologique, statistique et seuils réglementaires. Cybergeo : Euro. J. of Geography, Environnement, Nature, Paysage, mis en ligne le 30 Novembre 2011. URL: http//journals.openedition.org/cybeo/24827.

Larbi, I. (2019). Assessment of climate and land use change impacts on the water balance components in the vea catchment, west africa (DOCTOR of). Abomey-Calavi.

Larbi, I., Nyamekye, C., Dotse, S. Q., Danso, D. K., Annor, T., Bessah, E., … Yomo, M. (2022). Rainfall and temperature projections and the implications on streamflow and evapotranspiration in the near future at the Tano River Basin of Ghana. *Scientific African*, *15*, e01071. https://doi.org/10.1016/j.sciaf.2021.e01071

Le Moine, N. (2008). *Le bassin versant de surface vu par le souterrain : une voie d'amélioration des performances et du réalisme des modèles pluie-débit ?* 348. Retrieved from http://www.cemagref.fr/webgr/Download/Rapports_et_theses/2008-LE_MOINE-

THESE.pdf

Mangoua, M. J., Gone, D. L., Kouassi, K. A., N rsquo guettia, K. G., Douagui, G. A., Savane, I., & Biemi, J. (2015). Hydrogeochemical assessment of groundwater quality in the Baya watershed (Eastern of Cte dIvoire). *African Journal of Agricultural Research*, *10*(49), 4477–4489. https://doi.org/10.5897/ajar2015.10212

Mangoua, M. J., Kouassi, K. A., Douagui, G. A., Savané, I., & Biémi, J. (2019). Remote Sensing and GIS Contribution for Groundwater Mapping Reservoirs in the Baya Watershed (Eastern Region of Côte d'Ivoire). *Journal of Geography, Environment and Earth Science International*, *23*(3), 1–14. https://doi.org/10.9734/jgeesi/2019/v23i330169

McGinnis, S., Nychka, D., & Mearns, L. O. (2015). *A New Distribution Mapping Technique for Climate Model Bias Correction BT - Machine Learning and Data Mining Approaches to Climate Science* (V. Lakshmanan, E. Gilleland, A. McGovern, & M. Tingley, eds.). Cham: Springer International Publishing.

Michel, K. A., Asaph, G., Joel, Y., Armel, Y. C., & Emilienne, N. G. N. G. (2021). Etude d ' impact prospective des débits de crues dans un contexte de changements climatiques en Afrique de l ' O uest : Cas du bassin versant du N ' zo (Sassandra , Ouest de la Côte d ' Ivoire) [Prospective impact study of flood flows in a context of . 57(2), 117–131.

Miessan Germain, A., Edoukou Jacques, D., Okon Franck-Armstrong, D., Privat, T., Kan Jean, K., & Jean Patrice, J. (2019). Apport de l'Analyse Hydrologique et de la Modélisation de la Relation Pluie-Débit dans le Suivi Quantitatif des Ressources en Eau dans un Contexte de Variabilité Climatique: Cas du Sous-Bassin Versant du Kouto (Nord de la Côte d'Ivoire). *European Journal of Scientific Research*, *154*(2), 192–212. Retrieved from http://www.europeanjournalofscientificresearch.com

MINAGRA (Ministère de l'Agriculture et de la Production Animale) 2001. Recensement national de l'agriculture 2000-2001. Direction des Statistiques de la documentation et de l'informatique, Abidjan (Côte d'Ivoire), 90 p.

N'da S.A, K. K., Etilé, R. N., Blahoua, G. K., Bi, G., Paul, E. K., & Valentin, N. (2018). Composition and distribution of zooplankton in relationship to environmental parameters in tropical river (sassandra river basin , Côte d ' Ivoire). *Journal of Global Biosciences,*

7(5), 5423–5438.

N’Dri, W. K. C., Pistre, S., Jourda, J. P., & Kouamé, K. J. (2019). Estimation of the Impact of Climate Change on Water Resources Using a Deterministic Distributed Hydrological Model in Côte d’Ivoire: Case of the Aghien Lagoon. Journal of Geoscience and Environment Protection, 07(07), 74–91. https://doi.org/10.4236/gep.2019.77007

N’gnessan Bi Vami Hermann, SALEY Mahaman Bachir , OGA Yeï Marie Solange, YAPI Assa Fabrice, KOUADIO Boyossoro Hélène, BIEMI jean1, KOUADIO Affian & Département. (2017). Caractérisation de la sécheresse hydrologique dans la région de la Marahoué (Centre- ouest de la Côte d ’ Ivoire). *International Journal of Engineering Science Invention*, *X*(X ǁ XXXX. 2013 ǁ PP.), 12.

N’guessan, K. A., Diarrassouba, N., Alui, K. A., Nangha, K. Y., Fofana, I. J., & Yao-kouame, A. (2015). Indicateurs de dégradation physique des sols dans le Nord de la Côte d’Ivoire : cas de Boundiali et Ferkessédougou. *Afrique SCIENCE*, *11*(3), 115–128. Retrieved from http://www.afriquescience.info

N’guettia Kobenan Germain. (2021). Dynamique de l’occupation du sol et qualité physico-chimique des ressources en eau souterraine du bassin versant de la Baya (Est de la Côte d’Ivoire*).* (THESE UNIQ). Abidjan: Université Nangui Abrogoua.

N Guessan, A. K., Kouassi, M. A., GNABOA, R., TRAORE, K. ., & HOUENOU, P. . (2014). Analyse De Phenomènes Hydrologiques Dans Un Bassin Versant Urbanisé : Cas De La Ville De Yamoussoukro (Centre De La Cote D ’ Ivoire). *Larhyss Journal*, *17*(Mars 2014), 135–154.

Näschen, K., Diekkrüger, B., Evers, M., Höllermann, B., Steinbach, S., & Thonfeld, F. (2019). The Impact of Land Use/Land Cover Change (LULCC) on Water Resources in a Tropical Catchment in Tanzania under Different Climate Change Scenarios. *Sustainability (Switzerland)*, *11*(24). https://doi.org/10.3390/su11247083

Nash, J. E., & Sutcliffe, J. V. (1970). ’ L ~ E Empirical or Analytical Approaeb. *Journal of Hydrology*, *10*(3), 282–290. Retrieved from http://linkinghub.elsevier.com/retrieve/pii/0022169470902556

Nicholson, S. E., & Selato, J. C. (2000). The influence of La Nina on African rainfall.

International Journal of Climatology, *20*(14), 1761–1776. https://doi.org/10.1002/1097-0088(20001130)20:14<1761::AID-JOC580>3.0.CO;2-W

Nouaceur, Z. (2020). La reprise des pluies et la recrudescence des inondations en Afrique de l'Ouest sahélienne. *Physio-Géo*, (Volume 15), 89–109. https://doi.org/10.4000/physio-geo.10966

Noufou Coulibaly. (1998). Déforestation et activités agricoles en Côte d'Ivoire: recherche d'un nouvel équilibre. Thèse de doctorat, faculté des études supérieures de l'Université Laval, Québec, Canada,159 p.

OCHA. 2013. http://www.unocha.org/cotedivoire/maps-graphics/thematic-maps

Oguntunde, P. G., Abiodun, B. J., & Lischeid, G. (2011). Rainfall trends in Nigeria, 1901-2000. *Journal of Hydrology*, *411*(3–4), 207–218. https://doi.org/10.1016/j.jhydrol.2011.09.037

Oguntunde, P. G., Friesen, J., van de Giesen, N., & Savenije, H. H. G. (2006). Hydroclimatology of the Volta River Basin in West Africa: Trends and variability from 1901 to 2002. *Physics and Chemistry of the Earth, Parts A/B/C*, *31*(18), 1180–1188. https://doi.org/https://doi.org/10.1016/j.pce.2006.02.062

Okafor, G. C., Larbi, I., Chukwuma, E. C., Nyamekye, C., Limantol, A. M., & Dotse, S.-Q. (2021a). Local climate change signals and changes in climate extremes in a typical Sahel catchment: The case of Dano catchment, Burkina Faso. *Environmental Challenges*, *5*, 100285. https://doi.org/https://doi.org/10.1016/j.envc.2021.100285

Okafor, G. C., Larbi, I., Chukwuma, E. C., Nyamekye, C., Limantol, A. M., & Dotse, S. Q. (2021b). Local climate change signals and changes in climate extremes in a typical Sahel catchment: The case of Dano catchment, Burkina Faso. *Environmental Challenges*, *5*(June), 100285. https://doi.org/10.1016/j.envc.2021.100285

Oleyiblo, J. O., & Li, Z. J. (2010). Application of HEC-HMS for flood forecasting in Misai and Wan'an catchments in China. *Water Science and Engineering*, *3*(1), 14–22. https://doi.org/10.3882/j.issn.1674-2370.2010.01.002

Oularé, S., Adon, G. C., Akpa, L. Y., Saley, M. B., Kouamé, F. K., & Therrien, R. (2017). Identification Des Zones Potentielles De Recharge Des Aquifères Fracturés Du Bassin

Versant Du N'zo (Ouest De La Côte d'Ivoire) : Contribution Du SIG Et De La Télédétection. *European Scientific Journal, ESJ*, *13*(36), 192. https://doi.org/10.19044/esj.2017.v13n36p192

Ozer, P., LaminouManzo, O., Tidjani, A., Djaby, B., & DeLongueville, F. (2017). Recent evolution of rainfall extremes in Niger (1950-2014)Evolution récente des extrêmes pluviométriques au Niger (1950-2014). *J*, *41*(3).

Patchali, T. E., Ajide, O. O., Matthew, O. J., Salau, T. A. O., & Oyewola, O. M. (2020). Examination of potential impacts of future climate change on solar radiation in Togo, West Africa. *SN Applied Sciences*, *2*(12), 1941. https://doi.org/10.1007/s42452-020-03738-3

Perrin, C., Michel, C., & Andréassian, V. (2003). Improvement of a parsimonious model for streamflow simulation. *Journal of Hydrology*, *279*(1–4), 275–289. https://doi.org/10.1016/S0022-1694(03)00225-7

Piani, C., Weedon, G. P., Best, M., Gomes, S. M., Viterbo, P., Hagemann, S., & Haerter, J. O. (2010). Statistical bias correction of global simulated daily precipitation and temperature for the application of hydrological models. *Journal of Hydrology*, *395*(3–4), 199–215. https://doi.org/10.1016/j.jhydrol.2010.10.024

Piniewski, M., Marcinkowski, P., & Kundzewicz, Z. W. (2018). Trend detection in river flow indices in Poland. *Acta Geophysica*, *66*(3), 347–360. https://doi.org/10.1007/s11600-018-0116-3

Renard, B. (2006). *Détection et prise en compte d ' éventuels impacts du changement climatique sur les extrêmes hydrologiques en*.

RCN,2021: https://www.floodmanagement.info/floodmanagement/wp-content/uploads/2021/02/Report_Nat_Consult_CI_FR__reviewCIMA_def_7jan2021.pdf

RGPH. (2022). *Rgph-2021 résultats globaux*. 1–37.

Robinson, M., & Cosandey, C. (2002). Impact de la forêt sur les débits d'étiage. Http://Dx.Doi.Org/10.1051/Lhb/2002044, 88. https://doi.org/10.1051/lhb/2002044

Rouse J.w. & Haas R.H., 1973. Monitoring vegetation in the great plain with ERTS, Third

ERTS Symposium, washington DC: NASA, p309-307

Saley, M.B. (2003) Système d'information hydrogéologique à référence spatiale, discontinuités pseudo-images, et cartographie thématique des ressources en eau de la région semi-montagneuse de Man (Ouest de la Côte d'Ivoire). Thèse unique de doctorat, Université de Cocody, Abidjan.

Saley, M. B., Kouamé, F. K., Penven, M. J., Biémi, J., & Boyossoro Kouadio, H. (2005). Cartographie Des Zones À Risque D ' Inondation Dans La Région Semi-Montagneuse À Louest De La Côte D ' Ivoire : Apports Des Mna Et De L ' Imagerie Satellitaire. *Télédétection, 5*(1-2–3), 53–67.

Sandeep K. P., Nicole O'Br. Modifiedmk: Modified Versions of Mann Kendall and Spearman's Rho Trend Tests,2021, R package version 1.6. https://CRAN.project.org/package=modifiedmk

Sankare, Y., Avit, F.-B. L. F., Egnankou, W., & Saenger, P. (1999). Nationale Plantentuin van België Etude floristique des mangroves des milieux margino-littoraux de Cote d'Ivoire. *Bulletin Du Jardin Botanique National de Belgique*, *67*(1), 335–360.

Sardoii, E. R., Rostami, N., Sigaroudi, S. K., & Taheri, S. (2012). Calibration of loss estimation methods in HEC-HMS for simulation of surface runoff (case study: Amirkabir dam watershed, Iran). *Advances in Environmental Biology*, *6*(1), 343–348.

Serdeczny, O., Adams, S., Baarsch, F., Coumou, D., Robinson, A., Hare, W., … Reinhardt, J. (2017). Climate change impacts in Sub-Saharan Africa: from physical changes to their social repercussions. *Regional Environmental Change*, *17*(6), 1585–1600. https://doi.org/10.1007/s10113-015-0910-2

Seydou, D., Dabissi, N., Armand, T. B. Z., Amidou, D., Bamory, K., Rose, E. K., … Seguis, L. (2018). Effets De La Dynamique Du Couvert Végétal Sur Les Écoulements Dans Le Bassin Versant De La Lagune Aghien En Côte d'Ivoire. *European Scientific Journal ESJ*, *14*(36). https://doi.org/10.19044/esj.2018.v14n36p312

SODEMI (1972). Carte géologique de la Côte d'Ivoire

Soro, G E, A, G. B. I. T., Srohorou, B., & Savane, I. (2014). Caracterisation des sequences de secheresse meteorologique a diverses echelles de temps en climat de type soudanais : cas

de l ’ extreme nord - ouest de la *COTE D ’ IVOIRE*. 107–124.

Soro, Gneneyougo Emile. (2011). Modelisation statistique des pluies extremes *EN COTE D’IVOIRE* (THESE UNIQ; Université d’Abobo-Adjamé, ed.). Abidjan.

Soro, Gneneyougo Emile, Noufé, D., Bi, T. A. G., & Shorohou, B. (2016). Trend analysis for extreme rainfall at sub-daily and daily timescales in Côte d’Ivoire. *Climate*, *4*(3). https://doi.org/10.3390/cli4030037

Soro G., E. K. Ahoussi, E. K. Kouadio, T. D. Soro, S. Oulare, M. B. Saley et N. Soro, (2014). La dynamique de l’occupation du sol dans la région des Lacs (Centre de la Côte d’Ivoire). Afrique science, vol. 10, no. 3, pp. 146–160.

Switanek, M., Crailsheim, K., Truhetz, H., & Brodschneider, R. (2017). Modelling seasonal effects of temperature and precipitation on honey bee winter mortality in a temperate climate. *Science of The Total Environment*, *579*, 1581–1587. https://doi.org/https://doi.org/10.1016/j.scitotenv.2016.11.178

Sylla, M. B., Nikiema, P. M., Gibba, P., Kebe, I., & Klutse, N. A. B. (2016). *Climate Change over West Africa: Recent Trends and Future Projections BT - Adaptation to Climate Change and Variability in Rural West Africa* (J. A. Yaro & J. Hesselberg, eds.). https://doi.org/10.1007/978-3-319-31499-0_3

Teshome, A., Zhang, J., Demissie, T., & Ma, Q. (2022). Observed and Future Spatiotemporal Changes of Rainfall Extreme Characteristics and Their Dynamic Driver in June-August Season over Africa. *Atmospheric and Climate Sciences*, *12*(02), 358–382. https://doi.org/10.4236/acs.2022.122022

Thapa, S., Baral, S., Hu, Y., Huang, Z., Yue, Y., Dhakal, M., … Wu, Y. (2021). Will climate change impact distribution of bats in Nepal Himalayas? A case study of five species. Global Ecology and Conservation, 26. https://doi.org/10.1016/j.gecco.2021.e01483

the Status of the Global Climate in 2006. (2006). *Organization*, (1016).

Thorsten Pohlert Trend: Non-Parametric Trend Tests and Change-Point Detection,2020, R package version 1.1.4. https://CRAN.R-project.org/package=trend

Touré, N. O., Dia Kane, Y., Diatta, A., Ba Diop, S., Niang, A., Ndiaye, E. M., … Hane, A. A.

(2007). Tuberculose et diabète. *Revue Des Maladies Respiratoires*, *24*(7), 869–875. https://doi.org/https://doi.org/10.1016/S0761-8425(07)91389-3

Tyson, P. D., Dyer, T. G. J., & Mametse, M. N. (1975). Secular changes in South African rainfall: 1880 to 1972. *Quarterly Journal of the Royal Meteorological Society*, *101*(430), 817–833. https://doi.org/10.1002/qj.49710143008

Tucker, (1979). "Red and photographic infrared linear combinations for monitoring vegetation", Remote Sensing of the Environment, no.8, pp.127-150

Ul Moazzam, M. F., Rahman, G., Munawar, S., Tariq, A., Safdar, Q., & Lee, B. G. (2022). Trends of Rainfall Variability and Drought Monitoring Using Standardized Precipitation Index in a Scarcely Gauged Basin of Northern Pakistan. *Water (Switzerland)*, *14*(7). https://doi.org/10.3390/w14071132

United Nations Development Programme (UNDP). (2018). Water Resources of Côte d'Ivoire.

Valéry, A., Andréassian, V., & Perrin, C. (2014). 'As simple as possible but not simpler': What is useful in a temperature-based snow-accounting routine? Part 2 – Sensitivity analysis of the Cemaneige snow accounting routine on 380 catchments. *Journal of Hydrology*, *517*, 1176–1187. https://doi.org/https://doi.org/10.1016/j.jhydrol.2014.04.058

Vissin, E. W. (2007). Impact de la variabilité climatique et de la dynamique des états de surfacesur les écoulements du bassin béninois du fleuve Niger. *Centre de Recherches En Climatologie (CNRS-UMR 5210)*, *Thèse de d*, 310p.

Wagener, T., McIntyre, N., Lees, M. J., Wheater, H. S., & Gupta, H. V. (2003). Towards reduced uncertainty in conceptual rainfall-runoff modelling: Dynamic identifiability analysis. *Hydrological Processes*, *17*(2), 455–476. https://doi.org/10.1002/hyp.1135

WMO (2006). Organization, (1016)

Yao, A. B. (2015). *Evaluation Des Bassin Versant De La Lobo En Vue D ' Une Ge Stion Rationnelle (Centre- Ouest De La Cô Te D ' Ivoire)*. 225.

Yao, A. B., Akaffou, F. H., Eblin, S. G., & Komey, A. K. (2023). *Impacts of climatic extremes on the production of hydroelectric energy from the Faé dam in San-Pédro (*

South-West Côte d ' Ivoire). (May), 5194.

Yao, A. B., Eblin, S. G., Brou, L. A., Kouassi, K. L., Ouede, G. B., Salifou, I., … Péné, B. C. (2021). Characterization of the variability in climate extremes in the Ferkessédougou sugar complexes (Northern Cote d'Ivoire). *Proceedings of the International Association of Hydrological Sciences*, *384*, 203–211. https://doi.org/10.5194/piahs-384-203-2021

Yao, A. B., Tié, B., Goula, A., Kane, A., Jules, O. M., & Kouassi, K. A. (2016). Cartographie du potentiel en eau souterraine du bassin versant de la Lobo (Centre-Ouest , Côte d ' Ivoire) : approche par analyse multicritère. *Hydrological Sciences Journal*, *61*(5), 856–867. https://doi.org/10.1080/02626667.2014.932360

Yao, J., Chen, Y., Zhao, Y., Mao, W., Xu, X., Liu, Y., & Yang, Q. (2018). Response of vegetation NDVI to climatic extremes in the arid region of Central Asia: a case study in Xinjiang, China. *Theoretical and Applied Climatology*, *131*(3), 1503–1515. https://doi.org/10.1007/s00704-017-2058-0

Yèkambèssoun N'Tcha M'Po Agnidé Emmanuel Lawin, Ganiyu Titilope Oyerinde, Benjamin Kouassi Yao, A. A. A. (2017). Comparison of Daily Precipitation Bias Correction Methods Based on Four Regional Climate Model Outputs in Ouémé Basin, Benin. *Hydrology*, *4*(6), 58. https://doi.org/10.11648/j.hyd.20160406.11

Yusop, Z., Chan, C. H., & Katimon, A. (2007). Runoff characteristics and application of HEC-HMS for modelling stormflow hydrograph in an oil palm catchment. *Water Science and Technology*, *56*(8), 41–48. https://doi.org/10.2166/wst.2007.690

Zhu, L., He, L., Shang, P., Zhang, Y., & Ma, X. (2018). Influencing factors and scenario forecasts of carbon emissions of the Chinese power industry: Based on a generalized divisia index model and monte carlo simulation. *Energies*, *11*(9). https://doi.org/10.3390/en11092398

ANNEX

Annex 1: List of Publications

Amichiatchi, N. J. M. C., Soro, G. E., Hounkpè, J., Goula Bi, T. A., & Lawin, A. E. (2023). Evaluation of Potential Changes in Extreme Discharges over Some Watersheds in Côte d'Ivoire. *Hydrology*, *10*(1). https://doi.org/10.3390/hydrology10010006 (Published)

N'da Jocelyne Maryse Christine Amichiatchi, Jean Hounkpè, Gneneyougo Emile Soro, Ojelabi Oluwatoyin Khadijat, Isaac Larbi, Andrew Manoba Limantol, Abdul-Rauf Malimanga Alhassan, Tie Albert Goula Bi, Agnidé Emmanuel Lawin; Analysis of past and projected changes in extreme precipitation indices in some watersheds in Côte d'Ivoire. Journal of Water and Climate Change 1 February 2024; 15 (2): 392–406. doi: https://doi.org/10.2166/wcc.2023.365 (Published)

Ojelabi Oluwatoyin, Oluwasemire Olatunji, Amichiatchi Jocelyn, Agnide Lawin (2023). Impacts of Anthropogenic Activities on Land use land cover changes dynamics in Ogun River basin Nigeria (Pending review)

Miss AMICHIATCHI N'da Jocelyne Maryse Christine was born in Abobo, Abidjan, Cote d'Ivoire in 1987. I am 36 years old and mother of one (1) baby girl since 2017. I attended my primary school at Toumodi, in the Centrale region of Cote d'Ivoire and the senior high school in this same town. I got my Baccalaureate at Lycee Mamie Adjoua, one of the excellent female schools in the Centrale region of Cote d'Ivoire in 2008. I rejoined Abidjan in 2009 for the university studies at University of Nangui Abrogoua from 2009 to 2017 where I got my Master degree. From 2010 to 2013, due to the war in my country, Universities were closed. I got my Bachelor degree in 2015 and in 2017, I got Master degree in Hydrology and Environment on the topic of impact of climate change impact on water inflows to the Kossou dam. After, my Master degree, I got a training from 12-04-2019 to 12-07-2019, a 4 months' internship in the Climate Change Directorate of the Environmental Information System (EIS). Since September 2019, I joined West African Science Service Center on Climate Change and Adapted Land Use (WASCAL) doctoral program in climate change and water resource. Concerning some of my qualities, I would describe myself as hard-working woman, open-minded, able to work alone or with team, I can work under pressure, disciplined, enthusiastic and Christian.

Abstract: This study assessed the impact of climate change on hydrological extremes (rainfall and discharge) in different climatic zones of Cote d'Ivoire. The objectives of this work were (i) to analyze the historical hydroclimatic trends (rainfall and discharge) from 1970 to 2017 and the effect of rainfall variability on low and high discharge in selected watersheds (ii) to analyze the effectiveness of the GR4J, GR5J and HEC-HMS hydrological models in simulating low flows and floods in selected river basins and (iii) examine the impact of climate change on extreme hydroclimatic events under the RCP4. 5 and RCP8.5 climate scenarios by 2050. Daily rainfall, discharge and evapotranspiration data (observed and future) and satellite images were the main data used in this research. Several methods where used to reach our objectives such us the standard homogeneity test and the modified Mann-Kendall test to analyze the historical hydro-climatic trends (rainfall and discharge), calibration and validation process to access the performance of the hydrological models in simulating low flows and floods in selected river basins and analysis on impact on land used future trend pattern were assessed on climate change on extreme hydroclimatic events under the RCP4. 5 and RCP8.5 Thus, this work has shown that the extreme indices have experienced a downward trend for extreme rainfall and a mixed trend (increase and decrease) for the flows for the data observed from our different study stations that are subject to the influence of high climate variability. As for the hydrological models, they showed a good performance overall both in calibration and validation with le Nash value around 0.7 for most of the watershed but the GR5J model showed a better performance on all the study basins and was therefore used in the simulation of futurs flows on its different basins. Under the RCP 4.5 and RCP 8.5 scenarios, the CNRM, CM5A and MPI climate models showed a fairly relative result dominated by a non-significant trend in the extreme indices used. Several methods were used to evaluate the dynamics of land use at the extremes, showing that all our study basins have been dynamically affected, either positively or negatively. Also, the relationship between changes in the vegetation index (NDVI) and extreme rainfall indices showed a non-significant negative correlation in general over the catchment areas studied, which would indicate that the recurrence of flooding or drought in Côte d'Ivoire is linked to the loss of vegetation cover. Similarly, this analysis revealed a positive correlation between vegetation indices (NDVI) and extreme flow indices as a whole. And finally, the analysis of the impact of climate change showed a decrease in annual rainfall, an increase in mean temperature and an alternation of decrease and increase in evapotranspiration analyzed and a great change on the discharge under RCP8.5 scenarios.

Key words: Climate variability, trend analysis on extreme indices, performance evaluation of hydrological models, climate change impact analysis.

PhD

Amichiatchi N' da Jocelyne Maryse Christine

ASSESSMENT OF THE IMPACT OF CLIMATE CHANGE ON HYDROLOGICAL EXTREMES IN COTE D' IVOIRE